Performance of Cement Paste with Polypropylene Fibre and Powder at High Temperature

Daha Shehu Aliyu

A thesis presented for the degree of
Doctor of Philosophy

School of Engineering,
Newcastle University, United Kingdom

August 2024

ABSTRACT

This research focuses on enhancing the elevated temperature by using ultraviolet (UV) treatment for polypropylene fibres (PPF) and powder (PPP). Cement paste is considered in this research to avoid the compounding effect of aggregate. The strength of cement paste relies on the presence of calcium silicate hydrate (C-S-H). However, at elevated temperatures, C-S-H decomposes, leading to stress and potential damage. The use of PPF and PPP in concrete initially reduced compressive strength due to poor cohesion between polypropylene and cement paste. Various experiments were conducted to evaluate these effects, including residual compressive strength testing under different humidity conditions, compressive strength and stiffness analysis at hot temperatures, microstructure investigation, and transient thermal creep testing. The use of UV-treated PPF and PPP significantly improved the compressive strength at all temperatures. The compressive strength at hot temperatures increased due to transforming the hydrophobic nature of polypropylene to hydrophilic.

Additionally, UV-treated PPF improves cement stiffness at high temperatures but showed little difference at room temperature. Microstructure investigations revealed that UV-treated PPF exhibited stronger bonding with cement paste, enhancing contact at room temperature, and UV-treated PPP reduced crack formation at 20°C. Both PPF and PPP melted at around 160ºC, leading to increased porosity in the cement paste. The microstructure remained unchanged until 200°C, but at 200°C, PPF and PPP melted, creating interconnected pores while PP remains in the sample. At 350°C, increased pore formation was observed. Thermal strain and transient thermal creep results indicated the impact of PPF in cement paste. Thermal expansion occurred up to 150°C, followed by contraction due to chemical reactions such as dehydration of calcium hydroxide, decomposition of calcium silicate hydrate, and decomposition of ettringite. The inclusion of UV-treated PPF reduced thermal expansion at 150°C by approximately 41%, enhancing dimensional stability. Thermal strain under constant load is reduced by approximately 50% at 100°C. Transient thermal creep increased with rising temperatures, while PPF did not affect TTS. A review of existing models and their predictions was carried out in relation to the TTS behaviour measured in this work. The review identifies limitations in current models, particularly above 200°C, and highlights the minimal effect of polypropylene fibres on TTS, advocating for improved models to enhance accuracy in predicting cement paste behaviour under high-temperature conditions.

ACKNOWLEDGMENT

In the name of Allah, the Most Gracious, the Most Merciful. All praise is due to Allah, the Lord of the world, who has enabled me to complete my PhD thesis. Without His grace and guidance, this accomplishment would not have been possible.

I sincerely thank my supervisor, Dr. Colin T Davie, for all his help and support during my research. His priceless advice and criticism were quite helpful in developing my work. I also thank Dr Enrico Masoero and Prof. Sean Wilkinson for their thoughtful assistance from the beginning of the study and their great contribution to me. I owe a debt of gratitude to Engineering's faculty and staff, mostly laboratory technologists, who have supported me throughout my academic career and given me a wonderful academic environment.

I am grateful to have had amazing people in my life, including friends and colleagues from inside and outside the institution, who have provided support, inspiration, and assistance throughout the years. Their kindness and generosity have helped me navigate the challenges of the PhD program.

I am thankful for the love and support I have received from my family, especially my parents, as I have pursued my academic goals. Their support and inspiration have been what has propelled my accomplishment. Special thanks to my wife and her parents for their unwavering support, love, and encouragement throughout this journey. My wife's patience, understanding, and sacrifices have been invaluable to me, and I am forever grateful for her presence in my life.

I am immensely grateful to Allah for blessing me with the gift of a beautiful newborn baby boy along my PhD journey. This bundle of joy has brought immense happiness and motivation to my life, and I thank Allah for this precious blessing. My thanks go to my lovely daughter for her daily prayer when leaving home for school for my success in my studies.

Finally, I want to express my sincere gratitude to the Petroleum Technology Development Fund (PTDF) for providing me with a scholarship for the duration of my studies. In addition to allowing me to continue my PhD, this grant has given me priceless chances to advance my academic and scientific abilities.

Table of contents

LIST OF TABLES

TABLE OF FIGURES

LIST OF EQUATIONS

ABBREVIATION

PP	Polypropylene
PPF	Polypropylene fibre
PPP	Polypropylene powder
C-S-H	Calcium silicate hydrate
RSC	Residual compressive Strength
RH	Relative humidity
SEM	Scanning electron microscope.
UV	Ultraviolet
MIP	Mercury Intrusion Porosimetry
XRD	X-ray diffraction
TTS	Transient thermal strain
RILEM	International Union of Laboratories and Experts in Construction Materials

NOMENCLATURE

Symbol	Term	Unit
ε_{th}	Thermal strain	
ε_{creep}	Creep strain	
ε_{tts}	Transient thermal strain	
T	Temperature	^{o}C
Es	Elastic modulus of the sample	MPa
Ks	Stiffness of the sample	N/mm
As	Cross-sectional area of the sample	m^2
Ls	Length of the sample	m
M	Mass	kg
V	Volume	m^3
D	Density	kg/m^3
σ_i	Initial compressive stress before heating	
σ_{uo}	Uniaxial compressive strength of the concrete	
$\varepsilon_{0.3}$	TTS at a stress/strength ratio of 0.3	
V_a	Volume of aggregate	m^3

Chapter 1: INTRODUCTION

1.1 Background

Concrete, a widely used construction material, relies on cement paste as its binding material. The strength of cement paste is primarily attributed to the presence of calcium silicate hydrate (C-S-H) (Colina & Sercombe, 2004). However, when subjected to elevated temperatures, C-S-H undergoes thermochemical reactions, leading to the release of water from nanopores into larger pores, a phenomenon referred to as dehydration in the cement paste literature. This dehydration process can introduce significant stress and potential damage to the C-S-H due to the removal of the firmly bound water within nanopores (Gawin et al., 2004). Consequently, high-temperature effects on cement-based materials encompass various fundamental phenomena, including dehydration of the pore system, thermal deformations, chemical phase transformations, drying creep, shrinkage, decomposition of hydration products, and microstructure destruction (Davie et al., 2010; Khoury, 1992a; Sarshar & Khoury, 1993; Schneider et al., 1997; Wang et al., 2019; Zhang & Davie, 2013) all of which contribute to structural damage.

Various applications can subject concrete to high temperatures, such as exposure to fire in buildings and structures, high-temperature industrial processes like furnaces and reactors, hot climates with prolonged sunlight exposure, geothermal projects, concrete pavements and roads in hot regions, high-temperature steam curing during construction, and concrete repair and retrofitting works involving high-temperature materials or processes. In these scenarios, the potential for thermochemical reactions in the calcium silicate hydrate (C-S-H) within the cement paste, leading to dehydration and structural damage, becomes a concern.

To mitigate the detrimental effects of high temperatures on concrete, researchers have explored the addition of polypropylene fibres. Several studies (Kalifa et al., 2002; Noumowe, 2005; Zeiml et al., 2006) have demonstrated the potential of polypropylene fibres to improve the performance of concrete exposed to high temperatures. Among various types of fibres, polypropylene fibre has shown particular effectiveness in enhancing the properties of cementitious materials (Kalifa et al., 2002; Zheng & Feldman, 1995).

However, adding polypropylene fibres reduces the compressive strength of hardened cement paste at ambient temperature (Bei-xing et al., 2004) and at high temperatures (Abaeian et al., 2018). This loss can be attributed to the hydrophobic nature of polypropylene, which hampers the cohesion between polypropylene and cement hydrate (Ossola & Wojcik, 2014).

Addressing the issue of reduced compressive strength, modifying the surface chemistry of polypropylene offers a potential solution by minimising its hydrophobicity. Such surface modifications can improve the final composite without compromising the workability of the mix and concurrently enhance the strength of the hardened paste (Coopamootoo & Masoero, 2018).

In light of these considerations, this study aims to investigate the effects of modifying the surface chemistry of polypropylene fibres and powder on the high-temperature performance of cement paste. By exploring the impact of surface modifications on the cohesion between polypropylene and cement hydrate, this research seeks to enhance the understanding of the mechanisms involved in improving the high-temperature properties of concrete reinforced with modified polypropylene fibres and powder. The findings of this study can contribute to the development of more durable and reliable concrete structures, particularly in applications where exposure to high temperatures is a concern.

1.2 Aim and Objectives

This study aims to investigate the effects of modifying the surface chemistry of polypropylene fibres and powder on the high-temperature performance of cement paste. This cement paste material will provide fire safety when used in tunnel linings and oil well grout.

The research aim will be achieved through the following objectives.

1) To identify the effect of humidity on the residual strength of cement paste samples heated to elevated temperatures that contain UV-treated or non-UV-treated polypropylene fibre and polypropylene powder.
2) To identify the microstructural changes using scanning electron microscopy (SEM) of cement paste samples heated to elevated temperatures that contain UV-treated or non-UV-treated polypropylene fibre and polypropylene powder.
3) To quantify the compressive strength and stiffness of the cement paste containing polypropylene fibres with and without UV treatment at a temperature ranging from ambient to 350°C.
4) To quantify the transient thermal creep of cement paste containing polypropylene fibres with and without UV treatment.

The decision to focus solely on polypropylene fibre (PPF) for objectives 3 and 4 is based on the observation made during the experiment for objective one. It was found that PPF yielded better results compared to PPP. Consequently, PPF was exclusively chosen for the subsequent experiments to save time, given the unexpected time constraints that disrupted the laboratory experiment.

1.3 Research knowledge contribution

This study aims to contribute to the knowledge gap regarding the effect of high temperatures on cement paste and its impact on concrete structures. Previous literature has established that elevated temperatures adversely affect cement paste, resulting in deterioration and mechanical changes. While some studies have explored the use of polypropylene fibre to enhance concrete properties at ambient and high temperatures, they have mostly reported the negative effects of polypropylene addition to the cement paste matrix at ambient and high temperatures. However, there is a lack of research on applying surface-treated polypropylene to improve cement paste performance.

This study takes a new approach by utilising ultraviolet treatment (UV) of polypropylene to mitigate the negative effects when added to cement paste, especially at high temperatures. The research focuses on critical parameters like residual compressive strength, compressive strength at high temperatures, and transient thermal creep of UV-treated polypropylene in cement paste under extreme conditions. By doing so, the study aims to comprehensively understand the behaviour of UV-treated polypropylene in cement paste.

This study develops a novel material that effectively reduces high-temperature effects on cement paste. This finding can potentially improve the design and construction of fire-resistant concrete structures, enhancing their durability and safety in high-temperature environments. These findings have practical implications for the construction industry, leading to the development of strong and fire-resistant concrete structures.

1.4 Justification of the research

The utilization of ultraviolet (UV) treatment for polypropylene in cement paste represents a crucial advancement in the field of construction materials. The decision to incorporate UV-treated polypropylene from the observed benefits it imparts to the mechanical properties of cement paste under varying temperature conditions. In prior research, non-UV-treated polypropylene had been employed, leading to a significant drawback in the mechanical performance of concrete at both ambient and high temperatures. This decline in mechanical properties raised concerns about the overall durability and structural integrity of the resulting concrete structures, highlighting the necessity for an alternative approach to enhance the material's resistance and strength. Recognizing this limitation, the integration of UV-treated polypropylene becomes imperative, as it offers the potential to counteract the observed decline and fortify the cement paste against the detrimental effects of both ambient and high-temperature environments.

The justification for employing UV treatment on polypropylene in cement paste is further underscored by its ability to induce positive alterations in the microstructure of the material. UV treatment has been shown to influence the molecular and surface characteristics of polypropylene, leading to improved adhesion and compatibility with the cement matrix. This enhanced compatibility contributes to the overall cohesion and integrity of the cement paste, resulting in superior mechanical properties.

1.5 Scope and limitation of the research

The research scope is limited to the effect of high temperature on the cement paste containing polypropylene fibre and polypropylene powder in the form of additives. Therefore, there are certain limitations of this research as follows:

1. The research considered compressive strength (hot and residual) and stiffness among the properties changes on cement paste. The research did not consider other properties, such as tensile and flexural strength.
2. In the case of microstructure investigation, the research is limited only to scanning electron microscopes. Other microstructures, such as mercury intrusion Porosimetry (MIP) and X-ray diffraction (XRD), were not included due to unexpected time constraints.
3. In transient thermal creep, only one sample was used in the experiment. Initially, 3 samples were planned, but due to time constraints as a result of Covid-19, it was not possible to run all the 3 samples for the experiment.

The tests conducted during the research were based on the International Union of Laboratories and Experts in Construction Materials, Systems, and Structures (RILEM). Some tests were conducted using other methods developed in the previous literature.

1.6 Thesis structure

Chapter 1: This chapter comprises an introduction that gives an overview of the effect of fire on cement paste and brief information on how some studies employed polypropylene to mitigate the effect. It briefly explained how adding polypropylene negatively affects compressive strength at ambient and high temperatures. There is also a brief explanation of how surface treatment of polypropylene improves mechanical properties. The aim and objectives, research knowledge contribution and research structure are also provided.

Chapter 2: This chapter presents a comprehensive review of concrete/cement paste at a high temperature, which comprises the effect of temperature on cement paste, decomposition of hydration products in cement paste at high temperatures, behaviour of cement paste at high temperature, effect of fibre in cement paste/concrete, effect of polypropylene fibre on mechanical properties of heated concrete/cement paste, Microstructure characterisation, Transient thermal creep of concrete, Effect of Polypropylene fibre on transient thermal creep behaviour of concrete

Chapter 3: This section discusses the chemistry of polypropylene (PP). A comprehensive literature on polypropylene includes physical and chemical properties, non-polarity of polypropylene, bonding between polypropylene and cement paste, Surface modification techniques for PP used in concrete/cement paste and quantification of hydrophilicity of PP are also discussed in this section.

Chapter 4: This chapter outlines the methodology used in this research, including the experimental program, UV treatment of PP, sample preparation, water retention test, residual compressive strength test, compressive strength at hot temperature, Microstructure characterisation using Scanning Electron microscopy (SEM) and Transient thermal strain test. All of these elements were connected to the overall objectives of the study.

Chapter 5: The result and analysis of the experiment were presented in this chapter; all the result analysis and discussion were given based on the methodology carried out from Chapter 4.

Chapter 6: The final chapter of this thesis presents the conclusions and recommendations drawn from the research conducted in the previous chapters and suggestions for future work.

Chapter 2: GENERAL LITERATURE ON CONCRETE/CEMENT PASTE AT HIGH TEMPERATURE

2.1 Introduction

In addition to traditional steel reinforcement, various types of fibres are utilised to enhance concrete's mechanical properties and durability, particularly for improving its tensile strength. The four primary categories of fibres that can be employed to reinforce concrete are steel, glass, natural, and synthetic fibres (Rico et al., 2017). Steel fibres can significantly enhance concrete's tensile and flexural strength by absorbing energy and controlling cracks, as demonstrated in the literature (Buratti et al., 2013; Beglarigale & Yazıcı, 2015). Furthermore, steel fibres' electrical, magnetic, and heat conductivity properties make them suitable for specialised applications (Sukontasukkul et al., 2010; Al-mattarneh, 2014). However, steel fibre corrosion can have a detrimental impact on concrete structures, leading to rapid deterioration (Söylev & Özturan, 2014). On the other hand, glass fibre has been found to have excellent strengthening properties, but its alkali resistance is poor (Sayyar et al., 2013). Natural fibres, such as wood (Torkaman et al., 2014), sisal (Silva et al., 2010), coconut (Ali & Chouw, 2013), sugarcane bagasse (Ramírez et al., 2012), palm (Nora et al., 2014), and vegetable fibres (Torgal & Jalali, 2011), are inexpensive and readily available, but they are not very durable. Synthetic fibres, such as those made of polyolefin (Alberti et al., 2014), acrylic (Oliveira et al., 2012), aramid (Vincent & Ozbakkaloglu, 2013), and carbon (Chaves & Cunha, 2014), can help prevent plastic shrinkage cracks in fresh concrete and enhance the post-cracking behaviour of concrete (Pujadas et al., 2014).

This chapter encompasses sections 2.2 to 2.9, which provide an in-depth analysis of various aspects related to the behaviour of cement paste and concrete under high temperatures.

The study utilised cement paste to focus solely on understanding the fundamental properties of cementitious materials at high temperatures. By excluding aggregates and other additives present in concrete, researchers could isolate these properties, offering valuable insights into concrete behaviour.

The following is a comprehensive overview of each section:

Section 2.2 focuses on the general effect of temperature on concrete/cement paste.

Section 2.3 provides a literature review on the decomposition of hydration products in cement paste under high-temperature conditions.

Section 2.4 explains the behaviour of cement paste at high temperatures. Here, the mechanical properties of cement paste at elevated temperatures are thoroughly examined. The section explains the effects of high temperatures on cement paste's strength and stiffness.

Section 2.5 deals with the effect of Fibers in Concrete/Cement Paste: This section presents a detailed review of the influence of fibres in concrete and cement paste. It encompasses an analysis of different types of fibres utilised in concrete and their mechanical effects on the overall behaviour of the material.

Section 2.6 focuses on the specific impact of polypropylene fibre on the mechanical properties of concrete and cement paste subjected to high temperatures. The discussion primarily revolves around the compressive strength of the material.

Section 2.7 reviews the utilisation of scanning electron microscopy (SEM) for microstructural characterisation in cement paste and concrete. This section examines the application of SEM to study the internal structure and properties of these materials.

Section 2.8 presents a literature review on concrete's transient thermal creep behaviour. It explores the creep phenomenon under temporary thermal conditions and investigates the thermomechanical and thermohygral processes involved.

The final section, 2.9, gives the literature on the effect of polypropylene fibre on concrete's transient thermal creep behaviour. It examines the influence of the fibres on the creep properties of concrete under varying temperature conditions.

2.2 Effect of temperature on cement paste

Concrete is vulnerable to high temperatures when exposed to accidental building or tunnel fires and when situated near furnaces and reactors (Oktar, 1996). This exposure can significantly decline its mechanical properties, including strength, modulus of elasticity, and volume deformation, leading to unfavourable structural degradation (Georgali & Tsakiridis, 2005). Several important considerations, such as loss of strength (Felicetti & Gambarova, 1998), elastic modulus (Saad, et, al,. 1996), cracking, spalling, ductility, and loss of bond with steel reinforcement, should be taken into account (Dotreppe et al., 1997). Research has shown that hardened cement paste is crucial to the deterioration process. The phase composition and pore structure of hardened cement paste have a complex relationship with the loss of structural quality of concrete, particularly concerning strength and fracture (Bournazel and Moranville 1997).

High temperatures cause a reduction in the strength and elasticity of cement paste by altering its physicochemical composition (Kim et al., 1998). The form of stress-strain curves is affected by factors such as the type of binder, aggregate, admixtures, aggregate-cement ratio, and storage conditions (Bournazel and Moranville 1997). The deterioration of the structural quality of concrete due to temperature rise is caused by changes in the basic processes of cement hydration and hardening of the binding system in the cement paste (Cong & Kirkpatrick, 1995; Vodák et al., 1997). The sensitivity of the calcium silicate hydrate (C-S-H) gel to temperature is demonstrated by the average C-S-H composition at 25°C ($C_{1.88}SH_{1.52}$) and 100°C ($C_{2.04}SH_{0.98}$), which affects the C/S and H/S ratios of C-S-H gel. Thermal treatment reduces the amount of bound water in the C-S-H gel while increasing the calcium content (Handoo et al., 2002).

High temperatures have a profound effect on the formation of ettringite. At temperatures between 60 and 80°C, the stability of ettringite decreases significantly, leading to dehydration and disintegration of ettringite hydrates (Saad, et al., 1996). This disintegration also reduces the OH^- content in the pore water solution (Georgali & Tsakiridis, 2005). $Ca(OH)_2$ crystals have a sheet-like and extended form at room temperature (Afridi et al., 2001). However, the spatial distribution of $Ca(OH)_2$ crystals becomes more compact as the temperature rises, indicating the presence of smaller crystals per unit volume of cement mix (Mehta & Monteiro, 2014). This decrease in crystal size is linked to the significantly reduced solubility of $Ca(OH)_2$ at higher temperatures. In contrast, hydrated cement pastes at lower temperatures are more likely to include larger masses of $Ca(OH)_2$with a well-developed morphology. High temperature also alters the pore structure of cement paste by reducing the specific surface of hydration products.

The initial heating process induces considerable changes in the cement paste, making it highly unstable within concrete. Substantial physical and chemical alterations take place during this stage. The presence of evaporable moisture has a significant influence at lower temperatures, approximately between 100°C and 200°C, while temperatures beyond 100°C mark the crucial point where chemical decomposition and the release of bound water become important. Notably, thermal impacts become considerably significant at temperatures exceeding approximately 600°C, eventually resulting in melting. Once the cooling phase commences, the behaviour of cement paste primarily revolves around absorbing moisture from the surrounding environment (Khoury, 1992b)

When cement paste is exposed to high temperatures, its microstructure becomes more varied, and its pore structure becomes coarser, according to studies by Khoury, et al., (1985); Noumowé, (2003). The loss of engineering properties at high-temperature attack is mainly caused by a decrease in the volume of the hydrate phase and $\mathrm{Ca(OH)_2}$, as well as an increase in the coarseness of the pore structure of concrete.

The microstructure of hardened concrete significantly impacts its properties, including strength, shrinkage, and permeability. A thorough understanding of the pore structure is crucial in revealing the mechanisms behind enhancing concrete properties. Concrete structures are prone to damage caused by the penetration of harmful solutions through their porous microstructure. Therefore, the penetration of aggressive agents into the concrete system relies on factors such as pore structure, porosity, and microstructure. Aside from pore geometry considerations, the reaction of penetrating aggressive solutions, such as chloride ions and carbon dioxide, also affects concrete's physical and chemical properties. Porosity, especially capillary porosity, significantly influences concrete permeability through factors such as interconnectivity, volume, and surface area, affecting void transport processes**.** To make durable concrete materials, it is reasonable to aim for lower permeability and pore diameters, which can lead to reduced flow of penetrating substances. Simply knowing the pore size distribution of a paste is not enough for predicting properties; measurements of pore volume, surface area, distribution, and connectivity are required for permeability prediction.

Other investigations conducted by Zhang et al., (2013); and Zhang & Ye, (2011), it was discovered that heating cement paste in the range of 105°C to 400°C leads to a lower density of the hydration product, C-S-H, due to the dehydration of calcium hydroxide and reduced volume of the hydrated gel. Simultaneously, clinker phases experience increased density through sintering effects and enhanced crystallization, contributing to an overall higher density of clinker.

. This finding suggested that the hydration product's density decreased while the clinker's density increased as the temperature increased.

The coarsening of the pore structure became more pronounced as the temperature increased. It was hypothesised that this coarsening could be viewed as the formation of equivalent cracks, which could lead to a deterioration in the mechanical behaviour of the cement paste. This hypothesis was particularly relevant when no chemical degradation of the cement paste occurred below 350°C as reported by Peng & Huang, (2008).

2.3 Decomposition of hydration products in cement paste at high temperatures

When cement paste is subjected to high temperatures, the different hydration products gradually lose water, resulting in mass loss. According to Ruiz et al., (2005) & Khoury, (1992b;) in a well-hydrated cement paste, the evaporation of free water and the dehydration of hydration products release water vapour, which is almost entirely complete at around 500°C. Ettringite, a crucial crystalline component of hydrated Portland cement, remains stable when in contact with a self-generated atmosphere up to temperatures of 114°C (Glasser, 2002). While CH loses water between 400 and 500°C, it can form calcium carbonate ($CaCO_3$) above 400°C if CO_2 is available. Additionally, decomposed calcium hydride can rapidly reform when cooling down to ambient temperature, as observed by Henry et al., (2016).

The decomposition of calcium silicate hydride (C-S-H), the primary binding phase and hydration product of cement, is a complex process due to its amorphous structure and bound water. Henry et al., (2016) reported that this reaction occurs between a wide temperature range and is a multi-step process. Fordham & Smalley (1985) suggested dehydration of capillary pore, interlayer, and absorbed water in C-S-H occurs below 400 ºC. However, some TGA studies (Khoury et al., 2002; Zhang & Ye, 2012) indicate that the temperature range for dehydration of C-S-H is significant, ranging from 105 to about 1000ºC. According to their X-ray diffraction (XRD) results, Peng & Huang (2008) found that C-S-H decomposition begins at 560 ºC but becomes significant only above 600ºC. Their thermogravimetric analysis (TGA) results also reported a primary dehydration of C-S-H between 105 and 300 ºC followed by the secondary range of C-S-H dehydration between 650ºC and 800ºC. The summary is shown in table 2-1 .

Table 2- 1: Type of damage of the concrete at high temperature

Temp °C	Type of Damage	References
105 - 400	Dehydration of the C-S-H within the capillary pore	Fordham & Smalley, (1985)
400 - 500	Loss of absorbed water withing calcium hydrate	Henry et al., (2016)
500	Evaporation of water and the dehydration of C-S-H. Mass loss of the sample	Alarcon-Ruiz et al., (2005); Khoury, (1992)
560 - 1000	Decomposition of hydration product (C-S-H)	Peng & Huang (2008); Khoury et al., (2002); Zhang & Ye, (2012)

2.4 Behaviour of cement paste at high temperature

In this section, the experimental investigation of the properties of cement paste material at a high-temperature ware reviewed.

2.4.1 Strength

The compressive and tensile strength of cement paste represents the maximum amount of stress that can be sustained by a material sample under compression or tension. Numerous studies have investigated the compressive strength of concrete and cement paste under high-temperature conditions. The primary factors affecting concrete strength at elevated temperatures include those identified by (Khoury et al., 2002) and (Ahmad et al., 2014).

- High-temperature exposure
- Type of concrete
- Rate of heating and cooling cycle
- Thermal cycle
- Relative humidity
- Applied load during heating

In studies investigating the effect of temperature on the strength of cement paste, various factors have been identified, each with a distinct impact on the material's strength. In general, as the temperature rises, the strength of the cement paste decreases. However, some studies have found that the strength of sealed samples may increase to around 6.6% to 13% at temperatures below 200°C (Khoury et al., 2002; Xu et al., 2001; Janotka & Nürnbergerová, 2005). However, a similar finding with a slightly different limit by Ahmad et al., (2014) observed an increase in strength of up to 5% at 100°C. Beyond this temperature, the compressive strength curve declined, as Figure 2-1 shows. This could be attributed to the hardening of the sample caused by drying and hydration of cement paste, as reported by Xu et al., (2001), who observed an increase in strength at 250°C.

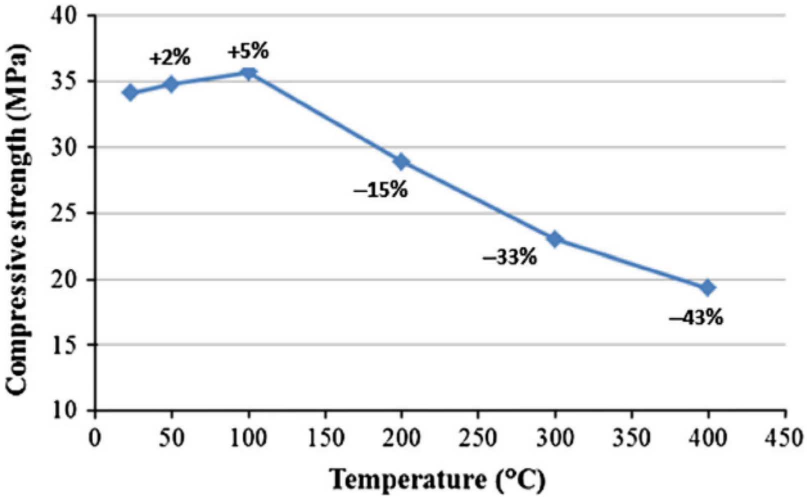

Figure 2- 1: Variation of compressive strength of mixture M0 with temperature (% changes in compressive strength calculated concerning strength at 23°C) (Ahmad et al., 2014).

Relative humidity also plays a role in affecting the strength of concrete/cement paste. The study conducted by Kirchhof et al., (2020), showed that the absorption of moisture into the gel pores results in a phenomenon known as a transverse bursting effect. This effect becomes increasingly noticeable as the external compressive load is imposed on the cement paste. Consequently, the overall behaviour and compressive strength characteristics experience a substantial decline due to moisture in the cement paste.

2.4.2 Stiffness

The relationship between temperature and stiffness in concrete has been extensively investigated. Studies consistently demonstrate that stiffness and compressive strength tend to decrease as temperature and cooling rate increase. Microcracking caused by water expansion and evaporation is the primary mechanism leading to stiffness degradation. Various factors influence concrete's elastic modulus, including cement paste and aggregate properties, concrete density, compressive strength, capillary voids, humidity, and test and loading conditions.

The impact of temperature on the stiffness of concrete and cement paste samples has been extensively studied, with consistent findings indicating a strong relationship between these factors. (Lee et al., 2007) conducted an experiment that revealed a noticeable decrease in stiffness and compressive strength as the temperature and cooling rate increased, as shown in Figure 2-2. This trend was consistent with the reduction in stiffness observed by Petkovski, (2010) in heated concrete under compression, where the decrease in stiffness became more prominent with higher cooling rates.

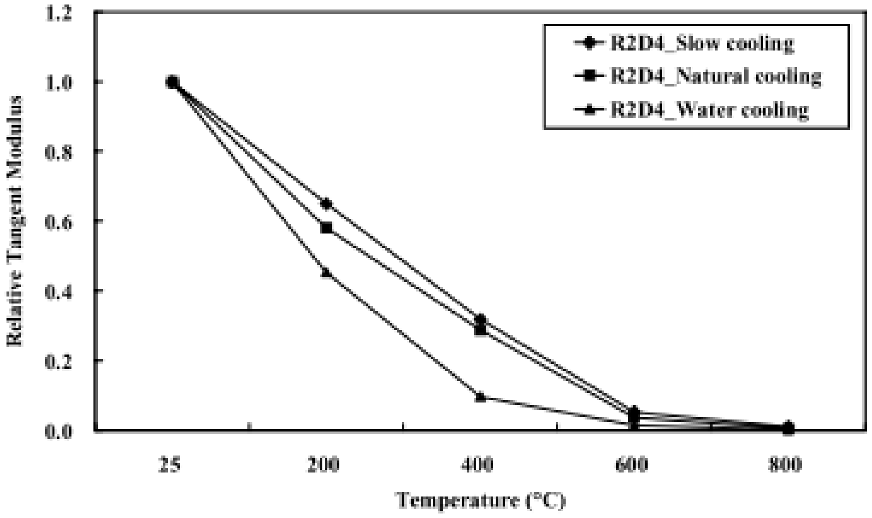

Figure 2- 2: Relative initial tangent modulus vs. temperature (Lee et al., 2007)

Research by Odelson et al. (2007) shed light on the mechanisms underlying stiffness degradation in cement paste exposed to elevated temperatures. The study found that the primary cause of stiffness loss, regardless of mix design, occurred below 120°C, as shown in Figure 2-3. This indicates the significant influence of microcracking from water expansion and evaporation within the porous structure. Chemical changes, on the other hand, were deemed insignificant once microcracking had already occurred. These results emphasise that even relatively low elevated temperatures can lead to significant damage in cement paste or concrete, highlighting the critical role of temperature in stiffness deterioration.

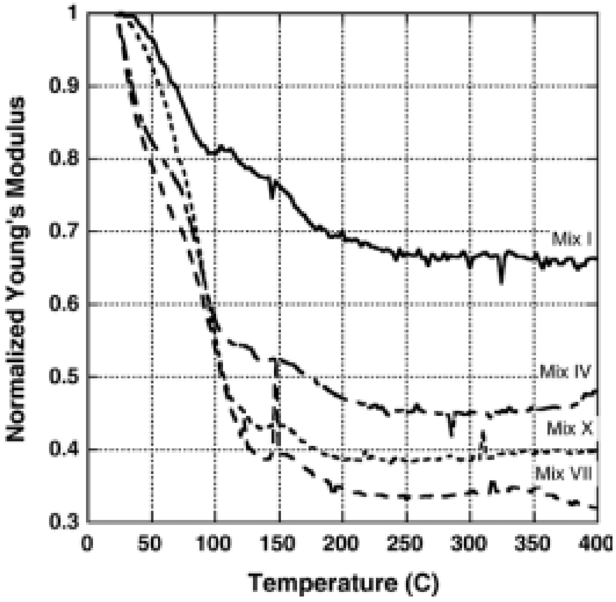

Figure 2- 3: Normalised modulus vs. temperature of cement paste (Odelson et al., 2007)

Furthermore, Masse et al., (2002) conducted ultrasonic measurements to evaluate the elastic modulus of cement paste, mortar, and micro concrete samples. The study demonstrated excellent reproducibility, with scattering below 3% in echo or transmission modes, even when samples were coupled or decoupled with transducers. The results confirmed that the elastic modulus increased with decreased water-cement ratio, indicating decreased porosity. However, an increase in temperature during thermal treatments led to a decrease in elastic modulus due to the decomposition of portlandite, resulting in microstructural changes, gaseous emission, cracking, and increased porosity, as shown in Figure 2-4.

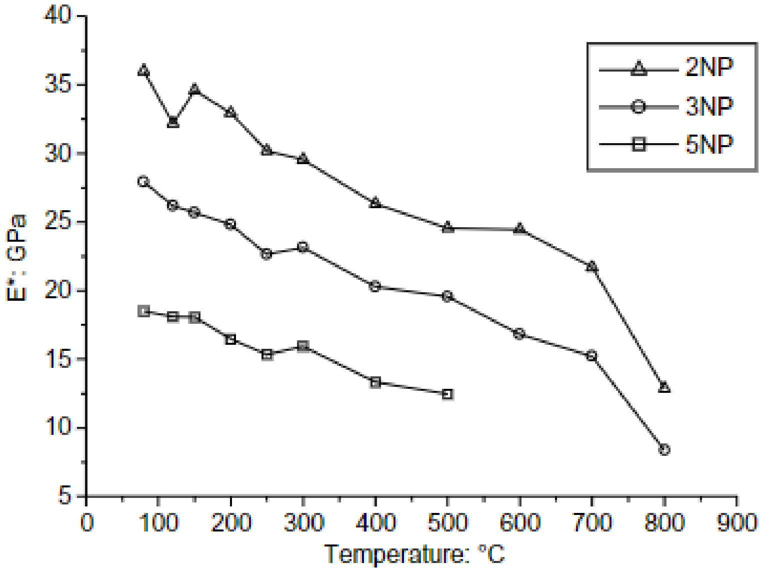

Figure 2- 4: Elastic modulus vs temperature (Masse et al., 2002)

In Figure 2-5, the results presented by Dias et al., (1990) showed relatively constant moduli within the range of 50 to 90 °C, suggesting the loss of physically held water. Moreover, the modulus values were greater than the initial modulus up to 120 °C. This could be attributed to a physical densification effect caused by drying, loading during the creep test, and the cooling phase. These findings indicate the complex interplay between temperature, loading, and moisture content in determining the stiffness of concrete.

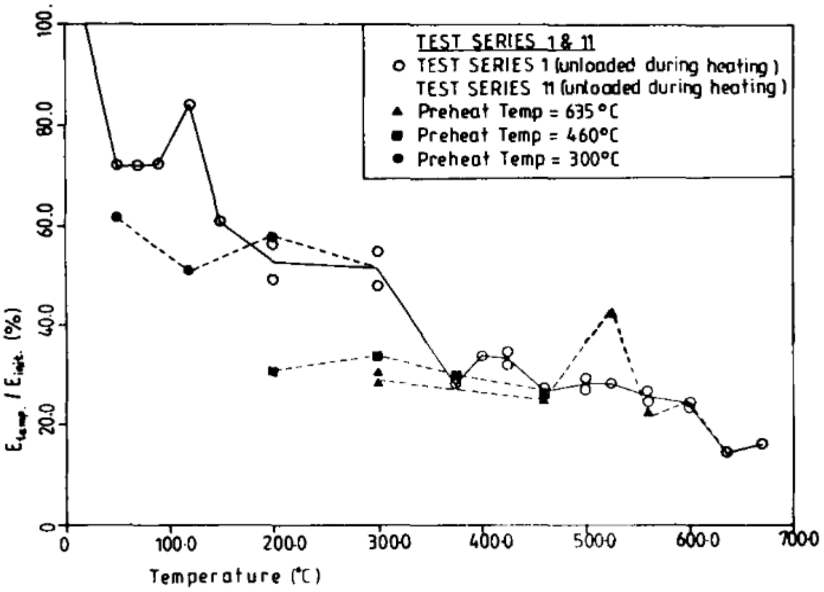

Figure 2- 5: modulus of elasticity at a temperature (Dias et al., 1990)

2.5 Effect of fibre in cement paste/concrete

The brittle nature of concrete and its weakness in tension are well-known. Enhancing the properties of construction materials by incorporating fibres is not new, as it has been used in the past by adding straw to mud bricks, horsehair to plaster, and asbestos to pottery. Incorporating fibres into concrete improves its strength and ductility (Khan et al., 2023). The addition of fibres leads to a homogeneous and isotropic material. When concrete cracks, the randomly arranged fibres start functioning by preventing the creation and propagation of cracks, thereby enhancing the strength and ductility of the material (Faisal, 1990).

There is a continued need to address the brittleness of concrete, and research on the effects of fibres with different diameters and properties on concrete can be useful. Fibres are often added to concrete to improve its technical properties and performance. Metals such as steel, organic, and inorganic fibres have been employed, with polypropylene (PPF) and glass fibres (GF) commonly used in the concrete industry. Studies have extensively examined the mechanical properties of PPF and GF-reinforced concrete, which have been shown to increase flexural strength, compressive strength, toughness, splitting tensile strength, and long-term durability. Fibre can also toughen while bridging cracks and prevent crack propagation by acting as a bridge in the cracking region, taking part or all of the tensile stress. Recent studies have found that including glass fibres Cem-FIL Anti-Crack HD with a modulus of elasticity 72 GPa, Filament diameter of 14 microns, and length of 12 mm in concrete mixes can decrease bleeding, improving surface integrity, homogeneity, and fracture resistance (Chandramouli et al., 2010). Adding glass fibre has also effectively controlled shrinkage fractures in concrete (Shakor, 2011). Polypropylene fibres have become widely accepted for use in concrete to improve the resistance to shrinkage cracking and the hardness of plain concrete. PPF enhance the mechanical properties of cementitious materials, with their effectiveness influenced by key variables such as aspect ratio, form, and length. A higher aspect ratio (l/d), typically ranging from 20 to 100, improves tensile strength and crack resistance. The form of PPF whether crimped, fibrillated, or monofilament affects the bond with the cement matrix, with crimped and fibrillated fibers enhancing toughness and crack control, while monofilament fibres focus on early-age crack prevention. The length of PPF, typically ranging from 6 to 60 mm, is chosen based on the application, with longer fibres contributing more to toughness and post-cracking performance and shorter fibres being more effective for controlling micro-cracks and improving surface durability. (Alhozaimy et al., 1996).

Furthermore, Karahan & Atiş (2011) examined the effects of polypropylene fibres on the drying shrinkage of fly ash concrete samples with varying fibre percentages. The results show that adding polypropylene fibres of 12mm length to concrete or fly ash concrete can reduce drying shrinkage by 1%, 4%, and 11% for samples with 0%, 15%, and 30% fly ash content, respectively, as shown in Figure 2-6. Moreover, according to Kene (2012), incorporating glass fibres into concrete can improve its mechanical strength compared to standard concrete without fibre.

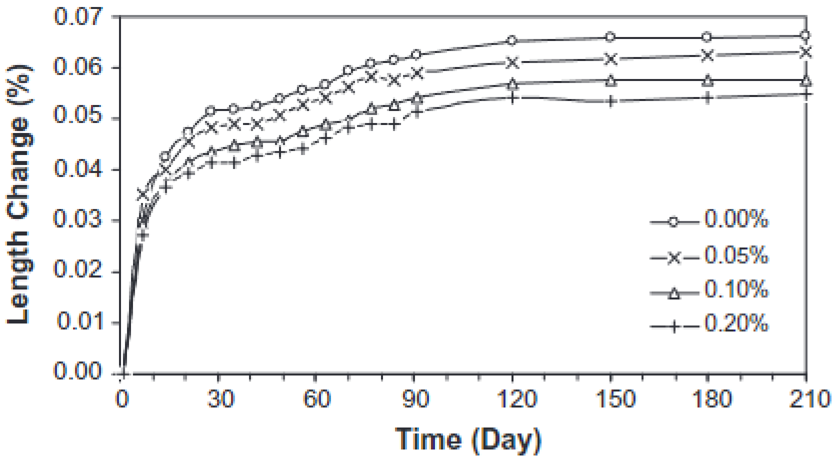

Figure 2- 6: Shrinkage of polypropylene fibre-reinforced Portland concrete (Karahan & Atiş, 2011)

Chandramouli et al. (2010) suggest incorporating fibres into concrete can increase compressive strength, flexural strength, and splitting tensile strength. Specifically, adding glass fibre has enhanced compressive strength by 20-25% and flexural and splitting strength by 15-20% after 28 days. In addition, Shi, (2015) has developed a method to produce recycled polypropylene fibre with excellent results in mechanical properties for reinforcing concrete.

Furthermore, some investigation by Murahari, (2013) found that using a small amount of polypropylene fibre in concrete improved the compressive strength at room temperature. Similarly, adding polypropylene fibre in less amount, i.e., 0.1% to 0.3% by mass of cement, increased the compressive strength of concrete, which could be due to the efficient filling effect of polypropylene fibre in concrete specimens that reduced the crack propagation and crack width. The strength is reduced when the addition percentage reaches 0.6 (Alhozaimy et al., 1996; Arunachalam & Jayakumar, 2015), as shown in Figure 2-7. The result presented by Bei-xing et al., (2004) shows that the compressive strength tends to reduce due to the presence of polypropylene fibre in the concrete. At 0.91$\boldsymbol{kg/m^3}$ content of polypropylene, the compressive strength tends to reduce by an average of 2.1% compared with the control sample. The loss of compressive strength is associated with the hydrophobic nature of polypropylene, which causes poor cohesion between polypropylene fibre and cement hydrate (Ossola & Wojcik, 2014).

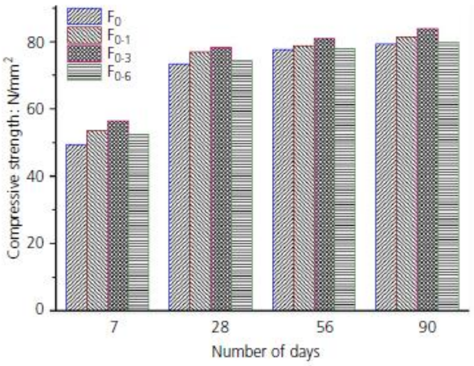

Figure 2- 7: Compressive strength of concrete containing polypropylene fibre (Arunachalam & Jayakumar, 2015)

Afroughsabet & Ozbakkaloglu (2015) show that incorporating 0.15%, 0.3%, and 0.45% by volume of polypropylene fibres significantly increased compressive strength. The result shows that the increase in compressive strength is about 5% to 15% because of the addition of polypropylene to the mix, as shown in Figure 2-8. This increase in compressive strength can be explained by the ability of the fibres to restrain the extension of cracks, reduce the extent of stress concentration at the tip of cracks, change the direction of cracks, and delay the growth rate of cracks. There is great potential for using these fibres in different concrete applications, such as footpaths and precast concrete elements, which provides an attractive avenue for recycling plastic waste.

The applications of fibres in concrete industries depend on the designer and builder to take advantage of this new material's static and dynamic characteristics (Faisal, 1990). The main areas of fibre applications in concrete are runways, aircraft parking, pavements, tunnel lining, slope stabilisation, thin shells, dams, and hydraulic structures.

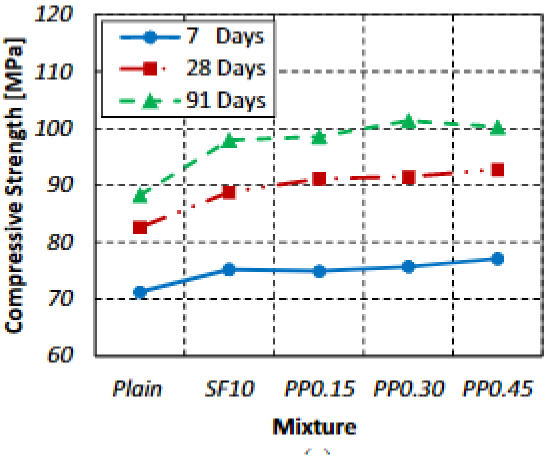

Figure 2- 8

Figure 2-8: Compressive strengths of polypropylene fibre-reinforced concrete (Afroughsabet & Ozbakkaloglu, 2015)

2.6 **Effect of heat on mechanical properties of concrete/cement paste containing polypropylene fibre**

The impact of high temperatures on concrete containing 1.0 kg/m^3 of polypropylene fibres was investigated by observing the microstructure of specimens heated to 200°C at different durations of 20 min, 6 h, and 2 days, respectively (Bo & Hahn, 2013). The study found that the cement matrix suffered extensive micro-cracking, partially due to the fast cooling after the first exposure to the open environment, and the contact fibre-cement matrix had certain flaws and initial micro-cracks. These factors, combined with the difference in thermal dilation between the cement matrix and polypropylene, could cause micro-cracking even with slower cooling rates. However, the presence of polypropylene fibre in the concrete specimens was observed to be good, as shown in Figure 2-9.

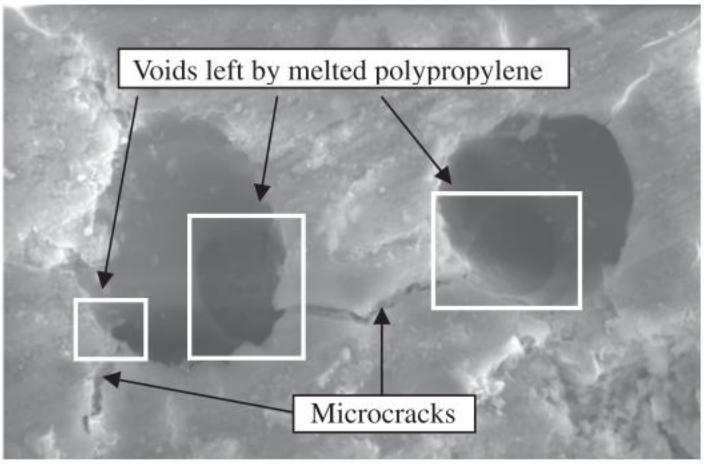

Figure 2- 9: Scanning electron microscope photos of the virgin concrete with the addition of polypropylene fibre exposed to 200 °C for 2 days (Bo & Hahn, 2013)

In another study, the effect of heating on high-strength concrete containing polypropylene fibres was investigated by observing both non-heated and heated specimens using SEM (Noumowe, 2005). The results showed that polypropylene fibres melted and volatilised at 200°C, creating additional pores and channels in the concrete that may act to relieve high internal moisture pressures, as shown in Figure 2-10. SEM analysis revealed traces of melted fibres, and the fibres were observed to decrease in length under heating. The use of fibre affects the porosity of the concrete at high temperatures, which may decrease the pore pressure inside the material and affect the release of moisture.

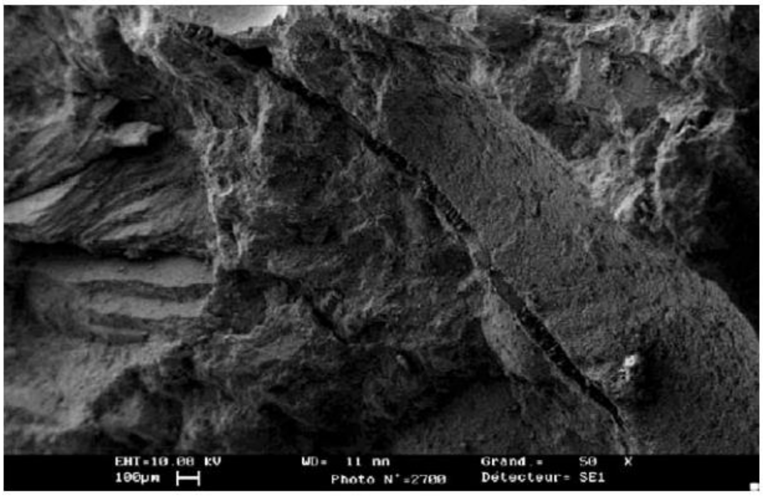

Figure 2- 10: melted fibres in high-strength concrete (Noumowe, 2005)

PP fibres are commonly used in concrete due to their ability to melt and vaporise at lower temperatures (160-180°C), creating free space in the micro-channels of the concrete matrix (Ding et al., 2012). This process reduces tension stress in the capillaries and decreases compression stress in the concrete matrix, making it a desirable characteristic for enhancing the mechanical properties of concrete. Another study by Ding et al., (2012) shows the beneficial effect of PP fibre on the residual strength of concrete after high-temperature exposures. On of the important reasons is that PP fibres melt and vaporise due to the lower melting point (160–180 °C) during the rapid temperature increasing process, which makes free space in the micro-channels in the concrete matrix shown in Figure 2-11, decreasing tension stress in the capillary that reduces the compression stress in the concrete matrix.

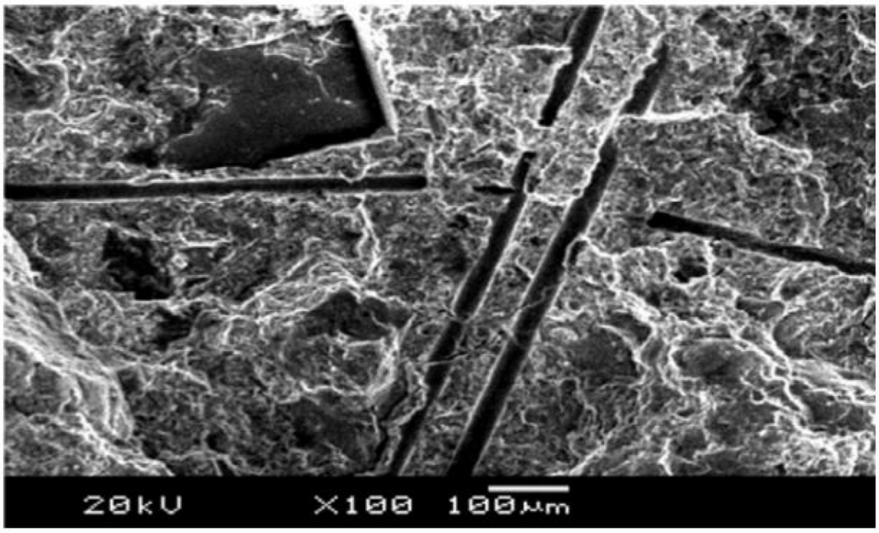

Figure 2- 11: Micro channels due to melting of PP fibre (Ding et al., 2012)

Polypropylene was introduced to improve the mechanical effect of concrete at high temperatures. Much research has been carried out, which shows the positive impact of adding polypropylene into concrete for improving the mechanical properties of concrete. Research made by Petrus et al. (2016), shown in Figure 2-12, found that the compressive strength of concrete containing polypropylene increases with an increase in temperature up to 300°C. This increase in compressive strength happens when polypropylene melts under high temperatures and forms new channels to release the thermally induced stress and, therefore, avoid excessive loss of compressive strength. This internal stress is trying to counterbalance the external load, acting as prestressing within the sample (Xiao & Falkner, 2006). The melting of polypropylene fibres generates not only new channels but also creates microcracks at the tip of fibres connecting the already existing pores and increasing the permeability (Bilodeau et al., 2004; Ozawa & Morimoto, 2014) carried out permeability tests on high-strength concretes (72 MPa), including 0.15% by volume of PPF. Results showed the residual permeability increased 12 times after heating the PPF concrete to 500 °C compared to the reference concrete.

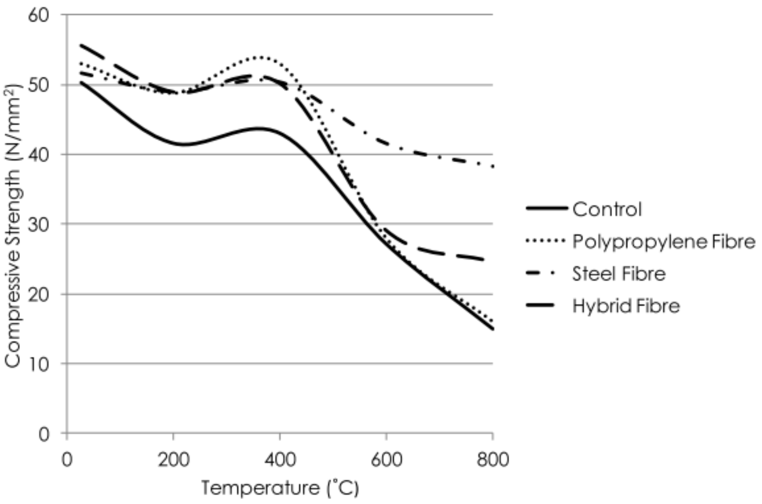

Figure 2- 12: Compressive strength of concrete containing Fibres (Petrus et al., 2016)

2.7 Microstructure characterisation

As an engineering material, concrete is complex. It exhibits varying properties that largely depend on its microstructure, which undergoes changes over time and varies depending on several factors such as cement type, mix proportions, curing conditions, heat treatment, and use of supplementary cementing materials. Additionally, the microstructure of concretes in real-world applications is susceptible to deterioration from various processes, which can ultimately affect their end-use properties.

Furthermore, information on the mechanical properties of the solid phases and their bonds may be necessary to predict strength and deformation. Sant et al. (2011) suggest that there are many microscopic techniques available for studying cementitious materials before and after hydration, including optical microscopy, transmission electron microscopy (TEM), scanning electron microscopy (SEM), and computed tomography scanning.

However, Diamond, (2004) explained the essential features of cement hydration paste and concrete using backscatter scanning electron microscopy (SEM) in a 'visual primer' approach. SEM techniques involve directing a high-velocity electron beam at a specific spot on a sample surface and scanning the beam in a raster pattern over a limited area to generate an image. Backscatter-mode SEM is one of the various SEM imaging methods. Combined with energy-dispersive X-ray spectroscopy (EDX), it can provide rapid and precise chemical composition information for specific spots or sections of the SEM image. This feature makes backscatter SEM a potent tool for concrete studies. Feng et al. (2004) utilised a scanning electron microscope point-counting technique to estimate the degree of hydration of plain Portland and blended cement pastes containing fly ash or slag. The results revealed that the SEM point-counting technique is a dependable and effective analysis tool for estimating the degree of hydration of Portland cement and the reaction of mineral admixtures blended in Portland cement pastes. Over the past few years, scanning electron microscopy (SEM) has been crucial in examining the intricate internal structure of hydrated cement pastes, mortars, and concretes (Diamond, 2004).

2.8 Transient thermal creep of concrete

When exposed to thermal and structural loading, concrete structures may undergo creep under different moisture and temperature conditions. The maximum limit for creep response occurs when the load is applied during the first heating of moist concrete, referred to as transient thermal creep. To tackle this issue, it is essential to identify and verify the limiting conditions through experiments.

In this research, hardened cement paste testing was preferred over concrete testing as it reduces the variability that aggregate types can cause. Moreover, cement paste is the main material that experiences creep in concrete, yet limited data exist in the literature (Mindeguia et al., 2013a; Hager & Pimienta, 2005a) on its basic creep above 100°C.

As expressed by Mindeguia et al., (2013b), transient thermal strain, also known as transient thermal creep, is a phenomenon that occurs in concrete when it is subjected to non-stationary heating under load. The standard for concrete design, ENV 1992-1-2 Eurocode 2, specifies that the strain (ε) in a concrete element that is subjected to both mechanical and thermal strain under loads is equal to:

$$\boldsymbol{\varepsilon = \varepsilon_{\sigma} + \varepsilon_{th} + \varepsilon_{creep} + \varepsilon_{tr}} \qquad \textit{2- 1}$$

Where ε_{σ} = is the instantaneous stress-dependent strain.

$\boldsymbol{\varepsilon_{th}}$ = is the free thermal strain

$\boldsymbol{\varepsilon_{\sigma}}$ = is the thermal strain under load

$\boldsymbol{\varepsilon_{creep}}$ = is the creep strain

$\boldsymbol{\varepsilon_{tr}}$ = is the transient thermal strain

Thermal strain εth and thermal strain under load $\boldsymbol{\varepsilon_{\sigma}}$ Measurements determine transient thermal strain (ε_{tr}). Assuming that classical material creep is negligible due to the relatively short duration of the experiment. This value is equal to:

$$\varepsilon_{tr} = \varepsilon_0 - \varepsilon_{th} \qquad 2\text{-}2$$

In earlier research conducted by Khoury, Grainger, Sullivan, et al., (1985); Torelli et al., (2016), it was observed that the sequence of applying heating and loading impacts the behaviour of thermally mechanically loaded concrete. Application of a pre-compressive load before heating results in a significant reduction in the free thermal expansion of concrete. This reduction is referred to as Transient Thermal Creep (TTC), a unique property specific to concrete. TTC can prove to be advantageous for a structural element that is partially or wholly constrained to prevent tensile cracks and compressive stresses caused by thermal incompatibility between the cement matrix and aggregates, as observed by , et al., (2019);Dejian, et al., (2019). However, at high temperatures, TTC could exceed the mechanical strain of the concrete, resulting in an unexpected additional deformation in the loading direction. Moreover, since it is mostly irreversible, TTC may exacerbate concrete damage during the cooling phase. Therefore, TTC should be considered when designing thermally mechanically loaded concrete structures.

Over the past 50 years, numerous experimental studies (Khoury, Grainger, Sullivan, et al., 1985; Gabriel A. Khoury et al., 1986; DiFonzo & Bordia, 1998; Sabeur & Colina, 2015; Mindeguia et al., 2013b; Pan et al., 2014) have been conducted to investigate Thermochemical changes in concrete. Initially considered quasi-instantaneous, TTC was found to be significantly nonlinear with respect to temperature and influenced by mechanical stress. It was observed that TTC occurs during the initial heating of the virgin pre-loaded sample and is largely irreversible with temperature changes.

Gawin, and Majorana, (2001) proposed that TTC is affected by physicochemical changes in the C-S-H and the creation of microcracks in concrete during heating. Thermo-chemical damage, coupled with the release of bound water, is believed to be the source of these strains (Noumowe et al., 1996; Davie et al., 2014). Temperature effects in concrete are also influenced by chemical alterations and moisture movement within the cement paste, along with the formation of microcracks resulting from temperature variations and inconsistencies in deformation between aggregates and the cement paste.

Georgali & Tsakiridis, (2005) Identified two primary factors responsible for thermal degradation in cement paste: the development of microcracks at the interface of dehydrated cement particles and the cement paste matrix, as well as changes in the microstructure of C-S-H. High-temperature exposure can lead to various types of cracks in concrete.

During the initial stage of concrete heating (500 °C), it was observed that pores and pre-existing microcracks close due to overall contraction. However, in the subsequent heating phase (>500 °C), bridge cracks emerge due to differential behaviour between aggregates and the mortar matrix, as reported by Henry et al., (2014); and Picandet et al., (2001)

The concept of "transient thermal creep" is essential for properly assessing concrete structures' performance at elevated temperatures, as reported by Khoury, Grainger, & Sullivan, (1985);. Schneider (1988) suggested that this phenomenon occurs due to the activation of concrete creep by temperature, resulting from the removal of interlayer water. Recent studies have focused on concrete behaviour under accidental conditions, examining heating rates greater than 0.5°C per minute and temperatures between 20°C and 800°C or above (K.-Ch. Thienel and F.S. Rostasy, 1996).

Transient thermal creep originates in the cement paste and is restrained by the aggregate, contributing to the thermal stability of heterogeneous concrete when subjected to initial heating. It helps prevent excessive heating-related damage and modifies thermal incompatibilities between the expanding gravel and shrinking cement paste, particularly around 100°C. However, transient thermal creep is restricted to the heating phase and does not occur during cooling, leading to irrecoverable strains (Khoury, 1992a).

Among the main publications written on TTC, we can mention those from Anderberg & Thelandersson, (1976); Khoury, Grainger, & Sullivan, (1985); Schneider, (1976). These research papers have been very useful when taking TTC. Recently, research has been conducted to evaluate and comprehend the mechanisms that activate TTS. The authors cited above frequently discuss two basic mechanisms.

2.8.1 Thermomechanical process

Transient thermal strain (TTS) can cause damage to concrete at various scales through different mechanisms. TTS can be caused by thermal gradients, dehydration-induced cement paste damage, and thermal strains caused by aggregates and cement paste incompatibility, as suggested by several studies (Bernhard. et al., 2002; Hertz, 2005). Some researchers have attempted to model TTS by incorporating the various types of damage using mesoscale models (Menou et al., 2008; Borderie et al., 2010). Others have directly linked TTS to the growth of cracks in the cement paste resulting from the thermal mismatch between the paste and aggregates (Hertz, 2005). These authors argue that this thermal mismatch generates tensile stresses in the matrix phase that can counteract the compression stresses brought on by external mechanical loading, thereby inducing contraction strain in the concrete. However, they agree that cracks only begin to appear in the matrix phase when the temperature reaches 200°C. Recent mesoscale calculations conducted by Sa & Benboudjema, (2011) have shown that the thermal strain increases up to around 400°C up to 400°C, as shown in Figure 2-13.

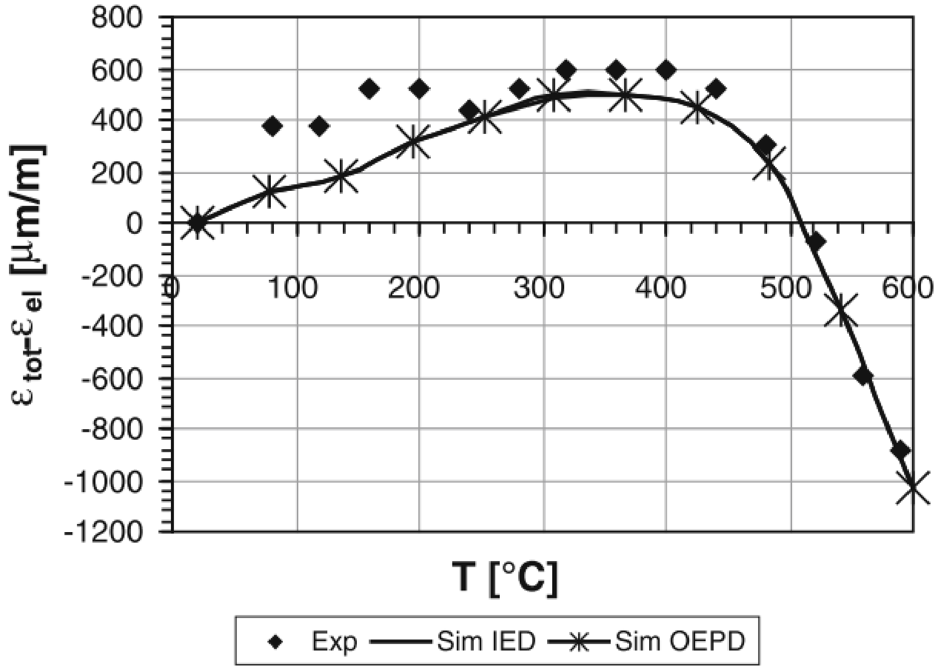

Figure 2- 13: Thermal strain of concrete (De Sa & Benboudjema, 2011)

Therefore, other processes should be primarily responsible for the occurrence of TTS below this temperature. But research conducted by Mindeguia et al., (2013a) reported that The thermal strain in pure cement paste verified the occurrence of transient thermal strains (TTS). The study tested a high-performance cement paste sample and analysed the thermal strains under compressive load and transient thermal strains, as shown in Figure 2-14. The results indicate that TTS occurs in the cement paste, with the expansion and subsequent shrinkage of thermal strain observed up to 150 °C. TTS becomes significant beyond 100 °C, with a maximum 10 μm/m value. The decrease in the slope of the TTS curve around 200 °C supports the occurrence of TTS in the cement paste. Up to 300 °C, TTS is primarily attributed to a thermo-hygral process rather than a thermomechanical process. The high TTS value in pure cement paste contributes to stress relaxation and limits crack formation between the paste and aggregates. This finding challenges previous assumptions that linked TTS to crack growth at the paste-aggregate interface.

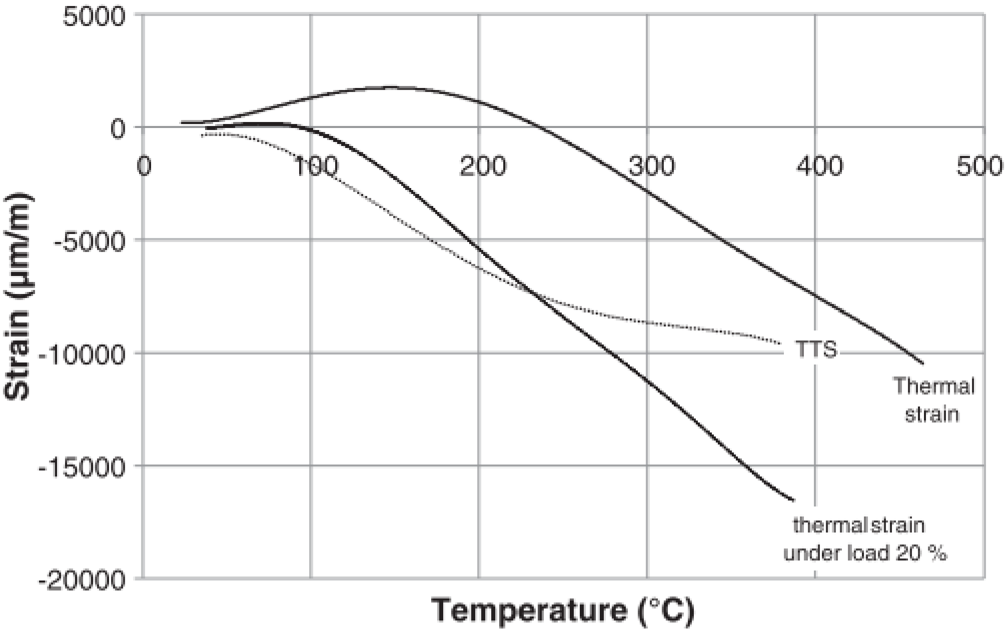

Figure 2- 14: Thermal strain, thermal strain under load and transient thermal strain of cement paste (Mindeguia et al., 2013a)

2.8.2 Thermo-hygral process

The moisture migration into the macropores and micropores of the C-S-H layers leads to an accelerated shear deformation at 20°C and sustained load, resulting in a delayed strain called "drying creep," which is known as the "Pickett Effect" (Acker & Ulm, 2001; Bažant et al., 2004). This specific creep can develop when the concrete undergoes the process of drying and re-humidifying. Water transfer in any direction affects this drying creep. When concrete is heated, physical and chemical changes occur in the cement paste, primarily the dehydration of C-S-H for temperatures ranging from 105°C to 300°C (Khoury, 1992b; DeJong & Ulm, 2007). This dehydration process involves water migration from the C-S-H layers (previously bound water) to the porous medium. The water movement under constant load accelerates the sliding of microstructure, causing additional delayed strain at high temperatures, known as "dehydration creep." The emergence of TTS may be attributed to this "dehydration creep," which is in addition to the "drying creep." Studies by Hassen and Colina, (2006);.. Sabeur, (2006); Sabeur & Meftah, (2008) have provided insight into this phenomenon.

2.9 Effect of Polypropylene fibre on transient thermal creep behaviour of concrete

Polypropylene (PP) fibres have gained significant attention in high-strength concrete (HSC) due to their ability to enhance concrete's mechanical and durability properties. However, limited research on PP fibres' influence on concrete's thermal strain at high temperatures is available.

Experimental studies by Huismann et al., (2011) and (Huismann et al., 2012) investigate the impact of PP fibres on the thermal strain of HSC at temperatures up to 750°C.

The study used acoustic emission (AE) analysis, ultrasound (US), and weight loss measurements to investigate the internal damage processes and explain the differences in the thermal strain of HSC with and without PP fibres. The results showed that the thermal strain of HSC with PP fibres significantly differed from that of plain HSC without PP fibres.

The study identified two distinct temperature ranges in which the PP fibres influence the thermal strain of HSC significantly. In the first range, between 200°C and 250°C, the thermal strain of the HSC containing PP fibres stagnated due to an accelerated moisture loss caused by the presence of fibre, which increased the permeability of the HSC. The fibre beds acted as defects in the cement paste matrix and favoured the nucleation of micro cracks, increasing the permeability of the concrete.

In the second temperature range, above 300°C, the thermal strain of HSC with PP fibres was lower than that of plain HSC without PP fibres. The difference became more significant at 600°C when the quartz transformation occurred, and the aggregates had the maximum thermal dilatation. The observations were explained by the different types of microcracking induced by the fibre beds, resulting in a more homogeneous distribution of the cracks and a lower thermal strain, as shown in Figure 2-15

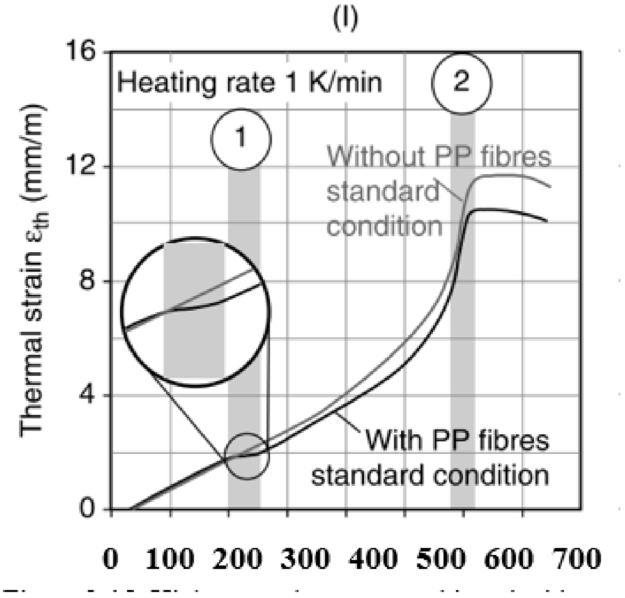

Figure 2- 15: High-strength concrete with and without polypropylene fibre (Huismann et al., 2011)

Huismann et al. (2012) conducted an experimental study on the transient strain of HSC under heating up to 750°C and the impact of PP fibres. The study determined the free thermal and mechanical strain during heating, which was experimentally determined for one HSC. The results showed that PP fibres prevented explosive spalling of HSC and enabled faster moisture flow of the free and physically bound water out of the concrete specimens in the temperature range from 200 to 250°C. The faster moisture flow-induced drying shrinkage counteracted the free thermal strain and caused stagnation of the thermal strain in this range. Above 250°C, PP fibres caused microcracking in the concrete, which became significant. The microcracking reduced the free thermal strain and increased the mechanically induced strain above 250°C compared to the HSC without PP fibres. At 600°C, the cracks in the HSC with PP fibres were smaller and higher in number than in the HSC without PP fibres.

Hou et al. (2019) investigated the effect of PP and hybrid (steel and PP) fibres on the creep behaviour of reactive powder concrete (RPC) at elevated temperatures. The study considered different thermo-mechanical regimes, including steady-state and transient conditions, and target temperatures ranging from 120 to 900°C. The study found that the short-term creep (STC) increased with increasing stress levels and higher target temperature. The STC developed below 500°C was low for both types of RPC, while above the transition stage of quartz aggregate, the evolution of STC was pronounced. The study also found that the STC of high-strength RPC (HRPC) was significantly higher than that of normal-strength RPC (PRPC) due to the presence of steel fibres. The transient strain at 60% strength ratio of PRPC is equal to the 40% transient strain ratio of HRPC, which has a different thermal expansion coefficient than the RPC matrix at high temperatures. Overall, the study found that the performance of PP fibre was better than the hybrid fibres on the creep behaviour of RPC, as shown in Figure 2-16.

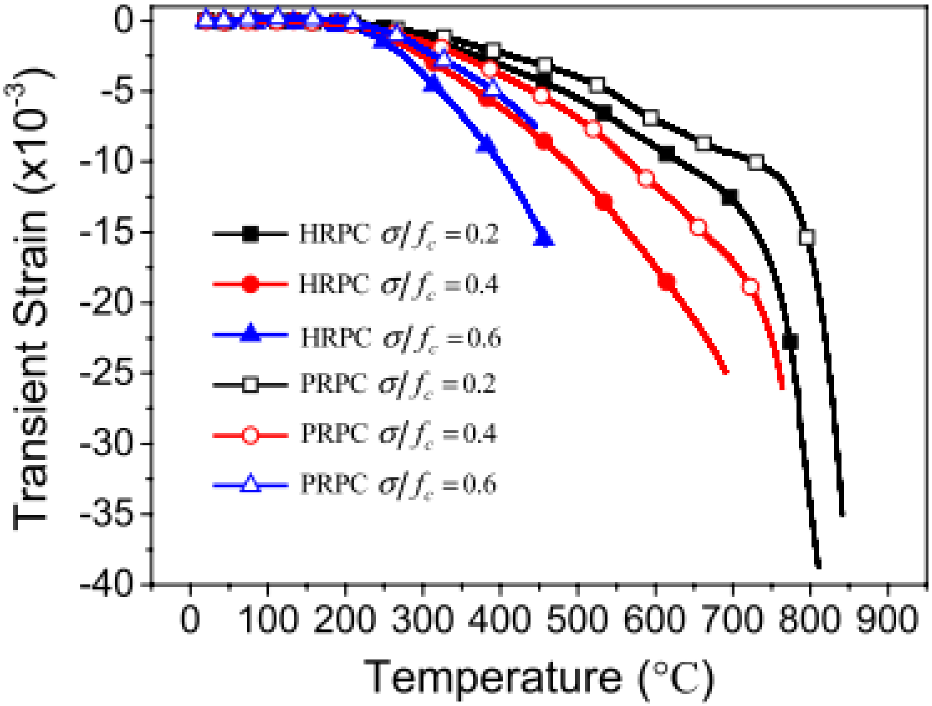

Figure 2- 16: Transient strain of HRPC and PRPC containing PP and steel fibre (Hou et al., 2019)

Alogla & Kodur (2020) investigated the development of temperature-induced transient creep strain in different types of concrete. The study measured creep strain by subjecting concrete specimens to heating and mechanical loading effects in the temperature range between 20°C and 800°C. The study found that transient creep strain constitutes a significant portion of total strain and that temperature range and stress level significantly influence the magnitude of transient creep strain, especially at temperatures above 500°C and stress (α) levels of 40% or more. The study also found that steel fibres in normal-strength concrete slightly reduced the extent of transient creep strain, while adding polypropylene fibres to high-strength concrete leads to higher transient creep strain, as shown in Figure 2-17. Finally, the study proposed a creep relation that expresses transient creep strain in terms of stress level, temperature, and the type of concrete. The proposed creep relation can be used in advanced analysis to explicitly account for reliable transient creep strain in predicting the fire resistance of concrete structures.

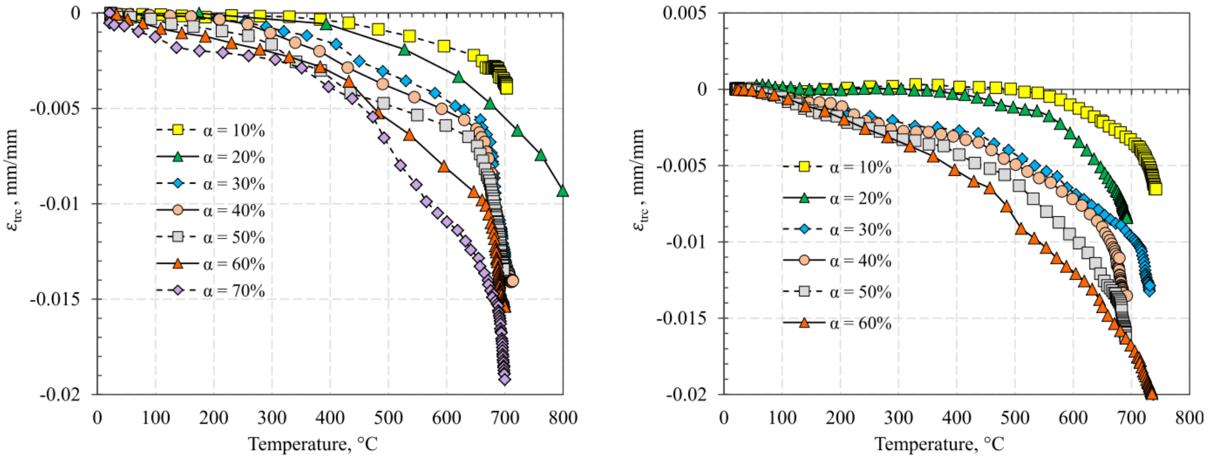

a) Transient creep strain NSC-Steel fibre b) Transient creep strain HSC- polypropylene fibre

Figure 2- 17: Transient thermal creep (Alogla & Kodur, 2020b)

Both studies investigated the effect of PP fibres on the creep behaviour of concrete at elevated temperatures, but the studies differed in their approach. (Hou et al., 2019) focused specifically on RPC and considered the effect of PP and hybrid fibres on creep behaviour under different thermo-mechanical regimes. The study found that the performance of PP fibre was better than that of hybrid fibres in terms of the creep behaviour of RPC. On the other hand, Alogla & Kodur (2020) investigated the development of temperature-induced transient creep strain in different types of concrete, including normal-strength and high-strength concrete with different types of fibres. The study found that temperature and stress level dominate the extent of transient creep generated in concrete, and adding polypropylene fibres to high-strength concrete leads to higher transient creep strain.

2.10 Concluding summary

The literature review provides a comprehensive overview of the effects of high temperatures on concrete and cement paste, highlighting key factors such as changes in physicochemical composition, decomposition of hydration products, and alterations in mechanical properties. It discusses how temperature-induced modifications, including the degradation of strength and elasticity, are influenced by factors like heating rate, relative humidity, and moisture content. Additionally, the review explores the role of fibres, particularly polypropylene and glass fibres, in enhancing concrete's mechanical properties and resistance to cracking. However, there are notable gaps in the literature, including a lack of discussion on the combined effects of temperature and fibres on concrete performance, limited exploration of long-term durability issues, and a need for deeper insights into the mechanisms underlying the interaction between fibres and hydration products at elevated temperatures and also the limited literature on polypropylene powder.

Furthermore, while the review provides valuable insights into the behaviour of fibre-reinforced concrete under thermal stress, research is needed to address these gaps comprehensively. Future studies could investigate the long-term durability of fibre-reinforced concrete exposed to high temperatures, including creep, fatigue, and ageing. Additionally, exploring novel fibre types or combinations that offer enhanced performance in high-temperature environments could provide valuable contributions to the field. Furthermore, deeper exploration into the microstructural changes and bond characteristics resulting from the interaction between fibres and hydration products at elevated temperatures could lead to more resilient and durable concrete materials for infrastructure applications.

Chapter 3: LITERATURE ON POLYPROPYLENE

3.1 Introduction

This literature related to the role of polypropylene (PP) fibres employed in concrete/cement paste to reduce the negative effect of the mechanical properties of concrete/cement paste at high temperatures. The literature explained an in-depth understanding of the role of PP fibres in heated concrete/cement paste, as well as the physical and chemical properties of the PP.

3.2 Chemistry of Polypropylene

In 1954, the discovery of polypropylene marked its widespread use compared to other commonly used plastics due to its low density. This material is highly resistant to various chemicals and can easily form into different shapes through injection moulding and extrusion. Its ability to withstand high temperatures makes it highly useful in clinical settings where items such as trays, funnels, and instrument jars need to be sterilised regularly. PP is a colourless material and possesses better mechanical properties than polyethylene. It is derived from the polymerisation of the olefin monomer propylene using heat, high-energy radiation, and a catalyst. Four main methods are used to enhance the polymerisation of any polymer: solution polymerisation, suspension polymerisation, bulk polymerisation, and gas-phase polymerisation. The properties of PP depend on several factors, such as the method of polymerisation, copolymer components, molecular weight, and molecular weight distribution. It is where each carbon atom is connected to a methyl group, and its molecular structure is depicted in Figure 3-1. (Hisham A. Maddah, 2016).

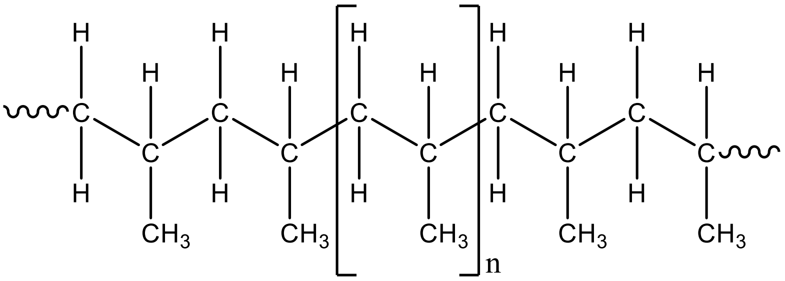

Figure 3- 1: Structure of Polypropylene

3.2.1 Molecular structure

Polypropylene (PP) is a linear hydrocarbon polymer that can be produced through Ziegler-Natta catalysed polymerisation technique or metallocene catalysis polymerisation using propylene monomer. PP has a vinyl polymer structure where every other carbon atom in the backbone chain is bonded to a methyl group, and it has little or no unsaturation in its chain structure. PP has similar features to polyethylene, such as swell in solution, and its properties depend on the molecular weight and grade. The Ziegler-Natta catalysts used in the polymerisation process have numerous active sites that lead to extensive tacticity and molecular weight dispersion of PP. Different types of catalysts and polymerisation processes can be employed to adjust the molecular configuration, resulting in three forms of PP (# Bárány, 2006). Polymer tacticity may be used to determine mechanical properties, solubility, and melt temperature (Arranz-Andrés et al., 2007). The properties of PP can vary depending on the arrangement of the methyl group in the PP carbon atom, which can be either isotactic, syndiotactic, or atactic. This arrangement is illustrated in Figure 3-2, and the presence of the methyl group in the PP backbone chain can give rise to several different properties for PP. (Ariff et al., 2012). The tacticity of PP is a crucial factor that affects its viscosity and final properties. Isotactic PP, which constitutes 90-95% of commercial PP, is made using a Ziegler-Natta catalyst and propylene monomer added from head to tail. Due to the stable arrangement of the methyl group on one side of the PP chain structure, isotactic PP does not form a zig-zag planar crystal structure but a helical crystal structure. As a result, the degree of crystallisation in isotactic PP can exceed 50%, leading to an increase in PP softening temperature and melt viscosity during processing. However, high processing temperatures can cause the methyl groups attached to the PP backbone to oxidise quickly, making them vulnerable to chemical assault by specific chemical agents.

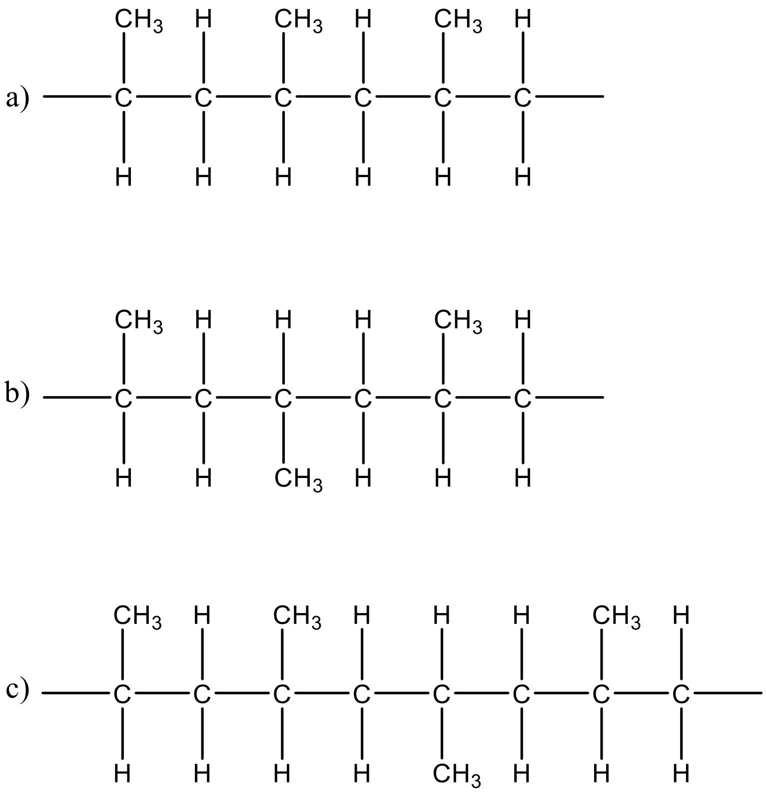

Figure 3- 2: The three basic forms of polypropylene are (a) isotactic, (b) syndiotactic, and (c) atactic

3.2.2 Molecular weight

The monomer propylene (C_3H_6) is a gaseous substance with a molecular weight (MW) of 42.1 Dalton. PP is a high-molecular-weight hydrocarbon, and its properties depend highly on its MW. Any form of chemical or thermal degradation leads to a decrease in MW and, consequently, a reduction in properties such as solid strength and melt viscosity. At room temperature, hydrocarbons with lower MWs (e.g., methane, ethane) exist as gases or vapours, while those with higher MWs (e.g., n-pentane) form liquids. Higher MWs are associated with an increased melting point, boiling temperature, and viscosity.

On the other hand, PP has a density of 18.02 Daltons, which is significantly higher than the values for lower MW hydrocarbons. Under experimental conditions, the average MWs of PP range from 75,000 to 200,000 Daltons. Commercially available PPs come in various grades, each with a specific MW range. (G. A. Khoury & Willoughby, 2008).

González-González et al. (1998) study found that the macromolecule degradation occurred primarily due to chain scission and no oxidation under the experimental conditions. This was supported by the absence of carbonyl groups and gel formation and a decrease in molecular weight and polydispersity. The molecular weight distribution curves indicated that chain scissions took place close to the macromolecule, which is in line with the Bueche hypothesis of mechanical degradation depicted in Figure 3-3. It was observed that there was no significant degradation up to 230°C; between 230 and 250°C, the number of chain scissions increased rapidly with increasing temperature; finally, from 250 to 270°C, there was no change in the number of chain scissions with increasing temperature.

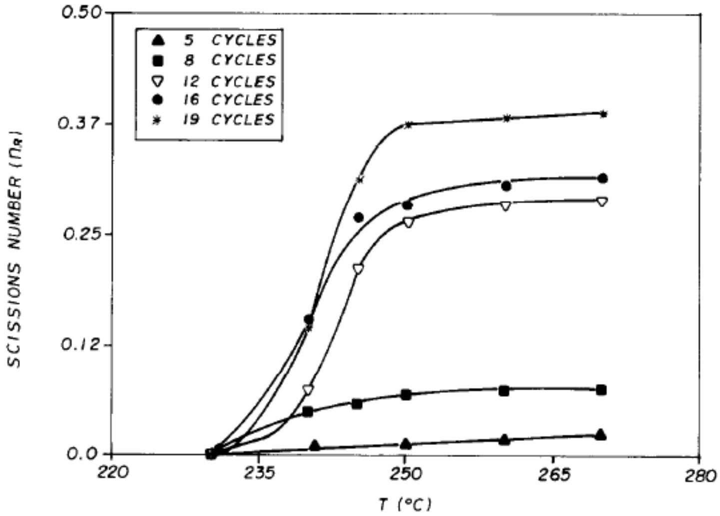

Figure 3- 3

Figure **3**-3: The average number of a chain as a function of die temperature (González-González et al., 1998)

3.2.3 Chemical reactivity

PP is an extremely chemically resistant material with high resistance to acids and alkalis, making it an ideal choice for chemical plant piping. Its resistance to alkaline concrete with a pH of 12 is also noteworthy. However, it is vulnerable to oxidation, so commercially made fibres are stabilised against this reaction. Despite this vulnerability, PP is still resistant to substances that can degrade many other materials. At room temperature, there are no known solvents for isotactic PP, making it an even more attractive choice for various industrial applications.

3.2.4 Melting of PP

3.2.4.1 Melting temperature

The melting process can happen at various temperatures, indicated by the range of temperatures displayed in the melting endotherm diagram Figure 3-4, which can start as low as 150°C. The commonly reported temperature for the maximum rate of melting $(\boldsymbol{T_m})$ is 165°C, which is the high point of the melting endotherm. It's important to note that the shape of the endotherm curve can be altered by changes in the test conditions, such as the polymer's heating rate and thermal history. The thermodynamic melting point, $\boldsymbol{T_{td-m}}$ is the temperature at which the ultimate crystallinity disappears, commonly referred to as the 'maximum' melting temperature, which is 176°C. (G. A. Khoury & Willoughby, 2008)

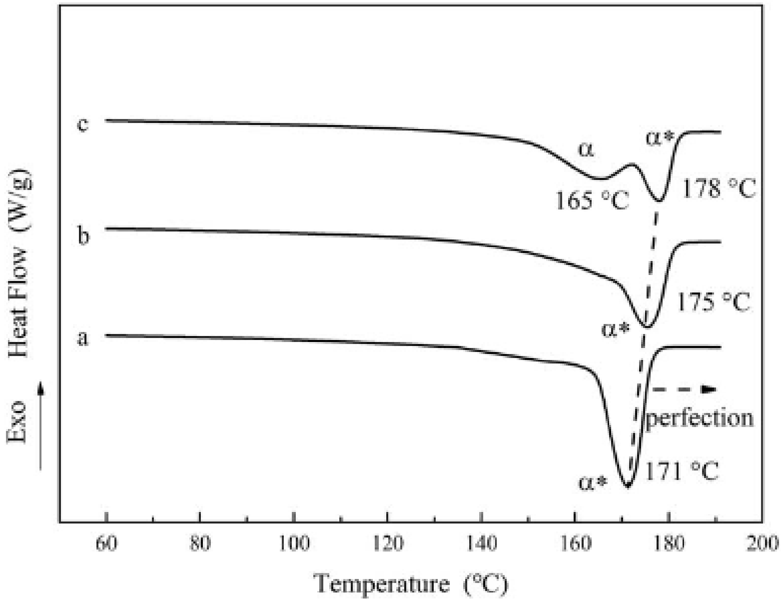

Figure 3- 4

Figure **3-**4: Melting endotherm range showing Tm as the peak in the endotherm (Yu et al., 2018)

3.2.4.2 Melt viscosity

The viscosity of a polymer melt is used to define its characteristics. The viscoelasticity of PP indicates the presence of structure inside a substance that is nominally classified as a liquid. Measuring the viscosity of a melt at a temperature near its melting point is a sensitive way of assessing polymer degradation, which becomes visible when heated beyond 270°C (Vinogradov & Prozorovskaya, 1964). When melted, the Arrhenius equation describes the shear viscosity of PP blends within a temperature range of 190°C to 290°C and a shear rate range of 10^{-2} to 10^{2} s^{-1}. Specifically, when the shear rate remains constant, the natural logarithm of the shear viscosity (η) measured in pascal seconds ($\boldsymbol{P_{a.s}}$) increases linearly with the reciprocal of the absolute temperature (1/T), as illustrated in Figure 3-5 (Liang & Peng, 2009).

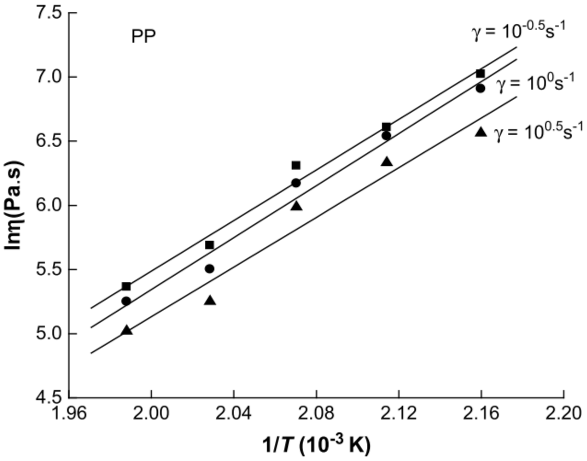

Figure 3- 5

Figure **3-**5: Influence of temperature on melt shear viscosity of PP (Liang & Peng, 2009)

According to Khoury & Willoughby, (2008), temperature has two effects on viscosity: it lowers it by increasing molecular energy and reducing molecular size through thermal degradation. However, applying the Arrhenius equation for polymer melts is challenging due to the reliance on shear, and the equation can only be used under constant shear rates. Figure 3-6 illustrates that at an extremely low shear rate, the viscosity coefficient at 230°C approaches or exceeds 500 $\boldsymbol{P_{a/s}}$

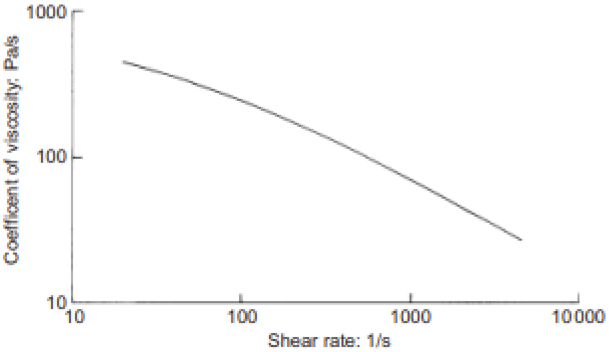

Figure 3- 6

Figure **3-**6: Coefficient of viscosity (Pa/s) against shear rate (1/s) for 22 MFI PP at 230◦C (G A Khoury & Willoughby, 2008)

3.2.4.3 Degradation in the melt (pyrolysis)

As the temperature of melted PP increases, the weakest carbon-carbon bonds in the carbon backbone start to break, referred to as the random scission process. This gradual breakdown leads to a decrease in molecular weight, commonly known as "thermal pyrolysis." The reduction in molecular weight can also cause the volatilisation of small molecules, which is an endothermic reaction with a gasification heat of 2kJ/g.(G A Khoury & Willoughby, 2008).

Between the temperature range of 200-300°C, oxygen was found to increase mass release from PP, producing refractory solid components that gradually transformed into volatiles at higher temperatures. The synthesis of peroxide on the tertiary carbon of PP played a key role in regulating the net mass release rate in the presence of oxygen, following first-order kinetics with respect to the oxygen partial pressure. At 250°C, about 90% of the PP underwent oxidative pyrolysis to form volatiles, with an activation energy of 60-70 kJ/mol. Around 350°C, energetic volatile species were observed to be produced, with larger molecular weights initially produced containing roughly 20-30 carbons. However, volatilisation was found to be impossible for polymers with more than 20-30 carbon atoms, and lighter molecular weight compounds were formed as the temperature increased. (Hayashi et al., 1998)

Extensive pyrolysis of PP, which is similar to thermal cracking in oil, results in the production of propylene volatile dimers and trimers, which are classified as alkanes (i.e., C_6H_{12} and C_9H_{18}), according to Jeffery et al,. (2001). All melted PP can be completely volatilised at a temperature of 470°C. At this temperature, the molecules in the gas phase act independently, providing an opportunity to examine the penetration of individual molecules into concrete. These molecules are highly active at elevated temperatures, with all the bonds undergoing rotations and vibrations, allowing the molecule to change its form rapidly.

3.2.5 Combustion

Various indicators such as the limiting oxygen index (LOI), carbonisation, smoke, mass loss, and heat release are used to quantify the physical and chemical changes that occur during material combustion. Commonly used tests to analyse the combustion properties of a material include the limiting oxygen index (LOI) test, thermogravimetric analysis (TGA), and cone calorimetric test (CCT). (Kim et al., 2017).

Savas et al. (2018) investigated how the carbon fibre content affects the flame retardancy of a retardant polypropylene composite. They found that the fibre length did not impact the composite's combustion properties, but the presence of carbon fibre did have an effect. As the fibre content increased, the oxygen index of the composite decreased because of the opposition of ammonium polyphosphate.

Polypropylene fibres are commonly used in concrete, and the maximum heat release due to oxidation of PP at around 500°C was calculated by determining the fibre content of 1-3 kg/m³. The maximum heat output due to full combustion or oxidation of hydrocarbon gases was between 473 and 356 kJ/m³ concrete, assuming a 15% porosity in the concrete filled with air and volatilised hydrocarbons mixed locally. This heat output is limited by the oxygen content in the concrete, which ranges from 37-28g. However, it is highly unlikely that even this degree of oxidation of the PP pyrolysis products will occur within the concrete due to the fate of the water in the concrete and the number of hydrocarbon products produced. If hydrocarbon gases and steam come into contact with the fire plume on the concrete surface, the gases may burn if the oxygen content is high enough. If the gases are released away from any flame, they will ignite on contact with oxygen at around 550°C but will ignite at about 350-400°C if a source fire is present. Perfect combustion produces only water and carbon dioxide, while imperfect combustion produces carbon monoxide, smoke, and mixed organic compounds. Under well-ventilated combustion conditions, the heat of combustion of PP is around 4600 kJ/kg (4.6 kJ/g). (G A Khoury & Willoughby, 2008)

3.2.6 Non-polarity of Polypropylene

For the bond to be non-polar or polar covalent is defined by electronegativity, which is a property of the bonding atoms. Electronegativity measures an atom's tendency towards attracting electrons (or electron density) to itself. This measure of atom tendency defines how the mutual electrons are distributed in a bond between the two atoms. The more strongly an atom attracts electrons in its bonds, the greater its electronegativity. Electrons are shifted towards atoms with more electronegative in a polar covalent bond. Therefore, the atom with the greater electronegative charge has a partial negative charge. The larger the difference in electronegativity, the more polarised the electron distribution and the higher the partial charges of the atoms. (Sharp et al., 2001). Water (H_2O) is one example of a polar molecule. The hydrogen atom has an electronegative charge value of 2.1, and the oxygen atom has 3.5. Therefore, the oxygen atom has a high electronegativity value, so it tends to pull the hydrogen tom's electron toward itself; the difference in electronegativity between hydrogen and oxygen is 1.4 and greater than 0.5. For an atom to be polar, the electronegativity difference must be ≥ 0.5. This difference in electronegativity shows that water has polar bonds. In analysing the geometry of water molecules, oxygen likes to form 2 bonds. It has 2 lone pairs of electrons because it is more electronegative and will have a partial negative charge δ-, and hydrogen has a partial positive charge δ+. The dipole moment is pulling toward the electronegative atom. The resultant vector of bond polarity in water indicates the polarity of molecules (Giovambattista et al., 2007), as shown in Figure 3-7.

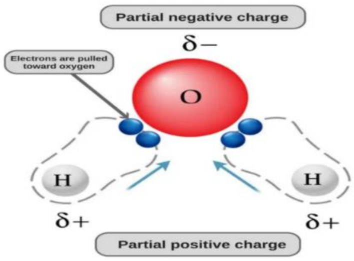

Figure 3- 7

Figure 3-7: Geometry of water molecule showing polar bond and dipole moment (Allot & Mindorrf, 2014)

In general, the molecules with high polarity are more likely to react with water because, when a polar material is placed in water, its positive ends attract the negative ends of the water molecules and vice versa. Because of the attraction, the molecules of the new material are uniformly mixed with the water molecules. Therefore, when taking PP, the carbon-hydrogen bond is non-polar because of the small difference in electronegativity in the C-H bond. The carbon atom has an electronegativity value of 2.5, and hydrogen has 2.1. The dipole moment is very small because the difference in electronegativity is 0.4, less than 0.5. This dipole moment pulls hydrogen's electron toward the carbon atom electron because carbon has a higher electronegativity than hydrogen. The dipole moment within the C-C bond is cancelled because they have the same electronegativity value, and the resultant vector between the C-C atom is zero. Therefore, polypropylene is a non-polar material because there is no significant dipole moment within the molecule since the dipole moment of C-H is very small and categorised as non-polar (Ingold, 1926)

3.2.7 The bond between PP and concrete/cement paste

The polarity of water and PP is completely different, as previously explained. Consequently, there is also a polarity mismatch between polypropylene and concrete, likely resulting in poor wettability at the interface between polypropylene and concrete. (G. A. Khoury & Willoughby, 2008). Hernández-Cruz et al. (2014) investigated the weak bonding between PP and concrete using Scanning Transmission X-ray Microscopy (STXM) analysis. The result of the experiment shows the absence of calcium (Ca) at the interface between the PP and cement paste in the hardened cement paste (HCP). As a result of this poor interface, there is a likelihood of a loss of strength in the cement paste.

3.3 Surface modification techniques for PP used in concrete/cement paste

3.3.1 Alkaline treatment

To improve the hydrophilicity of PP and enhance its adhesion with hydrated cement paste, an alkaline treatment can be employed, which involves immersing the material in a sodium hydroxide (NaOH) solution. Infrared analysis was conducted to compare the polarity of the treated PP with that of untreated PP to assess the effectiveness of this treatment. The results showed that the polarity of the treated and untreated PP was quite similar, indicating that the alkaline conditions of the treatment did not degrade the material. This finding is presented in Figure 3-8 (Buendía et al., 2013)

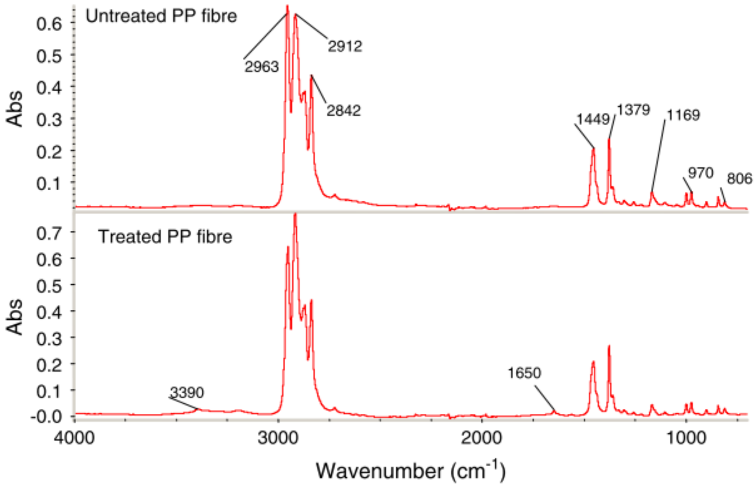

Figure 3- 8: Infrared spectrum of the surface of Treated and untreated Polypropylene (López-Buendía et al., 2013)

Other research results show some beneficial effects of using an alkaline solution on fibre treatment. Park et al. (2008) reported that the mechanical interlocking mechanism, which is attributed to the enhanced surface roughness of the material, is effective in the alkaline treatment of PP.

Using a basic alkali solution for treating PP fibres affects the cement matrix rather than the fibres. This treatment promotes the precipitation of hydration products on the surface of the fibres, which creates a rough surface that can generate frictional forces with the matrix. Even without direct bonding between the fibre and matrix, the Baggott & Gandhi (1981) model for steel reinforcement in cement is believed to apply to PP fibre reinforcement. In this study, micro defects were found on the surface of the PP fibres, which created a semi-interaction between the fibres and matrix. The basic alkali solution increased the wetness of water by 300 times, enhancing the wettability between the fibre surface and the cementitious matrix. This improved wettability increases the presence of rough surface asperities on the fibre surface, resulting in enhanced frictional forces between the fibres and matrix. It would also promote the formation of crystalline products during the hydration process, strengthening the bonding between the fibre surface and matrix, resulting in a 34% increase in compressive strength (Lovata & Fahmy, 1987).

3.3.2 Surface Oxidation treatment

Flame oxidation and wet-chemistry oxidation are two techniques used to oxidise the surface of PP fibres. The oxidation process involves mixing different types of gases in specific proportions and burning them on a distinct flame. This leads to the appearance of specific oxygen-containing groups on the surface of PP fibres. According to Pijpers & Meier, (2001), XPS analysis of PP fibres revealed a significant number of oxygen atoms on their surface after flame treatment. Figure 3-9 displays the anticipated oxidation pathway resulting from these flame treatments.

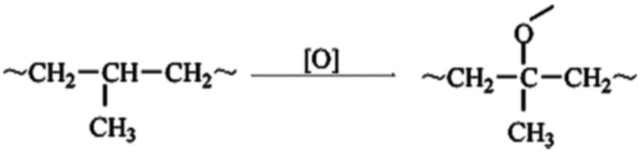

Figure 3- 9: mechanism during treatment of PP fibres by flame oxidation

The combination of potassium dichromate, sulfuric acid, and water is commonly used for wet-chemistry oxidation. This solution can remove dirt and amorphous areas from the surface of PP fibres, creating micro holes with complex shapes within the PP fibre body. Additionally, this solution can add hydrophilic groups to the surface of PP fibres, improving wetting ability and interfacial strength between PP fibres and cement matrices after treatment. The most likely oxidation mechanism produced by chromium acid treatment is depicted in Figure 3-10, as Wang et al. (2006) reported.

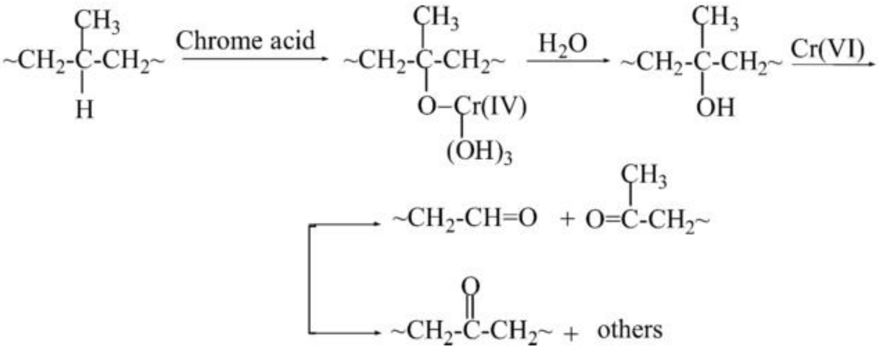

Figure 3- 10: Oxidation mechanism during treatment of PP by chromium acid (Wang et al., 2006)

3.3.3 Plasma treatment

Plasma is an intricate energy source used to modify various materials' surface characteristics through different surface modification techniques. Plasmas are chemically active media consisting of diverse components, such as excited and ionised atomic and molecular particles, photons, and radicals. These species possess enough energy to cause chemical reactions within the plasma volume and at the plasma-solid-surface interface. In contrast to other forms of plasma, cold plasmas do not generate heat damage to the materials they interact with. This unique property makes them ideal for low-temperature plasma chemistry and for treating heat-sensitive materials, such as polymers and biological tissues (Borcia et al., 2011). It is frequently observed that plasma treatments are employed to modify the surface characteristics of polymers, such as adhesion, dyeability, wettability, biocompatibility, friction, and penetrability, to suit specific applications (Wolf, 2010). Plasma-based techniques can bring about physical and chemical alterations in the surface properties of polymers through various simultaneous processes such as etching, grafting, polymerisation, cross-linking, and so on, depending on the treatment parameters, without altering their intrinsic bulk properties (Yasuda & Yasuda, 2000).

Plasma treatment leads to two alterations in materials, which ultimately enhance adhesion. When oxygen interacts with the polymer, it generates polar groups with two effects. Firstly, they increase the surface tension, which enables the adhesive or lacquer to wet the surface adequately. As a result, the adherence of the adhesive or lacquer to the modified PP molecules is improved. Secondly, the treatment results in an increase in surface roughness (Zeiler et al., 2000).

In their study, Feldman et al. (2000) examined how $SiCl_4$-plasma-treated PP fibres influence cement matrices. They found that those made with plasma-treated fibres exhibited greater flexural strength and toughness than untreated fibres. X-ray photoelectron spectroscopy (XPS) and attenuated total reflection Fourier transform infrared (ATR-FTIR) analyses revealed that the $SiCl_4$-plasma-treated PP fibres surfaces underwent substantial oxidation reactions, which led to the formation of functional groups such as C-O and C=O on the surface of the $SiCl_4$-plasma-treated PP fibres.

Although plasma treatment is a highly effective technology for altering polymer surfaces while preserving bulk structure and properties (Lin & Hsieh, 1997), manufacturers do not widely utilise it. This is partly due to its lack of cost-effectiveness and because various parameters, such as temperature, duration, and other variables, may influence the efficacy of plasma treatment. According to preliminary research (Feldman et al., 2000; Zhang et al., 2000;

Lin & Hsieh, 1997), different gases used in plasma treatment may be suitable for different types of polymeric fibres and may have varying effects on PP fibres.

3.3.4 LASER treatment

In recent years, laser technology has gained significant attention in various fields due to its precision and versatility in material processing. Among the plethora of laser systems available, the picosecond amplifier EKSPLA Atlantic 5 LASER stands out for its capability to deliver three distinct beamlines at 1064 nm, 532 nm, and 355 nm wavelengths, with a remarkably short pulse duration of approximately 10 picoseconds (Akand et al., 2018). This particular study focused on harnessing the 355 nm beamline to ensure optimal energy absorption for polymeric materials, thereby highlighting the versatility of the EKSPLA Atlantic 5 LASER in tailored material treatment applications.

The laser treatment methodology employed a systematic approach to specimen surface ablation, characterized by overlapped parallel scanlines oriented perpendicular to the long side of the polypropylene (PP) specimen shown in Figure 3-11. This configuration, combined with a fixed movement system, enabled simultaneous treatment of three specimens, demonstrating the system's capability for high-throughput processing. The choice of scanner strategy was instrumental in achieving uniform pulse distribution and energy deposition across the specimen surface, ensuring consistent treatment outcomes. Central to the study was the meticulous optimization of process parameters to achieve desired functionalization outcomes while mitigating undesirable effects such as surface burns. A comprehensive analysis encompassing six levels of laser power revealed a nuanced relationship between power settings and surface effects, ranging from negligible ablation at lower power levels to significant specimen damage at higher thresholds. This empirical investigation informed the selection of optimal process parameters, with due consideration given to both functionalization efficacy and surface integrity (Malchiodi et al., 2023).

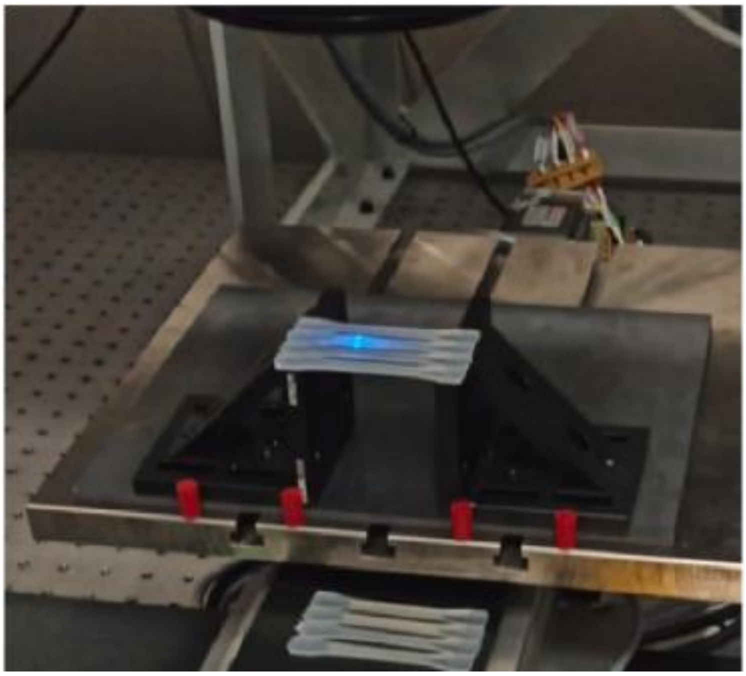

Figure 3- 11: LASER treatment of Polypropylene fibre

3.3.5 Ultra-violet light treatment

The modification of surface composition and wettability has been a widely investigated topic, with various techniques being explored, including the utilisation of UV-light exposure, as reported by Chylińska et al., (2020). Among the techniques for altering the surface properties of PP, the exposure of PP to UV light has been identified as one possible approach. This method has been found to increase PP's surface energy by breaking the molecular bond on the surface and adding polar oxygen atoms.

According to Nie et al. (1999), the surface adhesion force of polypropylene increased significantly after the modification process. This increase in adhesion force was attributed to the formation of mounds on the surface, which resulted from the production of low molecular weight oxidised materials. Additionally, the modification process increased the surface energy of polypropylene, consequently enhancing its hydrophilicity and adhesion performance.

Coopamootoo & Masoero (2018) have investigated the effects of UV treatment on polypropylene (PP) used in concrete and reported that the use of UV irradiation on PP can effectively restore the compressive strength of concrete to its original level, which is comparable to the strength of concrete made with untreated PP. This improvement in strength is primarily attributed to an enhancement in the interfacial bonding between the cement matrix and the PP. This effect, also observed by (Ossola & Wojcik, 2014) on cement-rubber composite, has suggested that pre-treating rubber crumbs with UV light could significantly reduce the composite's strength loss.

Moreover, precise control in UV treatment is emphasized in the literature, as highlighted by Malchiodi et al., (2023). This involves meticulous setup involving a UV LED lamp with specific parameters, including peak wavelength and maximum irradiance. Additionally, strategies are employed to maintain consistent conditions, such as controlling the distance from specimens and mitigating heat accumulation. Studies indicate that prolonged UV exposure enhances the wettability of PP, leading to a significant reduction in contact angle. However, the glossy surface of specimens may partially impede the effectiveness of UV treatment, possibly due to the reflection of the UV-LED source.

3.4 Quantification of hydrophilicity of PP

3.4.1 PP- water contact angle

Surface wetting is a commonly studied phenomenon, often assessed using optical contact angle measurements (Aurenty et al., 1997; Chen et al., 2016; Mandolfino et al., 2019; Tu et al., 1998). In order to determine the surface free energy component of a material, it is necessary to measure its contact angle. The contact angle is a critical parameter that characterises the extent of wetting of a liquid on a solid surface. Once the contact angle reaches a constant value under specific conditions, it can be inferred that thermodynamic equilibrium has been established at the interface. (Aurenty et al., 1997).

The study conducted by (Mandolfino et al., 2019) on the surface treatment of PP using low-pressure plasma has reported different results for contact angle measurements depending on the type of working gas used. Similarly, a study conducted by (Chen et al., (2016) found an increase in the hydrophilicity of PP following plasma treatment, as observed from the water contact angle measurement. Specifically, the water contact angle of untreated PP was found to be 97.1^{o}. However, by increasing the power input to 200W and extending the exposure time to 180s, the water contact angle significantly decreased, increasing wettability and decreasing the polar component. This finding is consistent with the results reported by (Chen et al., 2016), in which the contact angle was found to be approximately 98.5^{o} and decreased significantly to 20^{o} after being treated with various types of plasma, as depicted in Figure 3-12.

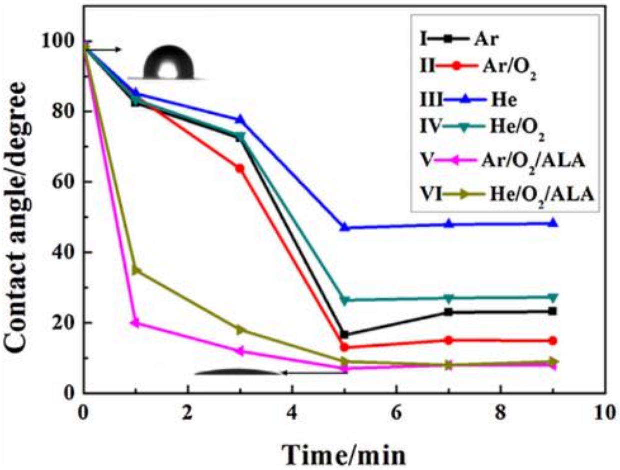

Figure 3- 12: Water contact angle of modified PP with different parameters (Chen et al., 2016)

One of the study's findings indicates a considerable improvement in the bonding between the PP fibres and the concrete matrix when treated with oxy-fluorination and evaluated using water contact angle measurement. As a result, the concrete's strength increased by 50-100% compared to the concrete with unmodified PP fibres (Tu et al., 1998).

3.4.2 Water retention test

However, the water retention method provides a balance between precision and simplicity that is appropriate for many experimental goals. Coopamootoo & Masoero (2018) used this method to study the surface modification of 10g of UV-treated PP. The samples were mixed with 50 ml V_1 of water and stirred for 10 minutes before being poured into a funnel lined with filter paper. The volume of the drained water V_2 was measured using a measuring cylinder, and this procedure was repeated for different UV-treated PP samples that were exposed to varying durations of UV radiation. The results show that longer exposure times (up to 72 hours) lead to greater surface modification, as indicated by increased water retention ($V_1 - V_2$), as shown in Figure 3-13.

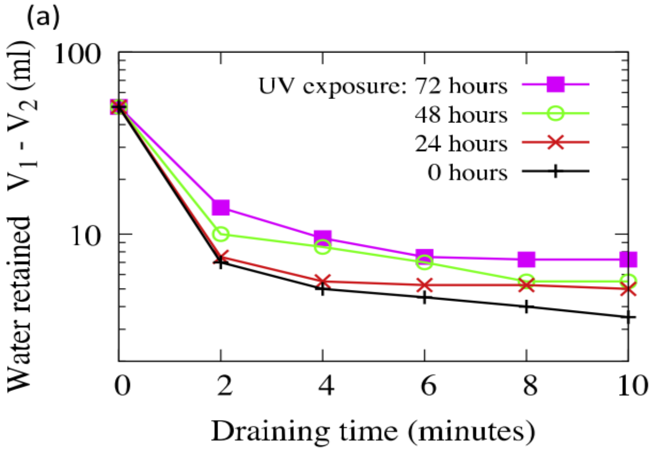

Figure 3- 13: water retention curves against draining time (Coopamootoo & Masoero, 2018)

V1 is the volume of water and the PP sample, V_2 is the volume of water drain in the cylinder, V_1-V_2 is the actual volume of retained water in the litmus paper

Ossola & Wojcik (2014) found similar results in an experiment concerning cement-rubber composites. Water retention increased due to the surface polarity, as demonstrated in Figure 3-14. This figure shows a continuous rise in water retention with time exposure, which indicates the benefit of UV treatment in terms of wettability

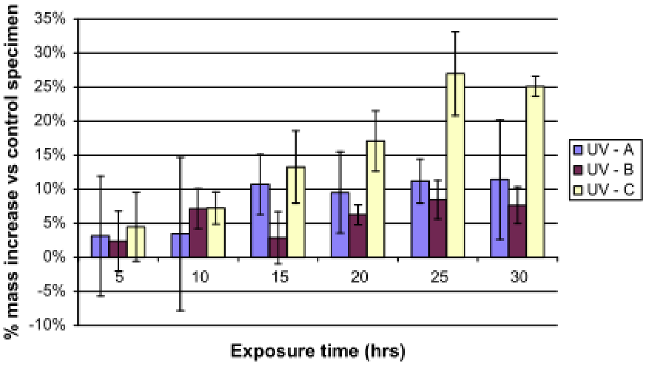

Figure 3- 14: Average water retention result for UV-treated rubber against time exposure

3.5 Concluding summary

The performance of cementitious composites with polypropylene fibres (PPF) is greatly influenced by the level of treatment applied to the fibres. Various surface modification techniques, such as alkaline treatment, surface oxidation, plasma treatment, and UV light exposure, have been investigated to enhance the compatibility of PPF with cement matrices. Among these techniques, UV treatment has shown promising results in altering the surface properties of polypropylene, leading to improved adhesion and bonding between the PPF and the cementitious material. This enhanced interface between the fibres and the cement paste is crucial for strengthening the composite and mitigating the adverse effects of high temperatures on its mechanical properties.

Studies have demonstrated the efficacy of UV treatment in increasing the hydrophilicity and surface energy of polypropylene fibres, which promotes better wetting and adhesion to the cementitious matrix. Additionally, UV treatment has been found to modify the chemical composition of the fibre surface, creating functional groups that facilitate chemical bonding with the cement paste. These modifications result in a stronger interfacial bond between the PPF and the cementitious matrix, leading to improved mechanical performance and durability of the composite, particularly in high-temperature environments where thermal stress can degrade the materials. Overall, the literature suggests that UV treatment is a promising method for enhancing the performance of cementitious composites with PPF reinforcement, offering potential solutions to challenges associated with high-temperature exposure.

Chapter 4: METHODOLOGY

4.1 Introduction

This chapter gives an outline of the experimental program. In this regard, the description of the materials used and their characteristics are explained in section 4.2.

Section 4.3 deals with the procedure for the treatment of polypropylene fibre (PPF) and polypropylene powder (PPP) using the ultraviolet light box for surface modification of PP. To this effect, some literature ware adopted for the treatment of polypropylene (PP), which is more economical and accurate.

Section 4.4 explains the preparation of the sample. Also, methods for mixing, casting, and curing samples following the method from the literature was adopted.

Sections 4.5 to 4.9 describe the procedures for the experimental plan. The experiment method comprises a water retention test adopted from the literature, residual compressive strength and compressive strength at hot temperature following ASTM standard, scanning electron microscopic using Tescan machine and transient thermal creep test following RILEM 129-MTH, 1997) recommendation.

4.2 Experimental program

The materials used in this study comprised Portland cement (CEM II/A-LL,32,5R) BS EN 197-1 standard. It contains cement clinker of about 80 to 94%, limestone of about 6 to 30% and other minor additions of about 0 to 5% (Cavalieri, 2001). Other materials include water, Polypropylene fibre, and polypropylene powder. The materials' sources, as well as their preparation, are described in the sub-section 4.2.1 to 4.2.3

4.2.1 Cement

CEM II/A-LL,32,5R cement was used throughout the experiment. The chemical composition of the cement is presented in Table 4-1. The chemical composition was found from the data sheet of the Quinn cement company.

Table 4- 1: Chemical composition of CEM IIA-LL,32,5R cement (Quinn Cement, 2011)

Oxide Composition (%)	MgO	Al_2O_3	SiO_2	SO_3	K_2O	C_aO	Fe_2O_3	Na_2O	Loss on Ignition
CEM II 35,5 R	1.54	23.55	45.98	1.47	1.8	18.67	4.91	0.24	3.88

4.2.2 Water

Deionised water, free from contaminants, was used to mix and cure cement paste. A deionisation water system consists of tanks designed to remove ions from water using the process of ion exchange. Deionized water was selected over tap water in this context to prevent any chemical interactions within the cement paste. This choice was made because tap water often contains impurities and minerals that can react with the cement components, potentially altering the properties of the paste and compromising the integrity of the results.

4.2.3 Polypropylene

Polypropylene fibre (PPF) and polypropylene powder (PPP), as shown in Figure 4-1. PPP was obtained from A. Schulman company, while PPF was bought from Amazon and manufactured by Goonvean fibres company. The properties are shown in Table 4-2. The properties were obtained from the manufacturing companies' data sheets.

Table 4- 2: Characteristics of Polypropylene fibre and polypropylene powder

	Length (l)mm	Diameter (d) (µm)	Tensile Strength (MP_a)	Melting Point (°C)	Specific gravity (g/cm^3)
Polypropylene Fibre	6	38	300-400	162-165	0.91
Polypropylene Powder	N/A	42	N/A	177.1	0.91

a) Polypropylene is in the form of powder

b) Polypropylene is in the form of fibre

Figure 4- 1: Polypropylene fibre and powder

4.3 Ultra-violet light treatment of Polypropylene

UV-C PPF and PPP exposure were carried out in the lightbox shown in Figure 4-2 below. The box was built for the purpose and fitted with 18W bulbs (254 nm wavelength). Samples were prepared by spreading the polypropylene within the UV lightbox to form a layer of uniform thickness of 1 mm, irradiating the PP sample at 0 hrs, 24 hrs, 48 hrs, and 72 hrs without interruption, respectively. The 72 hrs were chosen for this experiment. The samples were then allowed to settle at room temperature for certain minutes.

Experiments were conducted using irradiation durations exceeding 72 hours, but these led to the noticeable deterioration of the plastic specimens, which were subsequently discarded. Comparable findings, including an optimal irradiation period of 72 hours, were obtained in prior research on cement-rubber composites, where the enhanced retention of water was attributed to surface polarity (Ossola & Wojcik, 2014).

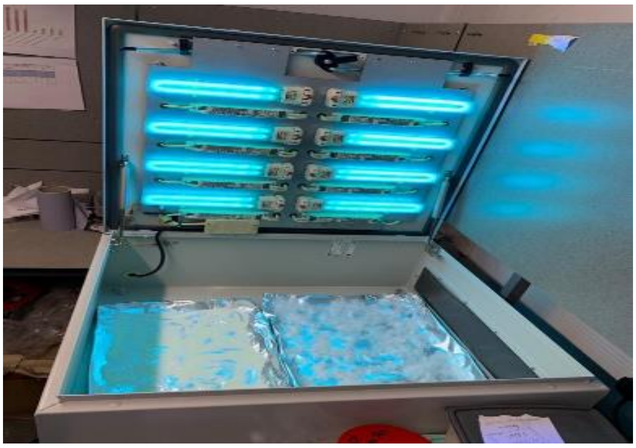

Figure 4- 2: UV box to treat Polypropylene

4.4 Preparation of specimen

4.4.1 Mixing of sample

Mixes consisting of only cement paste and water were prepared. Other aggregates were not involved to avoid other effects associated with the aggregate-polypropylene interaction at high temperatures. The water-cement ratio of 0.35 was kept constant throughout the experiment following the work of (Wong & Buenfeld, 2009), whereby in their experiment, good agreement was observed between the estimated and actual values for Portland cement pastes with a range of w/c ratios (0.25–0.50) and curing ages (3–90 days). The cement paste was cast in a small plastic cylindrical mould of a normal base diameter of approximately 40mm ±0.2 and a height of 80mm ±0.2

The reference mix in this work is Portland cement paste (CEM II/A-LL,32,5R) BS EN 197-1 standard. The mix containing only Portland cement containing polypropylene fibre was obtained by adding 2% polypropylene fibre, 3%, and 4% separately and polypropylene powder of 5%, 10% and 15%.

The selection of relevant percentages for polypropylene fibres (PPF) and polypropylene powder (PPP) was guided by existing literature. Murahari, (2013) suggested a minimum volume percentage of 2% for PPF, noting that as fibre volume increases, there tends to be a decrease in concrete compressive strength. Hence, additional percentages of 3% and 4% were included to assess the effects of PPF treatment on mechanical properties. Similarly, Coopamootoo & Masoero, (2018) research indicated that 15% was the maximum percentage for PPP, demonstrating a significant decrease in compressive strength. Consequently, percentages of 5% and 10% were chosen to investigate the impact of UV treatment on PPP in cement paste's mechanical properties.

The mix composition is shown in Table 4-3. All the materials were batched by weight, and the calculation showing each material's quantity is shown in Appendix I

First, all the required water was poured into the mixing machine, as shown in Figure 4-3. The cement was then added to the water, allowing 30 seconds to absorb water. The paste was mixed for 2 minutes at low speed, and the polypropylene was added, followed by another 2 minutes at low speed, followed by 2 minutes of final mixing at high speed, as prescribed by (American Society of Testing Materials, 2009).

Table 4- 3: Mixed Composition of cement paste

		Polypropylene (g)											
Cement (g)	**Water (g)**	**Non-TPPF**			**UV-TPPF**			**Non-TPPP**			**UV-TPPP**		
		2%	3%	4%	2%	3%	4%	5%	10%	15%	5%	10%	15%
1000	350	0	0	0	0	0	0	0	0	0	0	0	0
1000	350	13	19	25	13	19	25	32	63	95	32	63	95
1000	350	13	19	25	13	19	25	32	63	95	32	63	95
1000	350	13	19	25	13	19	25	32	63	95	32	63	95
1000	350	13	19	25	13	19	25	32	63	95	32	63	95

Figure 4- 3: Typical mixing machine

4.4.2 Casting of samples

The cement paste specimens were then placed in moulds in three layers following the general instructions for placing concrete in moulds given in (ASTM C 192/C 192M, 2002) and compacted on a vibrating table for 60 seconds. The cement paste samples were removed from the mould at the age of 24 hours and placed in water for curing at a temperature of 20 ± 3°C for up to 28 days.

The sample casting followed the established procedure, ensuring accurate mixture preparation, appropriate mould selection, careful elimination of air bubbles during casting, and curing of samples as stated above. A total of 509 cement paste samples were cast for this study, shown in Table 4-5, with specific sample allocations for each experimental condition. One hundred forty-one samples were cast for UV-treated PPF, with the aim of investigating the impact of UV treatment on the performance of PPF in cement paste. Similarly, 141 samples were cast for non-treated PPF. For UV-treated PPP, 90 samples were cast to analyse the behaviour of UV-treated PPP in cement paste, while an additional 90 samples were allocated for non-treated PPP. Finally, 47 samples were used for control samples, representing the standard behaviour of cement paste without PP in any form.

Three hundred sixty cement paste samples were used to assess residual compressive strength. Of these, 180 samples were tested under sealed conditions, and the remaining 180 were tested under unsealed conditions. The number of samples used for the RCS test for both the PP percentage for sealed and unsealed samples is shown in Table 4-4 below.

Table 4- 4: Number of samples for residual compressive strength test of cement paste

		Sealed RCS					**Unsealed RCS**					**Comp. at hot temp.**					**TTC**	
	Total	**20**	**50**	**100**	**200**	**350**	**20**	**50**	**100**	**200**	**350**	**20**	**50**	**100**	**200**	**350**	**FTS**	**LTS**
Control	47	3	3	3	3	3	3	3	3	3	3	3	3	3	3	3	1	1
TPPF 2%	47	3	3	3	3	3	3	3	3	3	3	3	3	3	3	3	1	1
TPPF 3%	47	3	3	3	3	3	3	3	3	3	3	3	3	3	3	3	1	1
TPPF 4%	47	3	3	3	3	3	3	3	3	3	3	3	3	3	3	3	1	1
NonTPPF 2%	47	3	3	3	3	3	3	3	3	3	3	3	3	3	3	3	1	1
NonTPPF 3%	47	3	3	3	3	3	3	3	3	3	3	3	3	3	3	3	1	1
NonTPPF 4%	47	3	3	3	3	3	3	3	3	3	3	3	3	3	3	3	1	1
TPPP 5%	30	3	3	3	3	3	3	3	3	3	3							
TPPP 10%	30	3	3	3	3	3	3	3	3	3	3							
TPPP 15%	30	3	3	3	3	3	3	3	3	3	3							
NonTPPP 5%	30	3	3	3	3	3	3	3	3	3	3							
NonTPPP 10%	30	3	3	3	3	3	3	3	3	3	3							
NonTPPP 15%	30	3	3	3	3	3	3	3	3	3	3							

A sealed cement paste sample is a sample that has been heated to the peak temperature and then placed inside an airtight container. Sealing the sample in an airtight container prevents it from coming into contact with environmental humidity, thus avoiding any potential reaction with moisture. This sealed condition is maintained 24 hours before conducting a compressive strength test. Sealing the cement paste sample helps preserve its moisture content when it reaches the peak temperature. Preventing the environmental humidity from interacting with the sample ensures that the moisture content remains constant during the 24 hours. This controlled environment allows a more accurate assessment of the cement paste's compressive strength, as any moisture content changes could affect the test results.

On the other hand, an unsealed cement paste sample is also heated to the specified peak temperature, but it is left to cool down inside the furnace for up to 24 hours. In this case, the sample is exposed to the surrounding environmental humidity in the furnace. As a result, the sample's moisture content can change due to the interaction with the ambient moisture. The purpose of using unsealed samples is to assess the influence of environmental humidity on the properties of the cement paste. Exposing the sample to environmental humidity allows for a more realistic evaluation of how the cement paste would behave when it is subject to moisture.

Table 4- 5: Total number of tests of the different mixes of polypropylene

		Polypropylene											
MIX	CONTROL	UV-T PPP			NON-T PPP			UV-T PPF			NON-T PPF		
Ratio of PP	0%	5%	10%	15%	5%	10%	15%	2%	3%	4%	2%	3%	4%
Temperature °C	20		20			20			20			20	
	50		50			50			50			50	
	100		100			100			100			100	
	200		200			200			200			200	
	350		350			350			350			350	
Number of samples													
TTC	2	0	0	0	0	0	0	2	2	2	2	2	2
RCS	30	30	30	30	30	30	30	30	30	30	30	30	30
CS at HT	15	0	0	0	0	0	0	15	15	15	15	15	15
Total number of samples	509												

PPP= Polypropylene powder, PPF= Polypropylene fibre, NON-T= Non treated, UV-T= Ultraviolent treated, TTC= Transient thermal creep, CS= Compressive strength, HT= High temperature, RCS = Residual compressive strength

4.5 Water retention test

The experiment aimed to measure the extent of surface modification resulting from UV treatment. A water retention test was employed as the quantifying method. This method was developed from this research.

Polypropylene samples were measured as 0.15g of PPF and 0.9g of PPP. It was kept in the humidity chamber set at 20°C and 80% RH, as shown in figure 4-4. The mass M_2 (mass of sample + container) was recorded as a function of time; M_1 is the mass of the container. From the experiment, when taking the value of mass M_2, the moisture covered the remaining surface of the container, which had to be taken away from the container. A separate container was used to estimate moisture covered within the container. The container was placed empty in a humidity chamber, and the change in mass was recorded at an interval day equal to the days taken for the sample. The mass was subtracted from the M_2. The final result of $M_{2,}$ when M_1 is subtracted, is the measure of the final mass of the sample.

The result is the lower bound estimate, and it is the minimum that can be expected because assuming that the whole container is covered with moisture, and it absorbed some water.

The variation in mass observed between polypropylene fibre and polypropylene powder stems from their distinct physical forms, with one being in a powdered state and the other in a fibrous form. Consequently, their respective masses inherently differ. When equating the mass of polypropylene powder to that of polypropylene fibre, the ability of the powder to absorb moisture is not significantly enhanced, likely due to the larger quantity of polypropylene powder.

$$M_m = (M_3 - M_1) \quad \textbf{\textit{4- 1}}$$

$$Ms = M_2 – M_m – M_1 \quad \textbf{\textit{4- 2}}$$

Where, M_1 = Mass of container

M_2 = Mass of sample + container

M_3 = Mass of moisture + container

M_m = Mass of moisture

Ms = Actual mass of sample

The actual mass of a sample is given as

$$Ms = M_2 – M_m – M_1 \quad \textbf{\textit{4- 3}}$$

The mass of water retention was given as

$$Mt = \frac{\mathrm{Ms - Mo}}{\mathrm{Mo}} \quad \textbf{\textit{4- 4}}$$

Where Mt is the mass of water retention at a given time

Mo is the initial mass of the sample

The water retention offers a satisfactory compromise between precision and simplicity for the objectives of this study.

Figure 4- 4: Humidity Chamber

4.6 Evaluation of moisture absorption on cement paste sample

Three samples were utilised to assess the variances in moisture absorption by the cement paste under different conditions. The experimental procedure involved subjecting all three samples to a temperature of 200°C in a furnace. Once the peak temperature was reached, the samples were allowed to equilibrate for a duration of 2 hours to ensure temperature homogeneity throughout the specimens, reaching the centre of each sample. The weight of the samples was recorded under hot conditions.

Initially, when the samples were heated, the mass of each sample was recorded before heating and 24 hours after heating to determine the difference in mass between the initial hot condition and the mass after cooling. These differences in mass represent the amount of moisture absorbed by the samples within 24 hours. The recorded values are presented in Table 4-6.

Furthermore, the three samples were then placed in storage containers. The first sample was placed in an airtight container alongside the water in a small container, ensuring a relative humidity (RH) of 90% to 100% was maintained after heating at 200°C. The second sample was kept in an airtight container together with magnesium chloride, with the aim of maintaining the sample at approximately 33% RH. The third sample was placed in an airtight container (specifically, a paint tin) to maintain an environment of approximately 0% RH. All samples were left undisturbed for a duration of 46 days before conducting the compressive strength test. The results obtained in this study provide valuable insights into the relationship between relative humidity and the residual compressive strength of cement paste.

Table 4- 6: Comparison of moisture absorption of the cement paste after heating in a different environment

	Initial mass before heating (g)	Mass after heating (at hot) (g) (a)	Mass after cooling (g) (b)	Differences between the mass (b-a) (g)	Difference in (%)
Airtight container (Paint tin)	197.51	170.16	170.18	0.02	0.02
Airtight container with Magnesium chloride	195.95	170.06	170.65	0.59	0.34
Airtight container 100%RH	196.89	171.04	172.60	1.56	0.91

4.7 Residual compressive strength

After curing samples for 28 days, the samples were placed into the furnace and heated at 1°C/min, starting from room temperature (20 ± 3^{o}C). When the desired temperature (*T*c) reached (50, 100, 200, or 350^{o}C), the samples were kept for 2 hours in the Furnace at *T*c to homogenise the temperature in the specimen to reach the centre of the sample. The samples were then allowed to cool to the ambient temperature inside the furnace. (Schneider, 1988). During the cooling process, the sample's temperature gradually decreases after maintaining the peak temperature for 2 hours, following a rate of 1^{o}C /min heating process. The rate of temperature decrease depends on sample properties, environment, and cooling method. The cooling process involves a gradual temperature decrease from the peak, resulting in a lower temperature over time (Alonso & Fernandez, 2004).

The heating process was done in several steps, summarised in Figure 4-5 for each selected temperature.

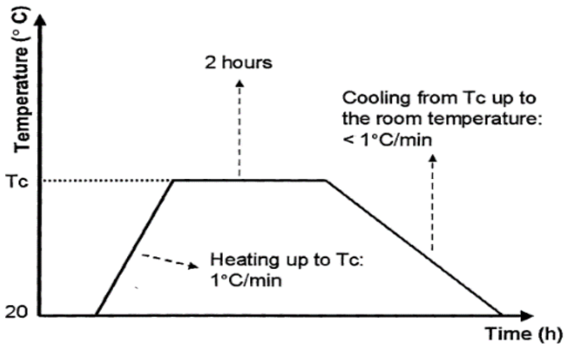

Figure 4- 5: The heating process of cement paste sample for the temperature of (50, 100, 200, and 350)(Alonso & Fernandez, 2004)

After this time, for the sealed samples, the samples were put into an airtight container (paint tin) for slow cooling down to room temperature for 24 hours. The following were used to put the sample into the airtight paint tin. The airtight paint tin is shown in Figure 4-6.

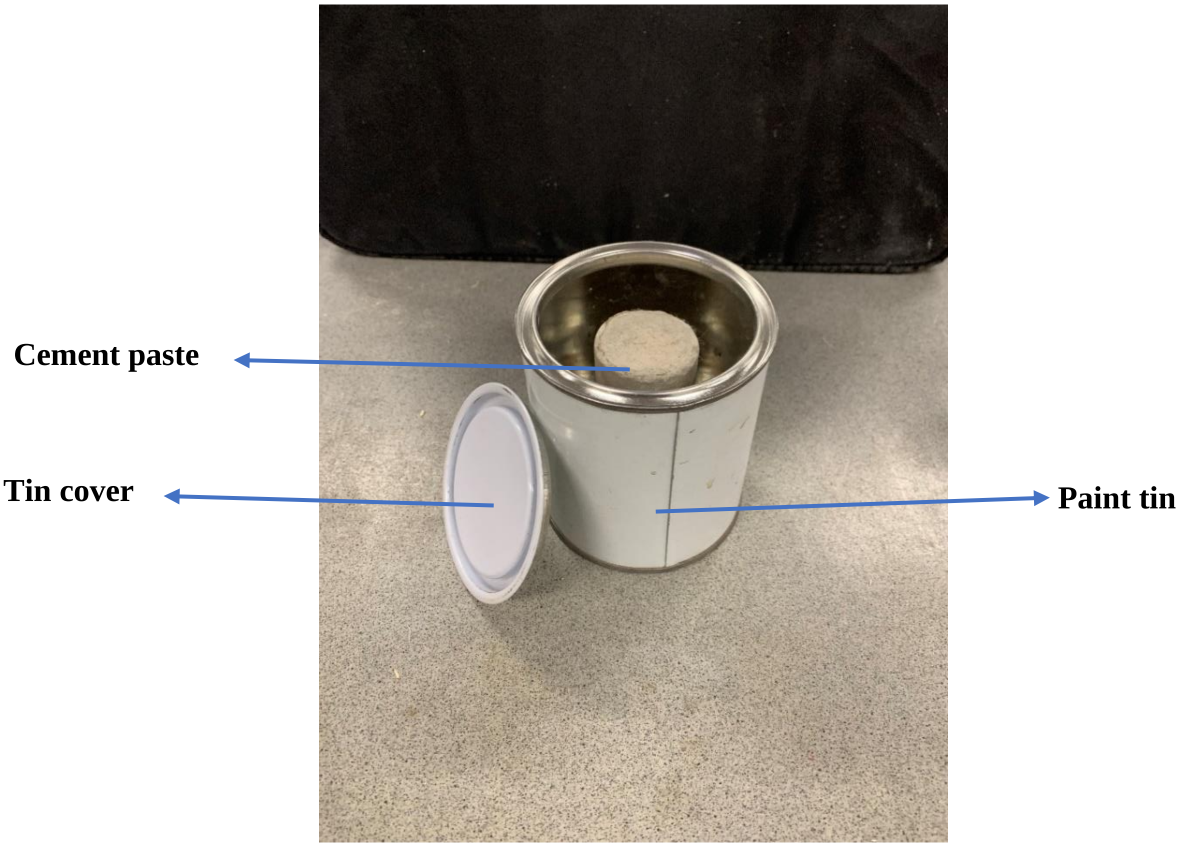

Figure 4- 6: Airtight paint tin container

1) Personal protective equipment (PPE) (Hot resistant hand glove, high-temperature resistance overall, and face visor attached with helmet) was worn to avoid direct contact with the heat.
2) A long tong (scissor) was used to remove the sample from the furnace.
3) The paint tin was placed on the heat mat, and the samples were then put into the paint tin and covered.
3) The sample in the paint tin was then moved to a storage place using the movable table.
4) A sign was placed near the storage place to stop lab users from the contact hot paint tin

The un-sealed samples were maintained in the furnace for slow cooling down to room temperature for 24 hours.

Three samples were tested for each heating temperature Tc for each 0%, 2%, 3%, 4% and 5%, 10%, and 15% for both treated and non-treated polypropylene fibre and polypropylene powder, respectively shown in table 4.4. According to (ASTM C109 2000), the compressive test was conducted with displacement control, and the displacement rate was 0.2 mm/m. on the Instron Machine with 250 kN capacity, shown in Figure 4-7. The compressive strength was computed from the recorded load taken on a computerised data acquisition system.

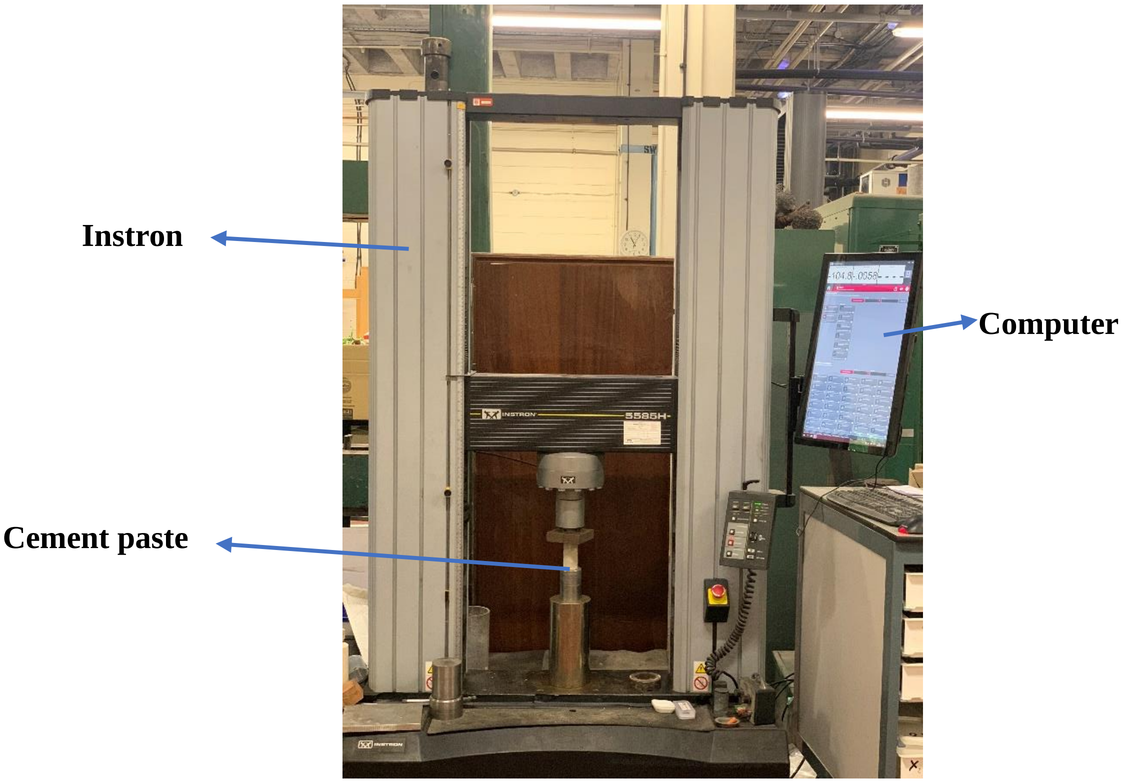

Figure 4- 7: Instron machine and computerised data acquisition system

4.8 Compressive strength at hot temperature

The test was conducted using the Instron universal testing system attached to an electric oven and the furnace close to the Instron machine. After curing samples for 28 days, the samples were placed into the furnace and heated at 1°C /min. When the desired temperature (*T*c) reached (50, 100, 200, or 350°C), the samples were allowed for 2 hours in the furnace at *T*c to homogenise the temperature in the specimen to reach the centre of the sample. The samples were then transferred to the oven and attached to the Instron machine at a temperature equal to the furnace temperature. The reason for heating samples into the furnace and transferring them to the oven is to have time to test 3 samples daily. Using only the oven attached to the Instron machine will allow testing of only 1 sample in a day.

The following steps were used to transfer the sample from the furnace to the oven, which was attached to the Instron.

1) PPE (Hot resistant hand glove, high-temperature resistance overall and face visor attached with helmet) was worn to avoid direct contact with the heat.

2) A long tong (scissor) was used for the removing of sample from the furnace

3) The plates (upper and lower plate) in the Instron machine were set, and the temperature was set in the oven, which is equal to that of the temperature in the furnace. The sample was placed

in the oven and attached to Instron directly after being removed from the furnace using a long tong (scissors) with heat-resistant hand gloves.

The compressive strength was computed from the recorded load taken on a computerised data acquisition system. According to (ASTM C109 2000), the compressive test was conducted with displacement control, and the loading speed was 0.2 mm/m. on the Instron Machine with 250 kN capacity, shown in Figure 4-8.

Three samples were heated and tested one after the other for each heating temperature Tc for each 2%, 3%, and 4% polypropylene fibre.

Figure 4- 8: Instron Machine attached to oven and Furnace

4.9 Microstructure characterisation using Scanning electron microscopic (SEM)

After each mechanical test for ambient temperature and heated cement paste sample for treated and non-treated PPF and PPP, the samples were taken and put in plastic bags for microscopic observation.

Cement paste samples with a size of 5mm taken from the crush cement paste sample were mounted on an aluminium stub with Achesons Silver Dag and dried overnight. The samples were coated with gold using a polaron sputter SEM coating unit. The coated samples were scanned using a Tescan Vega LMU scanning electron microscope, shown in Figure 4-9.

Figure 4- 9: Tescan Vega LMU scanning electron microscope

The images were collected on the testing surface through digital images from Tescan-supplied software. The coated samples were scanned under the SEM, and the magnification was set at 1000x and the scale bar length of (50µm) for the cement paste samples containing both treated and non-treated PP heated at 200^{o}C and 350^{o}C at a compromise image quality. For the samples at ambient temperature, the magnification was set at 100x magnification and the scale bar length of (500µm) on the cement paste sample at 20^{o}C, as it is the set magnification that will allow to see the fibre on the sample.

Different scales were employed for scanning the cement paste samples due to specific considerations. At 20°C, the polypropylene fibres within the samples cannot be adequately focused, hindering the observation of their dispersion within the cement paste when subjected to a scale of 50µm. Therefore, adjustments were necessary to ensure clear visibility of the fibres at this temperature. Conversely, for samples heated at 200°C and 350°C, the holes where the fibres melted were not visible at scales of 500 µm. Hence, the scale had to be adjusted until the microscopic channels within the cement paste samples became visible. Other researchers have successfully used this method to study PP fibres in their experiments, as explained in section 2.7.

4.10 Transient thermal strain test

The experimental method for the transient thermal creep test followed the guidelines provided by (RILEM TC 129-MHT, 1997) recommendations for accidental conditions were used. Cylindrical samples with a diameter of 40mm ±0.2 and a height of 80mm ±0.2 were utilised and cured for 28 days before being stored at a temperature of 20 ±2°C and an RH of 50 ±5%. The samples were at least 355 days old when the test began.

4.10.1 Heating condition

The heating condition utilised was for an accidental condition involving short-term exposure of drying samples to high temperatures. Based on RILEM recommendation, accidental conditions correspond to temperatures reaching 700°C or more, while service conditions rarely exceed 200°C.

4.10.2 Test procedure

The test was conducted using an Instron uniaxial compressive machine attached to an oven, shown in Figure 4-8, and a strain gauge (WK-06-250GB-350) was attached to the sample, as shown in Figure 4-10. The samples were kept at 50% humidity and 20°C temperature for up to 367 days before the commencement of the experiment. Subsequently, each sample was loaded into the uniaxial compressive machine, and the load was applied until the required loading level was reached. The constant load of the test was 20% of the cement paste's reference ‘cold’ compressive strength.

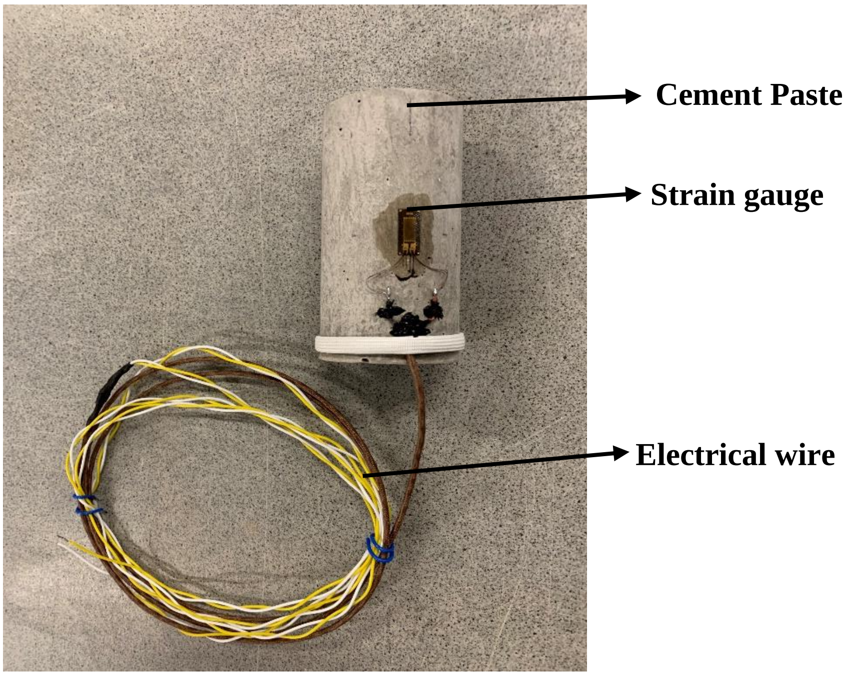

Figure 4- 10: strain gauge (WK-06-250GB-350) attached to the sample

The sample underwent a heating process at an average rate of 1^{o}C per minute. The temperature was gradually increased to reach four specific levels: 50^{o}C, 100^{o}C, 200^{o}C, and 350^{o}C. Each temperature level was maintained constant during heating for 1 hour to stabilise the temperature. Initially, it was planned to allow a maximum of 2 hours for the subsequent experiment, which would give the sample enough time to stabilise at the peak temperature. However, in this experiment, the maximum time allowed was reduced to 1 hour due to the extended testing time required for each sample. This decision was made based on findings from various literature sources (Hager & Pimienta, 2005b; Khoury, Grainger, & Sullivan, 1985), which suggested that 1 hour is sufficient for the sample to reach a stabilised state.

After the last temperature stage, the sample was cooled by turning off the heating device. The plan was to reach up to around 700^{o}C, but the oven's maximum temperature is 350^{o}C. This maximum temperature makes us limit the experiment to the maximum of 350^{o}C.

The elastic strain at ambient temperature was recorded during the specimen loading test. Then, this strain component was measured as 'hot' at the end of every temperature of 50^{o}C, 100^{o}C, 200^{o}C and 350^{o}C temperature stages by performing a quasi-instantaneous unloading-loading cycle as shown in Figure 4-11.

Finally, the free thermal strain was measured by performing a similar heating-cooling cycle on the sample without any applied load. After the experiment, the following curves were plotted: the free thermal strain of the sample (strain during heating and cooling without any loading), the thermal strain under constant load (20% of the cold compressive strength), and the transient thermal creep/strain (the difference between the free thermal strain and the thermal strain under load as defined above).

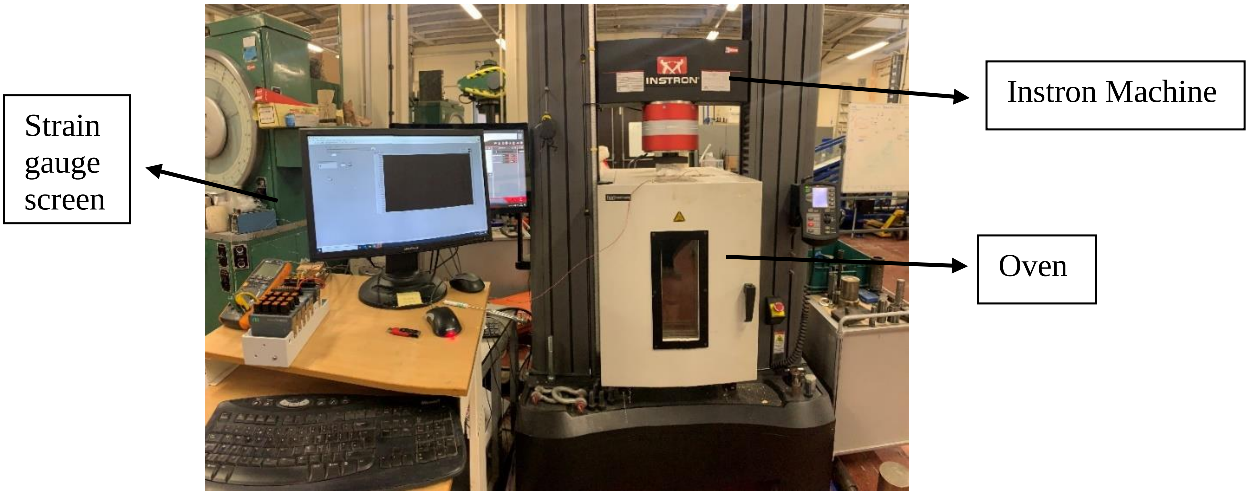

Figure 4- 11: Set of transient thermal strain equipment

4.11 Concluding summary

The methodologies outlined in this chapter play a crucial role in ensuring the reliability and validity of the research findings. By meticulously detailing the experimental program, including materials, procedures, and treatment methods, the study establishes a robust framework for experimentation.

The utilisation of established techniques from literature not only enhances the accuracy of the research but also contributes to cost-effectiveness. Adopting standardised methods for sample preparation, mixing, casting, and curing further ensures consistency and comparability of results.

Moreover, various experimental procedures, such as water retention tests, residual compressive strength analysis, scanning electron microscopy, and transient thermal creep tests, demonstrate a comprehensive approach to investigating the properties of cement paste containing polypropylene fibre and polypropylene powder.

Overall, the careful consideration and implementation of these methodologies underscore the importance of methodological rigour in scientific research, ultimately enhancing the credibility and significance of the study's findings.

Chapter 5: RESULTS AND DISCUSSION

5.1 Introduction

To meet the objectives of this research, the experimental work was carried out as per the methodology in sections (4.5 to 4.9) to test:

5) The effect of humidity on residual compressive strength of cement paste containing polypropylene fibre and powder with and without UV pre-treatment.
6) The compressive strength and stiffness at high temperatures of cement paste containing polypropylene fibres with and without UV pre-treatment.
7) The microstructural characterisation of cement paste containing polypropylene fibre and polypropylene powder with and without UV pre-treatment at high temperatures using SEM.
8) The transient thermal creep of cement paste containing polypropylene fibres with and without UV pre-treatment.

Section 5.2 presents and discusses the results of the experimental work of the water retention test. Likewise, the evaluation of residual compressive strength of unsealed cement paste compared with the literature is discussed in section 5.3. Section 5.4 gives the results and discussion of the residual compressive strength of sealed and unsealed cement paste containing polypropylene fibre (PPF) and polypropylene powder (PPP). Section 5.6 explains the effect of UV treatment on PPF and PPP. Section 5.8 explains the results of the compressive strength of cement paste containing PPF at hot temperatures. In addition, section 5.10 deals with the results of the elastic modulus of cement paste containing PPF. Accordingly, the results of scanning electron microscopic (SEM) were discussed in section 5.11. Free thermal strain and thermal strain under constant load were discussed in section 5.13. Finally, the result of transient thermal creep was discussed in section 5.14.

5.2 Water retention test

Following the literature discussed in section 3.2.6, it has been established that polypropylene (PP) exhibits non-polar characteristics, rendering it unresponsive to water due to its inherent properties. Consequently, due to its non-polar nature, PP demonstrates limited reactivity with cement paste. Surface treatment techniques were employed to modify the non-polarity of PP, enabling it to acquire a polar structure that exhibits enhanced reactivity with both water and cement paste, as explained in section 4.3.

In order to verify the effectiveness of the surface treatment in facilitating interaction between PP and water, a water retention test was conducted. The primary objective of this test was to ascertain whether the treated PP surface could effectively engage with water, consequently promoting a strong bond between PP and cement paste. Detailed information regarding the methodology employed for this test can be found in section 4.5 of this thesis.

Figure 5-1 shows the water retention capacity of the samples evaluated as a function of exposure time. It was observed that a prolonged exposure time of 72 hours significantly increased water retention for both polypropylene fibre (PPF) and polypropylene (PPP). This finding is consistent with the research conducted by (Coopamootoo & Masoero, 2018), providing further support for the notion that extended UV-C exposure leads to enhanced water retention properties in polypropylene.

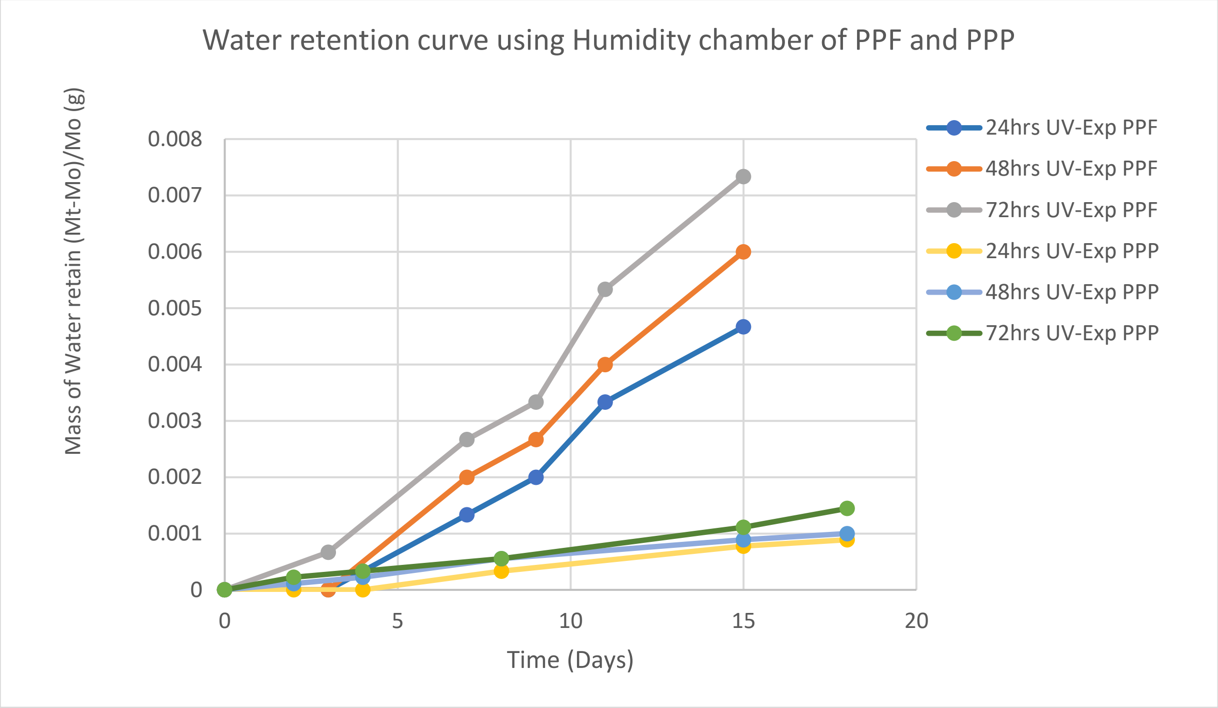

Figure 5- 1: Water retention curves using humidity chamber for PPF and PPP

Visual looking at the samples revealed noticeable surface modifications after exposure to UV-C radiation. The degree of surface modification was more pronounced in the case of PPP, with an exposure time of 72 hours, resulting in a high level of surface modification. Conversely, PPF exhibited a longer threshold for degradation, with exposure times beyond 72 hours leading to degradation.

Certainly! The comparison between PPF and PPP revealed notable differences in their ability to retain water over time. When subjected to water exposure for both 24 hours and 72 hours, PPF demonstrated a substantial 56.6% increase in water retention. In contrast, PPP exhibited a slightly lower increase of 44% in water retention under the same conditions.

This discrepancy suggests that there are distinct variations in how PPF and PPP interact with water within the polypropylene material. Essentially, PPF seems to have a higher capacity for absorbing and retaining water compared to PPP. This could be attributed to differences in their physical structures and surface properties, influencing their ability to bind and hold moisture within the polypropylene matrix.

These observations suggest that the surface modification behaviour differs between PPP and PPF when subjected to prolonged UV-C exposure. The implication of allowing the PPP to achieve a maximum time of more than 72 hours is that it will burn and cannot be used in our experiment, as reported by Coopamootoo & Masoero, (2018)

This result provides crucial information about the effectiveness of the surface treatment technique used to modify the non-polar structure of polypropylene (PP) and enhance its reactivity with water and cement paste. The result refers to the observations and analysis of PP samples' water retention capacity and surface modifications after exposure to UV-C radiation. These observations have important implications for the experiment, as they indicate that the surface modification technique effectively enhances the reactivity of PP with water and cement paste. However, they also highlight the importance of considering the degradation threshold of PP, as prolonged exposure beyond a certain point may make the material unusable for the intended purpose.

5.3 Evaluation of normalised residual compressive strength of unsealed cement paste samples

This section establishes a correlation between residual compressive strength (RCS) findings in cement paste between the experimental result and the literature. The choice to focus on unsealed cement paste stems from its significant presence in the existing literature. However, it is worth noting that certain results reported in the literature contradict some of the main research findings regarding the RCS of unsealed cement paste.

To address these differences, a comprehensive comparison was conducted between this research results and the findings of selected literature sources. This comparison aims to identify the factors or variables contributing to the observed differences. By analysing the contrasting results, the aim is to understand the underlying mechanisms influencing the RCS of unsealed cement paste.

By considering a range of literature, various experimental approaches, and methodologies, this finding comprehensively evaluates the factors influencing RCS in unsealed cement paste. This analysis will advance knowledge in this field and provide valuable insights for future research and practical applications.

Figure 5-2 illustrates the evaluation of the normalised residual compressive strength of unsealed cement paste samples, comparing them with experimental results obtained in the research of Komonen & Penttala, (2003) for cement paste with no polypropylene addition.

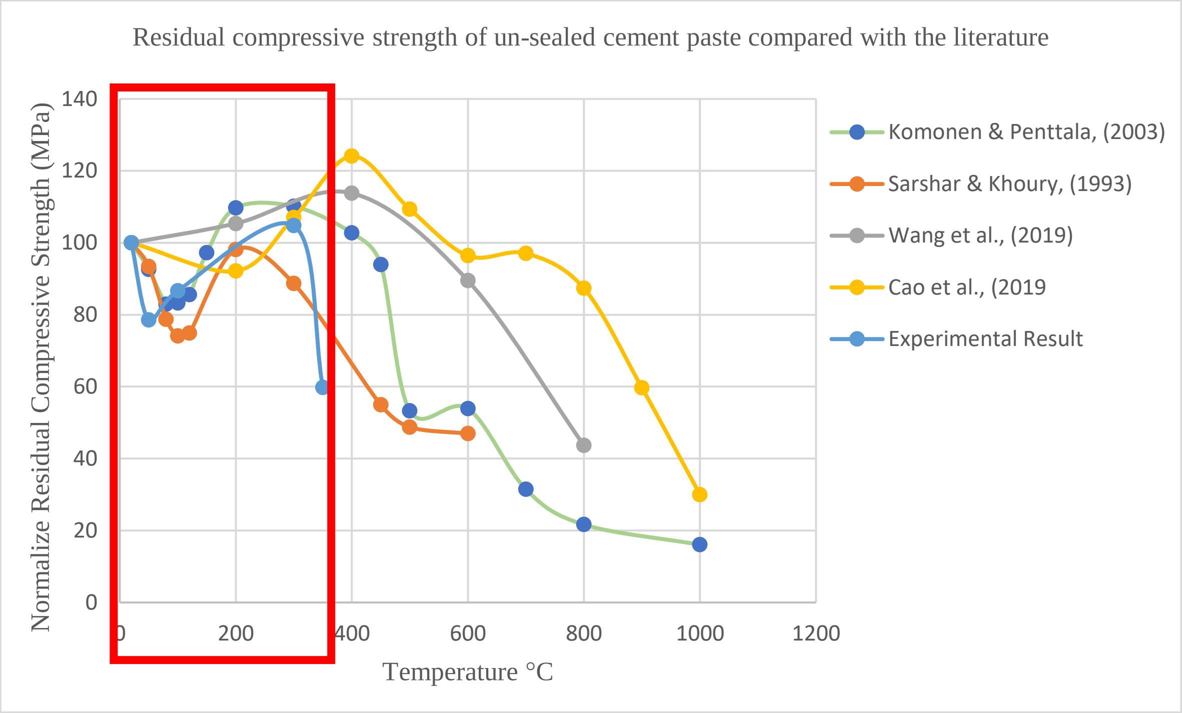

Figure 5- 2: Residual compressive strength of un-sealed cement paste compared with literature

The findings of this study demonstrate consistent trends with previous research conducted at temperatures of 100°C and 200°C. Specifically, the results align closely with the outcomes reported by Sarshar & Khoury, (1993) at 350°C, indicating a strong correlation between our experimental findings and the existing literature. The highlighted area in the graph is the main consideration portion where all the comparison is considered between 20°C to 350°C.

However, the experimental results from this study reveal a significant variation in the residual compressive strength of cement pastes between temperatures of 200°C and 350°C, excluding the results obtained by Sarshar & Khoury, (1993). The values of residual compressive strength observed in this experiment are lower than those reported in the literature. The discrepancy in residual compressive strength at 350°C can be attributed to the differing exposure times of the samples. While this experiment involved a 2-hour exposure period, the literature results were obtained after only 1 hour of exposure. Prolonged exposure beyond 1 hour substantially impacts the residual compressive strength, resulting in a notable decline in bulk strength within the initial 2-hour duration. This decline in strength is associated with the development of porosity, contributing to the overall reduction in strength (Naus, 2005).

Contrary to the prevailing literature on the behaviour of cement paste at high temperatures, the findings from Cao et al., (2019); Wang et al., (2019) indicate an increase in residual compressive strength at 400°C compared to the reference. According to the literature, the decomposition of calcium-silicate-hydrate (C-S-H) initiates between 200°C and 300°C, as confirmed by Alarcon-Ruiz et al., (2005); Khoury, (1992b). The unexpected increase in strength at 400°C is attributed to the low calcium-silica ratio (C/S) and reduced calcium hydroxide content of the cement. These factors, calcium-silica ratio (C/S) and reduced calcium hydroxide contribute to improved strength under hydrothermal conditions above 300°C, as verified by Kunther et al., (2017).

5.4 Residual compressive strength of cement paste containing PPF and PPP

This section presents the comprehensive analysis of the residual compressive strength (RCS) results obtained from cement paste samples containing polypropylene fibre (PPF) and polypropylene powder (PPP). The study investigates the effect of humidity on the RCS of cement paste samples containing UV-treated and non-UV-treated PPF and PPP, both in sealed and unsealed conditions.

The application of PPF and PPP in cementitious materials has garnered significant attention due to their potential to enhance various properties, which are highlighted in section 4.2.3. The analysis of RCS offers invaluable insights into the performance of these additives and their influence on the overall strength characteristics of cement paste.

An essential focus of this study delves into how PPF and PPP affect the RCS of cement paste. By examining RCS values, it becomes feasible to determine the degree to which these additives contribute to the compressive strength of the cement paste. Furthermore, the examination extends to the impact of surface treatment on PPF and PPP samples, aiming to evaluate how treating these additives influences RCS.

To understand the results, various comparisons were conducted. These comparisons evaluate the positive or negative effects of incorporating PPF and PPP into the cement paste matrix. Analysing the data makes identifying trends, patterns, and differences between different sample compositions and conditions possible.

Figure 5-3 below outlines the logical progression of the result analysis, presenting a structured overview of the key findings and their interrelationships. This flow chart serves as a visual guide, enabling a clear understanding of the analysis process and the organisation of the subsequent sections.

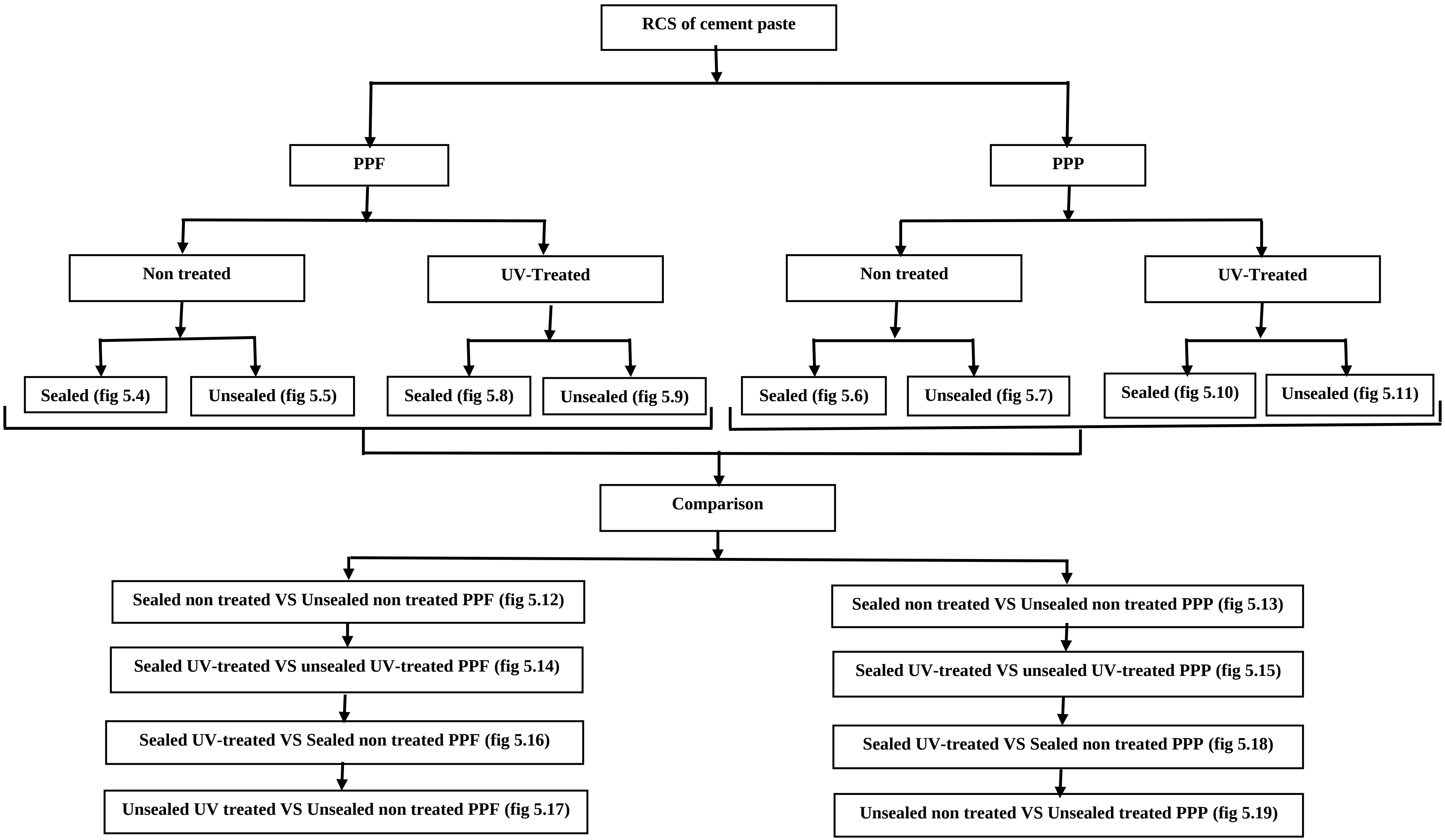

Figure 5- 3: Showing the category of polypropylene fibre and powder used for residual compressive strength of cement paste

5.4.1 Evaluation of moisture absorption on cement paste samples on residual compressive strength

A comparative analysis was conducted to evaluate the moisture absorption characteristics of cement paste samples in different environments. Analysing the data presented in Figure 5-4, it is evident that the sample exposed to around 100% relative humidity absorbed the highest amount of moisture compared to the samples covered with magnesium chloride and the airtight container alone, which exhibited negligible moisture absorption. Furthermore, the figure illustrates that the residual compressive strength at 100% relative humidity experienced a significant decrease of 33% compared to the 0% relative humidity condition and a 27% decrease compared to the 33% relative humidity condition. This finding indicates that the moisture absorbed into the gel pores of the cement paste contributes to a reduction in the residual compressive strength (Kirchhof et al., 2020)

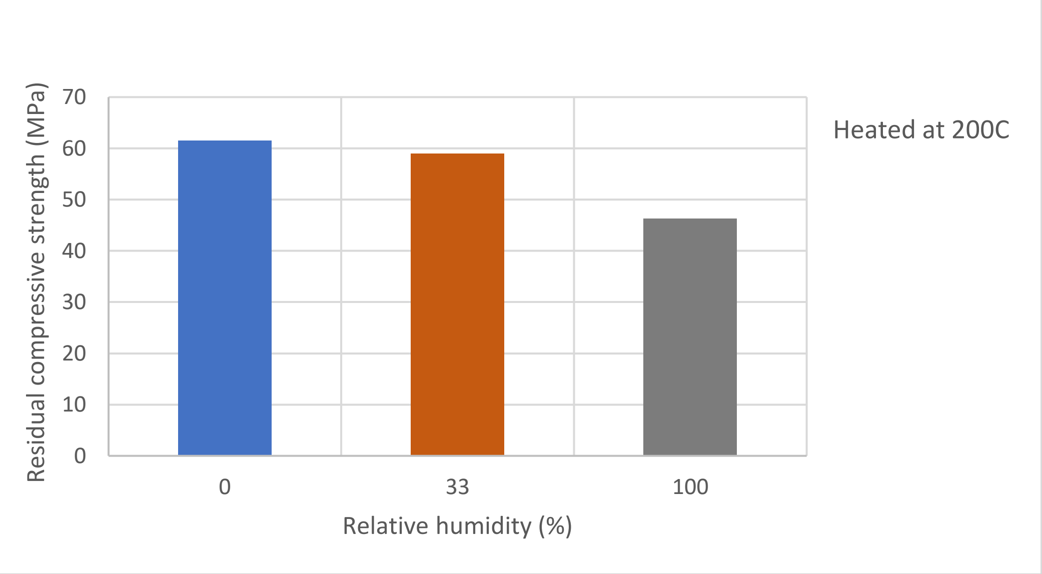

Figure 5- 4: Comparison of residual compressive strength of cement pastes under different relative humidity

The humidity level plays a crucial role in influencing the residual compressive strength of cement paste due to the chemical changes induced in the microstructure. Existing literature suggests that moisture absorption into the gel pores leads to a transverse bursting effect within the solid matrix of the cement paste. This effect becomes more pronounced with increasing external compressive load. Consequently, the compressive strength behaviour is significantly affected by the moisture content present in the cement paste. Studies conducted by Chen et al., (2012a); Glucklich & Korin, (1975); Kirchhof et al., (2020) have reported decreased compressive strength of concrete with higher moisture content.

The impact of humidity on cement paste's residual compressive strength (RCS) has been studied in the literature. However, this experimental finding revealed a relatively small difference in RCS between sealed and unsealed cement paste samples. The small differences can be attributed to the storage conditions of the samples, which were kept in a furnace at a relative humidity (RH) of 33% for 24 hours before the compressive test. It should be noted that this humidity level is considerably lower than the ambient humidity, which ranges from 90% to 100%.

This section explores the literature on the influence of humidity on RCS and establishes a link to the experimental findings of this study. The experimental data of this research suggest that minimising moisture absorption from the samples contributes to a lesser reduction in RCS.

By integrating relevant literature and presenting experimental evidence, this study enhances our understanding of the relationship between humidity and the residual compressive strength of cement paste.

In practical terms, designers must account for the effect of humidity on heated structures, particularly in relation to the residual compressive strength (RCS) of cement paste. Research indicates that humidity influences the microstructure of cement paste, with moisture absorption leading to a transverse bursting effect within the solid matrix, particularly under external compressive loads. This effect is well-documented in existing literature, with studies showing a decrease in compressive strength with higher moisture content.

Overall, designers should recognize relative humidity as a critical factor in assessing the residual compressive strength of cement paste. Failure to account for moisture-induced stress and chemical changes could compromise the structural integrity of concrete elements in heated environments. Thus, proactive measures to manage humidity levels are essential in ensuring the durability and stability of heated structures over time.

To mitigate the impact of humidity on RCS, designers should consider strategies to minimize moisture absorption. This may include controlling storage conditions and exposure to ambient humidity levels. Additionally, integrating relevant literature and experimental evidence can enhance understanding of the relationship between humidity and RCS.

5.4.2 Residual compressive strength of sealed and unsealed cement paste containing non-UV-treated PPF

Figure 5-5 and Figure 5-6 present the results of the residual compressive strength analysis of cement paste samples containing non-UV-treated polypropylene fibre (PPF). The samples were divided into sealed and unsealed categories, as explained in section 4.4.2. The findings indicate that adding PPF at concentrations of 2%, 3%, and 4% decreased strength compared to the original paste at ambient temperature. The strength reductions were observed to be 3%, 10%, and 16%, respectively. Previous studies conducted by Komonen & Penttala, (2003); Manolis et al., (1997) have noted that this decrease in strength can be attributed to the hydrophobic nature of polypropylene, which leads to poor bonding between the PPF and the cement paste.

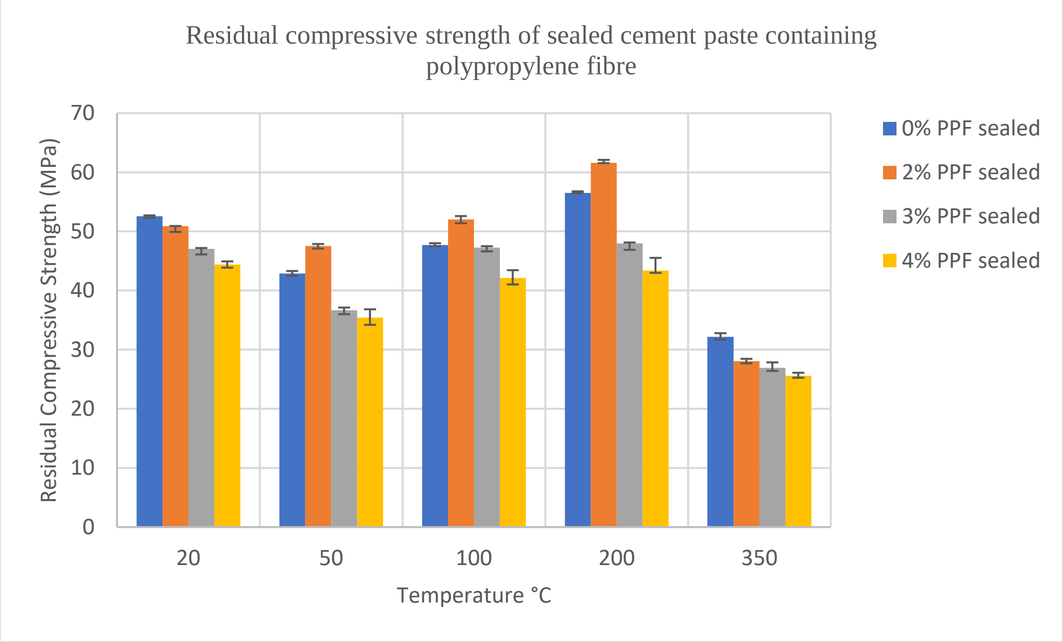

Figure 5- 5: Residual compressive strength of sealed cement paste sample containing non-UV treated PPF

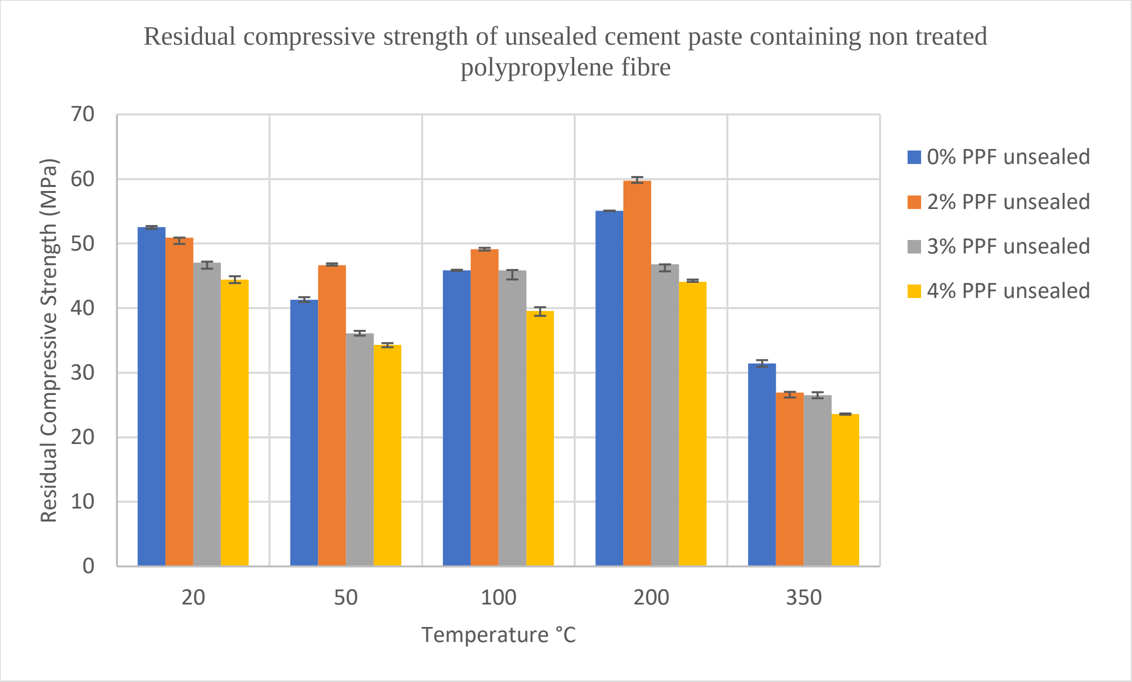

Figure 5- 6: Residual compressive strength of un-sealed cement paste sample containing non-UV treated PPF

Furthermore, it was observed that both the sealed and unsealed samples exhibited a decrease in residual compressive strength when exposed to a temperature of 50°C. The reduction in strength compared to the control sample was approximately 7%, 28%, and 25% for the sealed samples and 9%, 30%, and 29% for the unsealed samples corresponding to PPF addition of 2%, 3%, and 4% respectively compared to the control sample. This decrease in strength can be attributed to the loss of water from the capillary pores of the cement paste, as reported by Sarshar, (1989).

On the other hand, an increase in residual compressive strength was observed when the samples were subjected to temperatures ranging from 100°C to 200°C. At 200°C, the sealed samples with a 2% PPF addition exhibited a 14% increase in strength compared to the original paste at 20°C, while the unsealed samples demonstrated a 12% increase. This increase in strength can be associated with the rapid formation of calcium silicate hydride (C-S-H) and the loss of non-chemically bound evaporable moisture, as confirmed by Sarshar & Khoury, (1993).

However, it was found that the samples containing 3% and 4% PPF regained their initial strength at 200°C. This increase is attributed to melting PPF and forming new channels to release the thermally induced pressure within the sample. The transformation of solid fibres into a liquid state led to the generation of thermally induced pressures within the sample. This phenomenon occurs due to the expansion of the melted polypropylene, which occupies a larger volume compared to its solid state. As the material transitions from a solid to a liquid, it undergoes a phase change that involves an increase in volume and, therefore, avoids excessive loss of compressive strength, as suggested by Xiao & Falkner, (2006).

The decrease in strength was observed on non-UV-treated PPF samples, both under sealed and unsealed conditions, when the temperature exceeded 200°C, resulting in a strength decline of 47%. This decrease in strength was attributed to the formation of pores within the cement paste at 350°C, caused by the melting of PPF. Additionally, the decomposition of calcium silicate hydride (C-S-H) occurred within the temperature range of 200°C to 300°C, further contributing to the decline in strength (Khoury, 1992b).

5.4.3 Residual compressive strength of sealed and unsealed cement paste containing non-UV-treated PPP

Based on the results presented in Figures 5-7 and 5-8, a decrease in strength was observed in samples containing additions of polypropylene (PPP) at concentrations of 5%, 10%, and 15%. The decrease in strength was approximately 7%, 7.8%, and 8%, respectively, for both sealed and unsealed samples. The reduction in strength is similar to the one mentioned in section 5.4.2.

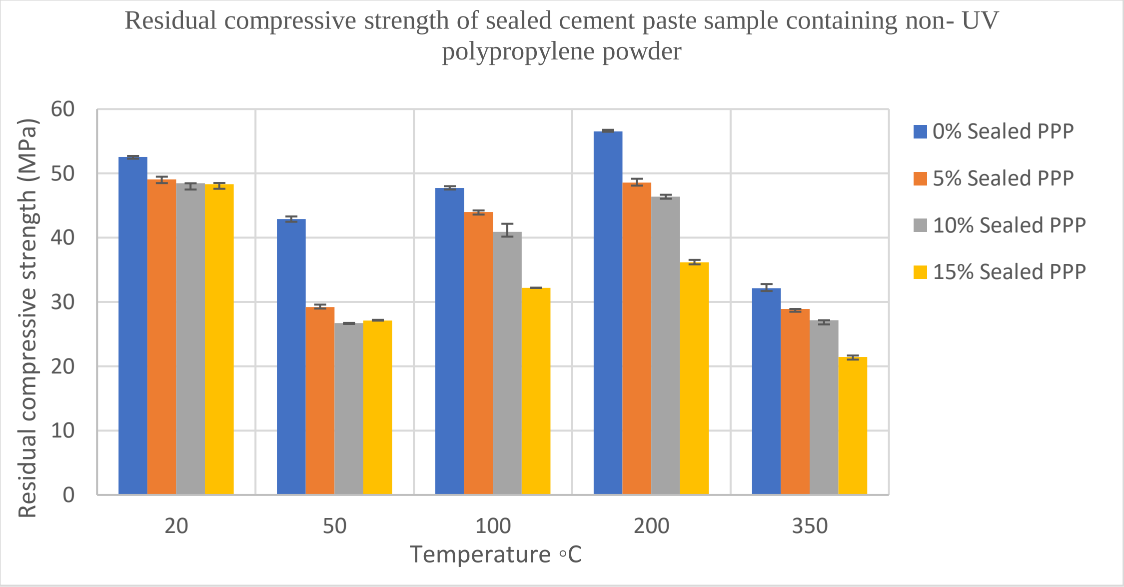

Figure 5- 7: Residual compressive strength of sealed cement paste sample containing non-UV treated PPP

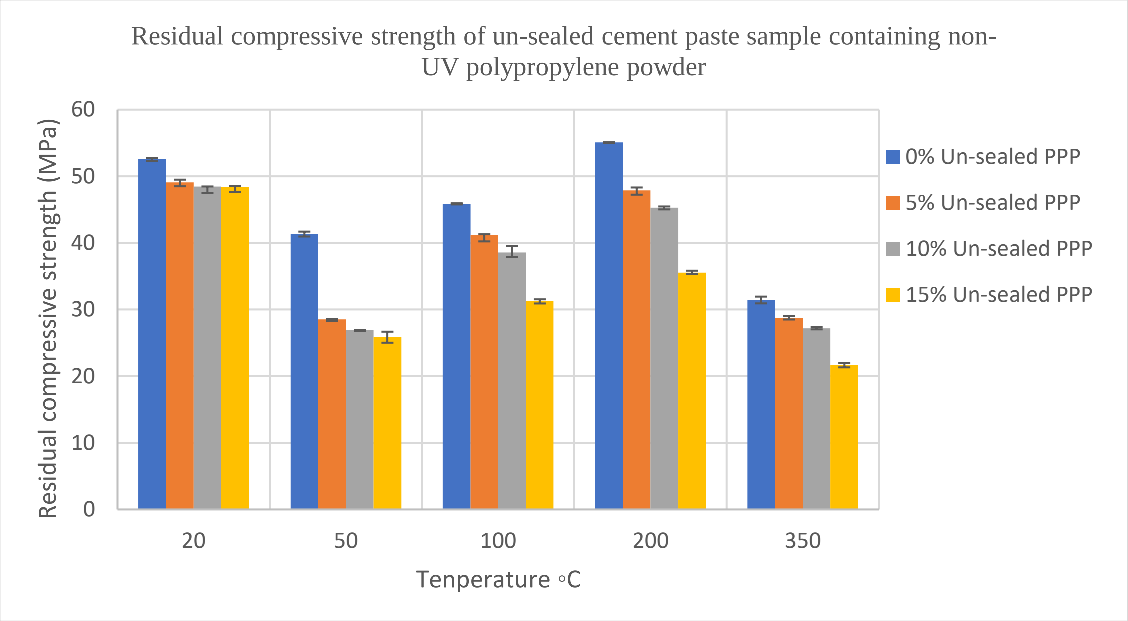

Figure 5- 8: Residual compressive strength of un-sealed cement paste sample containing non-UV treated PPP

The results showed that both sealed and unsealed samples experienced a reduction in strength when exposed to a temperature of 50°C. This decrease in strength was observed in the samples containing polypropylene powder (PPP) at various percentages. Adding 5%, 10%, and 15% PPP for the sealed samples resulted in an approximate reduction in strength of 40%, 55%, and 44%, respectively, compared to the control sample. Similarly, the unsealed samples with corresponding PPP concentrations decreased strength by approximately 41%, 44%, and 46%.

This decline in strength can be attributed to two factors. Firstly, the loss of water from the cement paste's capillary pores contributed to the strength reduction. Secondly, the presence of polypropylene in powder form resulted in a higher replacement of the binder in the matrix, leading to a decrease in overall strength.

At a temperature of 200°C, the strength of the samples was observed beyond that seen at 50^{o}C and 100^{o}C. However, even with the increase, the strength of the samples containing 5%, 10%, and 15% PPP remained lower than the strength observed at 20°C.

More specifically, the sealed samples exhibited reductions in strength of 1%, 4%, and 25%, respectively, for the addition of the corresponding percentages of PPP. In comparison, the unsealed samples showed even greater reductions in strength, with values of 2%, 7%, and 27% for the respective PPP percentage additions. Among all the samples, those containing 15% PPP displayed the most significant decrease in strength.

This decrease in strength can be attributed to the proportion of PPP present in the cement matrix, as it contributes to the formation of a higher number of pores within the cement paste. The presence of these pores weakens the overall structure and reduces the strength of the material.

On the other hand, the notable increase in strength observed at 200°C can be attributed to two factors. Firstly, the rapid formation of calcium-silicate-hydrate (C-S-H) improves strength. Secondly, there is a loss of non-chemically bound evaporable moisture, further enhancing the samples' strength.

When the temperature increased from 200°C to 350°C, a decline in strength was observed under both sealed and unsealed conditions. The decline in strength was approximately 41%, 44% and 55% for the sealed and unsealed conditions, respectively. This significant decline can be attributed to the formation of pores in the cement paste due to the melting of PPP, which creates additional pores within the samples. Additionally, the decomposition of calcium silicate hydrate (C-S-H) is known to occur within the temperature range of 200°C to 300°C, contributing to the observed decline in strength.

5.4.4 Residual compressive strength of sealed and unsealed cement paste containing UV-treated Polypropylene fibre

The treatment of polypropylene fibres (TPPF) with UV irradiation significantly improves the compressive strength of cement paste at ambient temperature. Adding 2%, 3%, and 4% TPPF leads to a respective increase in compressive strength by 31%, 20%, and 11%, as depicted in Figure 5-9. The trend observed in the results of the unsealed samples, as shown in Figure 5-10, is like that of the sealed samples, having the percentage increment of 24%, 16% and 10% for the 2%, 3% and 4% TPPF addition. This enhancement can be attributed to altering polypropylene (PP) surface chemistry through UV irradiation techniques, transforming its hydrophobic nature into hydrophilic. This transformation facilitates improved bonding between PP and cement paste. The treatment of PP is explained in section 4.3.

Upon heating the samples to 200°C, control samples and those containing TPPF exhibit increased residual compressive strength. Notably, the sample containing TPPF at 2%, 3%, and 4% shows strength improvements of 12%, 17%, and 12% under sealed environmental conditions while 5%, 8% and 1% under unsealed conditions. This strength increase can be associated with the relief of pressure caused by drying, resulting in higher van der Waals forces and a closer arrangement of capillary pores (Irshidat et al., 2020). However, heating beyond

200°C decreases strength due to the decomposition of C-S-H and the possible formation of additional pores caused by the molten PP within the cement paste.

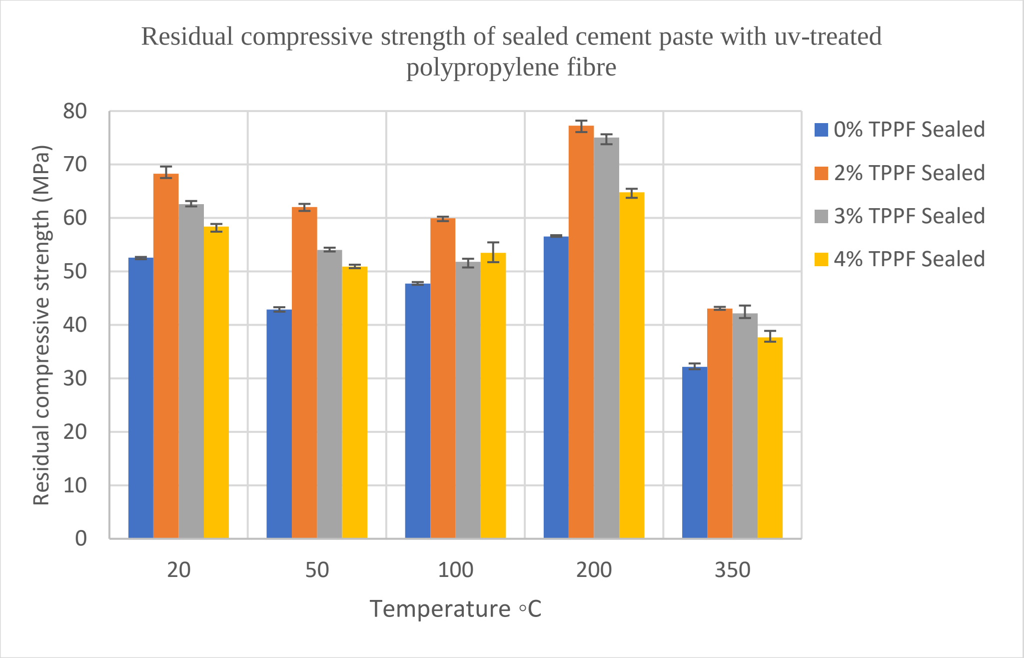

Figure 5- 9: Residual compressive strength of sealed cement paste sample containing UV-treated polypropylene fibre

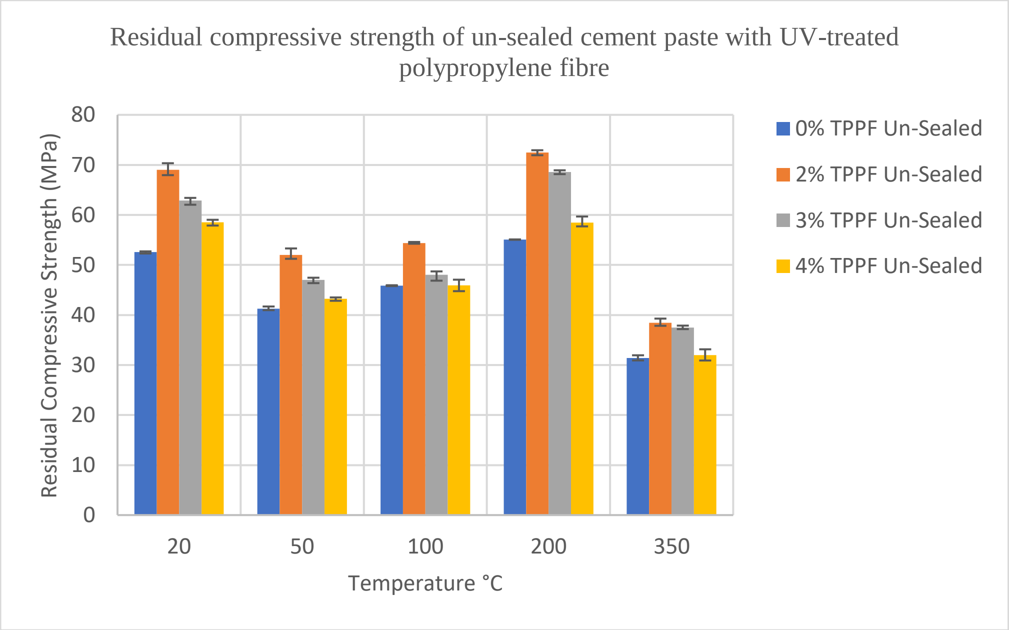

Figure 5- 10: Residual compressive strength of unsealed cement paste sample containing UV-treated polypropylene fibre

5.4.5 Residual compressive strength of sealed and unsealed cement paste containing UV-treated polypropylene powder

Figure 5-11 illustrates the residual compressive strength of cement paste containing UV-treated polypropylene powder (TPPP). The results indicate a significant difference with adding 5%

TPPP, increasing the strength by 10% compared to the original paste without PP. However, insignificant differences are observed with 10% and 15% TPPP additions, as the strength of the TPPP returns to a level comparable to the paste without PP.

The limited effectiveness of the 10% and 15% treated PPP can primarily be attributed to the higher proportion of PPP in the cement paste compared to the 5% treated PPP addition. Additionally, the substantial percentage occupied by PPP in the cement paste matrix further diminishes their impact. This suggests that the higher quantity of treated PPP may not significantly enhance the desired strength of the cement paste,

. However, the trend observed in the results of the unsealed samples, as shown in Figure 5-12, was similar to that of the sealed samples, also having additional enhancement in strength.

In cases where TPPP is absent, the strength of the samples with non-TPPP consistently remains lower than that of the original paste across all percentage additions. This observation is in line with a similar trend identified by Coopamootoo & Masoero, (2018)

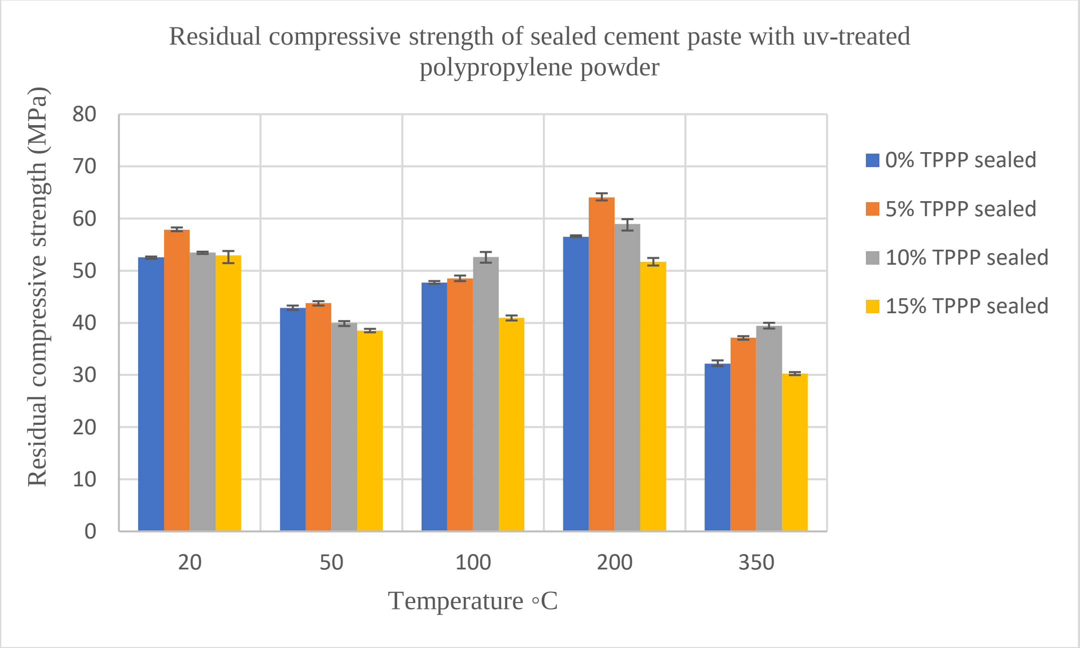

Figure 5- 11: Residual compressive strength of sealed cement paste sample containing UV-treated PPP

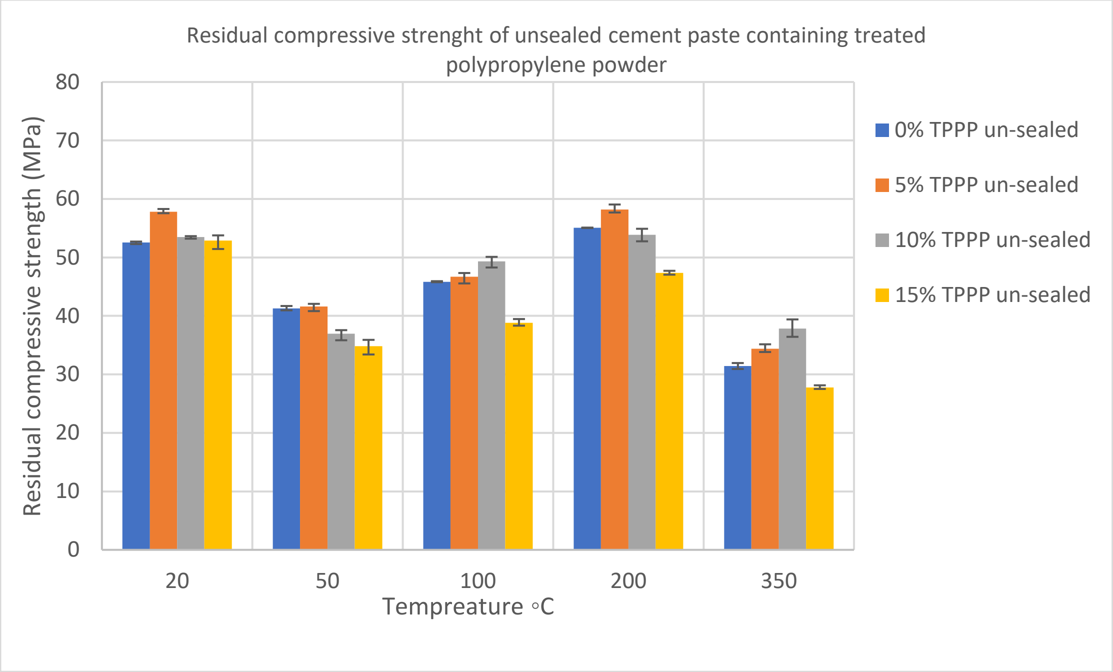

Figure 5- 12: Residual compressive strength of unsealed cement paste sample containing UV-treated PPP

This enhancement in strength for both sealed and unsealed cement paste samples containing TPPP can be attributed to the surface chemistry treatment of PP using UV irradiation techniques, which transform the hydrophobic nature of PP into a hydrophilic one, as explained in section 4.3. This transformation facilitates improved bonding between PP and the cement paste.

Furthermore, when the samples were heated up to 200°C, the control samples and those containing TPPP exhibited increased residual compressive strength in sealed and unsealed environments. Compared to the original paste at 20°C, the strength increase was 8% for 0% TPPP, 11% for adding 5% TPPP and 2% for adding 10% TPPP under sealed conditions. This increase in strength is similar to what was explained earlier in section 5.4.4.

5.4.6 Comparison between the sealed and un-sealed cement paste samples on residual compressive strength of non-UV treated PPF and PPP

The influence of humidity on the residual compressive strength is depicted in Figure 5-13 for samples containing polypropylene fibres (PPF) and Figure 5-14 for samples with polypropylene powder (PPP). When subjected to a temperature of 200°C, a significant difference in residual compressive strength UV-treated and non-UV-treated is observed for both PPF and PPP samples. The difference in residual compressive strength ranges from 3% to 5% for PPF samples with 0%, 2%, 3%, and 4% polypropylene fibre content, respectively, in the sealed condition for PPF. Conversely, for PPP samples, the residual compressive strength is insignificant at 200°C. Specifically, the different in residual compressive strength for sealed samples is measured at 3%, 1%, 2%, and 2% for PPP samples with 0%, 5%, 10%, and 15% PPP addition, respectively, compared to un-sealed samples.

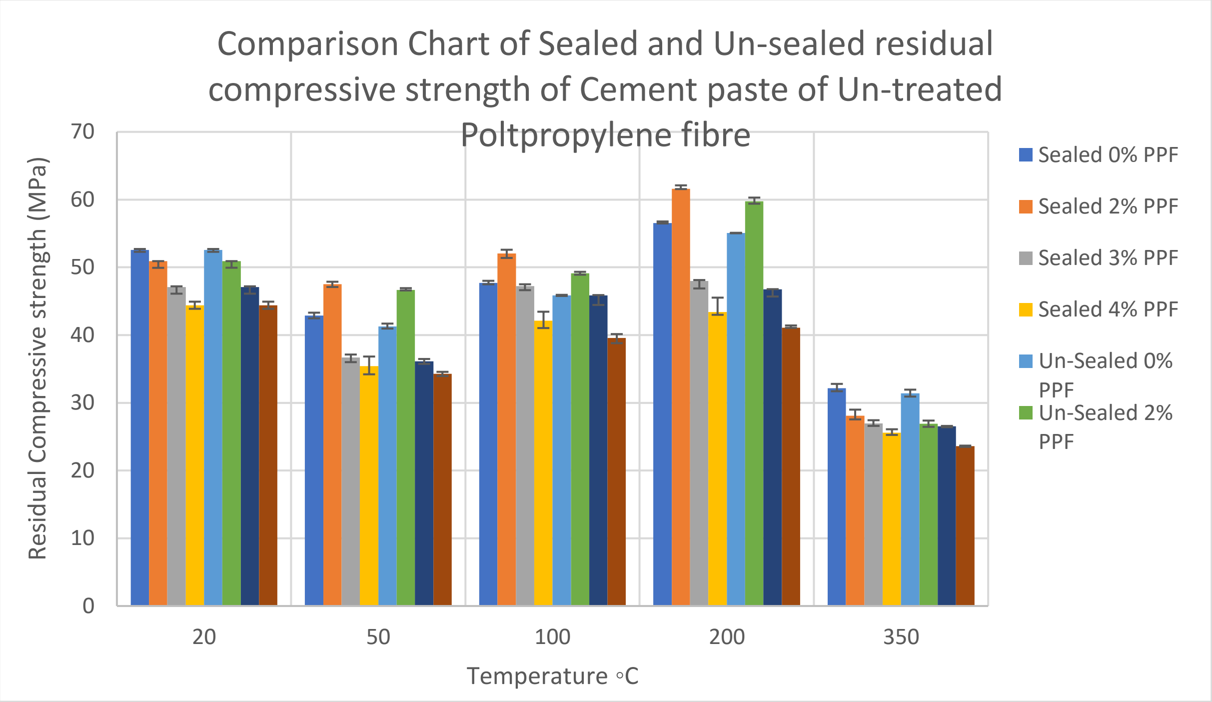

Figure 5- 13: Comparison of sealed and un-sealed residual compressive strength of cement paste containing non-UV treated PPF

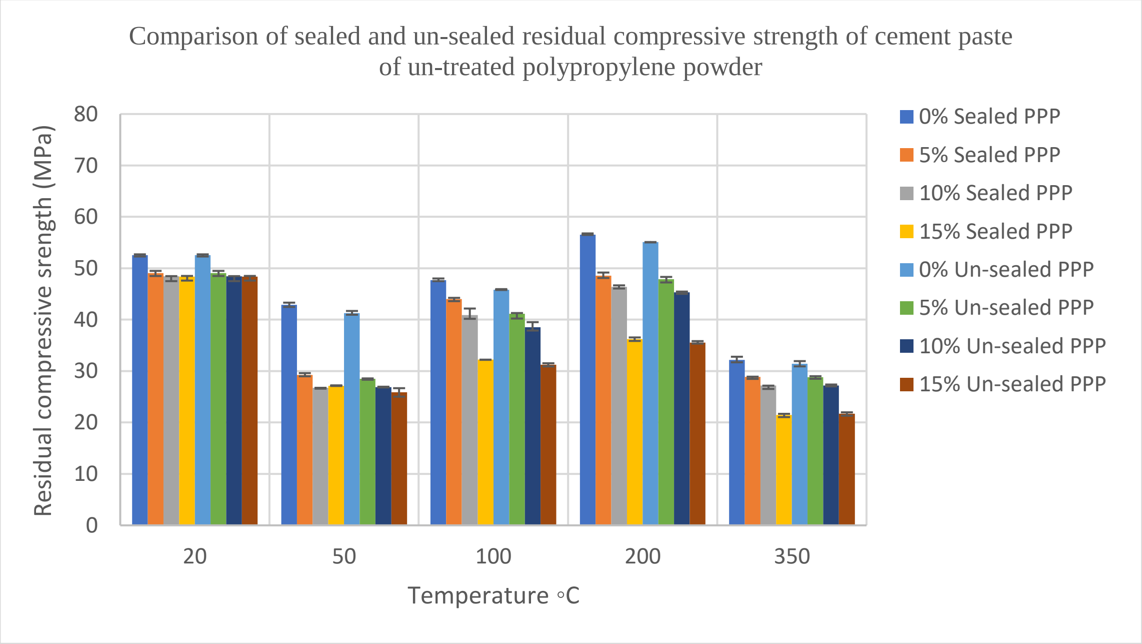

Figure 5- 14: Comparison of sealed and un-sealed residual compressive strength of cement paste containing non-UV treated PPP

Comparing the sealed PPF samples with their unsealed counterparts, the variation in residual compressive strength is found to be insignificant. This observation also holds true for PPP samples. These slight changes in residual compressive strength between the sealed and unsealed cement paste sample of both PPF and PPP are attributed to the unsealed samples being allowed to cool in the furnace until reaching ambient temperature, characterised by a lower relative humidity of approximately 33%, as opposed to the samples cooled in an open environment with relative humidity ranging from 80% to 85% as explained in section 5.4.1.

These findings align with the results reported by (Kirchhof et al., 2020), who observed a decrease in residual compressive strength with increased humidity levels.

5.4.7 Comparison between the sealed and un-sealed cement paste samples on residual compressive strength of UV-treated PPF and PPP

The impact of humidity on the residual compressive strength of cement paste incorporating TPPF and TPPP is illustrated in Figures 5-15 and 5-16, respectively. Both sealed and unsealed samples of TPPF and TPPP exhibit strength enhancement in sealed conditions at various temperatures. Notably, at 200°C, the most critical temperature point, a significant increase in strength is observed, followed by a notable decrease beyond that temperature. Specifically, at 200°C, the addition of 0%, 2%, 3%, and 4% TPPF to sealed samples resulted in strength increases of 2.6%, 6%, 9%, and 10%, respectively, in residual compressive strength. Similarly, sealed TPPP samples demonstrated strengthened characteristics, with increases of approximately 2.6%, 9%, 8.6%, and 8% for the respective additions of 0%, 5%, 10%, and 15% TPPP in the cement paste samples. The discrepancies in residual compressive strength variations observed between sealed and unsealed TPPF and TPPP samples, in comparison to untreated samples, are explained in Section 5.4.6.

The increase in strength from the sealed samples is attributed to the conditioning of the samples, which were allowed to cool in a furnace to reach ambient temperature; additionally, another reason is explained in section 5.4.3.

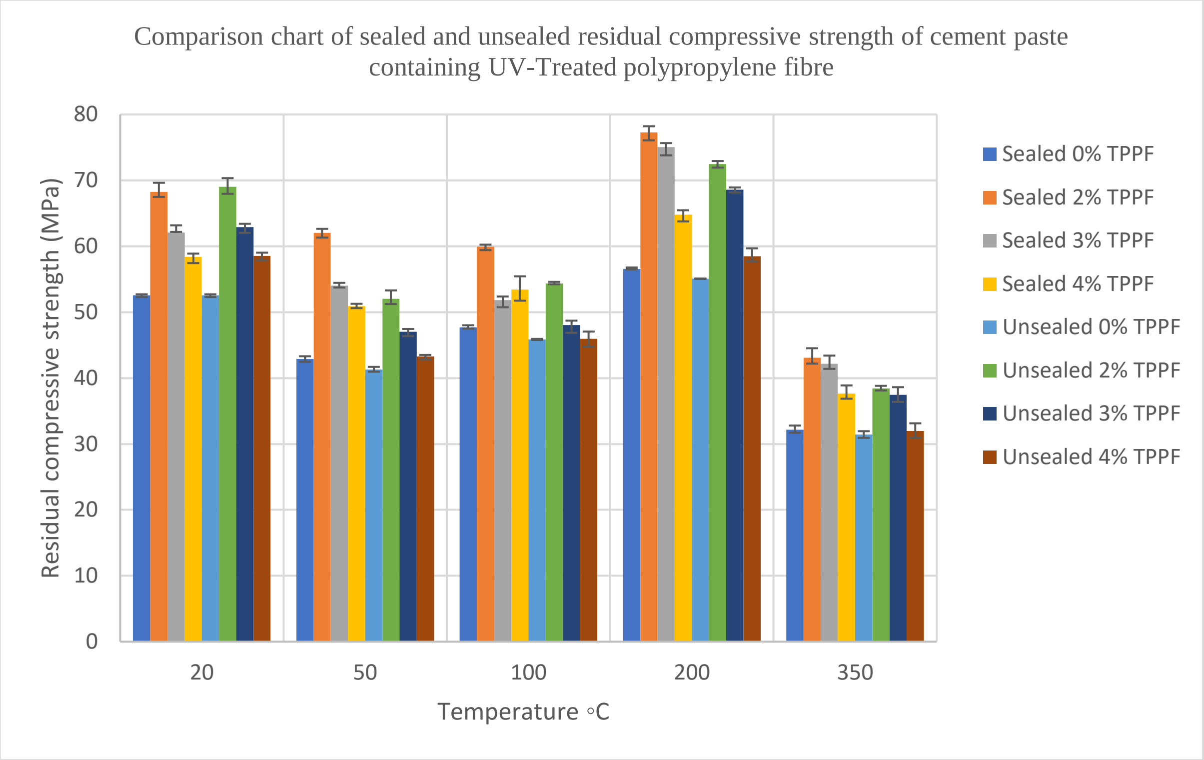

Figure 5- 15: Comparison of sealed and unsealed residual compressive strength of cement paste containing UV-treated PPF

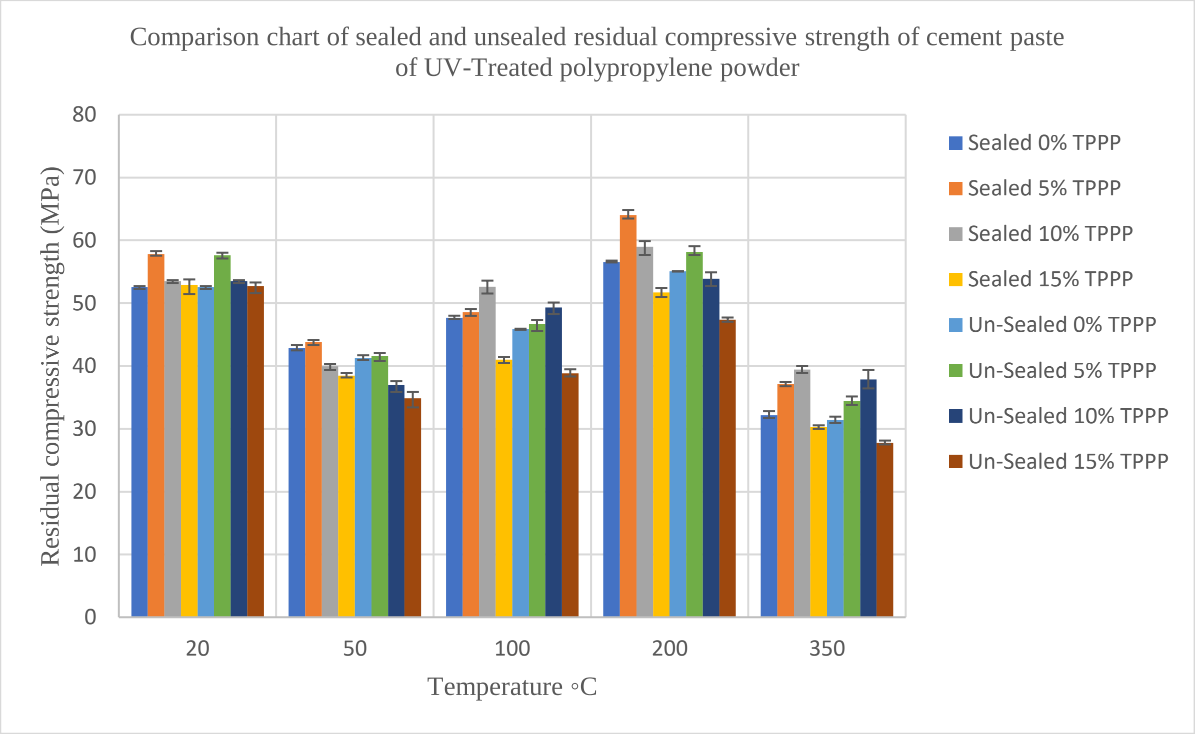

Figure 5- 16: Comparison of sealed and unsealed residual compressive strength of cement paste containing UV-treated PPP

This experimental result shows little effect between the sealed and unsealed sample in the residual compressive strength of cement paste for both with and without polypropylene.

The findings of this study have important implications for the field of cement paste research, particularly in the context of enhancing residual compressive strength. The investigation revealed that sealing the cement paste samples resulted in higher residual compressive strength than the unsealed samples, regardless of the temperature. This suggests that the sealing process contributed to an increase in strength.

5.4.8 Comparison between Polypropylene fibre and polypropylene powder

In this study, we evaluated the residual compressive strength (RCS) of cement paste containing two distinct additives: polypropylene fibres (PPF) and polypropylene powder (PPP). PPF and PPP were subjected to UV treatment and untreated conditions to explore their impact on RCS. Moreover, we examined the influence of sealed samples on RCS for both PPF and PPP under both UV-treated and untreated conditions. This result has been explained in section 5.4.

Our results revealed a noteworthy discrepancy in RCS between cement paste incorporating UV-treated and untreated PPF and that containing PPP, regardless of UV exposure. This disparity can be attributed to the differing percentages of each additive used and their distinct physical properties.

Firstly, the varying percentages of PPF (2%, 3%, and 4%) and PPP (5%, 10%, and 15%) introduced into the cement paste could lead to differences in pore distribution and interfacial interactions within the matrix. Studies have indicated that a higher percentage of PPP may increase porosity due to agglomeration, potentially reducing compressive strength. In contrast, incorporating PPF at lower percentages has been shown to enhance the mechanical properties of cementitious composites by bridging cracks and improving stress transfer mechanisms.

Secondly, the physical form of the additives significantly influences pore formation and distribution within the cementitious matrix. PPP in powder form tends to create more voids and interfacial gaps during mixing, resulting in higher porosity and reduced strength. Conversely, PPF, with its fibrous morphology, can act as reinforcement within the matrix, mitigating crack propagation and enhancing overall structural integrity.

5.5 Concluding Summary

The conclusion drawn from the results of this study underscores several significant points regarding the effects of humidity on heated cement paste containing treated polypropylene fibre (TPPF) and treated polypropylene powder (TPPP). Firstly, it underscores the critical importance of sealing cement paste samples to maintain the integrity of the experimental conditions and to accurately assess the effects being studied. Additionally, the findings suggest promising potential benefits associated with incorporating TPPF and TPPP in cement paste, particularly in terms of enhancing residual compressive strength. This indicates a potential avenue for improving the durability and performance of cement-based materials in various applications.

Furthermore, the results shed light on the intricate interplay between temperature, humidity, and the strength properties of cement paste samples. Understanding these influences is crucial for optimizing the design and performance of concrete structures, especially in environments where temperature and humidity variations are significant factors.

In a broader context, these insights contribute to advancing our understanding of cement paste behaviour, providing valuable knowledge for researchers, engineers, and practitioners involved in construction materials science and concrete technology. By elucidating the effects of humidity and the role of additives like TPPF and TPPP, this study contributes to ongoing efforts aimed at developing more resilient and sustainable construction materials for the built environment.

5.6 Effect of UV treatment of polypropylene in cement paste

A comparison was made in this section to check the effect of UV treatment on polypropylene in the case of fibre and powder. As explained in the literature in section 3.3, the treatment of polypropylene helps in changing the surface chemistry of polypropylene. The method used in treating polypropylene surfaces was discussed in section 4.3. Furthermore, the results of the residual compressive strength of cement paste containing both treated PP, and non-treated PP were presented in the sealed and unsealed conditions in sections 5.4.1 to 5.4.5. This section compares the results of the following:

- Sealed cement paste sample containing UV-treated PPF and Sealed cement paste sample containing non-treated PPF
- Unsealed cement paste sample containing UV-treated PPF and Unsealed cement paste sample containing non-treated PPF
- Sealed cement paste sample containing UV-treated PPP and Sealed cement paste sample containing non-treated PPP
- Unsealed cement paste samples containing UV-treated PPP and Unsealed cement paste samples containing non-treated PPP

By comparing these scenarios, this study aims to identify UV treatment's beneficial effects on polypropylene. The evaluation of the residual compressive strength of the cement paste specimens in each case will provide insights into how UV treatment influences the performance of polypropylene in cement-based materials.

5.6.1 Sealed cement paste sample containing UV-treated PPF and sealed cement paste sample containing non-treated PPF

Figure 5-17 compares cement paste samples containing UV-treated PPF and non-treated PPF under sealed conditions. The result shows that the RCS result of cement paste containing UV-treated PPF is higher than that of non-treated PPF. For the 2%, 3% and 4% fibre addition at each temperature stage, the percentage increase is 25%, 25%, and 24% at 20^{o}C. At 50^{o}C, the percentage increase is 23%, 32% and 30%. At 100^{o}C, the percentage increase is 13%, 9% and 21%. At 200^{o}C, the percentage increase is 20%, 36%, and 33%. At 350^{o}C, the percentage increase is 35%, 36% and 32%, respectively.

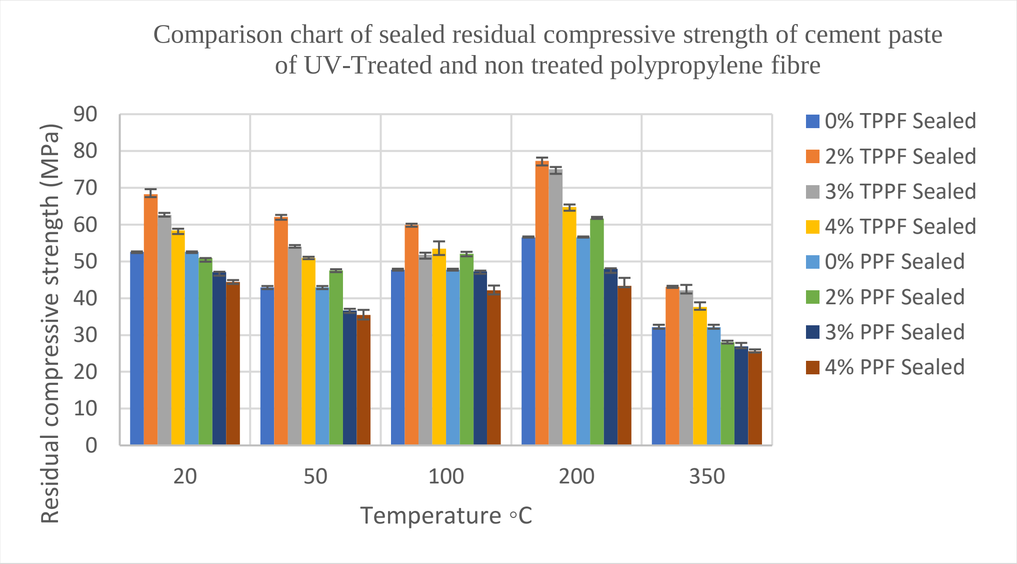

Figure 5- 17: Comparison of sealed residual compressive strength of cement paste of UV-Treated and non-treated PPF

5.6.2 Unsealed cement paste sample containing UV-treated PPF and unsealed cement paste sample containing non-treated PPF

Figure 5-18 compares cement paste samples containing UV-treated PPF and non-treated PPF under unsealed conditions. The result shows that the RCS result of cement paste containing UV-treated PPF is higher than that of non-treated PPF. For the 2%, 3% and 4% fibre addition at each temperature stage, the percentage increase is 25%, 25%, and 24% at 20^{o}C. At 50^{o}C, the percentage increase is 10%, 23% and 21%. At 100^{o}C, the percentage increase is 10%, 5% and

14%. At 200°C, the percentage increase is 18%, 32%, and 25%. At 350°C, the percentage increase is 30%, 29% and 26%, respectively.

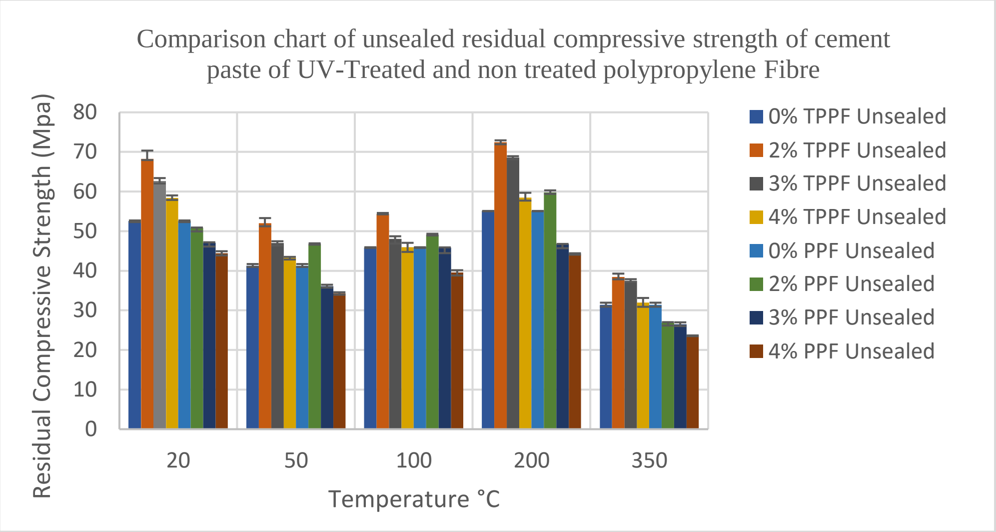

Figure 5- 18: Comparison of unsealed residual compressive strength of cement paste of UV-Treated and non-treated PP

5.6.3 Sealed cement paste sample containing UV-treated PPP and sealed cement paste sample containing non-treated PPP

Figure 5-19 compares cement paste samples containing UV-treated PPP and non-treated PPP under sealed conditions. The result shows that the RCS result of cement paste containing UV-treated PPP is higher than that of non-treated PPP. For the 2%, 3% and 4% fibre addition at each temperature stage, the percentage increase is 15%, 9%, and 9% at 20°C. At 50°C, the percentage increase is 33%, 33% and 30%. At 100°C, the percentage increase is 9%, 22% and 21%. At 200°C, the percentage increase is 24%, 21%, and 30%. At 350°C, the percentage increase is 22%, 31% and 29%, respectively.

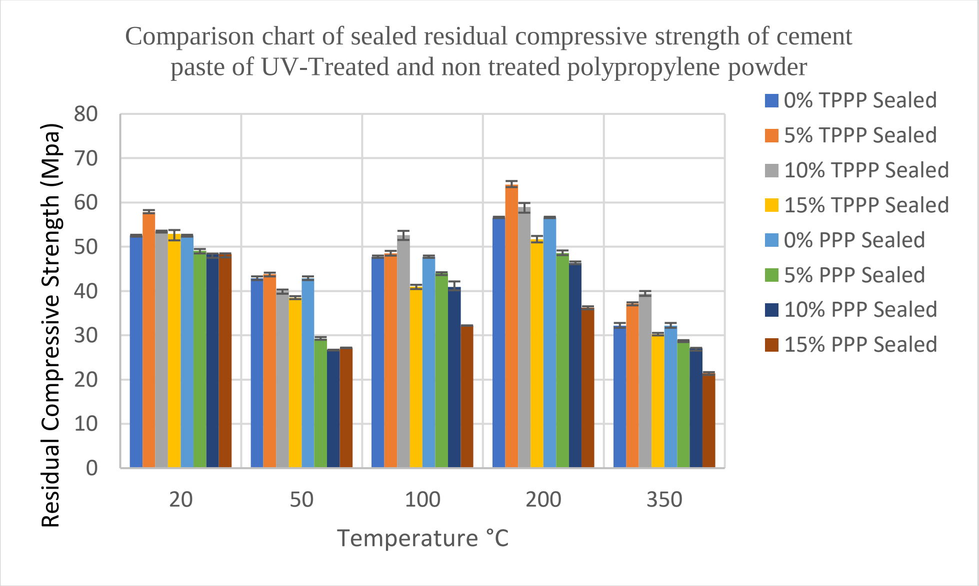

Figure 5- 19: Comparison of sealed residual compressive strength of cement paste of UV-Treated and non-treated PPP

5.6.4 Unsealed cement paste samples containing UV-treated PPP and unsealed cement paste samples containing non-treated PPP

Figure 5-20 compares cement paste samples containing UV-treated PPP and non-treated PPP under unsealed conditions. The result shows that the RCS result of cement paste containing UV-treated PPP is higher than that of non-treated PPP. For the 2%, 3% and 4% fibre addition at each temperature stage, the percentage increase is 15%, 9%, and 9% at 20°C. At 50°C, the percentage increase is 32%, 27% and 26%. At 100°C, the percentage increase is 12%, 22% and 19%. At 200°C, the percentage increase is 18%, 16%, and 25%. At 350°C, the percentage increase is 16%, 28% and 22%, respectively.

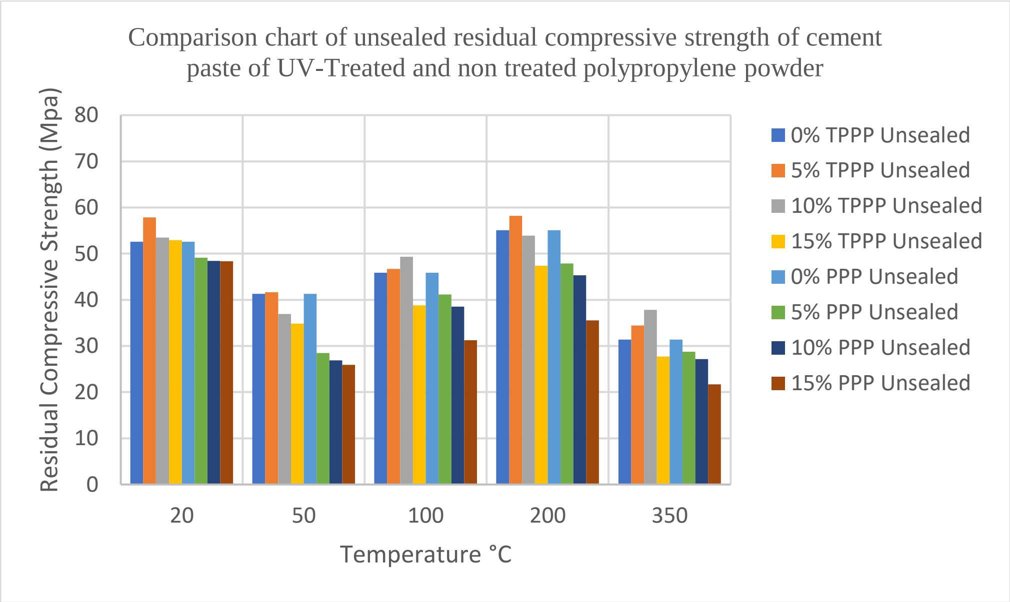

Figure 5- 20: Comparison chart of unsealed residual compressive strength of cement paste of UV-Treated and non-treated PPP

In general, the comparison made from section 5.4.8.1 to 5.4.8.2 on UV-treated PP and non-treated PP, both in the case of sealed and unsealed conditions, shows that at each stage of temperature, the UV-treated PPF and PPP exhibit high RCS than that of non-treated PPF and PPP.

The enhanced RCS observed in UV-treated PPF and PPP can be attributed to the surface treatment of PP, which was discussed in section 5.4.4. The surface treatment appears to impart a beneficial effect on the material, leading to improved mechanical performance.

These findings benefit UV-treated polypropylene's potential applications and advantages in construction and engineering.

5.7 Concluding summary

The study's findings underscore the potential advantages of incorporating treated polypropylene fibre (TPPF) and treated polypropylene powder (TPPP) in enhancing the residual compressive strength of cement paste. Additionally, they highlight the significant influence of temperature and humidity on the strength properties of cement paste samples. These insights deepen our understanding of cement paste behaviour, offering valuable implications for concrete structures.

From a practical perspective, the experiment's results suggest several crucial considerations for concrete construction. Firstly, the understanding that structures are never entirely sealed upon cooling underscores the importance of comprehending how environmental factors, particularly moisture, can impact the long-term performance of concrete. The assessment of residual compressive strength (RCS) under various conditions provides crucial insights into how moisture influences the durability of cement paste, which is essential for predicting the structural integrity of concrete in real-world applications.

A significant outcome of the study is the recognition of property adjustments following damage. Understanding how moisture affects the RCS of cement paste enables engineers to anticipate and mitigate potential degradation in concrete structures, leading to more effective maintenance and repair strategies.

Furthermore, the evaluation of RCS contributes to understanding the residual structural capacity of concrete elements over time. By considering environmental factors such as moisture, engineers can more accurately estimate the remaining strength of concrete structures throughout their service life, aiding in developing more precise inspection and monitoring protocols.

The greatest impact of UV treatment on polypropylene fibre (PPF) and polypropylene powder (PPP) lies in its ability to enhance bonding with cement paste, thereby improving the overall strength properties of the composite material.

For PPF, UV treatment transforms its hydrophobic nature to hydrophilic, leading to better compatibility and bonding with the cement paste. This UV treatment significantly improves strength, particularly at ambient temperatures and up to 200°C. However, beyond 200°C, the strength begins to decline due to the decomposition of calcium silicate hydrate (C-S-H) and potential pore formation from melted PPF.

Similarly, UV treatment of PPP enhances its bonding with the cement paste, particularly through surface chemistry modifications induced by UV irradiation techniques. This improves strength, especially at higher temperatures, such as 200°C. However, like PPF, strength may decrease at even higher temperatures due to C-S-H decomposition and additional pore formation from melted PPP.

5.8 Compressive strength of cement paste containing PPF at hot temperature.

Assessing the compressive strength of cement paste at elevated temperatures is crucial for understanding its performance under heat exposure. Compressive strength at hot temperatures evaluates the material's ability to withstand compressive forces in high-temperature environments like engines and furnaces, aiding in material selection and design optimization. Conversely, residual compressive strength assesses the material's ability to withstand loading despite existing damage, guiding safety assessments and maintenance decisions for degraded structures. These results highlight the importance of testing concrete compressive strength at elevated temperatures to ensure the resilience and reliability of structures in heat-prone environments, informing decisions on material selection, design improvements, and compliance with industry standards. Ultimately, such testing contributes to the safety and sustainability of infrastructure under thermal stress.

5.8.1 Compressive strength of cement paste containing UV-treated PPF and non-treated PPF at hot temperature

The results of the hot compressive strength tests conducted on cement pastes and cement paste samples containing polypropylene fibre at different percentages (2%, 3%, and 4%) are depicted in Figure 5-21. It was observed that adding polypropylene fibre at 2%, 3%, and 4% reduced the cement paste's compressive strength by approximately 3%, 10%, and 16%, respectively, at ambient temperature. This decrease in strength was attributed to the hydrophobic nature of polypropylene, which led to poor bonding between the cement paste and polypropylene, as reported by Hernández-cruz et al., (2014). Generally, the trend of the graph is similar to the graphs in residual compressive strength.

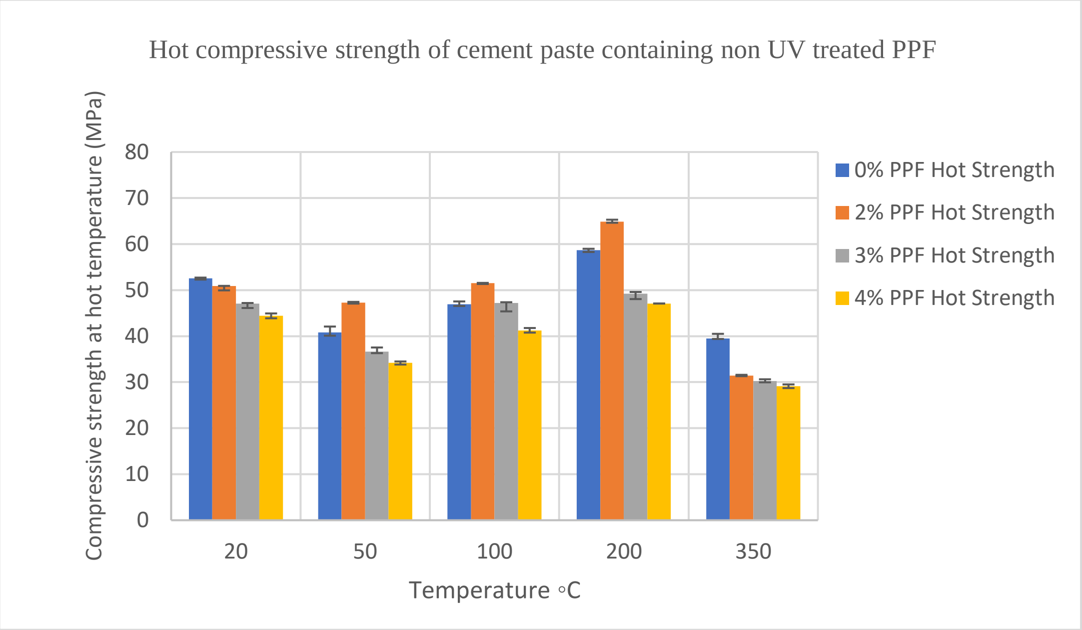

Figure 5- 21: Hot compressive strength of cement paste containing non-UV treated PPF

At a temperature exposure of 50°C, the hot strength of the samples was found to be approximately 22% lower compared to the reference sample tested at 20°C. This decrease in strength can be attributed to the dispersion of evaporable water within the sample, causing a weakening of the van der Waals forces. But at 50°C, the increase in strength above the sample containing 0% PPF was attributed to the lower fibre percentage added to the cement paste, which resulted in increased toughness and reduced plastic shrinkage crack due to water lost at 50°C. However, as the temperature increased to 200°C, the strength of all samples gradually increased. Notably, at 200°C, the reference sample exhibited approximately 12% higher strength than the reference sample at 20°C. This increase could be attributed to the rapid formation of calcium silicate hydride (C-S-H) and the loss of non-chemically bonded evaporable moisture, as mentioned by Sarshar & Khoury, (1993). This phenomenon was observed in both samples containing polypropylene fibre.

Furthermore, the results demonstrated a significant 21% increase in strength at 200°C for the sample containing 2% polypropylene fibre, compared to the same sample tested at ambient temperature. The reason for this increase is explained in section 5.4.1. However, the increase in strength for samples containing 3% and 4% polypropylene fibre additions was found to be insignificant, amounting to only 4% and 6%, respectively, due to the fibre content being higher than that of 2% PPF as explained in section 2.5 according to Bei-xings et al., (2004). The small increase also benefits the cement paste because the strength at 200°C is higher than the strength at ambient temperature. The reason for the change in compressive strength generally is explained in section 5.4.1.

A decline in strength was observed for all samples with 0%, 2%, 3%, and 4% polypropylene fibre additions when exposed to temperatures ranging from 200°C to 350°C. The decrease in strength at 350°C was measured as 33%, 62%, 56%, and 52% compared to the strength of the samples tested at ambient temperature, respectively. This decline in strength was attributed to the formation of additional pores within the samples due to the molten polypropylene in samples with polypropylene fibre addition, as well as the decomposition of C-S-H, which is responsible for the strength of cement paste. This decomposition typically occurs between temperatures of 200°C and 300°C.

Figure 5-22 results demonstrate the strength of samples containing treated polypropylene fibre (TPPF) at elevated temperatures. The trend of the graph observed for these samples is similar to those without treated polypropylene fibre. Notably, there was a significant increase in strength at 20°C for the samples with 2%, 3%, and 4% treated TPPF compared to the samples without polypropylene fibre, with increases of approximately 30%, 18%, and 11%, respectively. This increase in strength can be attributed to the treatment of PPF through UV irradiation, which reduced the hydrophobic nature of the fibres.

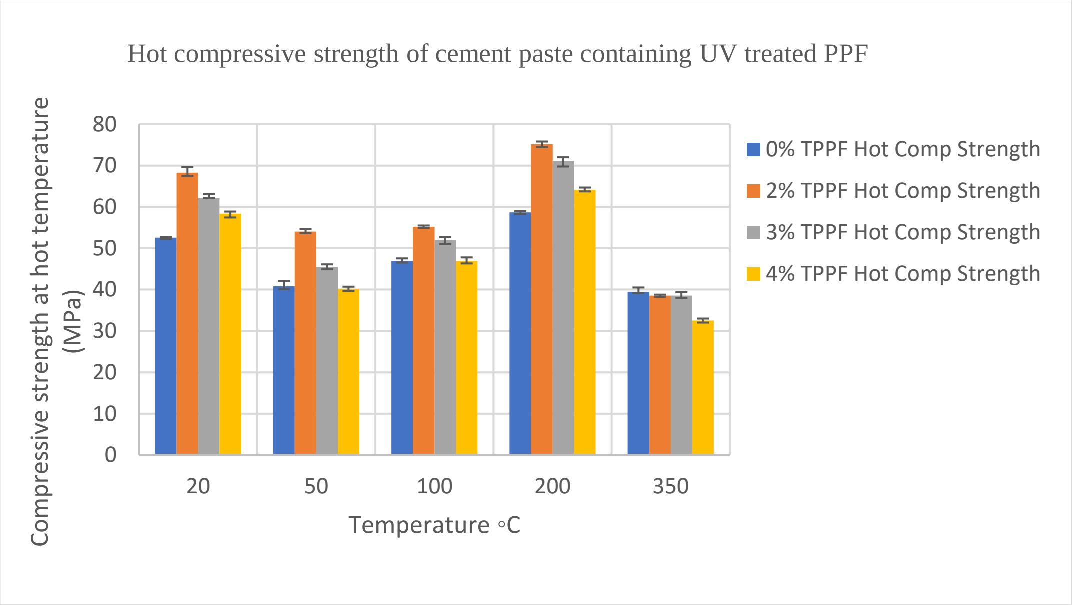

Figure 5- 22: Hot compressive strength of cement paste containing UV-treated PPF

At a temperature of 200°C, a significant increase in strength of approximately 10%, 9%, 8% and 9% was observed for the sample with 0%, 2%, 3% and 4% TPPF addition, respectively. The significant increase in strength for the 2% treated TPPF sample can be attributed to the lower percentage of polypropylene fibre added to the cement paste compared to the 3% and 4% TPPF additions and the surface treatment of polypropylene fibre. The increase in strength was observed for all percentage additions, indicating a positive correlation between the increase in temperature, the removal of moisture content, the lower amount of polypropylene content in the cement paste matrix, and the increase in surface force between gel particles as explained by Behnood & Ghandehari, (2009). Additionally, the possible thermally induced stress generated by polypropylene within the sample during melting may have contributed to the observed increase in strength reported by Xiao & Falkner, (2006).

A decline in strength was observed for all samples, including those with 0%, 2%, 3%, and 4% non-UV-TPPF and UV-TPPF additions when exposed to temperatures ranging from 200°C to 350°C. The decrease in strength for non-UV TPPF was measured as 24%, 38%, 36%, and 34%, while for treated TPPF, the decrease was 25%, 44%, 38%, and 44%, respectively, compared to the strength of the samples tested at ambient temperature. The reason for the declination in strength is explained in section 5.4.1.

5.8.2 Comparison between hot compressive strength of cement paste containing UV-treated PPF and non-treated PPF

Figure 5-23 demonstrates that the hot compressive strength of polypropylene fibre treated with UV irradiation is significantly higher than untreated polypropylene fibre. The findings indicate that the compressive strength of TPPF was higher than non-treated PPF at different temperatures. At a temperature of 50°C, adding 2%, 3%, and 4% TPPF resulted in strength improvements of 13%, 19%, and 15%, respectively, compared to non-treated PPF. Similarly, at 100°C, TPPF exhibited higher strength values with improvements of 7%, 9%, and 12% compared to non-treated PPF at the corresponding fibre addition percentages.

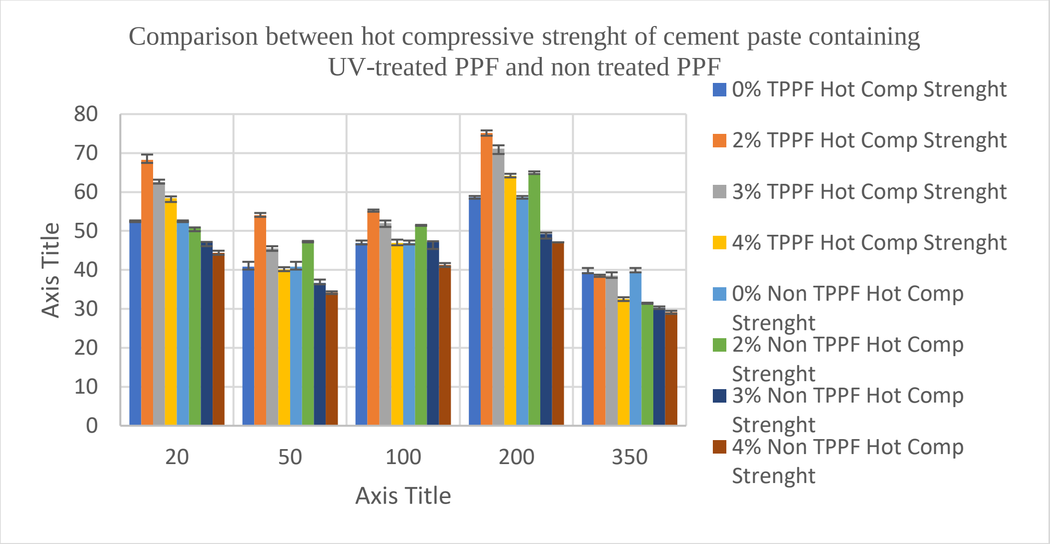

Figure 5- 23: Comparison between hot compressive strength of cement paste containing UV-treated PPF and Non treated PPF

Furthermore, at 200°C, the strength difference between TPPF and non-treated PPF became more pronounced. The increment of TPPF by 2%, 3%, and 4% led to strength enhancements of 14%, 31%, and 27%, respectively, demonstrating the positive impact of TPPF even at elevated temperatures despite the fibres melting.

However, the cement paste weakened when the samples were subjected to a temperature of 350°C, resulting in their melting of polypropylene. Nonetheless, the strength of TPPF remained higher than non-treated PPF, exhibiting increases of 19%, 22%, and 10% for 2%, 3%, and 4% TPPF addition, respectively.

These variations in strength can be attributed to the hydrophobic nature of non-treated PPF, which results in inadequate bonding between the polypropylene fibres and the cement paste matrix. Consequently, applying UV treatment to the polypropylene fibres improves compressive strength at ambient and elevated temperatures.

5.8.3 Comparison between hot and residual compressive strength of cement paste containing PPF

The observed trend in strength for the residual compressive strength of both treated and non-treated polypropylene samples, as shown in Figures 5-24 and 5-25, followed a similar pattern to that of the hot compressive strength. However, it was noted that the residual compressive strength was lower than the corresponding hot strength in both cases. At a temperature of 50°C, the difference in strength between the hot and residual compressive strength was very small for samples with and without treated polypropylene fibre (TPPF). This can be attributed to incomplete moisture escape from the hot compressive strength. For the treated PPF samples containing 2%, 3%, and 4% PPF addition, the difference in strength did not exceed 4%. Notably, as the temperature increased from 100°C to 200°C, the strength exhibited a more substantial increase, indicating the complete removal of moisture from the hot strength. At 100°C, the difference in compressive strength was approximately 8%, which further increased to around 10% at 200°C. At 350°C, the difference in strength was insignificant.

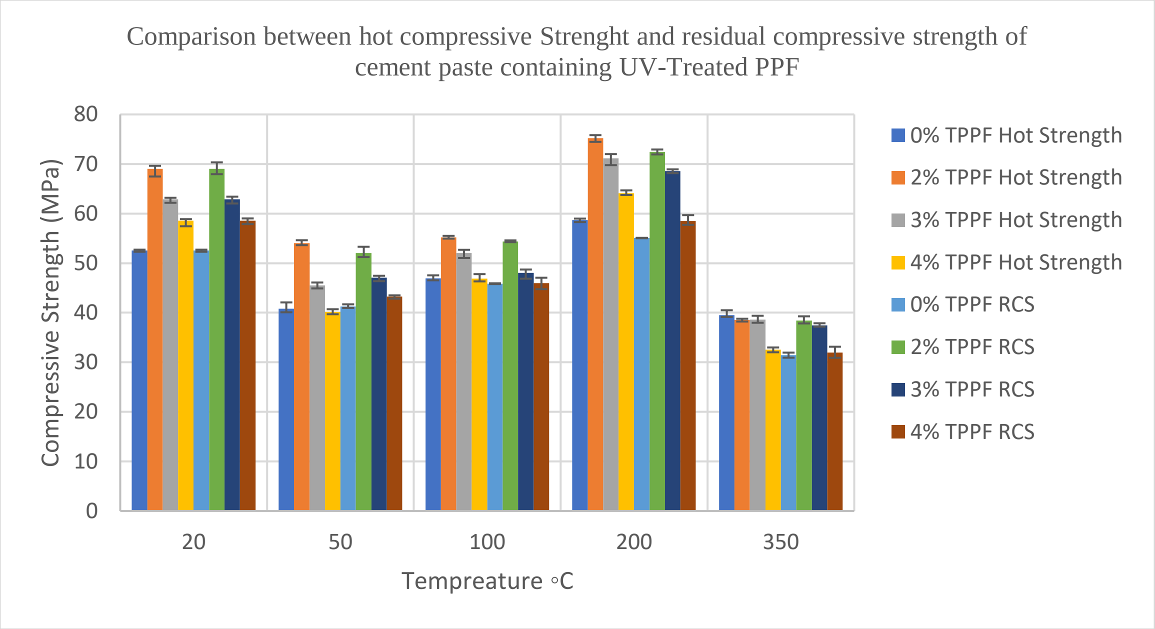

Figure 5- 24: Comparison of hot and residual compressive strength of cement pastes containing UV-treated polypropylene fibre

The observed reduction in the residual compressive strength can be attributed to moisture absorption from the surrounding environment. This moisture can affect cement paste's residual compressive strength, leading to damage caused by chemical changes in the microstructure, as previously reported in the literature (Chen et al., 2012).

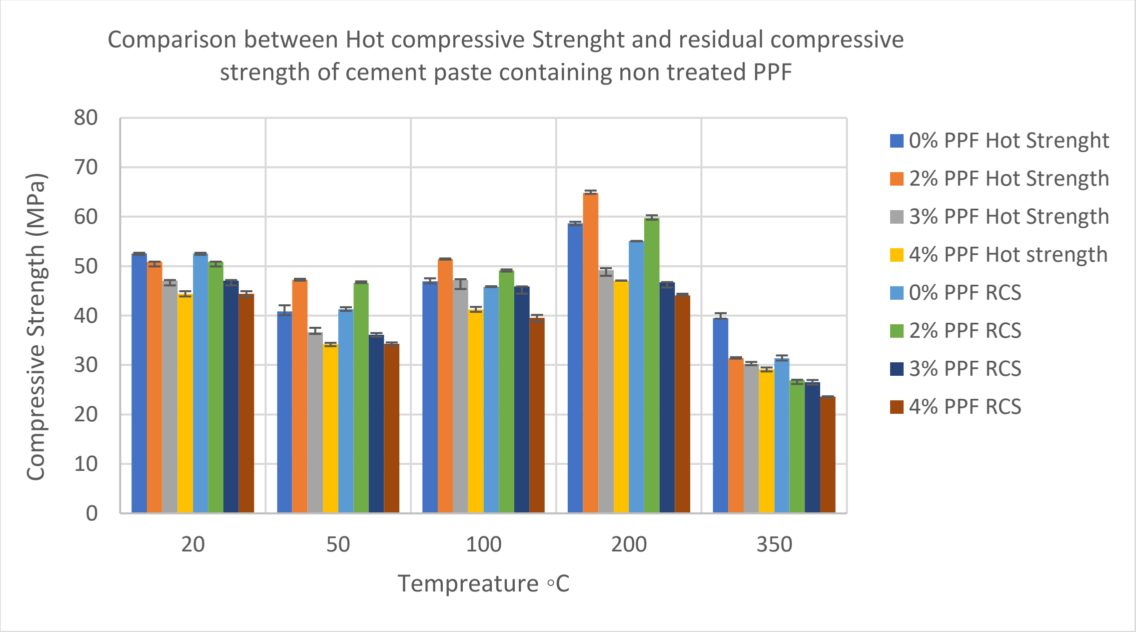

Figure 5- 25: Comparison of hot and residual compressive strength of cement pastes containing non-UV treated PPF

5.9 Concluding summary

Assessing the compressive strength of cement paste at hot temperatures provides crucial insights into its performance under conditions commonly encountered in high-temperature environments like engines and furnaces. One main benefit of such tests is evaluating the material's capacity to withstand compressive forces under elevated temperatures. This evaluation is essential for ensuring the durability and reliability of structures exposed to heat, guiding decisions on material selection, and design optimisation.

Moreover, testing the compressive strength of cement paste at hot temperatures enables the assessment of residual strength, which is vital for understanding the material's ability to withstand loading despite existing damage. This information is invaluable for conducting safety assessments and making maintenance decisions for structures that may have undergone degradation.

Furthermore, employing treated polypropylene fibres in cement paste offers distinct advantages. The treatment, often through UV irradiation, reduces the hydrophobic nature of the fibres, enhancing their compatibility with the cement paste matrix. This result improves the bonding between the fibres and the paste, enhancing mechanical properties, including increased compressive strength at elevated temperatures.

Overall, the primary advantage of testing cement paste compressive strength at hot temperatures lies in its ability to inform decisions regarding the resilience and reliability of structures in heat-prone environments. By providing insights into material behaviour under extreme conditions, such testing contributes to improved design, enhanced safety, and the long-term sustainability of infrastructure subjected to thermal stress.

5.10 Elastic modulus of cement paste containing polypropylene at a hot temperature

5.10.1 Elastic modulus of cement paste containing non-treated PPF at hot temperature

The elastic modulus of the samples was calculated using the elastic modulus equation written as equation (5.1). The general calculation is shown in Appendix II.

$$K = EA/L \quad \textbf{\textit{5- 1}}$$

Where E is the elastic modulus

K is the stiffness of the sample

A is the cross-sectional area of the sample.

L is the length of the sample.

To determine the stiffness of a compressive machine (Km), we undertake a process that amalgamates the intrinsic stiffness of the machine itself with that of the metal constituting its structure. This amalgamation is achieved by computing the parallel connection of these two stiffness values.

Mathematically, this is expressed as:

$$\frac{1}{K_{eq1}} = \frac{1}{K_m} + \frac{1}{K_{metal}} \qquad 5\text{- }2$$

Where K_{eq1} denotes the equivalent stiffness resulting from the combination of the machine's stiffness K_m and the stiffness of the metal K_{metal}. By equating this expression to the stiffness of the compressive machine K_m, we can isolate Km:

$$\frac{1}{K_m} = \frac{1}{K_{eq1}} - \frac{1}{K_{metal}} \qquad 5\text{- }3$$

Similarly, to ascertain the stiffness of the sample K_s, we consider the parallel connection of the sample's stiffness and that of the compressive machine:

$$\frac{1}{K_{eq2}} = \frac{1}{K_s} + \frac{1}{K_m} \qquad 5\text{- }4$$

Where K_{eq2} is the equivalent stiffness resulting from the combination of the machine's stiffness K_m and the stiffness of the sample K_s.

Rearranging this equation allows us to solve for Ks:

$$\frac{1}{K_s} = \frac{1}{K_{eq2}} - \frac{1}{K_m} \qquad 5\text{- }5$$

This systematic approach enables the determination of both the stiffness of the compressive machine K_m and the stiffness of the sample K_s.

Figure 5-26 illustrates the effect of adding PPF to the cement paste matrix on the elastic modulus of the paste. The results indicate that adding 2%, 3%, and 4% PPF decreases the elastic modulus of the cement paste by 4%, 13%, and 19%, respectively, compared to the original paste without PPF addition, at a temperature of 20°C. The extent of the decrease varies among the different PPF concentrations, which could be attributed to the fibres acting as microcracks, which disperse stress and prevent crack propagation, thereby reducing the material's overall stiffness.

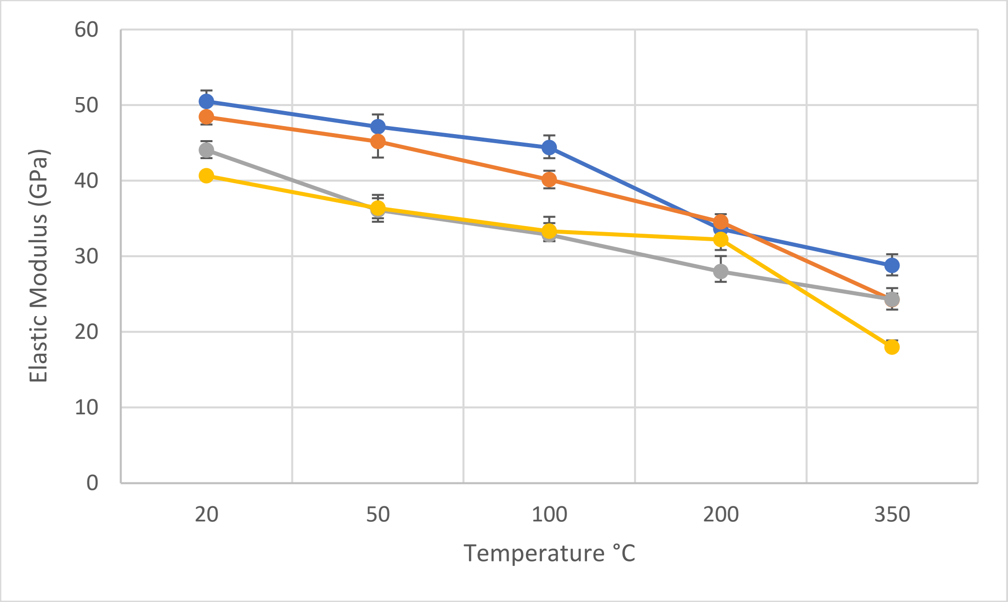

Figure 5- 26: Elastic modulus of cement paste containing non-UV treated PPF at hot temperature

The study investigated the effect of temperature on the elastic modulus of cement pastes, both with and without polypropylene fibres (PPF). The results showed that the elastic modulus gradually decreased with increasing temperature. For the control sample, when heated at 200°C, there was a significant loss of around 33% in the elastic modulus. This loss increased to 40% at 300°C, compared to the ambient temperature. These findings contradict the results of a previous study by Sercombe & Galle, (2003), who reported a loss of only 17% when the cement paste was heated to 300°C.

The disparity in results can be attributed to keeping the cement paste samples at a constant temperature of 20°C for up to 7 years, and they used a different type of cement (CEMI) in their experiment. These variations in experimental conditions likely contributed to the contrasting outcomes between the two studies. The reduction in the elastic modulus of cement paste can be attributed to some underlying mechanisms. Firstly, the dehydration and decomposition of C-S-H formed during the cement hydration play a crucial role. The elevated temperatures cause the breakdown of these hydrates, resulting in a decrease in the internal cohesive forces within the cement paste.

Consequently, the stiffness and elastic modulus of the material decreases as well. Moreover, the thermal expansion of cement particles and the formation of microcracks due to thermal stress further contribute to the loss of elasticity in cement paste when exposed to high temperatures. The thermal stresses induced by the temperature gradient lead to the formation of microcracks, weakening the overall structure of the material (Odelson et al., 2007)

Adding 2%, 3%, and 4% PPF resulted in a 50%, 49%, and 56% loss in elastic modulus when heated to 350°C compared to the initial value at 20°C. This finding aligns with the results reported by Leo & Horiguchi, (2006), who found that the loss in elastic modulus of concrete with PPF additions of P6-0.25, P6-0.5, and P30-0.25 was 71%, 70%, and 67%, respectively, in comparison to the original value when heated to 400°C. Here, P6 and P30 represent the fibre length, while 0.25 and 0.5 denote the fibre volume in the concrete.

The most significant reduction in elastic modulus occurs between 20°C and 200°C, which is attributed to transformations and chemical reactions within the cement paste, altering its material structure and compromising its mechanical properties. These alterations also contribute to the decrease in the elastic modulus (Odelson et al., 2007)

5.10.2 Difference of elastic modulus between treated and non-treated PPF

Based on the analysis presented in Figure 5-27, it can be observed that there was not much difference in the elastic modulus between the treated and non-treated PPF additions at a temperature of 20°C. The differences observed were 0.7%, 5%, and 4% for 2%, 3%, and 4% TPPF addition above non-treated PPF.

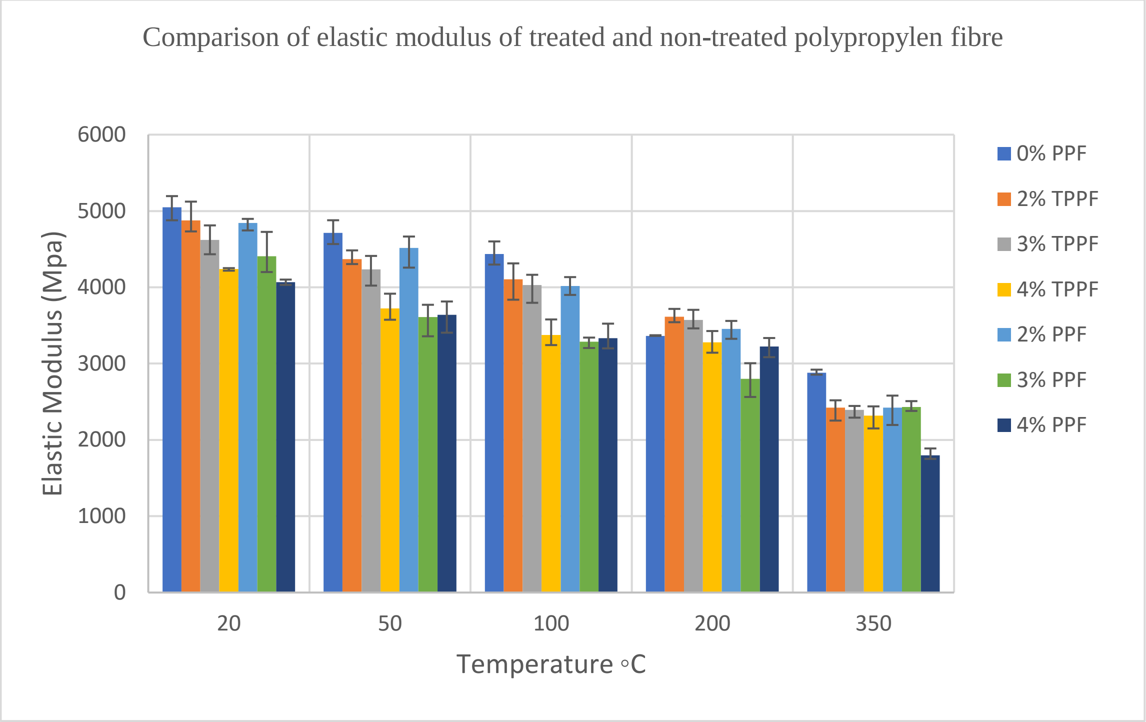

Figure 5- 27: Difference in elastic modulus between UV-treated and non-UV-treated PPF

Furthermore, at a temperature of 50°C, the differences in elastic modulus were found to be 3%, 15%, and 2% for 2%, 3%, and 4% TPPF addition, respectively, above non-treated PPF. Similarly, at a temperature of 100°C, the differences observed were 2%, 18%, and 1% for 2%, 3%, and 4% TPPF, respectively, above non-treated PPF. At a higher temperature of 200°C, the differences in elastic modulus were found to be 4%, 22%, and 2% for PPF additions of 2%, 3%, and 4% TPPF addition, respectively, compared to the non-treated PPF.

Likewise, at a temperature of 350°C, the differences observed were negligible, with a difference of 0.07% and 1.6% between TPPF and non-treated PPF additions of 2% and 3%, respectively. However, a difference of 22% was observed to be high for the 4% PPF addition above non-treated PPF. This difference could be due to the percentage difference of polypropylene in the cement matrix.

Adding UV-treated polypropylene fibre (TPPF) to cement paste shows some improvement in the elastic modulus, especially at elevated temperatures. However, the overall effect is not substantial, and there seems to be a limitation to how much TPPF can effectively improve the stiffness of the cement paste. The surface treatment of polypropylene fibres appears to play a role in the observed improvements.

5.11 Microstructure investigation of cement paste containing polypropylene

The present study focuses on investigating the microstructure of cement paste containing polypropylene fibres, aiming to assess the influence of fibre incorporation on the internal composition of the cementitious matrix at a microscopic level. Through an in-depth examination of the microstructure, valuable insights can be obtained regarding the interactions between the fibres and the cementitious matrix, including the dispersion and alignment of fibres within the paste. This investigation helps understand the impact of fibre content and distribution on the overall microstructure, pore connectivity, and the formation of cracks and propagation pathways. By gaining insights into the microstructural changes caused by polypropylene fibres, researchers can optimise the dosage and distribution of fibres to cement paste with improved mechanical performance and durability.

5.11.1 Cement paste sample containing 0% PP

The effect of temperature on porosity was investigated in this study. It was observed that as the temperature increased, there was a substantial rise in porosity due to two main factors: sample cracking and degradation of the cement paste. These factors happen due to the escape of bound water. The result agrees with the finding by Ye et al., (2007). They noted that temperature considerably impacted both the size and shape of pores.

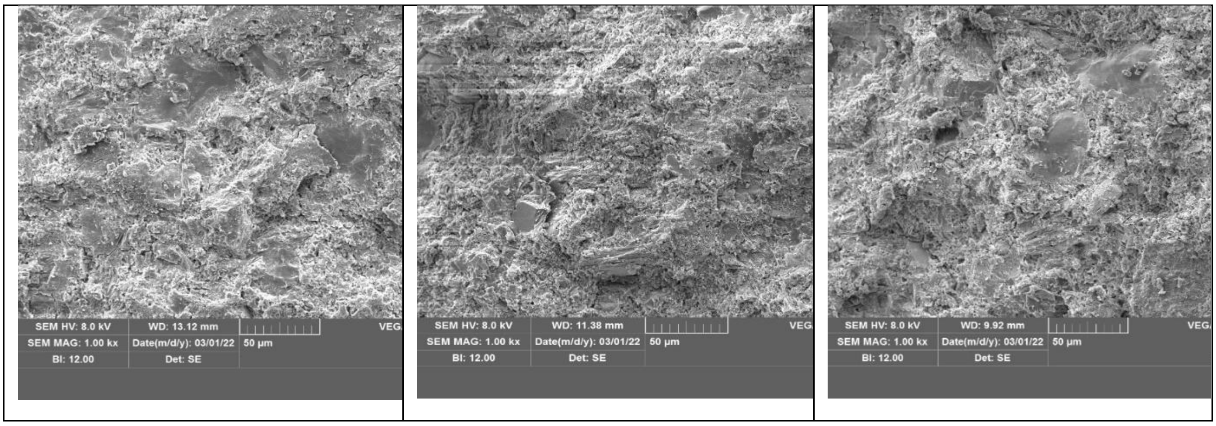

a) Cement paste sample with 0% PP at 20°C b) Cement paste sample with 0% PP at 200°C c) Cement paste sample with 0% PP at 350°C

Figure 5- 28: SEM images of cement paste containing 0% polypropylene

At temperatures below 200°C, porosity was lower, and the pores exhibited greater irregularity than those at 350°C. The physicochemical changes up to 350°C were primarily characterised by water loss and the disintegration of calcium silicate hydroxide. These changes caused the collapse of the gel structure and the creation of additional porosity. Alterations in the porous medium were responsible for these modifications. From 20°C to 200°C, no significant increase in porosity is observed.

Additionally, the brightness of the hydration product (C-S-H) remained almost unchanged at these temperatures, as depicted in Figure 5-28a and b, respectively. The importance of the hydration product of cement pastes remaining bright from 20°C to 200°C lies in its stability and durability. Cement paste is formed by the chemical reaction between cement and water, resulting in the formation of hydration products, mainly calcium silicate hydrates (C-S-H) and calcium hydroxide ($Ca(OH)_2$). The fact that the brightness colour of the hydration product remains consistent over this temperature range indicates that the microstructure of the cementitious materials remains intact and does not undergo significant thermal degradation. This stability at 200°C temperatures is crucial because it ensures that the compressive strength increment observed at 200°C is predominantly attributed to the maintenance and continued development of C-S-H bonds rather than the formation of new, possibly weaker, phases. As a result, concrete exposed to such elevated temperatures can retain a considerable portion of its original strength, making it particularly important for applications in high-temperature environments. However, an increase in porosity was observed when the temperature reached 350°C, as shown in Figure 5-27c. This result agrees with the findings reported by Fares et al., (2010; Malik et al., (2021). Concerning the compressive strength with the microstructure investigation, it can be said that the increase in strength at 200^{o}C is associated with the hydration product not changing the colour.

5.11.2 Non-UV treated PPF in cement paste at 20^{o}C

The non-heated cement paste samples containing various percentages of PPF (2%, 3%, and 4% additions) were examined using scanning electron microscopy (SEM) at a magnification of 100x. The SEM images in Figure 5-29 depict the distribution of PPF within the cement paste samples for the respective PPF additions (2%, 3%, and 4%, represented by labels a, b, and c, respectively). Notably, Figure 5-29c exhibits a higher quantity of fibres than Figures 5-28b and 5.29a. Figure 5-29b also displays a higher fibre content than Figure 5-29a. The variations in fibre quantities among the figures can be attributed to the differences in the percentages of fibres present in the three sample types, as indicated in the figures.

The SEM analysis reveals that the PPF particles have established good contact with the hydration products within the cement matrix. No distinct interface is observed between the PPF and the cement matrix. However, some instances of PPF fibres being pulled out from the cement paste are observed, likely due to the hydrophobic nature of PPF, which gives a poor bond between the fibre and cement paste. These findings align with those reported by Schutter, et al., (2008).

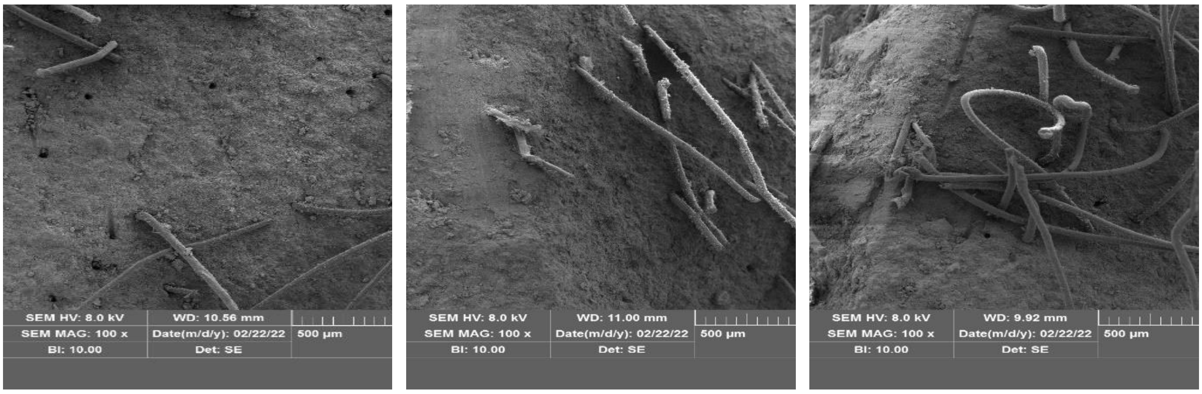

a) Cement paste containing 2%PPF at 20°C b) Cement paste containing 3%PPF at 20°C c) Cement paste containing 4%PPF at 20◦C

Figure 5- 29: Picture of the SEM for the sample containing non-treated PPF at 20ºC

5.11.3 UV-treated PPF in cement paste at 20°C

Non-heated cement paste specimens incorporating a varying percentage of ultraviolet (UV) treated polypropylene fibre (PPF) at 2%, 3%, and 4% were examined using scanning electron microscopy (SEM) at a magnification of 100x. As depicted in Figure 5-30, the obtained SEM images illustrate the distribution of UV-treated PPF within the cement paste samples, which is analogous to the distribution observed in cement paste specimens containing non-treated PPF. The analysis of these images reveals that the UV-treated PPF exhibits favourable interaction with the hydration products, establishing a sound interface with the cement paste matrix. Notably, the UV-treated PPF remains embedded within the cement paste matrix without experiencing detachment but rather undergoes breakage, indicating a strong bond between the UV-treated PPF and the cement paste matrix, contributing to increasing compressive strength, as explained in section 5.4.4. This enhanced bond can be attributed to the alteration of PPF's surface chemistry from hydrophobic to hydrophilic nature, consequently improving the interfacial compatibility with the cement paste.

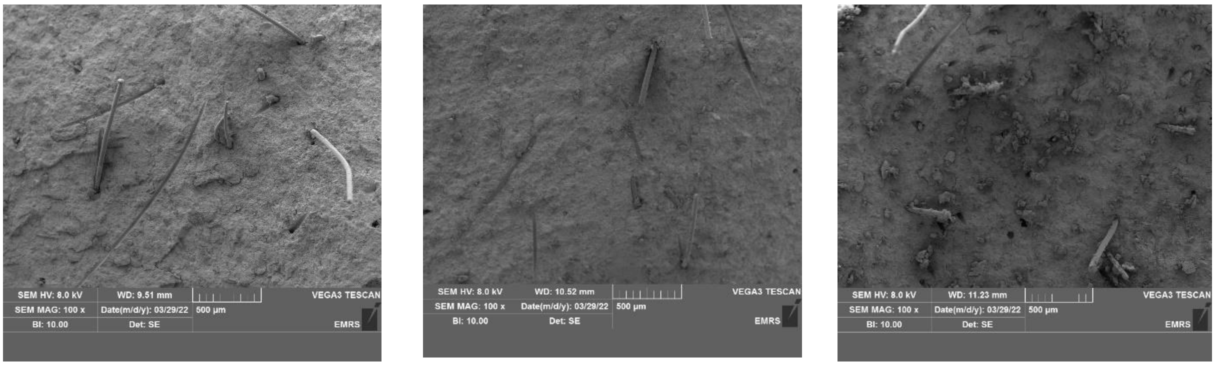

a) Cement paste with 2%TPPF at 20°C b) Cement paste with 3%TPPF at 20°C c) Cement paste with 4%TPPF at 20°C

Figure 5- 30: Picture of the SEM for the sample containing Treated PPF at 20ºC

5.11.4 Heated cement paste containing UV-treated PPF and Non treated PPF

Figure 5-31 results depict samples of UV-treated and non-treated PPF (polypropylene fibre) with varying additions of 2%, 3%, and 4% PPF. These samples were heated at 100°C, a temperature at which the fibre did not undergo melting. It is evident from the figure that the PPF has established a favourable contact with the hydration product, which is consistent with the findings reported by Schutter, et al., (2008). It should be noted that their study involved heating the result at 130°C, a temperature below the melting point of PPF.

From Figures 5-31a and b, a hole is observed, which can be attributed to the fibre being pulled during the sample preparation; this indicates a lack of strong bonding between PPF and the cement paste due to the hydrophobic nature of PPF.

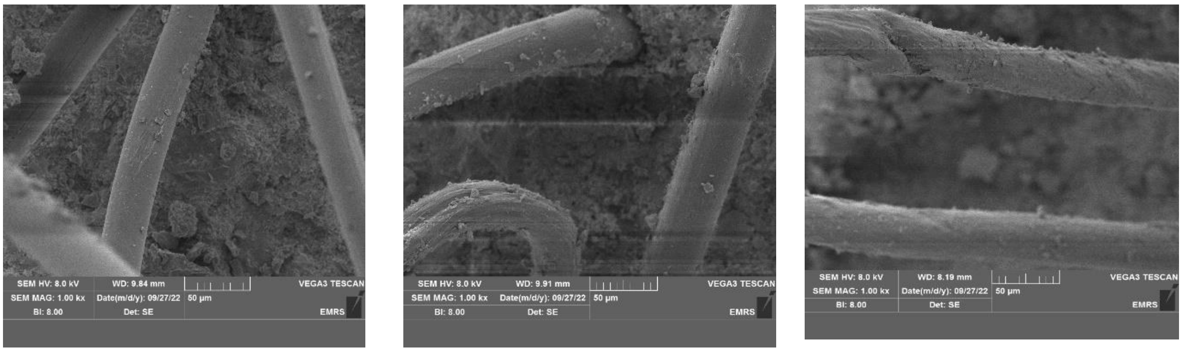

a): 2% Non-treated PPF at 100◦C b): 3% Non-treated PPF at 100◦C c): 4% Non-treated PPF at 100◦C

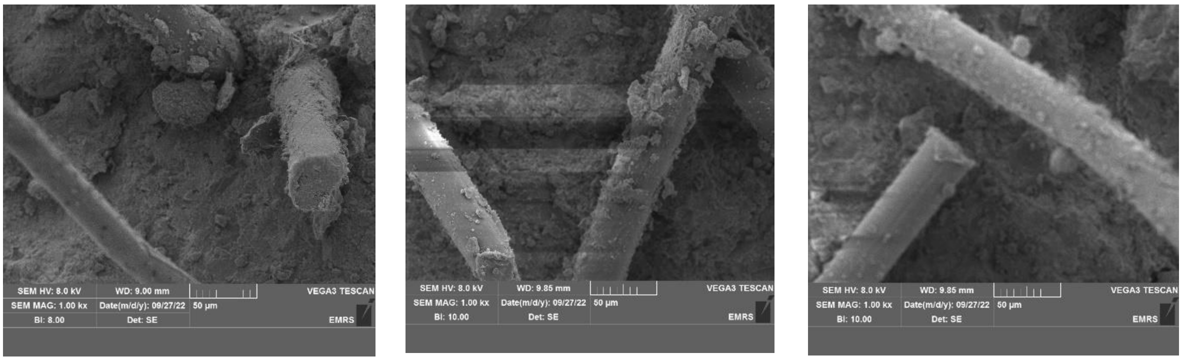

d): 2% UV-treated PPF at 100◦C e): 3% UV-treated PPF at 100◦C f): 4% UV-treated PPF at 100◦C

Figure 5- 31: Picture of the SEM for the sample containing non-treated PPF and UV-treated PPF at 100°C

After heating the samples in the furnace, UV-treated and non-UV-treated fibres melted and volatilised at 200°C, as demonstrated in Figure 5-32 under 1000x magnification. The melted fibres introduced additional pores and small channels in the cement paste, which could alleviate high internal pressure, as suggested by Noumowe, (2005). In a liquid state, these molten fibres permeated through the surrounding pores, enabling connectivity among the hydrated products. As the temperature increased, the melted PPF, both UV-treated and non-UV-treated, absorbed more energy. The melted fibre remains within the cement paste as it has not volatised completely. Volatile products combust at 350°C to 400°C under direct heat, as explained in section 3.2.5. Consequently, the remaining fibre channels and the flow path connected with each other, forming a more interconnected pore network, as reported by Schutter, et al., (2008).

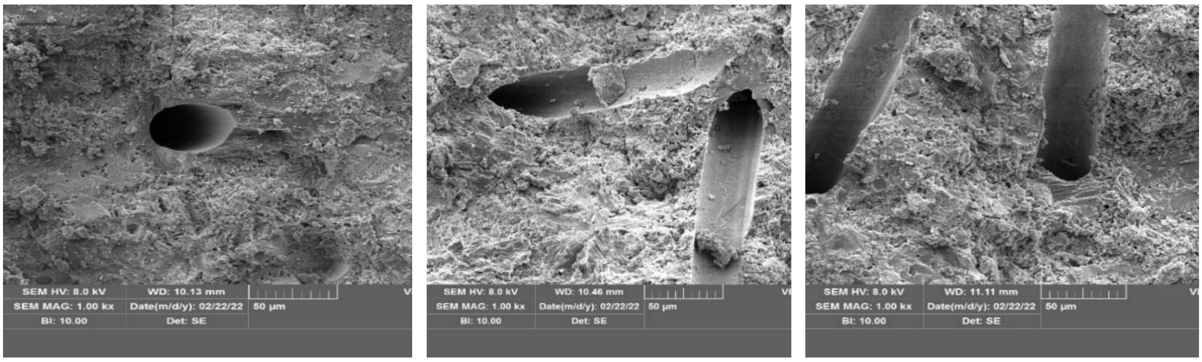

a): 2% Non-treated PPF at 200◦C b): 3% Non-treated PPF at 200◦C c): 4% Non-treated PPF at 200◦C

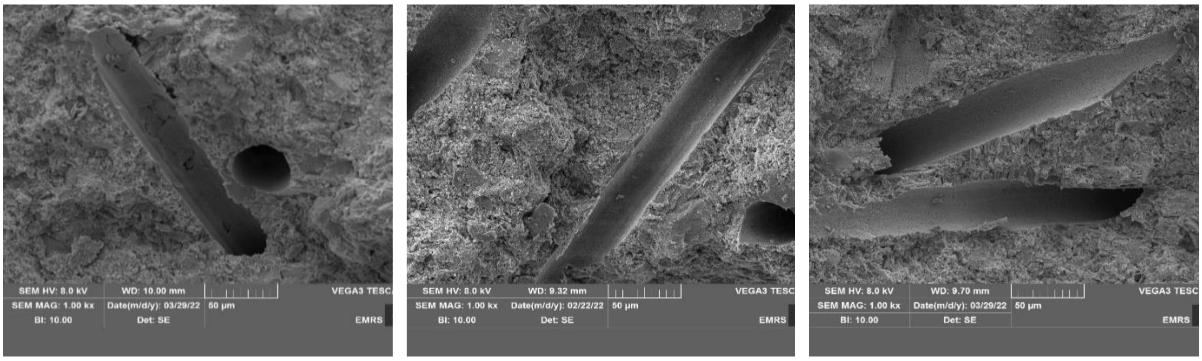

d): 2% UV-treated PPF at 200◦C e): 3% UV-treated PPF at 200◦C f): 4% UV-treated PPF at 200◦C

Figure 5- 32: Picture of the SEM for the sample containing non-treated PPF and UV-treated PPF at 200ºC

Figure 5-33 exhibits an image obtained from a sample containing non-treated PPF with additions of 2%, 3%, and 4%, as well as UV-treated PPF with the same additions, all heated at 350°C. Similar to the earlier discussion, the PPF remained melted at 200°C. The persistence of molten PPF creates pathways for moisture to escape. Consequently, after the PPF has melted, the area surrounding the fibre appears looser than the area without fibre. These phenomena were investigated and confirmed through three-dimensional tomography tests conducted by Park et al., (2008).

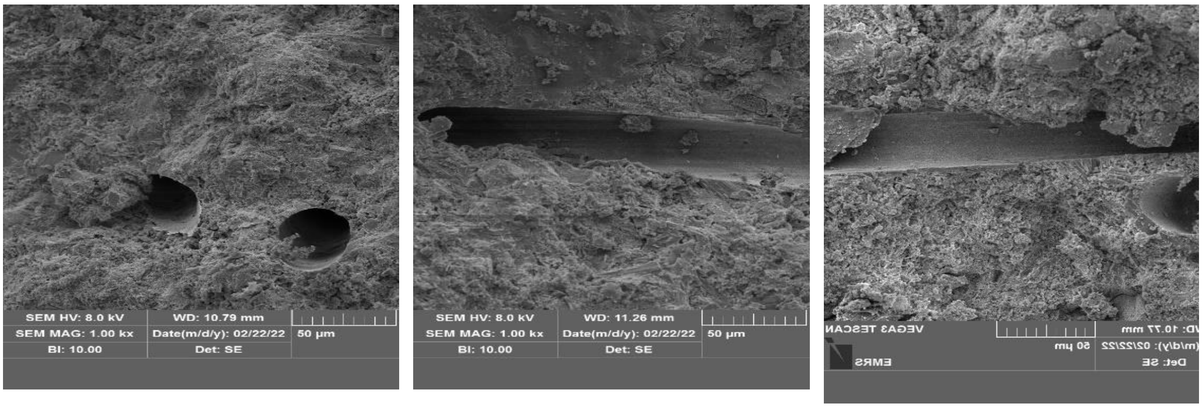

a): 2% Non-treated PPF at 350◦C b): 3% Non-treated PPF at 350◦C c): 4% Non-treated PPF at 350◦C

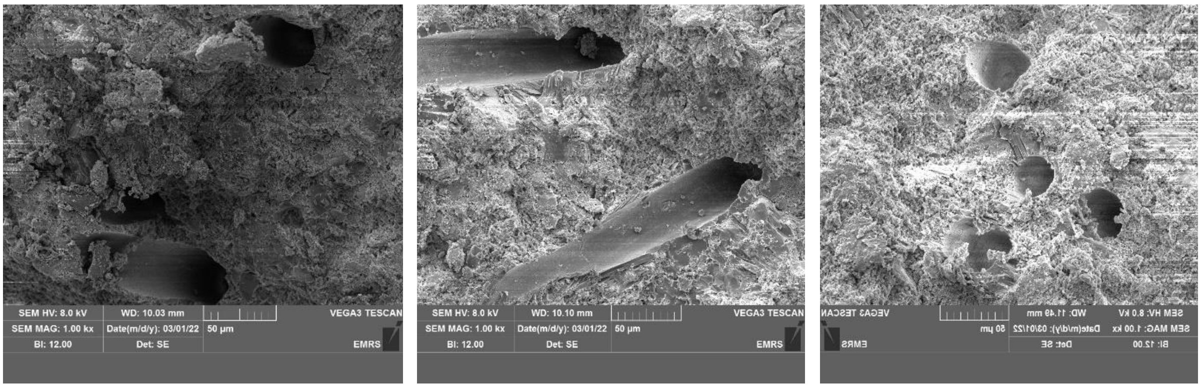

d): 2% UV-treated PPF at 350◦C e): 3% UV-treated PPF at 350◦C f): 4% UV-treated PPF at 350◦C

Figure 5- 33: Picture of the SEM for the sample containing non-treated PPF and UV-treated PPF at 350°C

5.11.5 Non-treated PPP and UV-treated PPP in cement paste at 20°C

The non-heated cement paste specimens containing non-UV treated PPP at 5%, 10%, and 15% addition and UV-treated PPP at the same addition levels were examined using scanning electron microscopy (SEM) at a magnification of 1000X. The results presented in Figure 5-34 indicate that both the non-treated and UV-treated PPP at 20°C did not exhibit observable presence within the cement paste matrix. However, the scanning images revealed the presence of cracks in all the samples with 5%, 10%, and 15% addition of non-treated PPP. These cracks were attributed to the hydration process occurring within the samples and the weakening of van der Waals forces due to the hydrophobic nature of PPP, which caused poor bonding between cement paste and PPP.

A significant reduction in crack formation was observed in the case of UV-treated PPP. This reduction in cracks can be attributed to the surface modification of PPP, which altered the hydrophobic nature of PPP and turned it hydrophilic. That is why the compressive strength at 20°C increased, as explained in section 5.4.5.

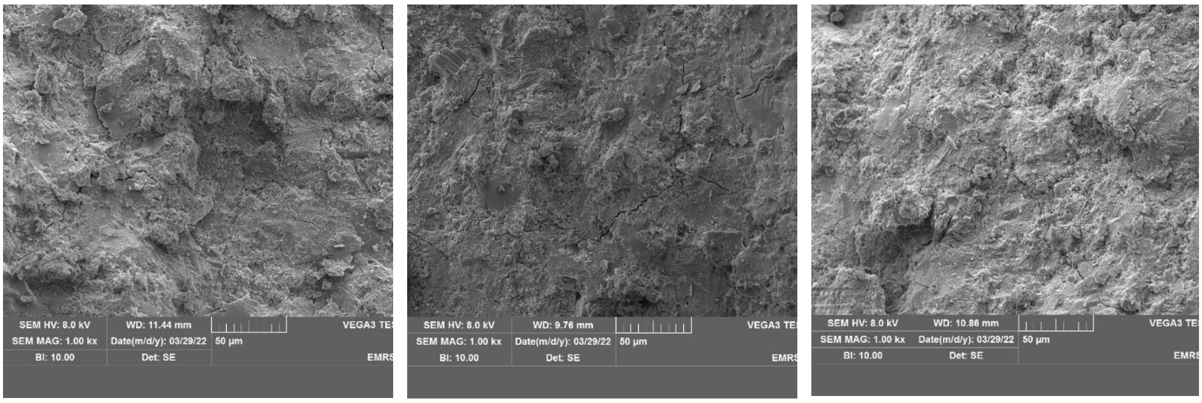

a) Cement paste containing 5%PPP at 20°C b) Cement paste containing 10%PPP at 20°C c) Cement paste containing 15%PPP at 20°C

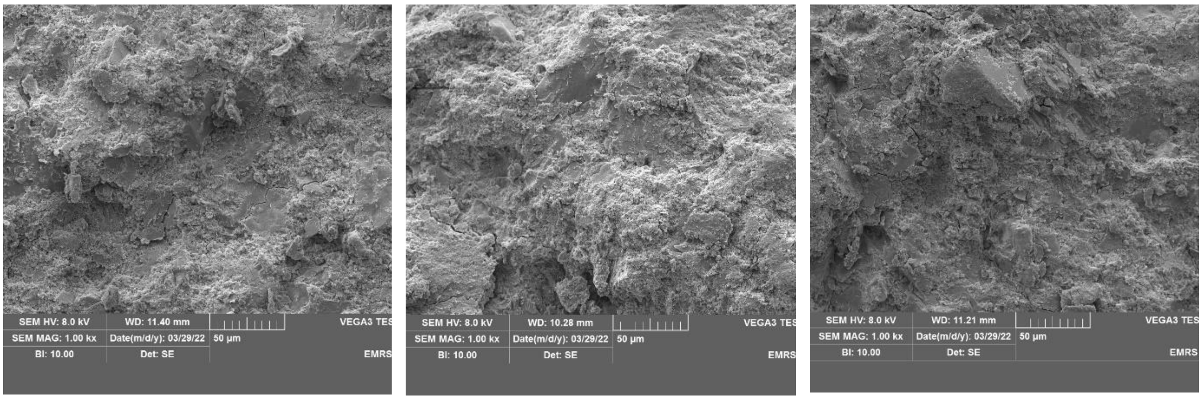

a) Cement paste containing 5%TPPP at 20°C b) Cement paste containing 10%TPPP at 20°C c) Cement paste containing 15%TPPP at 20°C

Figure 5- 34: Picture of the SEM for the sample containing non-treated PPP and UV-treated PPP at 20°C

5.11.6 Heated cement paste containing UV-treated PPP and non-treated PPP

Heating the sample in the furnace causes UV-treated and non-UV-treated PPP to melt and volatilise at 200°C, as depicted in Figure 5-35 under 1000x magnification. The melted PPP creates additional pores and small channels in the cement paste, which can alleviate high internal pressure (Noumowe, 2005). In their liquid state, these molten PPP particles pass through the surrounding pores, breaking the connection among hydrated products. The elevated temperature causes the melted PPP in both UV-treated and non-UV-treated samples to absorb more energy and undergo vaporisation. Consequently, the remaining PPP and the flow path become interconnected, forming a more connected pore network (Schutter, et al., 2008).

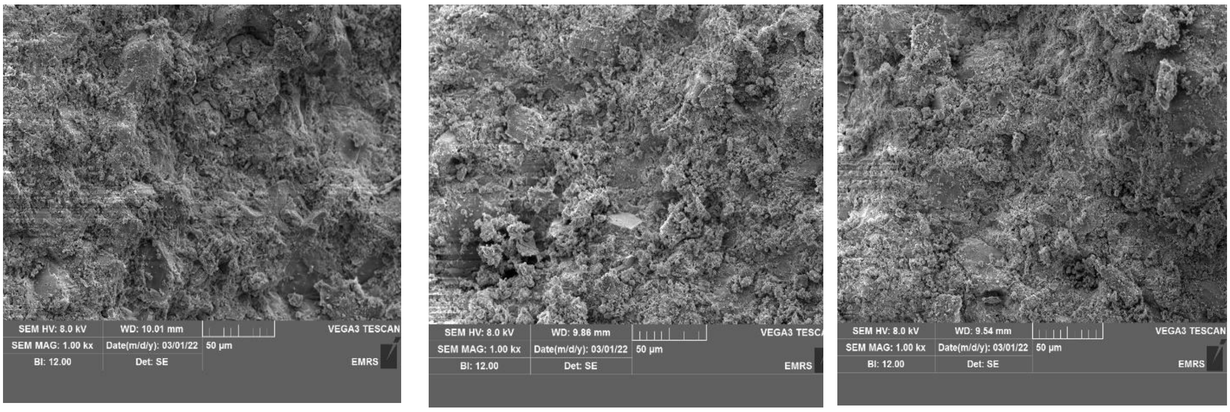

a) 5% Non-UV treated PPP at 200◦ b) 10% Non-UV treated PPP at 200◦C c) 15% Non-UV treated PPP at 200◦C

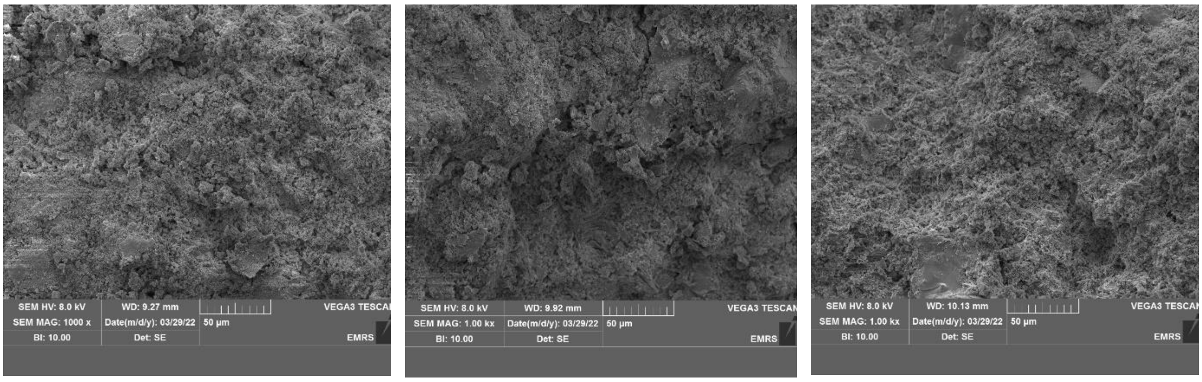

d) 5% UV-treated PPP at 200◦C e) 10% UV-treated PPP at 200◦C f) 15% UV-treated PPP at 200◦C

Figure 5- 35: Picture of the SEM for the sample containing non-treated PPP and UV-treated PPP at 200°C

The observed image reveals a higher number of pores than those generated by fibres within the cement paste sample. This increased pore formation is associated with PPP in a crystalline form, which disperses and mixes within the cement paste matrix. Due to the higher pore formation, the cement paste's strength decreases significantly compared to paste without PPP.

Figure 5-36 displays images taken from samples containing non-treated PPP with additions of 5%, 10%, and 15%, as well as UV-treated PPP with the same additions, all heated at 350°C. Similarly, the PPP remains melted and has no differences in physical observation as described earlier at 200°C. But in this case, the compressive strength is drastically reduced due to the disintegration of C-S-H that happens when the temperature exceeds 200^{o}C, as explained in section 5.4.5.

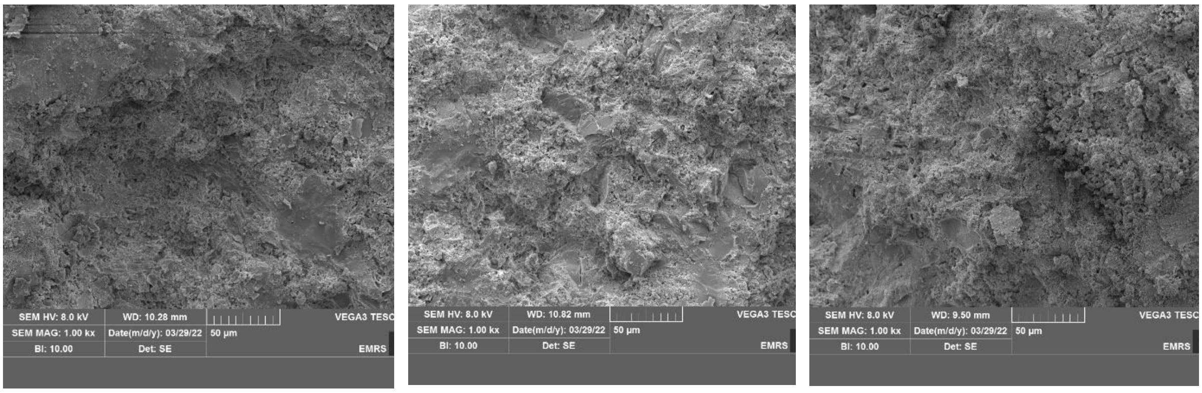

a) 5% Non-UV treated PPP at 350◦C b) 10% Non-UV-treated PPP at 350◦C c) 15% Non-UV treated PPP at 350◦C

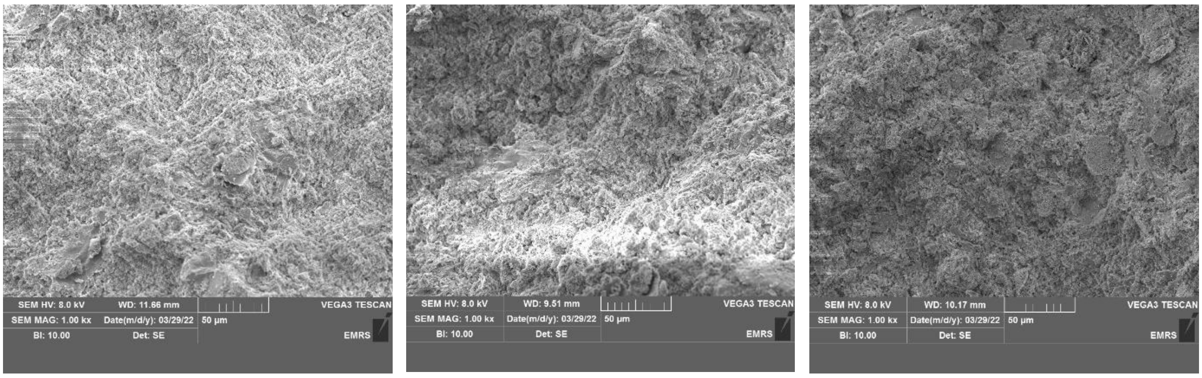

d): 5% UV-treated PPP at 350◦C *e): 10% UV-treated PPP at 350◦C* *f): 15% UV-treated PPP at 350◦C*

Figure 5- 36: Picture of the SEM for the sample containing non-treated PPP and UV-treated PPP at 350^{o}C

The microstructure plays a critical role in regulating water removal from cement paste under both normal and high-temperature conditions. When exposed to thermal conditions, the melting of polypropylene fibres or powder can positively influence the performance of the cement paste (Hertz, 1992). The melting of polypropylene fibres introduces additional porosity and small channels into the paste. It is important to note that the dimensions and quantity of the fibres or powder can influence the microstructural behaviour of cement paste under compressive strength, as discussed in section 5.8.1.

5.12 Concluding summary

The results examine the microstructural analysis of cement paste containing polypropylene fibres (PPF), aiming to determine their impact on the internal composition of the cementitious matrix at a microscopic scale. Through examination, this study sheds light on the interplay between the fibres and the cementitious matrix, encompassing aspects such as fibre dispersion, alignment, and their influence on pore connectivity and crack formation. The findings show that optimal dosage and distribution of PPF can enhance cement paste's mechanical robustness and durability.

Temperature variation emerges as a crucial factor affecting porosity within the cementitious matrix, with higher temperatures inducing increased porosity primarily due to sample cracking and cement paste degradation. Physicochemical changes up to 200°C are characterised by water loss and calcium hydroxide disintegration, maintaining the hydration product's stability (C-S-H) stability and preserving the microstructure's integrity. This stability at 200°C ensures that the increased compressive strength is predominantly attributed to the maintenance and development of C-S-H bonds rather than weaker phase formation, vital for applications in elevated temperature environments.

Scanning electron microscopy (SEM) analysis of cement paste specimens incorporating UV-treated PPF reveals a favourable interaction with hydration products, marked by enhanced bonding and integrity within the cement paste matrix. The UV treatment alters PPF's surface chemistry from hydrophobic to hydrophilic, facilitating improved interfacial compatibility and increasing compressive strength. Furthermore, heating of samples results in molten PPF formation, introducing additional porosity and channels within the cement paste, thereby aiding in pressure alleviation.

Moreover, the study underscores the influence of PPF on crack formation, with UV-treated PPF significantly reducing crack occurrence attributed to its altered surface properties. However, heating at higher temperatures reduces compressive strength due to the disintegration of C-S-H, emphasising the critical role of microstructure in governing the behaviour of cement paste under varying conditions.

The research highlights the importance of UV-treated PPF in enhancing cement paste's mechanical performance and durability, emphasising its potential to mitigate crack formation and maintain structural integrity under diverse environmental conditions. Additionally, it underscores the significance of microstructural analysis in optimising material composition and design for enhanced performance in real-world applications.

The significance of UV-treated polypropylene fibres (PPF) extends beyond the laboratory setting, finding practical relevance in real-world structural applications. UV-treated PPF offers tangible structural integrity and longevity benefits by enhancing cement paste's mechanical properties and durability. In constructions subjected to diverse environmental conditions, such as high temperatures, UV-treated PPF serves as a reliable reinforcement, mitigating crack formation and preserving the structural integrity of concrete elements.

However, excessive use of PPP might also increase the overall porosity of the cement paste, potentially weakening its mechanical properties. Additionally, the absence of fibre reinforcement could reduce crack bridging capability, potentially making the cement paste more susceptible to crack formation and propagation. Therefore, while higher amounts of PPP might improve certain aspects of the cement paste, careful consideration is necessary to balance the reinforcement benefits with potential drawbacks such as increased porosity.

In summary, UV-treated PPF in structural applications represents a practical approach to bolstering the resilience of concrete structures, underscoring the importance of advanced materials and microstructural analysis in engineering durable and sustainable infrastructure for the built environment.

5.13 Free thermal strain and transient thermal strain of a cement paste under load

Transient thermal strain analysis of cement paste plays a pivotal role in investigating the behaviour and performance of cement-based materials subjected to varying temperature conditions. When cement paste experiences changes in temperature, it undergoes thermal expansion or contraction, leading to thermal strain. This phenomenon can result in internal stresses that can potentially impact the cement paste's overall integrity. Thus, gaining insights into these transient thermal strains is essential for understanding the material's behaviour and facilitating preventive measures against potential damage.

The presentation and discussion of the results will be treated separately for the free thermal strain, thermal strain under load, and transient thermal strain. This division will enable a comprehensive understanding of the distinct behaviours exhibited by cement paste under different thermal conditions.

This study investigated cement paste's transient thermal creep behaviour containing polypropylene fibres (PPF). The effect of PPF on transient thermal creep was examined by incorporating different percentages (2%, 3%, and 4%) of PPF, both non-UV-treated and UV-treated, into the cement paste.

5.13.1 Free thermal strain

This study investigated the thermal strain of cement paste samples with different percentages of polypropylene fibre (PPF) additives. The measurements were carried out without applying any axial load, resulting in a stress level of zero. The relationship between the thermal strain increases and the temperature rise was analysed for each cement paste control sample and cement paste containing PP fibres. The results are presented in Figure 5-37 for cement paste with non-treated PPF and Figure 5-38 for cement paste with treated PPF.

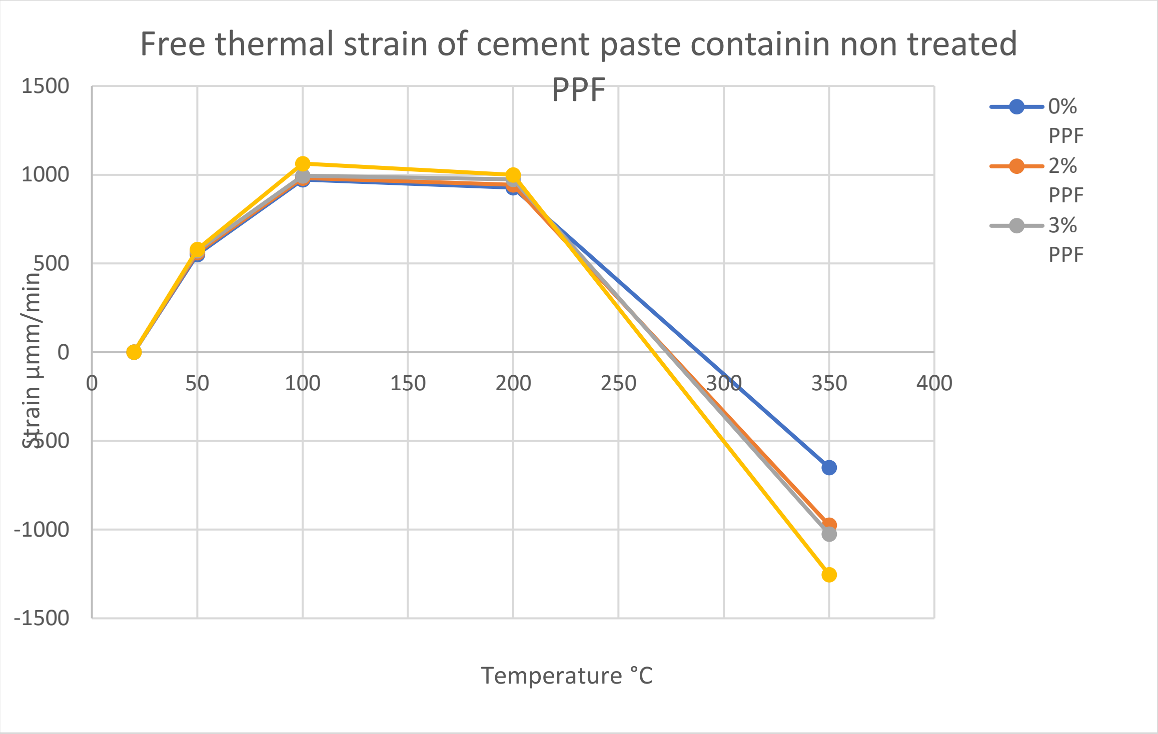

Figure 5- 37: Free thermal strain of cement paste containing non-treated PPF

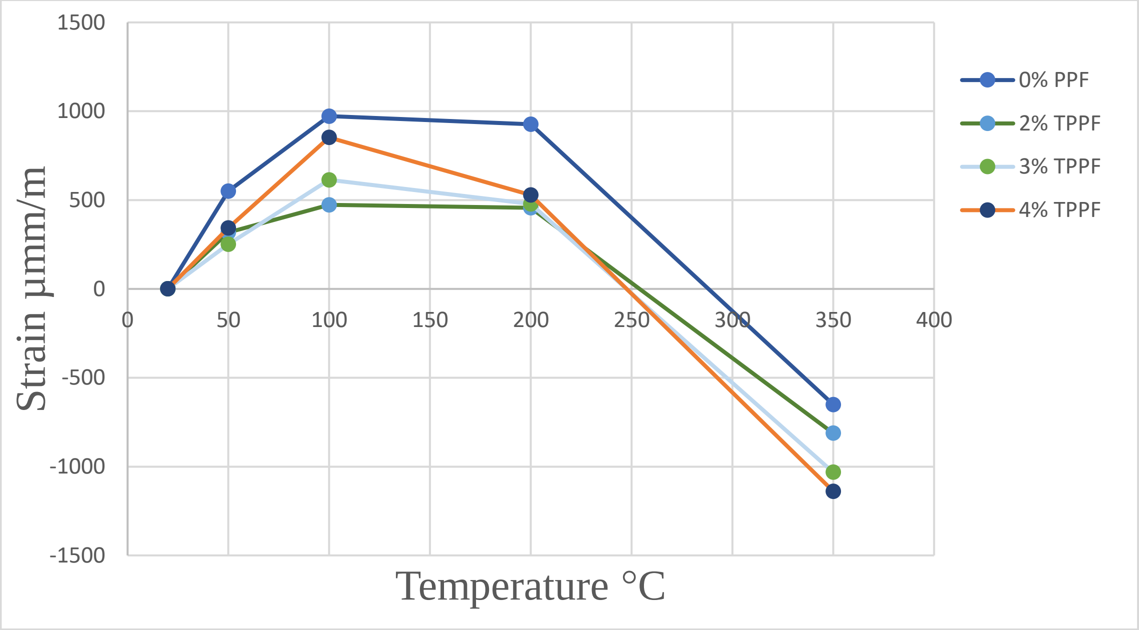

Figure 5- 38: Free thermal strain of cement paste containing UV-treated PPF

All the cement paste samples exhibited thermal expansion as the temperature increased from ambient to 150°C. This expansion was attributed to the increased kinetic energy of particles in the cement paste, resulting from higher temperature conditions. The enhanced particle movement caused the paste to occupy a larger volume. A similar behaviour was reported by Khoury, Grainger, & Sullivan, (1985).

However, as the temperature continued to rise beyond 150°C, the thermal strain gradually decreased and eventually contracted up to 350°C. This phenomenon was linked to specific chemical reactions within the cement paste, such as the decomposition of calcium silicate hydrates, which reduced particle movement and, consequently, decreased volume. Cruz & Gillen (1980) also noted this effect in their experiment.

A comparison of the measured thermal strains revealed that the control sample (cement paste without PPF) and samples containing 2%, 3%, and 4% non-UV treated PPF after 150°C exhibited very low differences. This indicated that the inclusion of PPF did not significantly reduce the thermal expansion of the cement paste. The presence of polypropylene fibres generally tends to restrain the overall expansion of the composite material during temperature changes due to their lower coefficient of thermal expansion compared to cement paste.

In contrast, adding UV-treated PPF in samples with 2%, 3%, and 4% contributed to a reduction in thermal expansion after 150^{o}C. The surface treatment of polypropylene fibres played a crucial role in this effect, mitigating the risk of cracking and enhancing dimensional stability.

At 350°C, the cement paste sample containing 4% non-UV treated PPF demonstrated the highest thermal strain, exhibiting a 23% difference compared to the reference cement paste without PPF. Additionally, as the percentage of non-UV treated PPF increased in other cement paste samples, the thermal strain also showed an increasing trend. Conversely, the thermal strain was reduced in the presence of UV-treated PPF due to the surface treatment, despite the fibres melting. The melted fibres remained within the cement paste samples, as they did not reach the combustion stage, typically occurring at temperatures above 350°C up to 400°C, as explained in section 3.2.5 of the literature.

These findings provide valuable insights into the thermal behaviour of cement paste with the incorporation of polypropylene fibres, emphasising the importance of surface treatment in achieving improved dimensional stability and reduced thermal expansion.

5.13.2 Thermal strain under constant load

The thermal strain exhibited by the sample under a load of 20% of the cold compressive strength of the sample was investigated and analysed. Due to time limitations, data collection was limited to a single sample for the experiment, precluding the originally planned averaging across three samples. Notably, the strain measurements displayed a consistent pattern across all the samples, as the data presented in Figure 5-39 revealed.

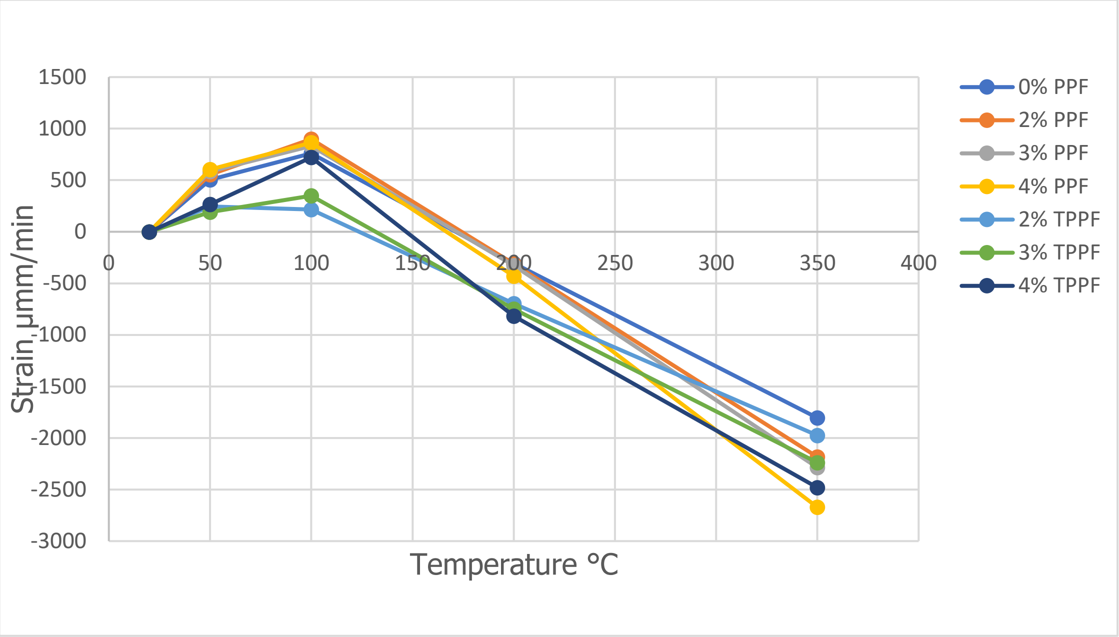

Figure 5- 39: Thermal strain under 20% cold compressive load

Upon subjecting the samples to an elevated temperature, it was observed that the thermal strain increased gradually from the ambient temperature up to 100°C. Subsequently, a noticeable shrinkage in the strain occurred as the temperature continued to rise, reaching 100°C. This contraction phenomenon persisted up to a temperature of 350°C. When examining the control sample, it exhibited a comparatively lower strain value at 350°C.

Adding UV-treated PPF in samples with 2%, 3%, and 4% contributed to a reduction in thermal expansion from 100°C. This result differs from free thermal strain, whereby the sample thermal expansion decreases around 150°C. The surface treatment of polypropylene fibres played a crucial role in this effect, mitigating the risk of cracking and enhancing dimensional stability, which is explained in section 5.13.1.

5.14 Transient thermal creep

To date, no direct experimental testing technique has been developed for measuring the transient thermal strain of concrete. However, since its initial introduction by Johansen and Best, as cited by Khoury, Grainger, & Sullivan, (1985), the transient thermal strain has been indirectly determined by subtracting the free thermal strain and elastic strain from the total strain.

5.14.1 Transient thermal creep behaviour of cement paste containing polypropylene fibre

Figure 5-40 presents the transient thermal creep (TTC) curves for each cement paste sample temperature stage without PPF (0% PPF). This figure shows that the transient thermal creep increases with temperature, particularly after 100°C. The transient thermal creep value at 200°C is -1235.28. The graph shows that transient thermal creep takes place around 100°C. A slight decrease in slope is observed up to around 200°C. These findings support the finding by Mindeguia et al., (2013b), who report the occurrence of transient thermal creep in cement paste at the same temperature range.

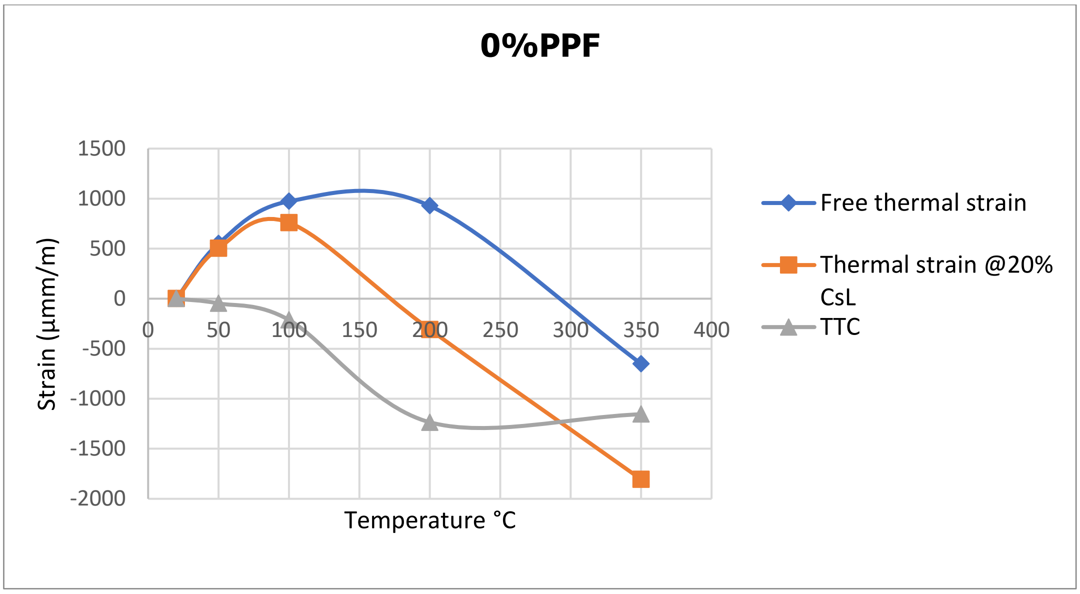

Figure 5- 40: Free thermal strain, thermal strain under load and transient thermal creep for cement paste

5.14.2 Effect of non-UV treated and UV treated PPF on transient thermal creep

Adding PPF, both non-UV treated and UV-treated, at different percentages (2%, 3%, and 4%) to the cement paste resulted in similar transient thermal creep behaviour to the cement paste without PPF.

For the cement paste sample containing 2% non-UV treated PPF shown in Figure 5-41, transient thermal creep was observed from 100°C to 200°C. At this PPF percentage, the strain value remained nearly constant up to 350°C, reaching -1209.74, 6% higher than cement paste without PPF. This difference in strain can be attributed to microstructural changes caused by the melting of PPF within the cement paste and the decomposition of cement hydrate components. This finding aligns with the research conducted by Alogla & Kodur, (2020b).

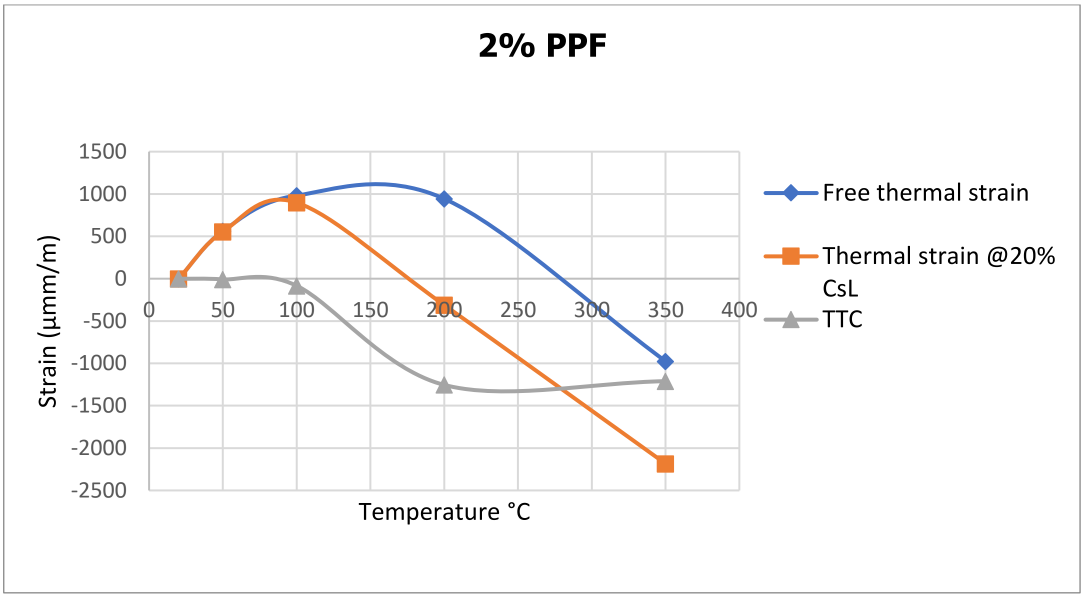

Figure 5- 41: Free thermal strain, thermal strain under load and transient thermal creep for cement paste containing 2% non-UV treated PPF

For the cement paste sample containing 2% UV-treated PPF shown in Figure 5-42, the strain value at 350°C reduced to -1163.01, indicating a reduction in strain of approximately 3.8% compared to the 2% non-UV treated PPF sample. This reduction can be attributed to the UV surface treatment of PPF, which transforms the hydrophobic nature of PPF to hydrophilic.

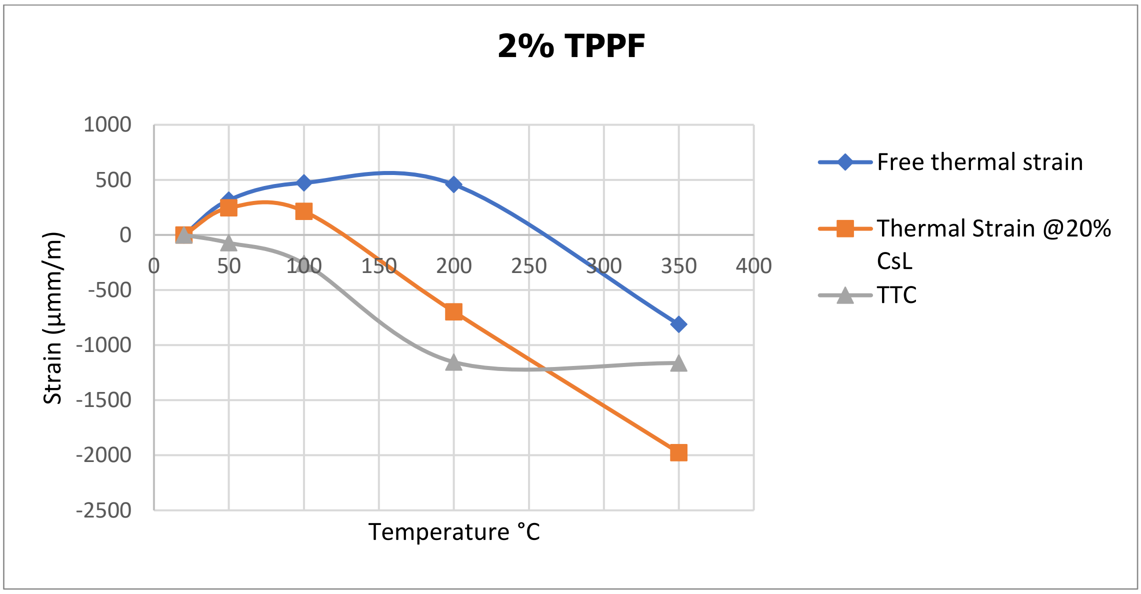

Figure 5- 42: Free thermal strain, thermal strain under load and transient thermal creep for cement paste containing 2% UV-treated PPF

The UV treatment of PPF modifies its surface properties, turning it into a hydrophilic material. This hydrophilic nature enhances the bonding and stress transfer between the TPPF fibres and cement paste matrix, leading to a reduction in strain when subjected to high temperatures. The reduced strain in the cement material makes it more suitable for applications where thermal stress and strain need to be minimised, improving the overall performance and durability of the material.

Similarly, for the cement paste sample containing 3% non-UV treated PPF shown in Figure 5-43, transient thermal creep occurred from 90°C to around 200°C. The strain value remains almost constant up to 350°C. The strain value is -1262.53 at 350ºC, which is 44% higher than the value for the sample with 2% non-UV treated PPF. This increase is associated with the higher quantity of polypropylene (3%) added to the cement paste, which accommodated more space within the cement matrix.

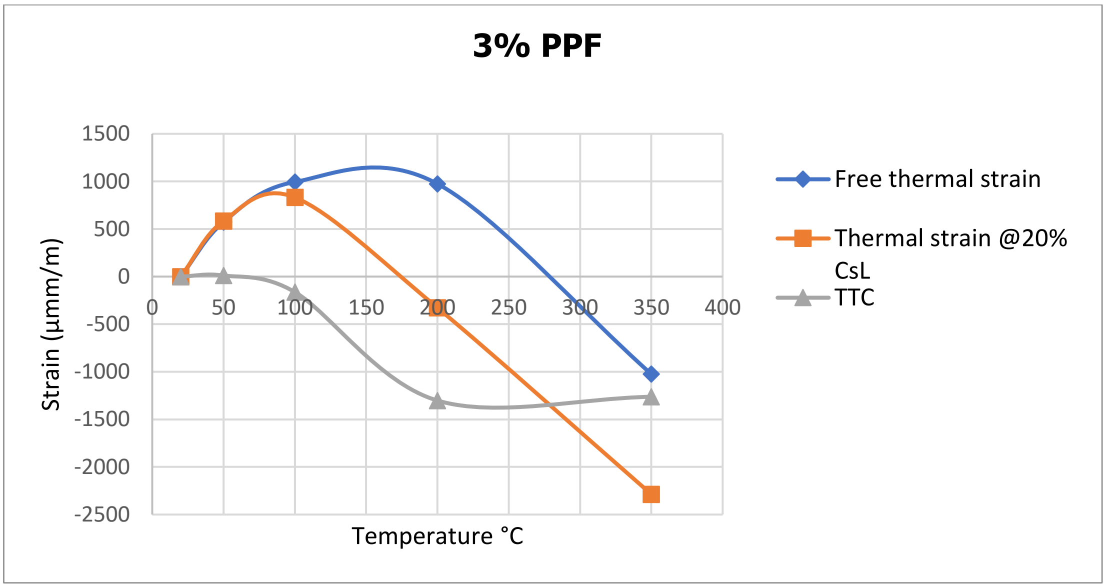

Figure 5- 43: Free thermal strain, thermal strain under load and transient thermal creep for cement paste containing 2% non-UV treated PPF

Incorporating 3% UV-treated PPF in the cement paste sample resulted in a strain value of 1206.42 at 350°C, indicating a reduction in a strain of approximately 4.4%, as shown in Figure 5-44. This reduction further supports the influence of UV surface treatment of PPF on transient thermal creep.

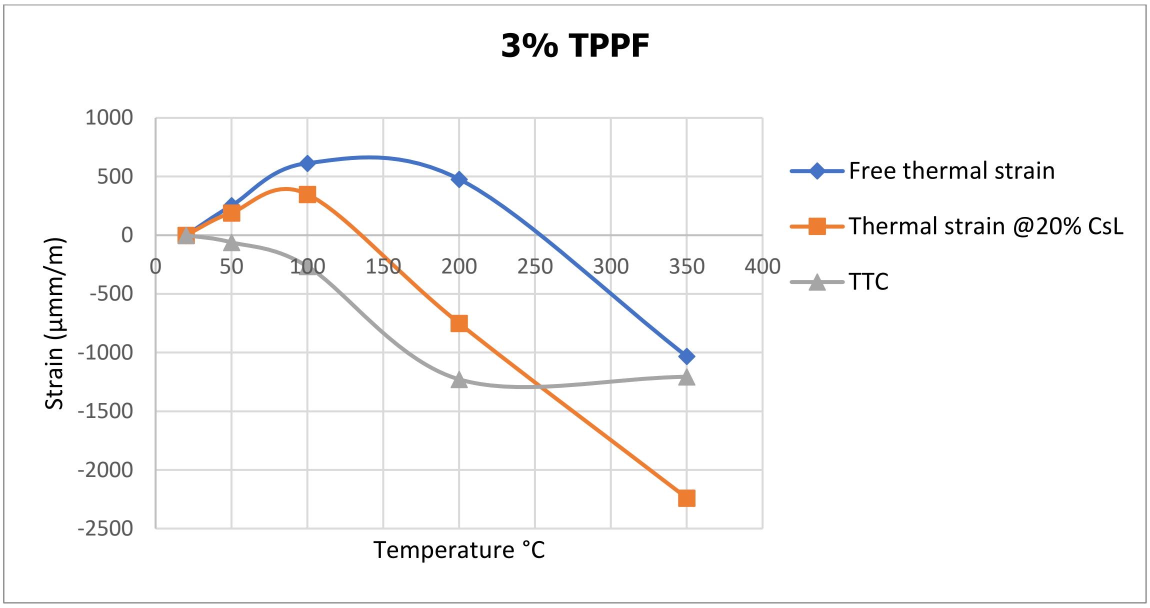

Figure 5- 44: Free thermal strain, thermal strain under load and transient thermal creep for cement paste containing 3% UV-treated PPF

For the cement paste sample containing 4% non-UV treated PPF shown in Figure 5-45, the transient thermal creep occurred from 60°C, and the decrease in slope reached up to 200°C. The strain value at 350°C was found to be -1418.34, reflecting the impact of the increased quantity of PPF (4%) in the cement paste.

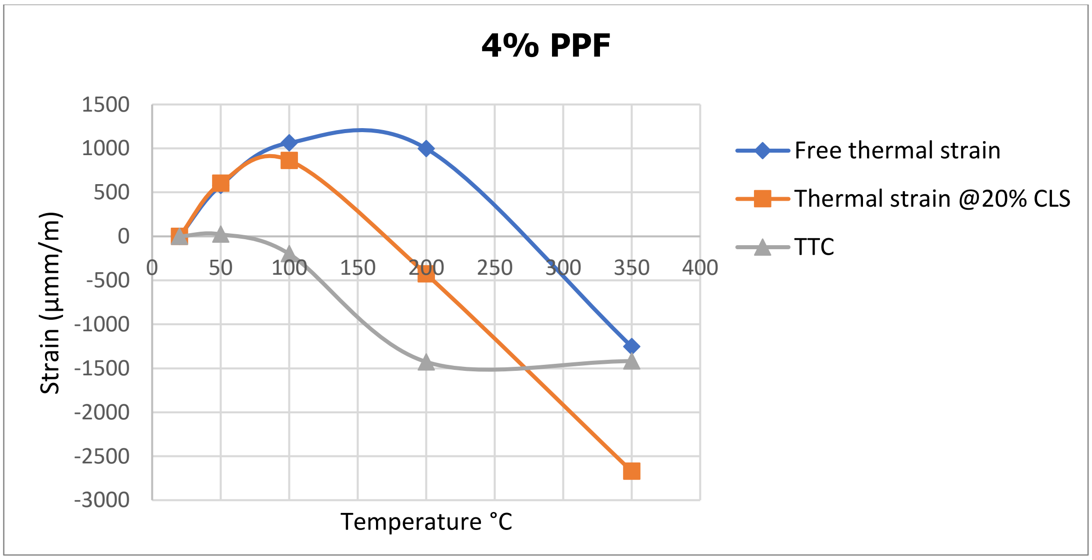

Figure 5- 45: Free thermal strain, thermal strain under load and transient thermal creep for cement paste containing 4% non-UV treated PPF

By incorporating 4% UV-treated PPF, the strain value at 350°C reduced to -1342.27, representing a reduction of approximately 5.7%, as shown in Figure 5-46. This reduction highlights the effect of UV treatment of PPF on transient thermal creep.

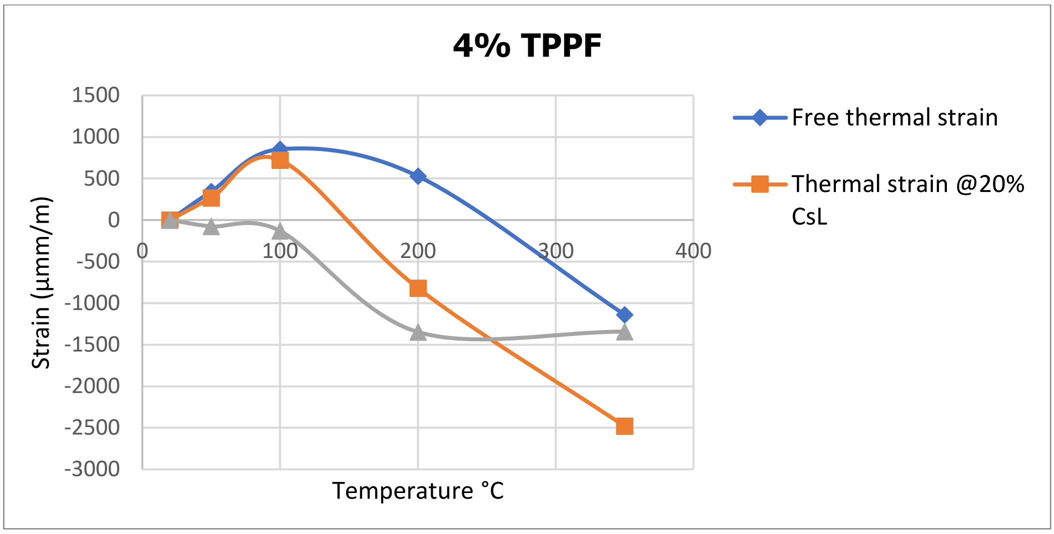

Figure 5- 46: Free thermal strain, thermal strain under load and transient thermal creep for cement paste containing 4% UV-treated PPF

5.14.3 Comparison between the TTS curve for the treated PPF and non-treated PPF

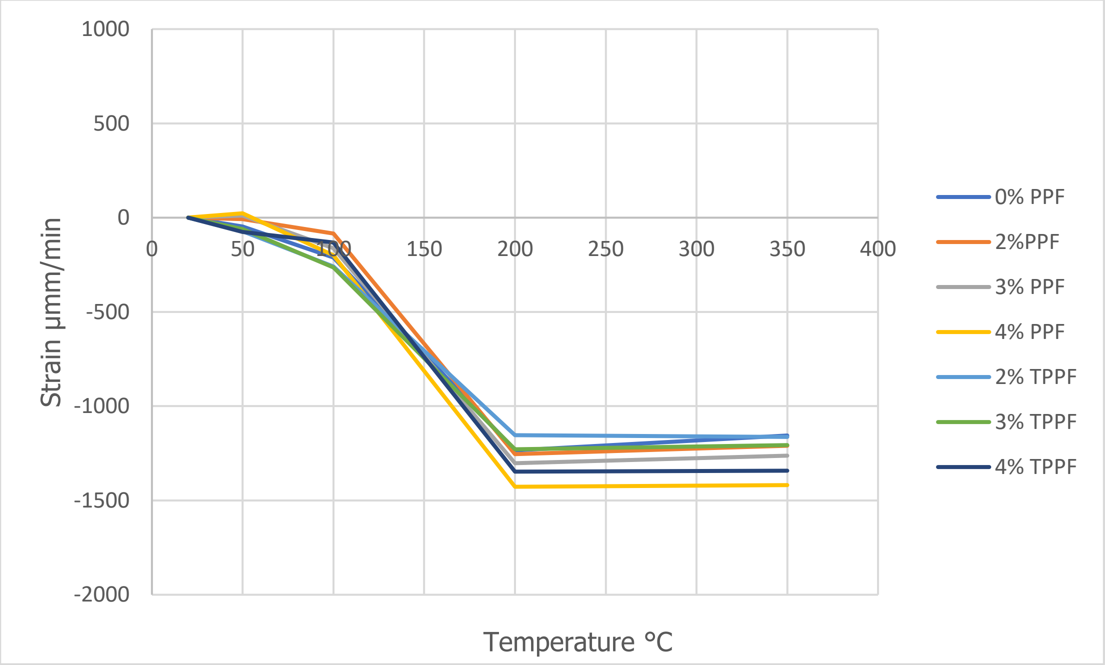

Figure 5- 47: comparison of transient thermal creep for cement paste containing UV-treated PPF and non-treated PPF

The response of various cement paste samples to temperature changes reveals a uniform pattern in their thermal strain behaviour. Initially, as the temperature increases from ambient to around 100°C, all samples have a slight expansion, likely due to thermal expansion, a common phenomenon where materials expand when heated. This expansion phase indicates the material's response to initial heat exposure before reaching a critical temperature threshold.

Upon exceeding this temperature range, all samples start to exhibit contraction, which intensifies as the temperature approaches 200°C. This contraction is primarily attributed to the dehydration of components in the cement paste, particularly the loss of free water and the onset of chemical decomposition of hydrates. As temperatures rise beyond 200°C, the rate of strain reduction slows and tends to be around 400°C. This behaviour suggests a slowdown in chemical decomposition or a stabilization effect where the impacts of thermal expansion and dehydration begin to balance out. The study also investigates the influence of PPF and TPPF on the thermal strain of cement paste. Samples with 3% and 4% PPF show less contraction compared to those with lower or no PPF content, indicating that PPF inclusion can moderate thermal strain.
Moreover, TPPF samples, particularly those with 2% and 3% fibre content, demonstrate even less strain at peak contraction compared to equivalent PPF samples, suggesting that TPPF might be more effective at these percentages. However, at 4%, the difference between PPF and TPPF becomes negligible, indicating a diminished fibre-type impact as the percentage increases. This result highlights the potential of both PPF and TPPF to enhance the thermal performance of cementitious materials, making them potentially more resilient in environments with significant temperature variations.

5.15 Concluding summary

The result presented in the study indicates the importance of considering transient thermal creep in the design of concrete structures exposed to varying temperatures. Transient thermal creep refers to the deformation in cement-based materials due to temperature changes. The study observed that creep increased as the temperature increased, particularly within the critical range of 80°C to 200°C. This finding emphasises the need for measures to mitigate deformation and damage in concrete structures subjected to such temperatures. To address this issue, the study explored using UV-treated polypropylene fibres (PPF) added to the cement paste. The addition of these fibres dissipates thermal stresses that develop during heating. They can accommodate some of the stress generated by temperature changes, reducing the overall thermal strain on the cement paste. The treatment transforms the hydrophobic nature of PPF to hydrophilic, leading to improved performance when incorporated into the cement paste.

Regarding the specific results of the study, when comparing cement paste samples containing different percentages of UV-treated PPF at 350°C:

- 2% UV-treated PPF resulted in a strain reduction of approximately 3.8% compared to the 2% non-UV-treated PPF sample.

- 3% UV-treated PPF led to a strain reduction of approximately 4.4%.
- 4% UV-treated PPF showed a strain reduction of approximately 5.7%.

The study shows the importance of considering transient thermal creep and offers a valuable approach to address this issue using UV-treated polypropylene fibres. This research contributes to the understanding of thermal behaviour in cement paste. It provides valuable insights for formulating strategies to improve the performance and longevity of concrete structures in varying temperature conditions. By adopting these findings and incorporating UV-treated PPF, construction projects can benefit from increased durability and reduced risks associated with thermal strains.

The study shows the importance of considering transient thermal creep and offers a valuable approach to address this issue using UV-treated polypropylene fibres. This research contributes to the understanding of thermal behaviour in cement paste. It provides useful insights for formulating strategies to improve the performance and longevity of concrete structures in varying temperature conditions. By adopting these findings and incorporating UV-treated PPF, construction projects can benefit from increased durability and reduced risks associated with thermal strains.

The main importance of considering transient thermal strain in real structural concrete lies in safeguarding the integrity and longevity of concrete structures exposed to varying temperatures. By acknowledging the impact of transient thermal creep, which causes deformation in cement-based materials due to temperature changes, engineers and designers can implement proactive measures to mitigate potential damage and deformation.

Including UV-treated polypropylene fibres (PPF) in cement paste presents a practical solution to address this issue. These fibres dissipate thermal stresses, reducing the cement paste's overall strain during temperature fluctuations. The observed strain reductions associated with incorporating UV-treated PPF highlight its effectiveness in enhancing the structural resilience of concrete.

Ultimately, construction projects can benefit from increased durability and reduced risks associated with thermal strains by considering transient thermal strain and adopting appropriate strategies, such as incorporating UV-treated PPF. This holistic approach contributes to the longevity and performance of concrete structures, ensuring their reliability under diverse temperature conditions.

Chapter 6: PRACTICAL APPLICATION OF TRANSIENT THERMAL STRAIN MODEL IN CONCRETE

6.1 Introduction

Concrete structures are routinely subjected to transient thermal conditions, such as fire exposure, which elicit intricate thermomechanical responses. These responses are pivotal in determining the structural integrity and safety (Khoury et al., 2004). A comprehensive understanding and precise modelling of these phenomena are paramount in ensuring concrete infrastructure's resilience and reliability under extreme thermal events (Torelli et al., 2016). This study delves into the diverse array of models proposed to elucidate the complex nature of transient thermal strain (TTS) in concrete, focusing on uniaxial formulations to capture the multifaceted behaviour of concrete under varying stress and temperature regimes.

The TTS lies in the interplay between free thermal strain (FTS) and load-induced thermal strain (LITS). FTS arises from the inherent response of concrete to temperature fluctuations, manifesting as strains independent of applied stress (Khoury, Grainger, & Sullivan, 1985). Characterized by low-order polynomial functions of temperature, FTS is pivotal for comprehending the baseline behaviour of concrete under thermal loading. Conversely, LITS represents the additional strain induced by the combined influence of thermal conditions and applied stress (Buttignol, 2020). Accurate prediction of LITS is essential for understanding the full spectrum of concrete behaviour during transient thermal events and is, therefore, a focal point of research in this domain.

In FTS modelling, various approaches have been proposed, ranging from simple polynomial functions to more sophisticated formulations tailored to specific conditions. Notably, the study by Lie, (1994) on linear function for the thermal expansion coefficient (α) offers a concise representation of FTS behaviour in normal-weight concrete with siliceous aggregates, yielding a parabolic strain curve. Moreover, efforts have been made to extend FTS models to encompass high-temperature scenarios (>600°C), as exemplified by Nielsen et al., (2002) and Pearce et al., (2004) formulation, which introduces a coefficient ($\boldsymbol{\alpha_T}$) to encapsulate the ratio of strain rate to temperature variation rate. Such advancements underscore the ongoing quest for robust and versatile modelling techniques capable of capturing the intricacies of concrete behaviour under extreme thermal conditions.

6.2 Models for Transient Thermal Strain (TTS) in Concrete

In concrete mechanics, the characterization and prediction of transient thermal strain (TTS) are critical for ensuring concrete structures' structural stability and performance, especially under varying temperature conditions. Over the years, researchers have developed several models to capture the complex relationship between TTS and temperature, each offering unique insights and methodologies. This introduction provides an overview of three notable models proposed by Nielsen, Diederichs, and Terro, highlighting their contributions to the field and discussing their respective strengths and limitations.

Nielsen, Diederichs, and Terro were considered for this study because their works demonstrate consistent results, validated by experimental data such as findings from Khoury et al., (1986). This consistency ensures high credibility and reliability in their models. Each author contributes unique strengths: Nielsen offers detailed and robust models, Diederichs provides innovative and accurate approaches, and Terro ensures practical relevance and usability. Their complementary strengths and the ability to address individual model limitations provide a balanced and thorough analysis grounded in both theoretical and experimental evidence.

6.2.1 Nielsen's model

Nielsen et al., (2002) proposed a novel TTS model, which offers a versatile approach to relating TTS to both applied stress and temperature. This model, designed to accommodate various concrete compositions and temperature conditions, presents a linear formulation that allows for the independent calibration of the TTS coefficient. By introducing a linear relationship between TTS and both applied stress and temperature, the model achieves a robust framework for understanding thermal strains in concrete.

The key equation proposed by Nielsen et al., (2002) is as follows:

$$\varepsilon_{tts} = \frac{\sigma}{\sigma_{uo}} \mathrm{a}(T - T_o) \qquad \text{6- 1}$$

Where,

ε_{tts} : Transient thermal strain

a : coefficient of free thermal strain

σ: is the initial compressive stress before heating.

σ_{uo}: Uniaxial compressive strength of the concrete

T_o: Initial temperature

T: is the current temperature

Here, the coefficient α is calibrated to 3.8×10^{-5}μs/°C ensuring the best fit of the TTS model across the temperature range of 20–500°C, as established in prior research (Nielsen et al., 2002).

This model offers practical utility, particularly in its ability to decouple the effects of TTS and thermal expansion, its linearity poses limitations. Notably, the formulation may not fully capture the sharp increase in LITS observed at elevated temperatures, typically exceeding 400–500°C. This limitation underscores the need for further refinement or alternative modelling approaches to depict TTS behaviour accurately under extreme thermal conditions.

6.2.2 Diederichs's model

Diederichs, (1987) introduced an innovative model that diverges from conventional linear formulations and captures the intricate nonlinear relationship between TTS and temperature. This departure from linearity is pivotal for accurately characterizing TTS behaviour, especially under extreme thermal conditions.

Central to Diederichs' model is the expression of TTS as a third-order polynomial function of temperature. This sophisticated approach enables a nuanced representation of TTS behaviour, accommodating the complexities inherent in concrete's response to temperature variations, particularly at elevated temperatures. By employing a third-order polynomial, Diederichs' model surpasses the limitations of linear formulations, offering a more precise depiction of LITS phenomena (Li & Purkiss, 2005).

The fundamental equation of Diederichs' model is as follows:

$$\varepsilon_{tts} = \frac{\sigma}{\sigma_{uo}} a_1(T - T_o) + a_2(T - T_o)^2 + a_3(T - T_o)^3 \qquad 6\text{-}2$$

Where,

ε_{tts}: Transient thermal strain

σ: Is the initial compressive stress before heating.

σ_{uo}: Uniaxial compressive strength of the concrete

a_1, a_2, a_3 : are coefficients that describe the relationship between the thermal strain and temperature changes.

T: is the current temperature.

T_o Is a reference temperature, often the initial or ambient temperature.

Here, the coefficients T_o, a_1, a_2, $and \quad a_3 \ are$ meticulously calibrated to experimental data provided by Diederichs. The calibration process ensures the optimal alignment of the model with empirical observations, facilitating accurate predictions of TTS across a range of temperatures. Specifically, the coefficients are determined as follows:

$$T_o = 20°C$$
$$a_1 = +0.0412 * 10^{-3}°C^{-1}$$
$$a_2 = -1.72 * 10^{-7}°C^{-1}$$
$$a_3 = +3.3 * 10^{-10}°C^{-1}$$

This meticulous calibration process underscores the rigour inherent in Diederichs' methodology, ensuring the fidelity of the model to experimental data.

While Diederichs' model entails a greater number of parameters compared to Nielsen's linear formulation, it offers significant advantages in terms of accuracy, particularly for temperatures exceeding 400–500°C. This heightened precision is attributed to the model's ability to capture the nonlinear nature of TTS, which is vital for accurately simulating concrete behaviour under extreme thermal conditions.

6.2.3 Terro's model

Terro's (1998) contribution to concrete mechanics is underscored by the development of the model, which is a significant advancement in the field. From prior research, Terro's model is grounded in identifying the TTS by Khoury et al., (1986), a pivotal reference point that serves as the foundation for subsequent modelling endeavours. By building upon this established framework, Terro effectively leverages existing knowledge to propel innovation in TTS characterization. The proposed equation considers the empirically observed relationship between TTS and the volume fraction of aggregates (Va). It applies to stress levels reaching up to 30% of the compressive strength.

$$\varepsilon_{tts} = \varepsilon_{0.3}(0.032 + 3.226\frac{\sigma_i}{\sigma_{uo}})\frac{V_a}{0.65} \quad 6\text{-}\ 3$$

Where

ε_{tts}: Transient thermal strain

σ_i Is the initial compressive stress before heating.

ε_{tts}: Transient thermal strain

σ_{uo}: Uniaxial compressive strength of the concrete

$\varepsilon_{0.3}$: TTS at a stress/strength ratio of 0.3

V_a: Volume of aggregate

For concrete with calcareous and lightweight aggregates, $\varepsilon_{0.3}$ is defined through a fourth-order polynomial function of temperature.

$$\varepsilon_{0.3} = a_o + a_1T + a_2\,T^2 + a_3\,T^3 + a_4\,T^4 \quad 6\text{-}\ 4$$

Where

$$a_o = -4.39 * 10^{-5}$$
$$a_1 = 2.73 * 10^{-6}$$
$$a_2 = 6.35 * 10^{-8}$$
$$a_3 = -2.19 * 10^{-10}$$
$$a_4 = 2.77 * 10^{-13}$$

Central to Terro's model (Terro, (1998)) aggregate content has been shown to influence concrete behaviour profoundly. By integrating this parameter into the model, Terro extends its applicability across diverse concrete compositions and loading conditions, thereby enhancing its versatility and utility in practical engineering contexts. This comprehensive approach ensures the model can accommodate the inherent variability encountered in real-world construction scenarios, where concrete formulations and environmental factors can vary significantly.

A distinguishing feature of Terro's model lies in its ability to provide a nuanced representation of TTS evolution with temperature. Terro captures the complex interplay between thermal effects and material properties through meticulous analysis and calibration, allowing for accurate TTS behaviour predictions across various temperature regimes.

In the model equation, the factor V_a describes the aggregate volume. It suggests a significant influence on strain behaviour. In practical terms, this relationship allows the model to be adjusted based on the actual aggregate volume to better fit experimental results. By tuning the parameter V_a the model can be calibrated to reflect the specific behaviour of concrete samples tested in experimental settings. This flexibility is crucial for accurately predicting the performance of different concrete mixes under thermal and mechanical loads, particularly in fire conditions.

However, if V_a is adjusted to zero, the entire expression for the ε_{tts} become zero, indicating that the strain induced by the load and temperature would theoretically disappear. This theoretical outcome significantly contrasts with experimental observations and other model predictions.

In reality, the strain induced by temperature and load does not disappear, even if the aggregate content is zero, as in cement paste. This discrepancy arises because V_a represents the volume fraction of aggregate, and eliminating it oversimplifies the complex interactions within the concrete matrix. Aggregates play a crucial role in the thermal and mechanical behaviour of concrete. They influence how heat is conducted through the material and how stress is distributed within the concrete.

6.3 Comparison of the models with experimental results

The three models—Nielsen's, Diederichs', and Terro's—provide a distinct perspective on TTS in concrete mechanics, reflecting varying approaches to capturing the relationship between TTS and temperature. However, all of the models were compared with the experimental results.

The existing literature predominantly addresses transient thermal strain (TTS) modelling within concrete, with limited or no literature on modelling the transient thermal strain of cement paste. This knowledge gap presents a significant challenge in establishing a direct correlation between the modelling methodologies applicable to concrete and those relevant to cement paste. Notably, despite the absence of literature on transient thermal strain modelling on cement paste, experimental findings indicate significant differences in the behaviour of transient thermal strain between concrete and cement paste, primarily attributed to the presence and influence of aggregates, particularly gravels.

Furthermore, the studies conducted by Huismann et al., (2011) and Alogla & Kodur, (2020) indicate that the addition of polypropylene fibre to the concrete matrix does not significantly impact the transient thermal strain (TTS) of concrete. Huismann's study focused on the thermal behaviour of fibre-reinforced concrete and showed that the incorporation of polypropylene fibres did not significantly alter the TTS characteristics of the concrete matrix. Similarly, Alogla and Kudur's research corroborates Huismann's findings by demonstrating that polypropylene fibres do not have a notable effect on the transient thermal strain of concrete. This consistency across different studies suggests that these fibres do not interact strongly with the concrete's response to thermal changes in a way that would affect TTS.

Given that the addition of polypropylene fibres does not markedly affect the transient thermal strain, existing TTS models, such as those proposed by Nielsen, Diederichs, and Terro, can be applied to concrete with polypropylene fibres without significant adjustments. These models primarily account for the thermal and mechanical interactions within the concrete matrix itself, and since polypropylene fibres do not alter these interactions significantly, the models remain valid.

Similarly, the findings from Mindeguia et al., (2013) indicate that transient thermal strain (TTS) primarily occurs in the cement paste, a conclusion that aligns with the results of this work on pure cement paste explained in section 5.14. The experiments conducted in this work also revealed that adding polypropylene fibre to the cement matrix does not significantly affect the TTS of the cement paste, similar to its impact on concrete.

Figure 6-1 compares the TTS behaviour of different models and experimental data for cement paste with and without polypropylene fibres across a range of temperatures. It shows that while the models by Terro, (1998) and Nielsen et al., (2002) generally align with experimental data at lower temperatures, discrepancies arise at higher temperatures. Specifically, the result of this work on cement indicates that the models are reliable up to 200°C. Beyond this point, the accuracy diminishes, likely due to the influence of aggregate materials such as gravel in concrete. These materials may alter the thermal response of the concrete matrix, leading to deviations from the predicted TTS values.

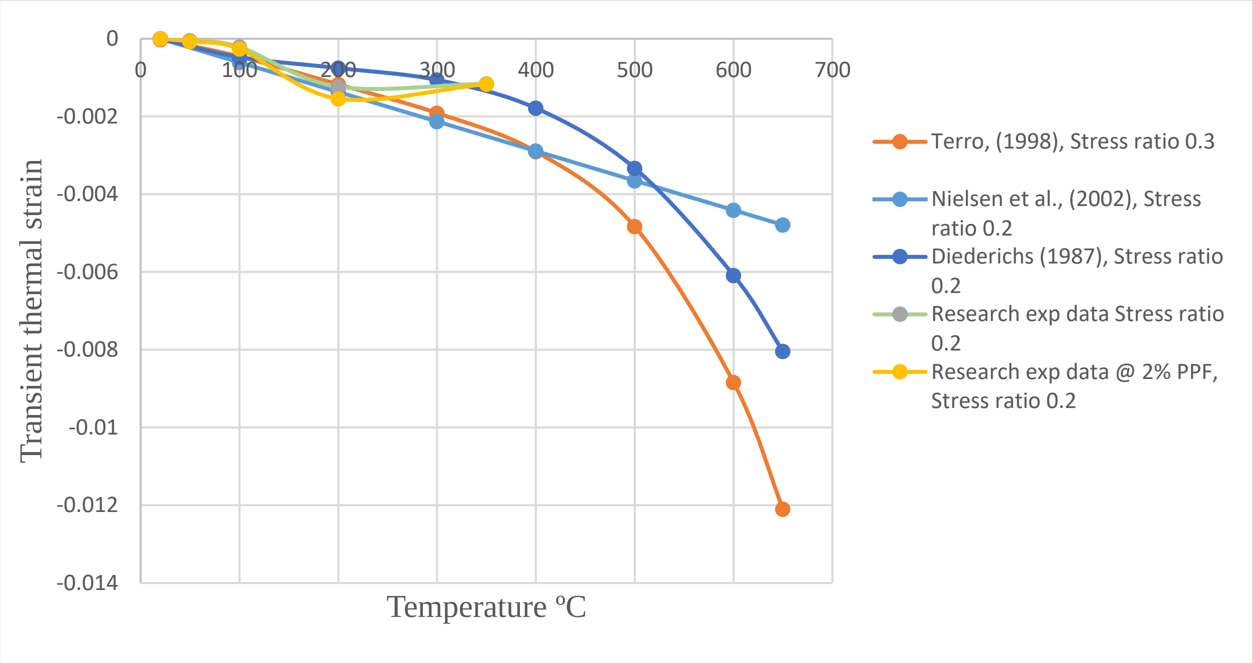

Figure 6- 1: Transient thermal strain. Parabolic model of 65% Va (Terro, 1998), (Nielsen et al., 2002) and (Diederichs, 1987) compared to the research experimental data

The Nielsen model predicts transient thermal strain (TTS) in concrete up to around 200°C, closely aligning with Terro's model and experimental data sets (with and without polypropylene fibres). However, as the temperature increases beyond 300°C, the model's linear approach begins to show limitations, underestimating the TTS compared to the experimental results, particularly at higher temperatures above 500°C. This suggests that while the Nielsen model is reliable for moderate thermal conditions, it does not fully capture the nonlinear increases in TTS observed at elevated temperatures, highlighting the need for more advanced or refined models for high-temperature applications.

Diederichs' model (1987), which uses a nonlinear, third-order polynomial approach, accurately captures the initial steep decline in TTS and also aligns well with experimental data up to approximately 200°C but again diverges at higher temperatures. The experimental data, particularly the dataset incorporating 2% PPF, aligns closely with Diederichs', Terro's, and Nielsen et al.'s models at lower to mid-range temperatures, validating their empirical accuracy.

This suggests that while current models are effective within a 200°C temperature range, the observed divergence at higher temperatures in all models above 200°C indicates that adjustments may be needed to account for the effects of aggregates at higher temperatures.

Typically, cement paste tends to have a higher transient thermal strain than concrete due to the inherent properties and interactions of their components. However, certain conditions can result in concrete exhibiting higher thermal strain than cement paste. For instance, if concrete includes a significant amount of aggregates with a higher thermal expansion coefficient than the cement paste, the concrete might display greater overall thermal strain (Mindess et al., 2003). This can happen with certain lightweight aggregates, as reported by Khoury et al., (1986).

Additionally, if there is poor bonding between the aggregates and the cement paste, the resulting differential thermal expansion can cause microcracking, which increases the overall thermal strain of the concrete (Gal & Kryvoruk, 2010). Concrete that is highly porous and contains a lot of moisture can undergo significant moisture movement during thermal cycles, leading to higher thermal strains due to water phase changes. In contrast, less porous cement paste might not show the same degree of moisture-related thermal strain (Mehta & Monteiro, 2014).

Moreover, the thermal strain response can vary based on the temperature range under certain conditions. Cement paste might demonstrate a more stable thermal response compared to concrete (Bažant et al., 1996). The effect of a constant temperature level on the thermal strain of concrete, as compared to cement paste, can be understood more comprehensively through the analysis presented by Khoury et al., (1986). According to their findings, at around 350°C, concrete exhibits an increase in thermal strain compared to cement paste.

At low temperatures (0°C - 200°C), both models show a similar trend, but the Terro model indicates a steeper initial increase in transient thermal strain compared to the experimental data. This increase in thermal strain of concrete more than that of cement paste might be the model design based on the high number of aggregates in the cement matrix, as reported by Mindess et al., (2003).

The volume fraction of aggregate V_a has a noticeable effect on Terro's model. When the aggregate content is reduced, Terro's model aligns more closely with the experimental results for cement paste, as shown in Figure 6-2, indicating that less aggregate reduces the discrepancies between model predictions and observed data. However, even with reduced aggregate content, Terro's model fails to capture the precise shape of the strain response for cement paste. This limitation becomes evident when V_a is set to zero, resulting in a theoretical elimination of strain, which does not align with experimental observations. Thus, while adjusting V_a can improve model alignment to some extent, it does not fully address the complexities of strain behaviour in cement paste, underscoring the need for models that can accurately account for aggregate effects without oversimplification.

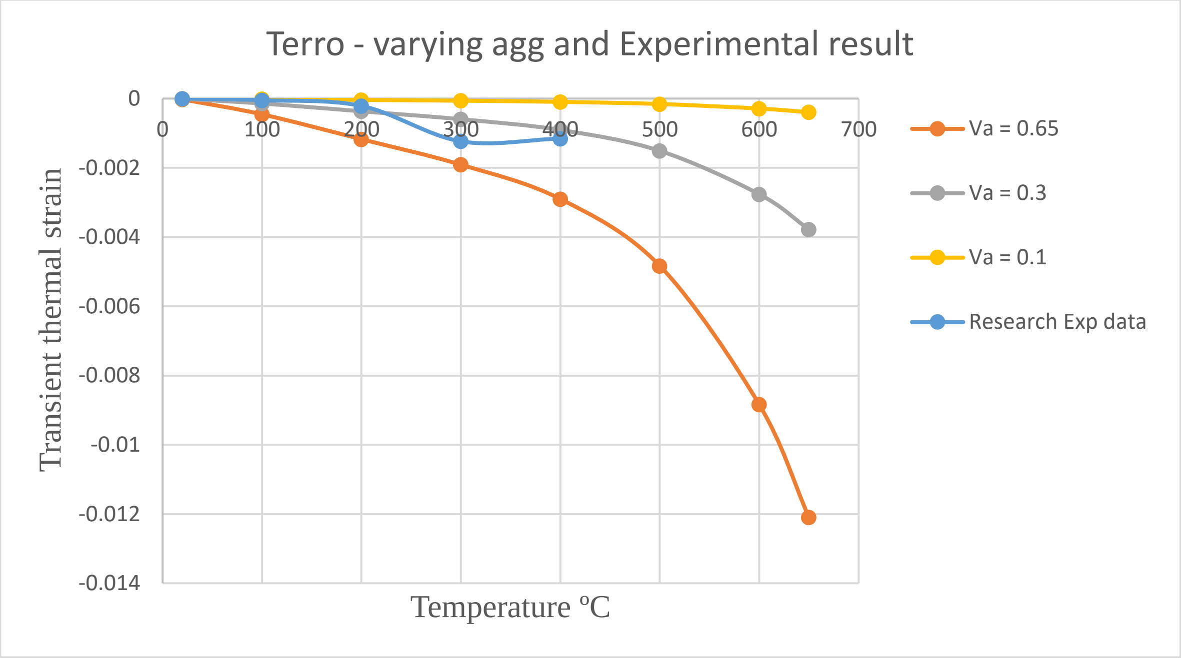

Figure 6- 2: Terro varying aggregate content and the research experimental curve

Additionally, concrete may experience a significant initial thermal strain compared to cement paste, likely because aggregates can initially restrict thermal expansion. The Nielsen model, however, fits with the experimental data in this range, indicating similar thermal strain behaviour between concrete and cement paste initially, despite the difference in composition. This initial similarity can be attributed to the dominant role of the cement matrix in both materials at lower temperatures.

As the temperature increases, both concrete and cement paste experience thermal strain. However, at around 350°C, the thermal strain in concrete, particularly gravel concrete and lightweight concrete, starts to rise sharply, whereas the thermal strain in cement paste increases at a slower rate initially. The figure illustrates that gravel concrete shows a notable increase in strain starting slightly before 350°C, while lightweight concrete shows an even more dramatic increase beyond 350°C.

This behaviour can be attributed to the heterogeneous nature of concrete, which consists of aggregates and cement paste. The aggregates in concrete expand at different rates than the cement paste when subjected to high temperatures. This differential expansion induces additional stresses within the concrete, leading to higher overall thermal strain. In contrast, cement paste, being a more homogeneous material, does not experience the same level of internal stress and thus has a relatively lower increase in thermal strain at 350°C.

6.4 Concluding Summary

This study investigates the behaviour of transient thermal strain (TTS) in cementitious materials under extreme thermal conditions, such as fire exposure, which is crucial for determining structural integrity and safety. This study explores TTS models for concrete to validate the transient thermal strain of cement paste, with a focus on uniaxial formulations. Several models for TTS have been reviewed, highlighting contributions from Nielsen, Diederichs, and Terro. Nielsen's linear model offers versatility and ease of calibration, while Diederichs' third-order polynomial model provides greater accuracy at elevated temperatures. Terro's model, which extends its applicability across diverse concrete compositions and loading conditions, enhances its practical relevance.

This study identifies significant gaps in the existing models, particularly under conditions where concrete exhibits higher thermal strain compared to cement paste, as previously explained. These gaps highlight the necessity for further research aimed at developing transient thermal strain models for concrete that align with experimental results for cement paste. Current models are accurate only up to approximately 200°C for cement paste and cement paste containing PP, indicating a limitation in their applicability to higher temperature ranges and concrete.

Studies by Huismann et al., (2011) and Alogla & Kodur, (2020) show that polypropylene fibres do not significantly affect the transient thermal strain (TTS) of concrete. Similarly, Mindeguia et al., (2013) confirm that TTS mainly occurs in cement paste and is consistent with concrete. This research has shown that adding polypropylene fibres does not notably change TTS in cement paste.

To address this, the development of new models for cement paste is essential. These models should extend the accuracy of thermal strain predictions beyond the current temperature threshold and ensure that the experimental results for cement paste are well-represented. By improving the accuracy of these predictions, particularly in laboratory settings where cement paste is used, the research will significantly contribute to our understanding of thermal behaviour in concrete.

Ultimately, these advancements in modelling will lead to the creation of more resilient concrete structures capable of withstanding extreme thermal events. Enhanced predictive accuracy will allow engineers to design structures that maintain their integrity and safety under high-temperature conditions, thereby extending the lifespan and reliability of concrete infrastructure in various applications.

Chapter 7: CONCLUSION AND FUTURE WORK

7.1 Conclusion

The main conclusions of this research are:

7.1.1 Effect of humidity on residual compressive strength of cement paste with polypropylene fibre and polypropylene powder for both UV-treated and non-treated at high temperatures

This research section aims to investigate the effect of humidity on the residual compressive strength of cement paste containing polypropylene fibre (PPF) and polypropylene powder (PPP), both with and without UV treatment, at high temperatures. The results revealed important insights into cement paste behaviour and polypropylene additives' role in strength enhancement under different conditions. The conclusions are listed below:

- For non-UV-treated PPF samples, it was observed that the addition of PPF at concentrations of 2%, 3%, and 4% led to a decrease in strength compared to the original paste at ambient temperature. This decrease was attributed to the hydrophobic nature of polypropylene, which resulted in poor bonding between PPF and the cement paste. When subjected to elevated temperatures up to 200°C, an increase in strength was observed, attributed to the rapid formation of calcium silicate hydrate (C-S-H) and the loss of non-chemically bound evaporable moisture. However, beyond 200°C, the strength declined due to the melting of PPF, leading to the formation of pores within the cement paste.
- Similarly, non-UV-treated PPP samples decreased strength at 50°C, attributed to the loss of water from the capillary pores and a higher replacement of the cement paste by PPP. The samples showed increased strength at 200°C due to the pressure relief caused by drying and improved arrangement of capillary pores. However, as the temperature increased, the strength declined, primarily due to the decomposition of C-S-H and the formation of additional pores caused by the molten PPP.
- UV-treated PPF samples showed significant strength improvement at ambient temperature, attributed to the transformation of the hydrophobic nature of polypropylene to hydrophilic, leading to enhanced bonding with the cement paste. The strength increase persisted until 200°C, after which it declined due to the decomposition of C-S-H and the possible formation of additional pores.

- For UV-treated PPP samples, a notable increase in strength was observed at 200°C, and this improvement was attributed to the surface chemistry treatment of PP using UV irradiation techniques, which improved bonding with the cement paste. However, at higher temperatures, the strength decreased due to the decomposition of C-S-H and the formation of additional pores caused by the molten PPP.
- For the influence of humidity on residual compressive strength, it was observed that sealing the cement paste samples led to a notable increase in their residual compressive strength when compared to the unsealed cement paste samples. While the difference in strength between the two groups was relatively small, this can be attributed to the storage conditions during the testing period, which maintained a relative humidity of 33%, significantly lower than the environmental humidity range of 90 to 100%.

  Despite the limited difference in strength under specific storage conditions, it is crucial to acknowledge that sealing the cement paste samples consistently improved compressive strength properties throughout the experimentation. These findings indicate that controlling humidity through sealing positively impacts the residual compressive strength of cement paste.

- The result shows significant differences between PPF and PPP in the RCS, which were closely linked to the varying percentages of additives and the distinct physical properties of polypropylene in its fibre and powder forms.

  Polypropylene fibres (PPF), when incorporated at lower percentages, demonstrated a notable improvement in the mechanical properties of the cement paste. This enhancement is primarily attributed to the fibre's ability to bridge cracks within the cement matrix, effectively mitigating the propagation of cracks and thereby increasing the material's overall strength. On the other hand, the use of polypropylene powder (PPP) resulted in an increase in porosity within the cement paste. The powder's fine particulate nature contributed to the formation of a more porous structure, which, in turn, affected the material's compressive strength.

  The study also explored the effects of UV treatment on both PPF and PPP. It was observed that the UV treatment had varying impacts on the RCS depending on whether fibres or powder were used. This variation suggests that the interaction between UV-treated polypropylene and the cement matrix is complex and dependent on the form and characteristics of the polypropylene additive.

7.1.2 The strength and stiffness at a high temperature of the cement paste containing polypropylene fibres with and without UV treatment

This study aims to investigate the compressive strength and stiffness directly measured at a high temperature of cement paste samples containing PPF with and without UV treatment. The results obtained from the experiments shed light on the behaviour of cement paste with varying percentages of PPF at different temperatures, providing valuable insights into the effects of polypropylene fibre addition and UV treatment on the mechanical properties of cement paste. The conclusion can be drawn as follows:

- Non-treated PPF indicates that adding polypropylene fibres negatively impacted the compressive strength of the cement paste at ambient temperature, with higher percentages of PPF leading to more significant reductions in strength. This decrease was attributed to the hydrophobic nature of polypropylene, which hindered proper bonding between the cement paste and fibres. However, at elevated temperatures of 200°C, the strength of all samples, including those containing polypropylene fibres, increased. This improvement was attributed to the rapid formation of calcium silicate hydride (C-S-H) and the loss of non-chemically bonded evaporable moisture.
- For samples containing UV-treated polypropylene fibres, the strength enhancement was more pronounced compared to non-treated polypropylene fibres at different temperatures. The UV treatment reduced the hydrophobic nature of the fibres, leading to improved bonding with the cement paste. At 200°C, treated TPPF samples exhibited significant increases in strength compared to non-treated PPF. However, when exposed to temperatures ranging from 200°C to 350°C, the compressive strength of all samples, both with and without TPPF, declined significantly. The melting of polypropylene and the decomposition of C-S-H contributed to this decline.
- The elastic modulus of the cement paste decreased with increasing temperature, and the addition of PPF also contributed to this reduction. However, the effect of UV-treated PPF on the elastic modulus was not substantially different from that of non-treated PPF at room temperature. At elevated temperatures, the differences in elastic modulus between treated and non-treated PPF were more pronounced, with the UV-treated PPF showing some improvement in stiffness.

7.1.3 The microstructural changes using scanning electron microscopic (SEM) of cement paste containing PPF and PPP for UV-treated and non-treated at high temperatures

This research section aims to investigate the microstructural changes in cement paste containing polypropylene fibres and polypropylene powder, both UV-treated and non-treated, at high temperatures using scanning electron microscopy (SEM). The results of this study shed light on various aspects of the cementitious matrix and its interactions with polypropylene additives, providing valuable insights into the potential improvements in mechanical performance and durability. The conclusion is listed below:

- Firstly, the investigation revealed that as the temperature increased, the porosity of cement paste increased significantly due to the escape of bound water, sample cracking, and degradation of the cementitious matrix. However, at temperatures up to 200°C, the microstructure of the cement paste remained intact, indicated by the consistent brightness of the hydration product (C-S-H). This stability ensured that the compressive strength increment observed at 200°C was predominantly attributed to the maintenance and continued development of C-S-H bonds, making it important for high-temperature applications.
- The microstructural analysis of cement paste containing non-UV treated polypropylene fibres at 20°C showed contact between the fibres and the hydration products. Still, some fibres were pulled out due to the hydrophobic nature of the fibres, resulting in a weaker bond between the fibre and cement paste. On the other hand, UV-treated polypropylene fibres exhibited a strong bond with the cement paste matrix due to their altered surface chemistry from hydrophobic to hydrophilic, contributing to increased compressive strength. Heating the samples at 200°C caused both UV-treated and non-treated polypropylene fibres to melt and volatilise, introducing additional pores and interconnected channels in the cement paste, which improved its performance under high temperatures. However, heating at 350°C reduced compressive strength due to the disintegration of C-S-H.
- Regarding polypropylene powder, both UV-treated and non-treated forms at 20°C did not exhibit a distinct presence within the cement paste matrix. However, due to the PP hydrophilic nature, UV-treated polypropylene powder showed a significant reduction in crack formation compared to non-treated powder. At 200°C, both UV-treated and non-treated polypropylene powder melted, creating additional pores and channels,

negatively affecting the cement paste's strength. At 350°C, the compressive strength was drastically reduced due to the disintegration of C-S-H.

In general, the microstructural investigation demonstrated the crucial role of polypropylene additives in regulating water removal and influencing the performance of cement paste under normal and high-temperature conditions. The dosage and distribution of these additives significantly affected the cementitious matrix's microstructural behaviour and compressive strength. By understanding these microstructural changes, researchers can optimise the use of polypropylene fibres and powder to enhance the performance and durability of cement paste in various applications, including those involving high temperatures.

7.1.4 The transient thermal creep of cement paste containing polypropylene fibres with and without UV treatment

This section aims to quantify the transient thermal creep of cement paste containing polypropylene fibres (PPF) with and without UV treatment. The investigation involved analysing free thermal strain, thermal strain under load, and transient thermal strain of cement paste samples subjected to varying temperature conditions. The conclusions are:

- The investigation into the free thermal strain of cement paste revealed that it exhibited thermal expansion as the temperature increased up to 150°C. Beyond this temperature, the thermal strain gradually contracted to 350°C, mainly due to specific chemical reactions within the cement paste. Adding PPF, non-UV-treated, shows a slight reduction in thermal expansion up to 150°C. However, the presence of UV-treated PPF significantly reduced the thermal expansion of the cement paste, indicating the importance of surface treatment in achieving improved dimensional stability and reduced thermal expansion.
- In the analysis of thermal strain under a constant load of 20% of the cold compressive strength, all samples exhibited a gradual increase in thermal strain up to approximately 80°C, followed by noticeable shrinkage as the temperature continued to rise to 350°C. Adding UV-treated PPF in samples reduced thermal expansion, showing a different behaviour compared to free thermal strain.
- The study observed that transient thermal creep increased with temperature, particularly after 100°C. Adding PPF, both non-UV treated and UV-treated, at different percentages to the cement paste resulted in similar transient thermal creep behaviour to the cement paste without PPF. However, the presence of UV-treated PPF contributed to a reduction in transient thermal creep, indicating improved performance.

- The study highlights the importance of accurately modelling transient thermal strain (TTS) in concrete, particularly under extreme thermal conditions like fire exposure. By examining key models from Nielsen, Diederichs, and Terro, the research identifies strengths and limitations in their ability to predict TTS in concrete and cement paste. The findings underscore a need for further research, particularly to develop models that accurately capture TTS in cement paste beyond 200°C. Improving these models is crucial for enhancing the resilience and safety of concrete structures in high-temperature environments.

Overall, the research contributes valuable insights into the thermal behaviour of cement paste and presents a practical strategy for mitigating the effects of transient thermal creep. By adopting UV-treated PPF and considering one of the models to develop the new model that will predict the TTS of cement paste at a temperature above 200°C. This will help in construction projects that can benefit from increasing the durability and reducing risks associated with thermal strains.

In general, the optimal polypropylene (PP) combinations for cement paste are UV-treated PPF at 2-3% for high-temperature strength and reduced thermal expansion, non-UV-treated PPP at 2% for enhanced porosity and water regulation; UV-treated PPP at less than 5% for high strength with humidity control; and non-UV-treated PPF at 2% for the strength retention up to 200°C. These combinations address the specific requirements of different applications, including thermal stability, porosity management, humidity control, and fire resistance, providing tailored solutions for enhancing the performance and durability of cement paste in various construction environments.

7.2 Future work

Future research should prioritise investigating the flexural strength and tensile strength of cement paste that incorporates UV-treated PPF under high-temperature conditions. Understanding how UV-treated PPF affects the mechanical properties of the cement paste at elevated temperatures is crucial for assessing its potential for real-world applications.

Additionally, it would be beneficial to explore other aspects of the cement paste's microstructure, such as mercury intrusion Porosimetry and X-ray diffraction. These analyses can provide valuable insights into the material's pore structure and crystallographic changes, shedding light on how UV-treated PPF influences the overall composition and performance of the cement paste.

Exploring the potential of UV-treated polypropylene fibres (PPF) within cement paste under high-temperature conditions opens avenues for bolstering the resilience and longevity of concrete structures. One promising direction is investigating the effects of higher temperatures and varying preload levels, providing crucial insights into material behaviour under extreme conditions. Understanding these dynamics is vital for ensuring the safety and reliability of concrete structures in real-world scenarios. Additionally, delving into the influence of different fibre percentages on mechanical properties offers opportunities to optimize reinforcement strategies, thus enhancing the material's resistance to thermal stresses.

Transitioning from cement paste to concrete, a material more representative of real-world structural compositions, offers an intriguing path for further research. By incorporating UV-treated PPF into concrete matrices, researchers can assess its impact on overall mechanical properties and durability under high temperatures. Prioritizing investigations into flexural and tensile strength provides essential data for designing reinforced concrete elements capable of withstanding both thermal stresses and structural loading. Moreover, analysing the microstructure of cement paste can offer deeper insights into the material composition and structural changes induced by UV-treated PPF, aiding in correlating macroscopic behaviour with microstructural features.

Conducting transient thermal creep tests on cement paste specimens containing UV-treated PPF can yield valuable data on long-term deformation behaviour under sustained thermal exposure. Assessing creep characteristics is crucial for evaluating dimensional stability and resistance to time-dependent deformation, which are essential considerations for practical applications. Addressing these research areas enhances our fundamental understanding of material behaviour and lays the groundwork for innovative, resilient construction materials tailored to meet the challenges of modern infrastructure demands.

By addressing these future research areas, a more comprehensive understanding of the effects of UV-treated PPF on cement paste behaviour under high-temperature conditions can be achieved. This knowledge will contribute to developing innovative and durable construction materials for various applications, ensuring the resilience and safety of concrete structures exposed to temperature variations.

Appendix I

Calculation of mix design of cement paste and polypropylene

Mass of dry cement = 1000g

Water /cement ratio = 0.35

Specific gravity of cement = $3.1 g/cm^3$

Specific gravity of water (Qw) = $1 g/cm^3$

Density of polypropylene = $0.946 g/cm^3$

Quantity of water = 1000 * 0.35 = 350g

Volume of cement $(V_c) = \frac{\text{mass of cement}}{\text{Specific gravity of cement}} = \frac{1000}{3.1} = 322.58 m^3$ *Appendix 1- 1*

Volume of water $(V_w) = \frac{\text{mass of water}}{\text{Specific gravity of water}} = \frac{350}{1} =$ 350g *Appendix 1- 2*

Total volume $(V_T) = (V_c) + (V_w) = 322.58 + 350 = 672.58$ *Appendix 1- 3*

Calculate the percentage of polypropylene in grams (g)

Volume of 2%PPF $(V_{PP}) = \frac{2}{100} * (V_T)$, therefore, mass (g) = Density of PP * V_{PP} Appendix 1- 4

Volume of 3%PPF $(V_{PP}) = \frac{3}{100} * (V_T)$, therefore, mass (g) = Density of PP * V_{PP} *Appendix 1- 5*

Volume of 4%PPF $(V_{PP}) = \frac{4}{100} * (V_T)$, therefore, mass (g) = Density of PP * V_{PP} *Appendix 1- 6*

Volume of 5%PPP $(V_{PP}) = \frac{5}{100} * (V_T)$, therefore, mass (g) = Density of PP * V_{PP} *Appendix 1- 7*

Volume of 10%PPP $(V_{PP}) = \frac{10}{100} * (V_T)$, therefore, mass (g) = Density of PP * V_{PP} *Appendix 1- 8*

Volume of 15%PPP $(V_{PP}) = \frac{15}{100} * (V_T)$, therefore, mass (g) = Density of PP * V_{PP} *Appendix 1- 9*

Appendix II

Calculation of elastic modulus (E)

The results contribute to a deeper understanding of the material's response to temperature variations and hold implications for enhancing the performance and durability of cement-based composites in various engineering applications.

$$K = \frac{\mathrm{EA}}{L} \qquad \textit{Appendix 2- 1}$$

Stiffness from the experiment is the slope from the compressive load against the extension, called equivalent stiffness. This equivalent stiffness comprises of stiffness of the machine and the stiffness of the sample.

K_{eq} = Equivalent stiffness

K_m = stiffness of the machine

K_s = stiffness of the sample

Therefore, to find the stiffness of the sample,

$$\frac{1}{K_{eq}} = \frac{1}{K_s} + \frac{1}{K_m} \qquad \textit{Appendix 2- 2}$$

$$\frac{1}{K_s} = \frac{1}{K_{eq}} - \frac{1}{K_m} \qquad \textit{Appendix 2- 3}$$

$$\frac{1}{K_s} = \frac{K_m - K_{eq}}{K_{eq}\, K_m} \qquad \textit{Appendix 2- 4}$$

$$K_s = \frac{K_{eq}\, K_m}{K_m - K_{eq}} \qquad \textit{Appendix 2- 5}$$

Therefore,

from equation (1)

$$E_s = \frac{K_s\,L_s}{A_s} \qquad \textit{Appendix 2- 6}$$

Were, E_s Is the Elastic modulus of the sample

K_s Is the stiffness of the sample

L_s Is the length of the sample

A_s Is the surface area of the sample.

Bibliography

A., S.B., E., M.C., A., K.G. & Dariusz, G. (2002) ‘Thermo-hydro-mechanical modelling of high performance concrete at high temperatures’, *Engineering Computations,* 19(7), pp. 787–819.

Abaeian, R., Behbahani, H.P. & Moslem, S.J. (2018) ‘Effects of high temperatures on mechanical behavior of high strength concrete reinforced with high performance synthetic macro polypropylene (HPP) fibres’, *Construction and Building Materials,* 165pp. 631–638.

Acker, P. & Ulm, F.J. (2001) ‘Creep and shrinkage of concrete: Physical origins and practical measurements’, *Nuclear Engineering and Design,* 203(2–3), pp. 143–158.

Afridi, M.U.K., Ohama, Y., Demura, K. & Iqbal, M.Z. (2001) ‘A note on the comparison of crack resistance of Ca(OH)2 crystals of unmodified and polymer-modified mortars in carbonated atmosphere’, *Cement and Concrete Research,* 31(11), pp. 1643–1645.

Afroughsabet, V. & Ozbakkaloglu, T. (2015) ‘Mechanical and durability properties of high-strength concrete containing steel and polypropylene fibers’, *Construction and Building Materials,* 94pp. 73–82.

Ahmad, S., Shaher, Y. & Al-hawas, M.A. (2014) *Effects of Key Factors on Compressive and Tensile Strengths of Concrete Exposed to Elevated Temperatures,* pp. 4507–4513.

Akand, L., Yang, M. & Wang, X. (2018) ‘Effectiveness of chemical treatment on polypropylene fibers as reinforcement in pervious concrete’, *Construction and Building Materials,* 163pp. 32–39.

Al-mattarneh, H. (2014) ‘Electromagnetic quality control of steel fiber concrete’, *Construction and Building Materials,* 73pp. 350–356.

Alarcon-Ruiz, L., Platret, G., Massieu, E. & Ehrlacher, A. (2005) *The Use of Thermal Analysis in Assessing the Effect of Temperature on a Cement Paste*. Vol. 35.

Alavéz-Ramírez, R., Montes-García, P., Martínez-Reyes, J., Altamirano-Juárez, D.C. & Gochi-Ponce, Y. (2012) ‘The use of sugarcane bagasse ash and lime to improve the durability and mechanical properties of compacted soil blocks’, *Construction and Building Materials,* 34pp. 296–305.

Alberti, M.G., Enfedaque, A. & Gálvez, J.C. (2014) ‘On the mechanical properties and fracture behavior of polyolefin fiber-reinforced self-compacting concrete’, *Construction and Building Materials,* 55pp. 274–288.

Alhozaimy, A.M., Soroushian, P. & Mirza, F. (1996) ‘Mechanical properties of polypropylene fiber reinforced concrete and the effects of pozzolanic materials’, *Cement and Concrete Composites,* 18(2), pp. 85–92.

Ali, M. & Chouw, N. (2013) 'Experimental investigations on coconut-fibre rope tensile strength and pullout from coconut fibre reinforced concrete', *Construction and Building Materials,* 41pp. 681–690.

Allot, A. & Mindorrf, D. (2014) *IB Biology Course Book: 2014 Edition: Oxford IB Diploma Program,* p. 728.

Alogla, S.M. & Kodur, V. (2020a) 'Temperature-induced transient creep strain in fiber-reinforced concrete', *Cement and Concrete Composites,* 113(July), p. 103719.

Alogla, S.M. & Kodur, V. (2020b) 'Temperature-induced transient creep strain in fiber-reinforced concrete', *Cement and Concrete Composites,* 113(December 2018), p. 103719.

Alonso, C. & Fernandez, L. (2004) 'Dehydration and rehydration processes of cement paste exposed to high temperature environments', *Journal of Materials Science,* 39(9), pp. 3015–3024.

American Society of Testing Materials (2009) *ASTM C 305 Standard Practice for Mechanical Mixing of Hydraulic Cement Pastes and Mortars of Plastic Consistency,* pp. 6–8.

Anderberg, Y. & Thelandersson, S. (1976) 'Stress and deformation characteristics of concrete: experimental investigation and material behaviour model', *Bulletin of Division of Structural Mechanics and Concrete Construction,* Bulletin54pp. 1–86.

Ariff, Z.M., Ariffin, A., Rahim, N.A.A. & Jikan, S.S. (2012) 'Rheological Behaviour of Polypropylene Through Extrusion and Capillary Rheometry', *InTech,* pp. 29–48.

Arranz-Andrés, J., Peña, B., Benavente, R., Pérez, E. & Cerrada, M.L. (2007) 'Influence of isotacticity and molecular weight on the properties of metallocenic isotactic polypropylene', *European Polymer Journal,* 43(6), pp. 2357–2370.

Arunachalam, A. & Jayakumar, K. (2015a) 'Briefing: Performance of polypropylene fibre in high-performance concrete', *Proceedings of the Institution of Civil Engineers - Construction Materials,* 168(6), pp. 263–266.

Arunachalam, A. & Jayakumar, K. (2015b) 'Briefing: Performance of polypropylene fibre in high-performance concrete', *Proceedings of Institution of Civil Engineers: Construction Materials,* 168(6), pp. 263–266.

ASTM C 192/C 192M (2002) 'Standard Practice for Making and Curing Concrete Test Specimens in the Laboratory', *Management,* 04pp. 1–8.

ASTM C109 (2000) 'Standard Test Method for Compressive Strength of Hydraulic Cement Mortars', *ASTM International, West Conshohocken,* pp. 1–6.

Atabek Savas, L., Mutlu, A., Dike, A.S., Tayfun, U. & Dogan, M. (2018) 'Effect of carbon fiber amount and length on flame retardant and mechanical properties of intumescent polypropylene composites', *Journal of Composite Materials*, 52(4), pp. 519–530.

Aurenty, P., Lanet, V., Tessadro, A. & Gandini, A. (1997) 'Apparatus for the characterization of the static and dynamic wettability of complex interfaces', *Annual Meeting - Technical Section, Canadian Pulp and Paper Association, Preprints*, Pt A(January 1997), .

Baggott, R. & Gandhi, D. (1981) 'Multiple cracking in aligned polypropylene fibre reinforced cement composites', *Journal of Materials Science*, 16(1), pp. 65–74.

Bažant, Z.P., Cusatis, G. & Cedolin, L. (2004) 'Temperature Effect on Concrete Creep Modeled by Microprestress-Solidification Theory', *Journal of Engineering Mechanics*, 130(6), pp. 691–699.

Bažant, Z.P., Kaplan, M.F. & Bazant, Z.P. (1996) *Concrete at high temperatures: material properties and mathematical models*. London: Addison-Wesley.

Beglarigale, A. & Yazıcı, H. (2015) 'Pull-out behavior of steel fiber embedded in flowable RPC and ordinary mortar', *Construction and Building Materials*, 75pp. 255–265.

Behnood, A. & Ghandehari, M. (2009) 'Comparison of compressive and splitting tensile strength of high-strength concrete with and without polypropylene fibers heated to high temperatures', *Fire Safety Journal*, 44(8), pp. 1015–1022.

Bilodeau, A., Kodur, V.K.R. & Hoff, G.C. (2004) 'Optimization of the type and amount of polypropylene fibres for preventing the spalling of lightweight concrete subjected to hydrocarbon fire', *Cement and Concrete Composites*, 26(2), pp. 163–174.

Bo, J. & Hahn, R. (2013) *Cement and Concrete Research Permeability measurement on high strength concrete without and with polypropylene fi bers at elevated temperatures using a new test setup*, 53pp. 104–111.

Borcia, C., Borcia, G. & Dumitrascu, N. (2011) 'Surface treatment of polymers by plasma and UV radiation', *Romanian Reports of Physics*, 56(1–2), pp. 224–232.

Borderie, C. La, Lawrence, C., N'Guyen, T. & Nahas, G. (2010) 'A mesoscopic approach for a better understanding of the transition from diffuse damage to localized damage', *Fracture Mechanics on Concrete and Concrete Structures, FraMCoS'7*,

Bournazel J. P. and Moranville M (1997) 'Durability of concrete: The crossroad between chemstry and mechanics', *Cement and Concrete Research*, 27(10), pp. 1543–1552.

Buratti, N., Ferracuti, B. & Savoia, M. (2013) 'Concrete crack reduction in tunnel linings by steel fibre-reinforced concretes', *Construction and Building Materials*, 44pp. 249–259.

Buttignol, T.E.T. (2020) 'A load induced thermal strain (LITS) semi-empirical model for plain and steel fiber reinforced concrete subjected to uniaxial compressive load', *Cement and Concrete Research*, 127(September 2019), p. 105896.

Cao, M., Li, L., Yin, H. & Ming, X. (2019) ‘Microstructure and Strength of Calcium Carbonate (CaCO 3) Whisker Reinforced Cement Paste After Exposed to High Temperatures’, *Fire Technology,*

Cavalieri, G. (2001) *British Standard A single copy of this British Standard is licensed to Workmanship on building sites —*, (May), .

Chandramouli, K., Rao, P.S.R., Narayanan, P., Sekhar tirumala, S. & Sravana, P. (2010) ‘Strength properties of glass fiber concrete’, *ARPN J Eng Appl Sci,* 5(January), pp. 1–6.

Chaves, L.P. & Cunha, J. (2014) ‘Design of carbon fiber reinforcement of concrete slabs using topology optimization’, *Construction and Building Materials,* 73pp. 688–698.

Chen, W.X., Yu, J.S., Hu, W. & Chen, G.L. (2016) ‘Partial hydrophilic modification of biaxially oriented polypropylene film by an atmospheric pressure plasma jet with the allylamine monomer’, *Applied Surface Science,* 387pp. 957–964.

Chen, X., Huang, W. & Zhou, J. (2012a) *Effect of moisture content on compressive and split tensile strength of concrete,* 19(December), pp. 427–435.

Chen, X., Huang, W. & Zhou, J. (2012b) ‘Effect of moisture content on compressive and split tensile strength of concrete’, *Indian Journal of Engineering and Materials Sciences,* 19(6), pp. 427–435.

Chylińska, M., Kaczmarek, H., Moszyński, D., Królikowski, B. & Kowalonek, J. (2020) ‘Surface studies of UV irradiated polypropylene films modified with mineral fillers designed as piezoelectric materials’, *Polymers,* 12(3), .

Colina, H. & Sercombe, J. (2004) ‘Transient thermal creep of concrete in service conditions at temperatures up to 300�C’, *Magazine of Concrete Research,* 56(10), pp. 559–574.

Cong, X. & Kirkpatrick, R.J. (1995) ‘Effects of the temperature and relative humidity on the structure of CSH gel’, *Cement and Concrete Research,* 25(6), pp. 1237–1245.

Coopamootoo, K. & Masoero, E. (2018) ‘Cement pastes with UV-irradiated polypropylene: Fracture energy and the benefit of adding metakaolin’, *Construction and Building Materials,* 165pp. 303–309.

Cruz, C.R. & Gillen, M. (1980) ‘Thermal expansion of Portland cement paste, mortar and concrete at high temperatures’, *Fire and Materials,* 4(2), pp. 66–70.

D.Gawin, C.E.Majorana, F.P.& B.A.S. (2001) ‘Modelling thermo-hygro-mechanical behaviour of High Performance Concrete in high temperature environments’. Fracture Mechanics of Concrete Structures p.pp. 199–206.

Davie, C.T., Pearce, C.J. & Bićanić, N. (2010) ‘A fully generalised, coupled, multi-phase, hygro-thermo-mechanical model for concrete’, *Materials and Structures/Materiaux et Constructions,* 43(SUPPL. 1), pp. 13–33.

Davie, C.T., Pearce, C.J. & Bićanić, N. (2014) ‘Fully coupled, hygro-thermo-mechanical sensitivity analysis of a pre-stressed concrete pressure vessel’, *Engineering Structures,* 59(March), pp. 536–551.

DeJong, M.J. & Ulm, F.J. (2007) ‘The nanogranular behavior of C-S-H at elevated temperatures (up to 700 °C)’, *Cement and Concrete Research,* 37(1), pp. 1–12.

Diamond, S. (2004) *The microstructure of cement paste and concrete — a visual primer,* 26pp. 919–933.

Dias, W.P.S., Khoury, G.A. & Sullivan, P.J.E. (1990) ‘Shrinkage of hardened cement paste at temperatures up to 670 C(1238 F)’, *ACI Materials Journal,* 87(3), pp. 204–209.

Diederichs, U. (1987) ‘Models for Describing Concrete Deformation at Steady Temperatures’, *Abschlubkolloquium Bauwerke unter Brandeinwirkung, Technische Universitat, Braunschweig,* 25p. 34.

DiFonzo, N. & Bordia, P. (1998) ‘Reproduced with permission of the copyright owner . Further reproduction prohibited without’, *Journal of Allergy and Clinical Immunology,* 130(2), p. 556.

Ding, Y., Azevedo, C., Aguiar, J.B. & Jalali, S. (2012) ‘Study on residual behaviour and flexural toughness of fibre cocktail reinforced self compacting high performance concrete after exposure to high temperature’, *Construction and Building Materials,* 26(1), pp. 21–31.

Dotreppe, J.C., Franssen, J.M., Bruls, A., Baus, R., Vandevelde, P., Minne, R., Van Nieuwenburg, D. & Lambotte, H. (1997) ‘Experimental research on the determination of the main parameters affecting the behaviour of reinforced concrete columns under fire conditions’, *Magazine of Concrete Research,* 48(6), pp. 117–127.

Faisal, F.W. (1990) ‘Properties and Applications of Fiber Reinforced Concrete’, *JKAU: Eng. Sci,* 2pp. 49–63.

Farah Nora, F.N.A., Bida, S.M., Nasir, N.A.M. & Jaafar, M.S. (2014) ‘Mechanical properties of lightweight mortar modified with oil palm fruit fibre and tire crumb’, *Construction and Building Materials,* 73pp. 544–550.

Fares, H., Remond, S., Noumowe, A. & Cousture, A. (2010) ‘High temperature behaviour of self-consolidating concrete. Microstructure and physicochemical properties’, *Cement and Concrete Research,* 40(3), pp. 488–496.

Feldman, D., Denes, F., Zeng, Z., Denes, A.R. & Banu, D. (2000) ‘Polypropylene fiber-matrix bonds in cementitious composites’, *Journal of Adhesion Science and Technology,* 14(13), pp. 1705–1721.

Felicetti, R. & Gambarova, P.G. (1998) ‘Effects of high temperature on the residual compressive strength of high-strength siliceous concretes', *ACI Materials Journal*, 95(4), pp. 395–406.

Feng, X., Garboczi, E.J., Bentz, D.P., Stutzman, P.E. & Mason, T.O. (2004) 'Estimation of the degree of hydration of blended cement pastes by a scanning electron microscope point-counting procedure', *Cement and Concrete Research*, 34(10), pp. 1787–1793.

Fordham, C.J. & Smalley, I. (1985) *A Simple Thermogravimetric Study of Hydrated Cement*. Vol. 15.

Gal, E. & Kryvoruk, R. (2010) *Properties of concrete*.

Gawin, D., Pesavento, F. & Schrefler, B.A. (2004) 'Modelling of deformations of high strength concrete at elevated temperatures', *Materials and Structures/Materiaux et Constructions*, 37(268), pp. 218–236.

Georgali, B. & Tsakiridis, P.E. (2005) 'Microstructure of fire-damaged concrete. A case study', *Cement and Concrete Composites*, 27(2), pp. 255–259.

George N., Freskakis, Richard C. Burrow, Debbas, E.B. (n.d.) *Strength Properties of Concrete, Elevated Temperatures*,

Giovambattista, N., Debenedetti, P.G. & Rossky, P.J. (2007) 'Effect of surface polarity on water contact angle and interfacial hydration structure', *Journal of Physical Chemistry B*, 111(32), pp. 9581–9587.

Glasser, F.P. (2002) *THE STABILITY OF ETTRINGITE*, (September), pp. 4–6.

Glucklich, J. & Korin, U.R.I. (1975) 'Effect of Moisture Content on Strength and Strain Energy Release Rate of Cement Mortar', *Department of Mechanics, Technion-Israel Institute of Technology, under Contract No NBS(G)- 101*, (2), pp. 517–521.

González-González, V.A., Neira-Velázquez, G. & Angulo-Sánchez, J.L. (1998) 'Polypropylene chain scissions and molecular weight changes in multiple extrusion *', *Polymer Degradation and Stability*, 60(1), pp. 33–42.

Hager, I. & Pimienta, P. (2005a) 'Transient thermal strains of High performance concretes', *Creep, Shrinkage and Durability of Concrete*, (February), pp. 461–472.

Hager, I. & Pimienta, P. (2005b) 'Transient thermal strains of High performance concretes', *Creep, Shrinkage and Durability of Concrete*, (January 2005), pp. 461–472.

Handoo, S.K., Agarwal, S. & Agarwal, S.K. (2002) 'Physicochemical, mineralogical, and morphological characteristics of concrete exposed to elevated temperatures', *Cement and Concrete Research*, 32(7), pp. 1009–1018.

Hayashi, J.I., Nakahara, T., Kusakabe, K. & Morooka, S. (1998) 'Pyrolysis of polypropylene in the presence of oxygen', *Fuel Processing Technology*, 55(3), pp. 265–275.

Henry, M., Darma, I.S. & Sugiyama, T. (2014) 'Analysis of the effect of heating and re-curing on the microstructure of high-strength concrete using X-ray CT', *Construction and Building Materials*, 67pp. 37–46.

Henry, M., R, K.H., Darma, I.S., Sugiyama, T., Vichit-vadakan, W., Kerr, E.A., Promentilla, M.A.B., Sugiyama, T., Darma, I.S., Sugiyama, T. & Promentilla, M. (2016) *Cracking and chemical composition of cement paste subjected to heating and water re-curing transport Heating and Water Re-Curing*, 14pp. 134–143.

Hernández-cruz, D., Hargis, C.W., Bae, S., Itty, P.A., Meral, C., Dominowski, J., Radler, M.J., Kilcoyne, D.A. & Monteiro, P.J.M. (2014) *Cement & Concrete Composites Multiscale characterization of chemical – mechanical interactions between polymer fibers and cementitious matrix*, 48pp. 9–18.

Hernández-Cruz, D., Hargis, C.W., Bae, S., Itty, P.A., Meral, C., Dominowski, J., Radler, M.J., Kilcoyne, D.A. & Monteiro, P.J.M. (2014) 'Multiscale characterization of chemical-mechanical interactions between polymer fibers and cementitious matrix', *Cement and Concrete Composites*, 48pp. 9–18.

Hertz, K.D. (2005) 'Concrete strength for fire safety design', *Magazine of Concrete Research*, 57(8), pp. 445–453.

Hertz, K.D. (1992) 'Danish investigations on silica fume concretes at elevated temperatures', *ACI Materials Journal*, 89(4), pp. 345–347.

Hisham A. Maddah (2016) 'Polypropylene as a Promising Plastic: A Review', *American Journal of Polymer Science*, (January), .

Hou, X., Abid, M., Zheng, W. & Hussain, R.R. (2019) 'Effects of Temperature and Stress on Creep Behavior of PP and Hybrid Fiber Reinforced Reactive Powder Concrete', *International Journal of Concrete Structures and Materials*, 13(1), .

Huismann, S., Weise, F., Meng, B. & Schneider, U. (2011) 'Influence of polypropylene fibres on the thermal strain of high strength concrete at high temperatures', *Journal of Structural Fire Engineering*, 2(3), pp. 173–179.

Huismann, S., Weise, F., Meng, B. & Schneider, U. (2012) 'Transient strain of high strength concrete at elevated temperatures and the impact of polypropylene fibers', *Materials and Structures/Materiaux et Constructions*, 45(5), pp. 793–801.

Ingold, C.K. & Ingold, E.H. (1926) 'CLXIX.—The nature of the alternating effect in carbon chains. Part V. A discussion of aromatic substitution with special reference to the respective roles of polar and non-polar dissociation; and a further study of the relative directive efficiencies of o', *Journal of the Chemical Society (Resumed)*, 129(0), pp. 1310–1328.

Irshidat, M.R., Al-nuaimi, N. & Rabie., M. (2020) *The Role of Polypropylene Microfibers in*

Thermal Properties and Post-Heating Behavior of Cementitious Composite, pp. 12–15.

Janotka, I. & Nürnbergerová, T. (2005) ‘Effect of temperature on structural quality of the cement paste and high-strength concrete with silica fume’, *Nuclear Engineering and Design*, 235(17–19), pp. 2019–2032.

Jeffery D. Peterson, Sergey Vyazovkin, C.A.W. (2001) *Macro Chemistry Physics - 2001 - Peterson - Kinetics of the Thermal and Thermo-Oxidative Degradation of Polystyrene (1).pdf*, 202pp. 775–784.

József Karger-Kocsis Tamás Bárány (2006) *Polypropylene handbook, Morphology, Blends and Composites*. Vol. 43. Budapest, Hungary: Springer Nature Switzerland AG.

K.-Ch. Thienel and F.S. Rostasy (1996) ‘Transient Creep of Concrete under Biaxial Strees and High Temperature’, *Cement and Concrete Research*, 26(9), pp. 1409–1422.

K. Murahari, R. mohan R. p (2013) ‘Effects of Polypropylene fibres on the strength properties Of fly ash based concrete’, *International Journal of Engineering Science Invention*, 2(5), pp. 13–19.

Kalifa, P., Chéné, G. & Gallé, C. (2002) ‘High-temperature behaviour of HPC with polypropylene fibres’, *Cement and Concrete Research*, 31(10), pp. 1487–1499.

Karahan, O. & Atiş, C.D. (2011) ‘The durability properties of polypropylene fiber reinforced fly ash concrete’, *Materials and Design*, 32(2), pp. 1044–1049.

Kene, K.S. (2012) ‘Experimental Study on Behavior of Steel and Glass Fiber Reinforced Concrete Composites’, *Bonfring International Journal of Industrial Engineering and Management Science*, 2(4), pp. 125–130.

Khan, M.S., Fuzail Hashmi, A., Shariq, M. & Ibrahim, S.M. (2023) ‘Effects of incorporating fibres on mechanical properties of fibre-reinforced concrete: A review’, *Materials Today: Proceedings*, (xxxx), .

Khoury, G.A. (1992a) ‘Compressive strength of concrete at high temperatures: A reassessment’, *Magazine of Concrete Research*, 44(161), pp. 291–309.

Khoury, G.A. (1992b) ‘Compressive strength of concrete at high temperatures: A reassessment’, *Magazine of Concrete Research*, 44(161), pp. 291–309.

Khoury, G. A., Dias, W.P. & Sullivan, P.J.E. (1986) ‘Deformation of concrete and cement paste loaded at constant temperatures from 140 to 724°C’, *Materials and Structures*, 19(2), pp. 97–104.

Khoury, G.A., Grainger, B.N. & Sullivan, P.J.E. (1985) ‘Transient Thermal Strain of Concrete: Literature Review, Conditions Within Specimen and Behaviour of Individual Constituents.’, *Magazine of Concrete Research*, 37(132), pp. 131–144.

Khoury, G.A., Grainger, B.N., Sullivan, P.J.E., Khoury, G.A., Sullivan, P.J.E. & Grainger, B.N. (1985) ‘Strain of concrete during first heating to 600°C under load’, *Magazine of Concrete Research*, 37(133), pp. 195–215.

Khoury, G.A., Majorana, Ã.C.E., Pesavento, F. & Schrefler, B.A. (2002) *Modelling of heated concrete*, (May 2014), .

Khoury, G.A., Majorana, C.E., Pesavento, F. & Schrefler, B.A. (2004) ‘Modelling of heated concrete’, *Magazine of Concrete Research*, 54(2), pp. 77–101.

Khoury, Gabriel A., Sullivan, P.J.E. & Grainger, B.N. (1986) ‘Strain of concrete during first cooling from 600°C under load’, *Magazine of Concrete Research*, 38(134), pp. 3–12.

Khoury, G. A. & Willoughby, B. (2008) ‘Polypropylene fibres in heated concrete. Part 1: Molecular structure and materials behaviour’, *Magazine of Concrete Research*, 60(2), pp. 125–136.

Khoury, G A & Willoughby, B. (2008) *Polypropylene fibres in heated concrete . Part 1 : Molecular structure and materials behaviour*, 9831(2), pp. 125–136.

Kim, J.-K., Moon, Y.-H. & Eo, S.-H. (1998) ‘Compressive Strength Development of Concrete With’, *Compressive Strength Development of Concrete With Different Curing Time and Temperature*, 28(12), pp. 1761–1773.

Kim, N.K., Lin, R.J.T. & Bhattacharyya, D. (2017) ‘Flammability and mechanical behaviour of polypropylene composites filled with cellulose and protein based fibres: A comparative study’, *Composites Part A: Applied Science and Manufacturing*, 100pp. 215–226.

Kirchhof, L.D., Cattelan, R., Lima, A. De, Carlos, L. & Filho, S. (2020) *Effect of Moisture Content on the Behavior of High Strength Concrete at High Temperatures Efeito do Teor de Umidade no Comportamento do Concreto de Alta Resistência em Altas Temperaturas*,

Komonen, J. & Penttala, V. (2003) ‘Effects of high temperature on the pore structure and strength of plain and polypropylene fiber reinforced cement pastes’, *Fire Technology*, 39(1), pp. 23–34.

Kumar Mehta, P.D. & Paulo J. M. Monteiro, P.D. (2014) *Concrete: Microstructure, Properties, and Materials, Fourth Edition*. 4th ed. New York: McGraw-Hill Education.

Kunther, W., Ferreiro, S. & Skibsted, J. (2017) ‘Influence of the Ca/Si ratio on the compressive strength of cementitious calcium-silicate-hydrate binders’, *Journal of Materials Chemistry A*, 5(33), pp. 17401–17412.

Lee, J.S., Xi, Y. & Willam, K. (2007) ‘Strength and stiffness of concrete under heating and cooling treatments’, *Fracture Mechanics of Concrete and Concrete Structures, Vols 1-3*, 1–3pp. 1709-17141886.

Leo, S. & Horiguchi, T. (2006) *Effect of short fibers on residual permeability and mechanical properties of hybrid fibre reinforced high strength concrete after heat exposition*, 36pp. 1672–1678.

LI Bei-xing, CHEN Ming-xiang, CHENG Fang, LIU Lu-ping (2004) 'The Mechanical Properties of Polypropylene Fiber Reinforced Concrete', *Journal of Wuhan University of Technology - Mater. Sci. Ed.*, 19(3), pp. 68–71.

Li, L.Y. & Purkiss, J. (2005) 'Stress-strain constitutive equations of concrete material at elevated temperatures', *Fire Safety Journal*, 40(7), pp. 669–686.

Liang, J.Z. & Peng, W. (2009) 'Melt viscosity of PP and FEP/PP blends at low shear rates', *Polymer Testing*, 28(4), pp. 386–391.

Lie, T.T. (1994) *Fire Resistance of Circular Steel Columns*, 120(5), pp. 1489–1509.

Liu, X., Ye, G., De Schutter, G., Yuan, Y. & Taerwe, L. (2008) 'On the mechanism of polypropylene fibres in preventing fire spalling in self-compacting and high-performance cement paste', *Cement and Concrete Research*, 38(4), pp. 487–499.

Liu, X, Ye, G., Schutter, G. De, Yuan, Y. & Taerwe, L. (2008) *On the mechanism of polypropylene fibres in preventing fire spalling in self-compacting and high-performance cement paste*, 38pp. 487–499.

López-Buendía, A.M., Romero-Sánchez, M.D., Climent, V. & Guillem, C. (2013) 'Surface treated polypropylene (PP) fibres for reinforced concrete', *Cement and Concrete Research*, 54pp. 29–35.

Lovata, N.L. & Fahmy, M.F. (1987) 'Interfacial bond study of a chemically treated polypropylene fibre-reinforced concrete', *Construction and Building Materials*, 1(2), pp. 83–87.

M. Saad, S.A. Abo-El-Eneini, G.B.H. and M.F.K. (1996) 'Effect of temperature on phsical and mechanical properties of concrete containing silica fume', *Cement and Concrete Research*, 26(5), pp. 669–675.

Malchiodi, B., Pelaccia, R., Pozzi, P. & Siligardi, C. (2023) 'Three sustainable polypropylene surface treatments for the compatibility optimization of PP fibers and cement matrix in fiber-reinforced concrete', *Ceramics International*, 49(14), pp. 24611–24619.

Malik, M., Bhattacharyya, S.K. & Barai, S. V. (2021) 'Microstructural Changes in Concrete: Postfire Scenario', *Journal of Materials in Civil Engineering*, 33(2), p. 04020462.

Mandolfino, C., Lertora, E., Gambaro, C. & Pizzorni, M. (2019) 'Functionalization of neutral polypropylene by using low pressure plasma treatment: Effects on surface characteristics and adhesion properties', *Polymers*, 11(2), .

Manolis, G.D., Gareis, P.J., Tsonos, A.D. & Neal, J.A. (1997) 'Dynamic properties of polypropylene fiber-reinforced concrete slabs', *Cement and Concrete Composites,* 19(4), pp. 341–349.

Masse, S., Vetter, G., Boch, P. & Haehnel, C. (2002) 'Elastic modulus changes in cementitious materials submitted to thermal treatments up to 1000°C', *Advances in Cement Research,* 14(4), pp. 169–177.

Menou, A., Mounajed, G., Boussa, H., La Borderie, C. & Lafdi, K. (2008) 'Thermal damage approach of concrete: Application to specimens subjected to combined compressive and high temperature loads', *High Temperature Materials and Processes,* 27(1), pp. 23–39.

Mindeguia, J.C., Hager, I., Pimienta, P., Carré, H. & La Borderie, C. (2013a) 'Parametrical study of transient thermal strain of ordinary and high performance concrete', *Cement and Concrete Research,* 48pp. 40–52.

Mindeguia, J.C., Hager, I., Pimienta, P., Carré, H. & La Borderie, C. (2013b) 'Parametrical study of transient thermal strain of ordinary and high performance concrete', *Cement and Concrete Research,* 48pp. 40–52.

Mindess, S., Young, J.F. & Darwin, D. (2003) 'Concrete Prentice Hall PTR', *Upper Saddle River,*

Naus, D. (2005) 'The Effect of Elevated Temperature on Concrete Materials and Structures — A Literature Review', *Contract,* 6283(1886), p. 184.

Nie, H.Y., Walzak, M.J., Berno, B. & McIntyre, N.S. (1999) 'Atomic force microscopy study of polypropylene surfaces treated by UV and ozone exposure: Modification of morphology and adhesion force', *Applied Surface Science,* 144–145pp. 627–632.

Nielsen, C. V., Pearce, C.J. & Bićanić, N. (2002) 'Theoretical model of high temperature effects on uniaxial concrete member under elastic restraint', *Magazine of Concrete Research,* 54(4), pp. 239–249.

Noumowe, A. (2005) 'Mechanical properties and microstructure of high strength concrete containing polypropylene fibres exposed to temperatures up to 200 °c', *Cement and Concrete Research,* 35(11), pp. 2192–2198.

Noumowé, A.N. (2003) 'Temperature Distribution and Mechanical Properties of High-Strength Silica Fume Concrete at Temperatures up to 200 °C', *ACI Materials Journal,* 100(4), pp. 326–330.

Noumowe, A.N., Clastres, P., Debicki, G. & Costaz, J.L. (1996) 'Transient heating effect on high strength concrete', *Nuclear Engineering and Design,* 166(1), pp. 99–108.

Odelson, J.B., Kerr, E.A. & Vichit-Vadakan, W. (2007) 'Young's modulus of cement paste at elevated temperatures', *Cement and Concrete Research,* 37(2), pp. 258–263.

Osman N. Oktar, H.M. and M.A.T. (1996) 'Factors Determining the correlations between concrete properties', *Cement and Concrete Research*, 26(11), pp. 1629–1637.

Ossola, G. & Wojcik, A. (2014) 'UV modification of tire rubber for use in cementitious composites', *Cement and Concrete Composites*, 52pp. 34–41.

Ozawa, M. & Morimoto, H. (2014) 'Effects of various fibres on high-temperature spalling in high-performance concrete', *Construction and Building Materials*, 71pp. 83–92.

Pacheco-Torgal, F. & Jalali, S. (2011) 'Cementitious building materials reinforced with vegetable fibres: A review', *Construction and Building Materials*, 25(2), pp. 575–581.

Pan, Z., Sanjayan, J.G. & Collins, F. (2014) 'Effect of transient creep on compressive strength of geopolymer concrete for elevated temperature exposure', *Cement and Concrete Research*, 56pp. 182–189.

Park, J.M., Kim, P.G., Jang, J.H., Wang, Z., Hwang, B.S. & DeVries, K.L. (2008) 'Interfacial evaluation and durability of modified Jute fibers/polypropylene (PP) composites using micromechanical test and acoustic emission', *Composites Part B: Engineering*, 39(6), pp. 1042–1061.

Pearce, C.J., Nielsen, C. V. & Bićanić, N. (2004) 'Gradient enhanced thermo-mechanical damage model for concrete at high temperatures including transient thermal creep', *International Journal for Numerical and Analytical Methods in Geomechanics*, 28(7–8), pp. 715–735.

Peng, G.-F. & Huang, Z.-S. (2008) *Change in microstructure of hardened cement paste subjected to elevated temperatures*. Vol. 22.

Pereira-de-oliveira, L.A., Castro-gomes, J.P. & Nepomuceno, M.C.S. (2012) 'Effect of acrylic fibres geometry on physical , mechanical and durability properties of cement mortars', *Construction and Building Materials*, 27(1), pp. 189–196.

Petkovski, M. (2010) 'Cement and Concrete Research Effects of stress during heating on strength and stiffness of concrete at elevated temperature', *Cement and Concrete Research*, 40(12), pp. 1744–1755.

Petrus, C., Ain Azhar, H., Dee, G.L., Ismail, R. & Alisibramulisi, A. (2016) 'Compressive strength of concrete with fibres at elevated temperature', *Jurnal Teknologi*, 78(5–4), pp. 71–74.

Piasta, J. (n.d.) *Heat deformations of cement paste phases and the microstructure of cement paste*, pp. 415–420.

Picandet, V., Khelidj, A. & Bastian, G. (2001) 'Effect of axial compressive damage on gas permeability of ordinary and high-performance concrete', *Cement and Concrete Research*, 31(11), pp. 1525–1532.

Pijpers, A.P. & Meier, R.J. (2001) 'Adhesion behaviour of polypropylenes after flame treatment determined by XPS(ESCA) spectral analysis', *Journal of Electron Spectroscopy and Related Phenomena*, 121(1–3), pp. 299–313.

Pujadas, P., Blanco, A., Cavalaro, S., Fuente, A. De & Aguado, A. (2014) 'Fibre distribution in macro-plastic fibre reinforced concrete slab-panels', *Construction and Building Materials,* 64pp. 496–503.

Quinn Cement (2011) *Quinn CEM II / A-L 32 , 5R General Purpose Cement (Bagged),* 44(1), p. 8866.

Rico, S., Farshidpour, R. & Tehrani, F.M. (2017) 'State-of-the-Art Report on Fiber-Reinforced Lightweight Aggregate Concrete Masonry', *Advances in Civil Engineering,* 2017.

RILEM TC 129-MHT (1997) 'Test methods for mechanical properties of concrete at high temperatures - Recommendations: Part 6 - Thermal Strain 3', *Materials and Structures,* (March), pp. 17–21.

De Sa, C. & Benboudjema, F. (2011) 'Modeling of concrete nonlinear mechanical behavior at high temperatures with different damage-based approaches', *Materials and Structures/Materiaux et Constructions*, 44(8), pp. 1411–1429.

Sabeur, F.M. and H. (2006) 'A THERMO-HYDRO–DAMAGE MODEL FOR THE DEHYDRATION CREEP OF CONCRETE SUBJECTED TO HIGH TEMPERATURE', *III European Conference on Computational Mechanics,*

Sabeur, H. & Colina, H. (2015) 'Effect of heating–cooling cycles on transient creep strain of high performance, high strength and ordinary concrete under service and accidental conditions', *Materials and Structures/Materiaux et Constructions*, 48(5), pp. 1561–1579.

Sabeur, H. & Meftah, F. (2008) 'Dehydration creep of concrete at high temperatures', *Materials and Structures/Materiaux et Constructions,* 41(1), pp. 17–30.

Sant, G., Lothenbach, B., Juilland, P., Saout, G. Le, Weiss, J. & Scrivener, K. (2011) 'The origin of early age expansions induced in cementitious materials containing shrinkage reducing admixtures', *Cement and Concrete Research,* 41(3), pp. 218–229.

Sarshar, R. (1989) 'Effect of elevated temperatures on the strength of different cement paste and concrete', *A thesis submitted for the Degree of Doctor of Philosophy of the University of London*, 6(6.1), p. 93.

Sarshar, R. & Khoury, G.A. (1993) 'Material and environmental factors influencing the compressive strength of unsealed cement paste and concrete at high temperatures', *Magazine of Concrete Research,* 45(162), pp. 51–61.

Sayyar, M., Soroushian, P., Maqbool, M., Balachandra, A. & Lu, J. (2013) 'Low-cost glass fiber composites with enhanced alkali resistance tailored towards concrete reinforcement', *Construction and Building Materials,* 44pp. 458–463.

Schneider (1976) 'Behaviour of concrete under thermal steady state and non-steady state conditions', *Fire and Materials,* (1), pp. 103–115.

Schneider, U. (1988) 'Concrete at high temperatures — A general review', *Fire Safety Journal,* 13(1), pp. 55–68.

Schneider, U., Alonso, M.C., Pimienta, P. & Jansson, R. (1986) *Physical properties and behaviour of high- performance concrete at high temperatures u. schneider, m. c. alonso, p.pimienta, r. jansson,* pp. 800–808.

Schneider, U., Schwesinger, P., Debicki, G., Diederichs, U., Franssen, J.M., Furamura, F., Jumppanen, U.M., Khoury, G.A., Millard, A. & Morris, W.A. (1997) 'Recommendations: Part 6 - Thermal strain', *Materials and Structures/Materiaux et Constructions,* 30(196 HS), pp. 17–21.

Sebeur Hassen and Horacio Colina (2006) 'Transient thermal creep of concrete in accidental conditions at temperatures up to 400C', *Magazine of Concrete Research,* 58(4), pp. 201–208.

Sercombe, J. & Galle, C. (2003) *Rehydration and microstructure of cement paste after heating at temperatures up to 300 ° C,* 33pp. 1047–1056.

Shakor, P. (2011) 'Glass Fibre Reinforced Concrete Use in Construction Related papers', *International Journal of Technology And Engineering System,* 2(2), .

Sharp, K.A., Madan, B., Manas, E. & Vanderkooi, J.M. (2001) 'Water structure changes induced by hydrophobic and polar solutes revealed by simulations and infrared spectroscopy', *Journal of Chemical Physics,* 114(4), pp. 1791–1796.

Shen, D., Liu, C., Li, C., Zhao, X. & Jiang, G. (2019) 'Influence of Barchip fiber length on early-age behavior and cracking resistance of concrete internally cured with super absorbent polymers', *Construction and Building Materials,* 214(1), pp. 219–231.

Shen, D., Liu, X., Li, Q., Sun, L. & Wang, W. (2019) 'Early-age behavior and cracking resistance of high-strength concrete reinforced with Dramix 3D steel fiber', *Construction and Building Materials,* 196pp. 307–316.

Shi, Y. (2015) *Development of recycled polypropylene plastic fibres to reinforce concrete. PhD thesis, James Cook University.,* p. 185.

Silva, F. de A., Filho, R.D.T., Filho, J. de A.M. & Fairbairn, E. de M.R. (2010) 'Physical and mechanical properties of durable sisal fiber-cement composites', *Construction and Building Materials,* 24(5), pp. 777–785.

Söylev, T.A. & Özturan, T. (2014) *Durability , physical and mechanical properties of fiber-reinforced concretes at low-volume fraction,* 73pp. 67–75.

Sukontasukkul, P., Pomchiengpin, W. & Songpiriyakij, S. (2010) ‘Post-crack (or post-peak) flexural response and toughness of fiber reinforced concrete after exposure to high temperature’, *Construction and Building Materials,* 24(10), pp. 1967–1974.

Terro, M.J. (1998) ‘Numerical modeling of the behavior of concrete structures in fire’, *ACI Structural Journal,* 95(2), pp. 183–193.

Torelli, G., Mandal, P., Gillie, M. & Tran, V.X. (2016) ‘Concrete strains under transient thermal conditions: A state-of-the-art review’, *Engineering Structures,* 127pp. 172–188.

Torkaman, J., Ashori, A. & Sadr Momtazi, A. (2014) ‘Using wood fiber waste, rice husk ash, and limestone powder waste as cement replacement materials for lightweight concrete blocks’, *Construction and Building Materials,* 50pp. 432–436.

Tu, L., Kruger, D., Wagener, J.B. & Carstens, P.A.B. (1998) ‘Surface modified polypropylene fibres for use in concrete’, *Magazine of Concrete Research,* 50(3), pp. 209–217.

Vincent, T. & Ozbakkaloglu, T. (2013) ‘Influence of fiber orientation and specimen end condition on axial compressive behavior of FRP-confined concrete’, *Construction and Building Materials,* 47pp. 814–826.

Vinogradov, G. V. & Prozorovskaya, N. V. (1964) ‘Rheology of polymers. Viscous properties of polypropylene melt’, *Rheologica Acta,* 3(3), pp. 156–163.

Vodák, F., Černý, R., Drchalová, J., Hošková, Š., Kapičková, O., Michalko, O., Semerák, P. & Toman, J. (1997) ‘Thermophysical properties of concrete for nuclear-safety related structures’, *Cement and Concrete Research,* 27(3), pp. 415–426.

Wang, W., Liu, X., Guo, L. & Duan, P. (2019) ‘Evaluation of properties and microstructure of cement paste blended with metakaolin subjected to high temperatures’, *Materials,* 16(6), .

Wang, W., Wang, L., Shi, Q., Yu, H., Chen, T., Wang, C. & Sun, T. (2006) ‘Progress of the surface modification of PP fiber used in concrete’, *Polymer - Plastics Technology and Engineering,* 45(1), pp. 29–34.

Wolf, R.A. (2010) *Plastic surface modification surface treatment and adhesion*. Munich [Germany] ; Cincinnati [Ohio]: Hanser.

Wong, H.S. & Buenfeld, N.R. (2009) ‘Determining the water-cement ratio, cement content, water content and degree of hydration of hardened cement paste: Method development and validation on paste samples’, *Cement and Concrete Research,* 39(10), pp. 957–965.

Xiao, J. & Falkner, H. (2006) ‘On residual strength of high-performance concrete with and without polypropylene fibres at elevated temperatures’, *Fire Safety Journal,* 41(2), pp. 115–121.

Xu, Y., Wong, Y.L., Poon, C.S. & Anson, M. (2001) *Impact of high temperature on PFA concrete*, 31(December 2000), pp. 1065–1073.

Yasuda, H. & Yasuda, T. (2000) 'Competitive ablation and polymerization (CAP) principle and the plasma sensitivity of elements in plasma polymerization and treatment', *Journal of Polymer Science, Part A: Polymer Chemistry*, 38(6), pp. 943–953.

Ye, G., Liu, X., Schutter, G. De, Taerwe, L. & Vandevelde, P. (2007) *Phase distribution and microstructural changes of self-compacting cement paste at elevated temperature*, 37pp. 978–987.

Yu, K., Jiang, H., Zhou, H., Mi, J., He, Y. & Wang, X. (2018) 'Evolution of double crystal melting peak in polypropylene foam assisted by β-nucleating agent and supercritical CO2', *Journal of Applied Polymer Science*, 135(12), pp. 1–10.

Zeiler, T., Kellermann, S. & Münstedt, H. (2000) 'Different surface treatments to improve the adhesion of polypropylene', *Journal of Adhesion Science and Technology*, 14(5), pp. 619–634.

Zeiml, M., Leithner, D., Lackner, R. & A. Mang, H. (2006) *How do polypropylene fibers improve the spalling behavior of in-situ concrete?* Vol. 36.

Zhang, H.L. & Davie, C.T. (2013) 'A numerical investigation of the influence of pore pressures and thermally induced stresses for spalling of concrete exposed to elevated temperatures', *Fire Safety Journal*, 59pp. 102–110.

Zhang, Q. & Ye, G. (2012) *Dehydration kinetics of Portland cement paste at high temperature*, pp. 153–158.

Zhang, Q. & Ye, G. (2011) 'Microstructure analysis of heated Portland cement paste', *Procedia Engineering*, 14pp. 830–836.

Zhang, Q., Ye, G. & Koenders, E. (2013) 'Investigation of the structure of heated Portland cement paste by using various techniques', *Construction and Building Materials*, 38pp. 1040–1050.

Zheng, Z. & Feldman, D. (1995) 'Synthetic fibre-reinforced concrete', *Progress in Polymer Science*, 20(2), pp. 185–210.